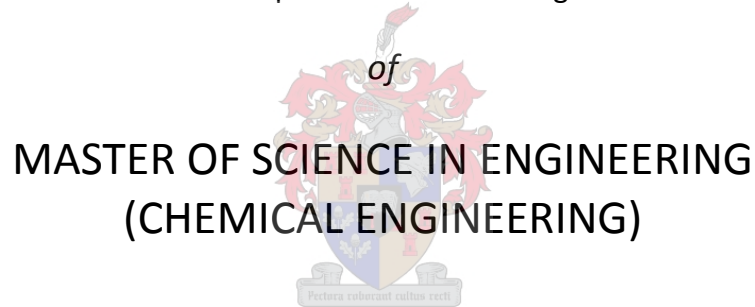


BACTERIAL PRODUCTION OF
ANTIMICROBIAL
BIOSURFACTANTS BY
Bacillus subtilis

by

Keenan Bence

Thesis presented in partial fulfillment
of the requirements for the Degree



in the Faculty of Engineering
at Stellenbosch University

Supervisor

Prof. K.G. Clarke

December 2011

Declaration

By submitting this thesis electronically, I declare that the entirety of the work contained therein is my own, original work, that I am the sole author thereof (save to the extent explicitly otherwise stated), that reproduction and publication thereof by Stellenbosch University will not infringe any third party rights and that I have not previously in its entirety or in part submitted it for obtaining any qualification.

Signature:.....

Date:.....

Copyright © 2011 University of Stellenbosch

All rights reserved

Abstract

Biosurfactants are microbially produced molecules that show excellent surface-active properties. *Bacillus subtilis* ATCC 21332 produces the biosurfactant, surfactin, which exhibits antimicrobial activity against bacteria as well as fungi. Although antimicrobial activity has been exhibited by a number of bacterially produced biosurfactants, notably the rhamnolipid from the pathogen *Pseudomonas aeruginosa*, the GRAS status *B. subtilis* makes the use of this organism preferable for large scale bioprocesses.

The objectives of this study were to: (1) evaluate the effect of different nutrient conditions on growth and surfactin production; (2) evaluate the growth of *B. subtilis* ATCC 21332 and associated surfactin production on a hydrocarbon substrate; (3) evaluate the antimicrobial activity of surfactin against *Mycobacterium aurum*, and (4) to establish whether active growth of *B. subtilis* ATCC 21332 and associated surfactin production can be extended during fed-batch culture.

B. subtilis ATCC 21332 was grown on low-nitrate; phosphate-limited and nutrient rich media with glucose as substrate during shake flask culture. Nitrate, phosphate, glucose and surfactin were quantified by HPLC analyses and growth via CDW and optical density measurements. Growth and surfactin production were further evaluated during shake flask culture on a hydrocarbon substrate replacing the glucose in the nutrient rich medium with an equivalent amount of *n*-hexadecane. The antimicrobial activity was quantified by growth inhibition of *M. aurum*.

Bioreactor batch and fed-batch studies were conducted to evaluate growth and surfactin production under controlled conditions. The fed-batch experiments included four constant dilution rate ($D=0.40\text{h}^{-1}$; $D=0.15\text{h}^{-1}$; $D=0.10\text{h}^{-1}$ and $D=0.05\text{h}^{-1}$) and two constant feed rate ($F=0.40\text{L/h}$ and $F=0.125\text{L/h}$) fed-batch strategies. The nutrient rich medium was used for these experiments and also as the feed medium for fed-batch experiments.

A CDW of 12.6 g/L was achieved in the nutrient rich medium during shake flask culture and was 2.5- and 1.6-fold higher than that achieved in the phosphate-limited medium and the low-nitrate medium respectively. A surfactin concentration of 652 mg/L was achieved in the nutrient rich medium, while a maximum surfactin concentration of 730 mg/L was achieved in the phosphate-limited medium. A surfactin concentration of only 172 mg/L was achieved in the low-nitrate medium.

Subsequently, growth and surfactin production were evaluated on *n*-hexadecane as sole carbon source. After inoculation, the CDW did not increase over a period of 119 h, which indicated that *B. subtilis* ATCC 21332 was unable to utilize *n*-hexadecane for growth and surfactin production.

The maximum CDW (27 g/L) and maximum surfactin concentration (1737 mg/L) achieved in the bioreactor batch experiments were 2.1- and 2.6-fold higher respectively than that achieved in the nutrient rich medium during shake flask experiments. These results served as a benchmark for further fed-batch experiments. During the fed-batch phase of the $D=0.40\text{h}^{-1}$ experiment, the biomass further increased by 9 g/h, which was 3.5-, 3.1- and 5.3-fold higher compared to the fed-batch phases of the $D=0.15\text{h}^{-1}$, $D=0.10\text{h}^{-1}$ and $D=0.05\text{h}^{-1}$ experiments respectively. Similarly, the biomass increased by 10.7 g/h during the fed-batch phase of the $F=0.40\text{L/h}$ experiment, which was 4.6-fold higher than that of the $F=0.125\text{L/h}$ experiment. The average rate of surfactin production was 633 mg/h during the fed-batch phase of the $D=0.40\text{h}^{-1}$ experiment, 29.4-, 5.4- and 34.2-fold higher compared to the fed-batch phases of the $D=0.15\text{h}^{-1}$, $D=0.10\text{h}^{-1}$ and $D=0.05\text{h}^{-1}$ experiments respectively. Analogously, the average rate of surfactin production (544 mg/h) of the $F=0.40\text{L/h}$ experiment was 9.4 fold higher than that of the $F=0.125\text{L/h}$ experiment.

The antimicrobial assay showed that surfactin inhibits *M. aurum* growth. An inhibition zone diameter of 4mm was measured at a surfactin concentration of 208 mg/L, which linearly increased to 24mm at a surfactin concentration of 1662 mg/L.

High feed flow rate strategies achieved higher rates of biomass increase and surfactin production and will thus decrease the production time required for large scale surfactin production. The antimicrobial activity of surfactin against *M. aurum* indicates that this biosurfactant has the potential to be used against *M. tuberculosis*, and as such has the potential to be used in the medical industry to reduce the spread of this, and other deadly diseases.

Uitreksel

Biosurfaktante is oppervlak-aktiewe molekules wat deur sekere mikro-organismes geproduseer word. *Bacillus subtilis* ATCC 21332 produseer 'n biosurfaktant genaamd surfactin, wat antimikrobiese eienskappe toon teen bakterieë sowel as fungi. Menige bakterieël geproduseerde biosurfaktante toon antimikrobiese eienskappe, vernaam die rhamnolipied van die patoog *Pseudomonas aeruginosa*, maar die algemene veiligheids-status van *B. subtilis* gee voorkeur aan hierdie organisme vir grootskaalse bioprosesse.

Die doelwitte van hierdie studie was: (1) om die effek van verskillende medium samestellings (in terme van voedingstowwe) ten opsigte van bakteriële seldigtheid en surfactin-produksie te evalueer; (2) om die bakteriële seldigtheid van *B. subtilis* ATCC 21332 en geassosieerde surfactin produksie vanaf 'n alkaan-substraat te evalueer; (3) om die antimikrobiese aktiwiteit van surfactin teen *Mycobacterium aurum* te evalueer; (4) om vas te stel of die aktiewe groei van *B. subtilis* ATCC 21332 en geassosieerde surfactin-produksie gedurende voer-lot kultuur verleng kan word.

B. subtilis ATCC 21332 was op lae-nitrat; fosfaat-beperkte en voedingstofryk-media met glukose as substraat in skudflesse gekultiveer. Nitrat, fosfaat, glukose en surfactin was deur hoëdruk vloeistofchromatografie gekwantifiseer en die seldigtheid deur middel van sel-droëmasse en optiese digtheid metings. Verder was die groei van *B. subtilis*, en geassosieerde surfactin produksie, vanaf 'n alkaan-substraat in skudflesse ge-evalueer deur die glukose in die voedingstofryke medium met 'n ekwivalente hoeveelheid van *n*-heksadekaan te vervang. Die antimikrobiese aktiwiteit van surfactin was deur die geïnhibeerde groei van *M. aurum* gekwantifiseer.

Bioreaktor lot en voer-lot studies was uitgevoer om die groei en surfactin produksie onder beheerde toestande te evalueer. Die voer-lot eksperimente het vier konstante verdunningstempos ($D=0.40\text{h}^{-1}$; $D=0.15\text{h}^{-1}$; $D=0.10\text{h}^{-1}$ en $D=0.05\text{h}^{-1}$) en twee konstante voertempos ($F=0.40\text{L/h}$ and $F=0.125\text{L/h}$) ingesluit. Die voedingstofryke medium was vir hierdie eksperimente en ook as die voermedium vir die voer-lot eksperimente gebruik.

'n Seldigtheid van 12.6 g/L is bereik gedurende skudfleskultuur in die voedingstofryk-media en was 2.5- en 1.6-voud hoër as die seldigthede wat in die fosfaat-beperkte en lae-nitrat media bereik is. 'n Surfactin konsentrasie van 652 mg/L is bereik in die voedingstofryke medium, terwyl 'n maksimum surfactin konsentrasie van 730 mg/L in die fosfaat-beperkte medium bereik is. 'n Surfactin konsentrasie van slegs 172 mg/L is in die lae-nitrat medium bereik.

Hierna was bakteriële seldigheid en surfactin produksie gevalueer met slegs *n*-heksadekaan as die enigste koolstof bron. Die bakteriële seldigheid het geen verandering getoon na inokulasie nie, wat aangedui het dat *B. subtilis* ATCC 21332 nie die vermoë beskik om *n*-heksadekaan vir groei en surfactin produksie te gebruik nie.

Die maksimum seldigheid (27 g/L) en maksimum surfactin konsentrasie (1737 mg/L) bereik in die bioreaktor lot eksperimente was 2.1- en 2.6-voud hoër onderskeidelik as dit bereik in die voedingstofryke medium gedurende skudfles eksperimente. Hierdie resultate dien as 'n basis vir verdere voer-lot eksperimente. Gedurende die voer-lot fase van die $D=0.40\text{h}^{-1}$ het die biomassa verder verhoog teen 9 g/h, wat 3.5-, 3.1- en 5.3-voud hoër was as dit van die $D=0.15\text{h}^{-1}$, $D=0.10\text{h}^{-1}$ en $D=0.05\text{h}^{-1}$ eksperimente onderskeidelik. Die biomassa het soortgelyk tydens die voer-lot fase van die $F=0.40\text{L/h}$ eksperiment teen 10.7 g/h verhoog, wat 4.6-voud hoër was as dit van die $F=0.125\text{L/h}$ eksperiment. Die gemiddelde tempo van surfactin produksie was 633 mg/h gedurende die voer-lot fase van die $D=0.40\text{h}^{-1}$ eksperiment, 29.4-, 5.4- en 34.2-voud hoër vergeleke met die voer-lot fases van die $D=0.15\text{h}^{-1}$, $D=0.10\text{h}^{-1}$ en $D=0.05\text{h}^{-1}$ eksperimente onderskeidelik. Die gemiddelde tempo van surfactin produksie (544 mg/L) was soortgelyk 9.4-voud hoër gedurende die voer-lot fase van die $F=0.40\text{L/h}$ eksperimente, vergeleke met die $F=0.125\text{L/h}$ eksperiment.

Die antimikrobiese toetse van surfactin teen *M. aurum* het positief getoets, wat aandui dat surfactin die groei van hierdie organisme inhibeer. 'n Inhibisie sone deursnee van 4mm was gemeet teen 'n surfactin konsentrasie van 208 mg/L, wat lineêr verhoog het tot 24 mm teen 'n surfactin konsentrasie van 1662 mg/L.

Hoë voertempo strategieë het hoër biomassa verhogingstempos en surfactin produksie tempos getoon en sal dus die produksietyd aansienlik verkort tydens grootskaalse surfactin produksie. Die antimikrobiese aktiwiteit van surfactin teen *M. aurum* toon dat hierdie biosurfaktant die vermoë het om gebruik te word teen *M. tuberculosis*. Daarom het surfactin die potensiaal om gebruik te word in die mediese industrie om die verspreiding van Tuberkulose, en ander dodelike patogene, te voorkom.

Acknowledgements

The following organizations and people are thanked for making this research possible:

- The National Research Foundation and the University of Stellenbosch for their financial assistance
- Prof. K.G. Clarke for supervising the project
- Mrs. H. Botha, Mrs. A. van Zyl, Mrs. M. Rossouw and Ms. L. Hamerse for their assistance with the surfactin-, glucose-, nitrate- and phosphate analyses
- Mrs. P. Snijman at the Department of Chemistry for the use of their tensiometer
- Prof. S. Reid (Department of Molecular and Cell Biology at the University of Cape Town) for kindly providing *Mycobacterium aurum*
- K. Hechter for her assistance with experiments. G. Griffen for evaluating the effect of phosphate concentration on the lag phase of *B. subtilis* growth.
- My wife, for her support and always believing in me
- My fellow students
- Jesus Christ, for His love and guidance

Table of Contents

| | |
|--|-----------|
| Declaration | ii |
| Abstract | iv |
| Uitreksel | vi |
| Acknowledgements | viii |
| List of figures | xiii |
| List of tables | xvi |
| Glossary and Nomenclature | xvii |
| Introduction | 20 |
| 1 Literature review | 21 |
| 1.1 Classification of biosurfactants | 21 |
| 1.1.1 Glycolipids | 21 |
| 1.1.2 Phospholipids and Polymeric biosurfactants | 22 |
| 1.1.3 Lipopeptides | 23 |
| 1.2 Properties of biosurfactants | 24 |
| 1.2.1 Surface tension | 24 |
| 1.2.2 Emulsification activity | 25 |
| 1.2.3 Foaming activity | 25 |
| 1.2.4 Biological activity | 26 |
| 1.3 Applications of biosurfactants | 31 |
| 1.3.1 Bioremediation applications | 32 |
| 1.3.2 Agricultural applications | 32 |
| 1.3.3 Biomedical applications | 33 |
| 1.4 Physiological roles of biosurfactants | 34 |
| 1.5 Location of biosurfactant in cell culture | 35 |
| 1.6 Association of biosurfactant and cell growth phase | 35 |
| 1.7 Quantification of biosurfactant characteristics | 35 |
| 1.7.1 Surface tension | 35 |
| 1.7.2 Quantification of surfactin concentration | 36 |
| 1.7.3 Emulsification activity | 37 |
| 1.7.4 Foaming activity | 37 |
| 1.7.5 Antimicrobial activity | 37 |

| | | |
|----------|--|-----------|
| 1.8 | Process conditions | 38 |
| 1.8.1 | Medium components..... | 38 |
| 1.8.2 | Process operation | 46 |
| 1.8.3 | Preferred process conditions for growth of <i>B. subtilis</i> and associated surfactin production | 57 |
| 1.9 | Hypotheses | 58 |
| 1.10 | Objectives | 58 |
| 2 | Materials and Methods | 60 |
| 2.1 | Micro-organisms and culture maintenance | 60 |
| 2.2 | Culture Media | 60 |
| 2.2.1 | Liquid media | 60 |
| 2.2.2 | Solid media | 63 |
| 2.3 | Experimental protocol..... | 63 |
| 2.3.1 | Inoculum development | 63 |
| 2.3.2 | Test flask experiments | 64 |
| 2.3.3 | Bioreactor experiments..... | 64 |
| 2.4 | Analytical Methods | 66 |
| 2.4.1 | Cell concentration..... | 66 |
| 2.4.2 | Surface tension | 68 |
| 2.4.3 | Surfactin concentration..... | 70 |
| 2.4.4 | Glucose concentration | 72 |
| 2.4.5 | Nitrate- and phosphate concentrations..... | 73 |
| 2.4.6 | Antimicrobial activity | 76 |
| 3 | Results and Discussion | 77 |
| 3.1 | Media requirements for growth and biosurfactant production | 77 |
| 3.1.1 | Media selection | 77 |
| 3.1.2 | Quantification of cell dry weight and surfactin concentration in selected glucose media | 77 |
| 3.1.3 | Influence of nutrient conditions on cell dry weight and surfactin concentration during shake flask culture | 79 |
| 3.1.4 | Quantification of cell dry weight and surfactin concentration in alkane media..... | 84 |
| 3.2 | Bioreactor batch culture of <i>B. subtilis</i> ATCC 21332 | 85 |
| 3.2.1 | Cell dry weight and surfactin concentration in bioreactor batch culture | 85 |

| | | |
|----------|--|------------|
| 3.2.2 | Influence of nutrient conditions on cell dry weight and surfactin concentration in bioreactor batch culture | 87 |
| 3.2.3 | Quantification of kinetics parameters of bioreactor batch cultures..... | 89 |
| 3.2.4 | Comparison of cell dry weight and surfactin concentration between bioreactor batch- and shake flask studies..... | 97 |
| 3.2.5 | Comparison of nutrient concentrations between bioreactor batch- and shake flask studies | 97 |
| 3.3 | Bioreactor fed- batch culture of <i>B. subtilis</i> ATCC 21332 | 99 |
| 3.3.1 | Quantification of cell dry weight and surfactin concentration in constant dilution rate fed-batch experiments..... | 99 |
| 3.3.2 | Comparison of rate of total biomass- and rate of total surfactin increase in constant dilution rate fed-batch experiments | 104 |
| 3.3.3 | Influence of nutrient conditions on cell dry weight and surfactin concentration in constant dilution rate fed-batch cultures | 105 |
| 3.3.4 | Quantification of kinetic parameters of constant dilution rate fed batch cultures | 108 |
| 3.3.5 | Quantification of cell dry weight and surfactin concentration in constant feed rate fed-batch cultures..... | 116 |
| 3.3.6 | Comparison of rate of total biomass- and rate of total surfactin increase in constant feed rate fed-batch experiments | 118 |
| 3.3.7 | Influence of nutrient conditions on cell dry weight and surfactin concentration in constant feed rate fed-batch cultures | 119 |
| 3.3.8 | Quantification of kinetic parameters of constant feed rate fed-batch cultures... | 120 |
| 3.4 | Surface activity of surfactin | 127 |
| 3.5 | Antimicrobial activity of surfactin against <i>Mycobacterium aurum</i> | 128 |
| 3.6 | Reproducibility of experiments | 130 |
| 3.6.1 | Shake flask experiments..... | 130 |
| 3.6.2 | Bioreactor experiments..... | 131 |
| 3.6.3 | Antimicrobial activity | 132 |
| 4 | Conclusions | 133 |
| 5 | Recommendations | 135 |
| | References..... | 137 |
| | Appendix A: Fed-batch Kinetics | 146 |
| | Derivation of unsteady-state rate equations..... | 146 |

| | |
|--|------------|
| Quasi-steady-state fed-batch operation | 149 |
| Derivation of exponential feed flow rate equation | 150 |
| Variation of dilution rate with constant feed rate | 152 |
| Appendix B: Predicted feed flow rates of constant dilution rate experiments | 154 |
| Appendix C: HPLC chromatograms | 157 |

List of figures

| | |
|--|----|
| Figure 1-1: R1-R4 Rhamnolipids (<i>Lang and Wullbrandt, 1999</i>) | 22 |
| Figure 1-2: A surfactin molecule | 23 |
| Figure 1-3: Schematic representation of membrane perturbation by fengycin (<i>Deleu et al., 2008</i>) | 30 |
| Figure 1-4: Assimilatory nitrate reduction pathway: Present in all bacteria that reduce nitrate to ammonia for subsequent conversion to nitrogenous cell constituents. Enzymes: 1 – nitrate reductase; 2 – nitrite reductase (<i>Redrawn from White, 2007</i>) | 45 |
| Figure 2-1: Illustration of stepwise increase in sterile feed flow rate to maintain a constant dilution rate | 66 |
| Figure 2-2: Relationship between CDW and Optical density | 68 |
| Figure 2-3: The du Noüy Tensiometer (With permission: University of Stellenbosch, Chemistry 324 Practical Guide 2009) | 69 |
| Figure 2-4: Surfactin standard curve | 71 |
| Figure 2-5: Glucose standard curve | 73 |
| Figure 2-6: Nitrate standard curve | 74 |
| Figure 2-7: Phosphate standard curve | 75 |
| Figure 2-8: Schematic representation of antimicrobial inhibition zones | 76 |
| Figure 3-1: Growth and surfactin production by <i>B. subtilis</i> ATCC 21332 from selected media.... | 78 |
| Figure 3-2: Influence of nutrient conditions on growth and surfactin production in medium A | 79 |
| Figure 3-3: Influence of nutrient conditions on growth and surfactin production in medium B | 80 |
| Figure 3-4: Evaluation of the effect of phosphate concentration on lag phase..... | 81 |
| Figure 3-5: Influence of nutrient conditions on growth and surfactin production in medium D | 82 |
| Figure 3-6: Influence of nutrient conditions on growth and surfactin production in medium C | 83 |
| Figure 3-7: Comparison of growth profiles between growth on glucose- and alkane media | 84 |
| Figure 3-8: CDW profiles of bioreactor batch experiments (configuration 1 and 2)..... | 86 |
| Figure 3-9: Dissolved oxygen concentration profiles of bioreactor batch experiments | 87 |
| Figure 3-10: Nutrient concentration profiles of batch culture in the bioreactor with configuration 1..... | 88 |
| Figure 3-11: Nutrient concentration profiles of batch culture in the bioreactor with configuration 2..... | 89 |
| Figure 3-12: $\ln(xV)$ versus time profiles of bioreactor batch experiments | 90 |
| Figure 3-13: Specific growth rate profiles of bioreactor batch experiments..... | 91 |
| Figure 3-14: Biomass yield on glucose profiles of bioreactor batch experiments | 92 |
| Figure 3-15: Surfactin yield on glucose ($Y_{p/s}$) profiles of bioreactor batch experiments..... | 94 |
| Figure 3-16: Surfactin yield on biomass profiles of bioreactor batch experiments | 95 |

| | |
|--|-----|
| Figure 3-17: Surfactin productivity and specific productivity profiles of bioreactor batch experiments | 96 |
| Figure 3-18: Comparison of growth and biosurfactant production in shake flasks and bioreactor | 97 |
| Figure 3-19: Comparison of glucose- and nitrate concentration profiles between bioreactor batch and shake flask studies | 98 |
| Figure 3-20: CDW profiles of fed-batch cultures (from 12 hours) during which exponential feeding strategies were applied | 101 |
| Figure 3-21: Total biomass profiles of fed-batch cultures during which exponential feeding strategies were applied | 102 |
| Figure 3-22: Surfactin concentration profiles of fed-batch cultures during which exponential feeding strategies were applied | 103 |
| Figure 3-23: Total surfactin profiles of fed-batch cultures during which exponential feeding strategies were applied | 104 |
| Figure 3-24: Average rate of biomass increase and average rate of surfactin production during fed-batch phases of constant dilution rate fed-batch experiments..... | 105 |
| Figure 3-25: Glucose concentration profiles of fed-batch cultures during which exponential feeding strategies were applied | 106 |
| Figure 3-26: Nitrate concentration profiles of fed-batch cultures during which exponential feeding strategies were applied | 107 |
| Figure 3-27: DO concentration profiles of fed-batch cultures during which exponential feeding strategies were applied | 108 |
| Figure 3-28: Specific growth rate profiles of fed-batch cultures during which exponential feeding strategies were applied | 109 |
| Figure 3-29: Biomass yield on glucose profiles of fed-batch cultures during which exponential feeding strategies were applied | 110 |
| Figure 3-30: Surfactin yield on glucose profiles of fed-batch cultures during which exponential feeding strategies were applied | 112 |
| Figure 3-31: Surfactin yield on biomass profiles of fed-batch cultures during which exponential feeding strategies were applied | 113 |
| Figure 3-32: Relationship between CDW and surfactin concentration during batch phases of fed-batch cultures during which exponential feeding strategies were applied | 114 |
| Figure 3-33: Surfactin productivity profiles of fed-batch cultures during which exponential feeding strategies were applied | 115 |
| Figure 3-34: Surfactin specific productivity profiles of fed-batch cultures during which exponential feeding strategies were applied | 116 |
| Figure 3-35: CDW and surfactin concentration profiles of fed-batch cultures during which constant feeding strategies were applied | 117 |

| | |
|---|-----|
| Figure 3-36: Total biomass and total surfactin profiles of fed-batch cultures during which constant feeding strategies were applied | 118 |
| Figure 3-37: Average hourly rate of biomass- and surfactin increases during the fed-batch phases of the constant feed rate fed-batch experiments..... | 119 |
| Figure 3-38: Glucose-, nitrate- and dissolved oxygen concentration profiles of fed-batch cultures during which constant feeding strategies were applied | 120 |
| Figure 3-39: Specific growth rate profiles of fed-batch cultures during which constant feeding strategies were applied | 121 |
| Figure 3-40: Biomass yield on glucose profiles of fed-batch cultures during which constant feeding strategies were applied | 123 |
| Figure 3-41: Surfactin yield on glucose profiles of fed-batch cultures during which constant feeding strategies were applied | 124 |
| Figure 3-42: Surfactin yield on biomass profiles of fed-batch cultures during which constant feeding strategies were applied | 125 |
| Figure 3-43: Surfactin productivity and specific productivity profiles of fed-batch cultures during which constant feeding strategies were applied..... | 127 |
| Figure 3-44: Plot of surface tension versus surfactin concentration..... | 128 |
| Figure 3-45: Relationship between surfactin concentration and antimicrobial activity (inhibition diameter) against <i>M. aurum</i> | 129 |
| Figure 3-46: Percentage reproducibility of key parameters of shake flask experiments..... | 130 |
| Figure 3-47: Percentage reproducibility of key parameters of bioreactor experiments..... | 131 |
| Figure A-1: Exponential increase in feed flow rate, while cell- and substrate concentration remains constant | 151 |
| Figure A-2: Change of dilution rate with time when a constant feed rate strategy is applied .. | 153 |
| Figure C-1: HPLC chromatogram of a 2.5 g/L surfactin standard | 157 |
| Figure C-2: HPLC chromatogram of a 2.0352 g/L glucose standard | 158 |

List of tables

| | |
|---|-----|
| Table 1-1: Organisms susceptible to antimicrobial action of biosurfactants produced by <i>B. subtilis</i> | 27 |
| Table 1-2: Antiviral activity of surfactin from <i>B. subtilis</i> | 29 |
| Table 1-3: List of media used in literature for biosurfactant production by <i>Bacillus subtilis</i> | 42 |
| Table 1-4: Process operating conditions and modes of operation used for <i>B. subtilis</i> culture from literature | 48 |
| Table 1-5: Feeding strategies applied for fed-batch culture of <i>B. subtilis</i> from literature | 54 |
| Table 2-1: Medium A and Medium B media components | 61 |
| Table 2-2: Trace element solution components for Medium A and Medium B | 62 |
| Table 2-3: Medium components of Medium C..... | 62 |
| Table 2-4: Trace element solution components for Medium C | 62 |
| Table 2-5: Derived media used for growth and biosurfactant production studies | 63 |
| Table 2-6: Predetermined feeding strategies for fed-batch fermentation | 65 |
| Table 2-7: Specifications of the HPLC column, mobile phase and absorbance..... | 70 |
| Table 2-8: HPLC specifications for glucose analyses | 72 |
| Table 2-9: Ion Chromatograph specifications for nitrate- and phosphate analyses | 74 |
| Table 3-1: Maximum CDWs and maximum surfactin concentrations achieved in selected media | 83 |
| Table B-1: Predicted feed flow rates according to Equation 2-1 to maintain a constant dilution rate of 0.05 h^{-1} , 0.10 h^{-1} , 0.15 h^{-1} and 0.4 h^{-1} (<i>continued</i>)..... | 156 |

Glossary and Nomenclature

| | |
|---|---|
| ATCC 21332 | Strain of <i>Bacillus subtilis</i> |
| aq | Aqueous |
| $\text{CaCl}_2 \cdot 4\text{H}_2\text{O}$ | Calcium chloride tetrahydrate |
| CDW | Cell dry weight |
| $\text{CoSO}_4 \cdot 7\text{H}_2\text{O}$ | Cobaltous sulphate heptahydrate |
| CMC | Critical micelle concentration |
| CuCl_2 | Copper chloride |
| $\text{CuSO}_4 \cdot 5\text{H}_2\text{O}$ | Copper sulphate pentahydrate |
| D | Dilution rate |
| DO | Dissolved oxygen |
| F | Flow rate |
| F_i | Flow rate at time i |
| F_0 | Initial flow rate at time 0 |
| $\text{FeSO}_4 \cdot 7\text{H}_2\text{O}$ | Ferrous sulphate heptahydrate |
| g | Gram |
| g | gravitational acceleration |
| h | Hour |
| HPLC | High pressure liquid chromatography |
| IR | Infra-Red |
| K_s | That substrate concentration at which half the maximum specific growth rate has been achieved |
| K_2HPO_4 | di-Potassium hydrogen orthophosphate |
| KCl | Potassium chloride |
| KNO_3 | Potassium nitrate |
| KH_2PO_4 | Potassium di-hydrogen orthophosphate |
| l | Contact perimeter of tensiometer ring with liquid surface |
| L | Litre |
| L/h | Litre per hour |
| M | Molar |
| m | mass |
| m_s | Specific rate of substrate uptake for maintenance activities |
| min | minute |
| ml | Millilitre |

| | |
|---|---|
| mL/min | Millilitre per minute |
| mg/L | Milligram per litre |
| mg/L/h | Milligram per litre per hour |
| mg/L/h/g _{cells} | Milligram per litre per hour per gram cells |
| MgSO ₄ ·7H ₂ O | Magnesium sulphate heptahydrate |
| MIC | Minimal inhibition concentration |
| mM | Millimolar |
| mm | Millimetre |
| mN/m | Milli-Newton per metre |
| MnSO ₄ ·H ₂ O | Hydrous manganese sulphate |
| MSM | Minimal salts medium |
| mV | Millivolt |
| NaCl | Sodium chloride |
| NaNO ₃ | Sodium nitrate |
| NaOH | Sodium hydroxide |
| (NH ₄) ₂ SO ₄ | Ammonium sulphate |
| nm | Nanometre |
| ρ | Density |
| ρ_i | Density at time <i>i</i> |
| ρ_0 | Initial density at time 0 |
| p | Product |
| P_i | Product concentration at time 'i' |
| P_0 | Initial product concentration |
| q_p | Specific rate of product formation |
| r_s | Rate of substrater uptake |
| r_p | Volumetric rate of product formation |
| r_x | Volumetric rate of biomass formation |
| R | Difference in weight measured before and after calibration of tensiometer |
| rcf | Relative centrifugal force |
| rpm | Revolutions per minute |
| s | Substrate |
| S_{fed} | Amount of substrate added during fed-batch culture |
| S_{feed} | Substrate concentration in feed stream |
| S_i | Substrate concentration at time 'i' |
| S_0 | Initial substrate concentration |
| $S_{reactor}$ | Residualsubstrate concentration in reactor |

| | |
|---|--------------------------------------|
| t | Time |
| TB | Tuberculosis |
| UV | Ultraviolet |
| μ | Specific growth rate |
| μ_{\max} | Maximum specific growth rate |
| μl | Microlitre |
| μM | Micromolar |
| μm | Micrometre |
| V | Volume |
| V_0 | Initial volume |
| v/v | Volume per volume |
| vvm | Volume per volume per minute |
| x | Cell concentration |
| X_i | Cell concentration at time 'i' |
| X_0 | Initial cell concentration |
| $Y_{p/s}$ | Product yield on substrate |
| $Y_{p/x}$ | Product yield on biomass |
| $Y_{x/s}$ | Biomass yield on substrate |
| Y_{PS} | True yield of product from substrate |
| Y_{XS} | True yield of biomass from substrate |
| $\text{ZnSO}_4 \cdot 7\text{H}_2\text{O}$ | Zinc sulphate heptahydrate |
| ZnCl_2 | Zinc chloride |

Introduction

Biosurfactants are surface-active molecules synthesized by numerous micro-organisms. One of the most intensively studied among these is *Bacillus subtilis*, which produces the surface-active molecule surfactin. The name surfactin was derived from its outstanding surfactant activity and was first discovered by Arima *et al.*, (1968), who reported the presence of a biologically active compound in the culture broth of a *B. subtilis* strain. A year later, the structure of this molecule was elucidated as that of a lipopeptide (Kakinuma *et al.* 1969a; Kakinuma *et al.* 1969b; Kakinuma *et al.* 1969 c).

Surfactin has the ability to reduce surface- and interfacial tensions and to form stable emulsions and foams. As such, surfactin has drawn much attention as a replacement to chemical surfactants as it offers distinct advantages over chemically synthesized surfactants, such as low toxicity, biodegradability, environmental compatibility and high selectivity and specific activity at extreme temperatures, pH and salinity. These properties have encouraged applications of surfactin in the minerals processing, food, environmental and cosmetics industries (Desai and Banat, 1997)

Studies on surfactin have shown that it also has biological properties, such as antibacterial (Haba *et al.*, 2001; Abalos *et al.*, 2002; Benincasa *et al.*, 2004; Bechard *et al.*, 1998), antiviral (Kracht *et al.*, 1999; Vollenbroich *et al.*, 1997; Makkar and Cameotra, 2002) and anticancer activities (Thanomsub, 2006; Seydlova *et al.*, 2008, Jing *et al.*, 2006), making it a promising agent for the biomedical industry. The aim of this study was to develop a process strategy for the enhanced production of surfactin for its use as antimicrobial agents. The process strategy was developed by considering appropriate environmental conditions, nutrient requirements and different process operations. This was initiated by means of an extensive literature survey on the production, properties and applications of biosurfactants, with focus on surfactin and the external factors that influence its production.

1 Literature review

1.1 Classification of biosurfactants

Biosurfactants are mainly classified according to their chemical structure and their microbial origin. Generally, their structure consists of a hydrophilic moiety and a hydrophobic moiety. The hydrophilic moiety usually consists of amino acids, anions or cations, or polysaccharides. The hydrophobic moiety, however, consists of saturated- or unsaturated fatty acids. Accordingly, the main classes of biosurfactants are glycolipids, phospholipids, polymeric biosurfactants and lipopeptides (Desai and Banat, 1997).

1.1.1 Glycolipids

Glycolipid biosurfactants are sugar-containing lipids in which a carbohydrate moiety is linked to a fatty acid moiety (Hommel & Ratledge, in N. Kosaric, 1993). The best known glycolipids are rhamnolipids, sophorolipids and trehalolipids, each of which is subsequently discussed (Desai and Banat, 1997).

1.1.1.1 Rhamnolipids

Rhamnolipids are probably the most common glycolipid and are produced by *Pseudomonas aeruginosa*. Rhamnolipids are formed by one or two rhamnose (hydrophilic) molecules linked to one or two fatty acids (hydrophobic), which are saturated or unsaturated C₈ – C₁₂ alkyl chains (Haba *et al.*, 2003). Consequently, many different homologues of rhamnolipids (as many as 28) have been identified and mixtures of these homologues can be produced by a single strain of *P. aeruginosa* (Abalos *et al.*, 2001). However, the types of rhamnolipids produced depend on the bacterial strain, the carbon source used and the process strategy (Lang and Wullbrandt, 1999; Déziel *et al.*, 1996; Itoh, 1971). Four homologues are most predominant. These four compounds are commonly referred to as R1-R4 rhamnolipids and are shown in Figure 1-1.

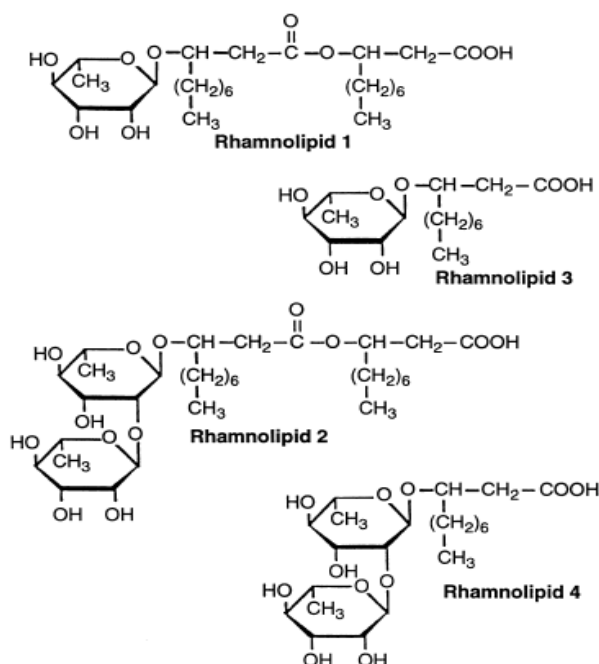


Figure 1-1: R1-R4 Rhamnolipids (Lang and Wullbrandt, 1999)

1.1.1.2 Sophorolipids and Trehalolipids

Sophorolipids and trehalolipids are similar in structure when compared to rhamnolipids (Cooper and Zajic, 1980). Sophorolipids consist of a dimeric sophorose molecule which is linked to a long chain hydroxy fatty acid and are mainly produced by the yeasts *Torulopsis bombicola* and *T. petrophilum* (Desai and Banat, 1997).

Trehalolipids are characterized by disaccharide trehalose linked at C₆ to two β-hydroxy-α-branched fatty acids. They have been isolated from several strains of *Arthrobacter*, *Mycobacterium*, *Brevibacterium*, *Corynebacterium* and *Nocardiaspp.* (Desai and Banat, 1997; Cooper and Zajic, 1980). The trehalolipids produced by these organisms differ in structure of fatty acids and the degree of unsaturation (Desai and Banat, 1997).

1.1.2 Phospholipids and Polymeric biosurfactants

Phospholipids are probably best known as a major constituent of all cell membranes. They consist of a fatty acid linked to a cationic phosphate group and have been reported to be produced by certain strains of *Acinetobacter sp.*, *Aspergillus sp.*, and *Theobacillus theooxidans* (Kosaric, 1993).

Polymeric biosurfactants are high molecular weight biopolymers which consist of a polysaccharide backbone to which fatty acid side chains are covalently linked (Desai and Desai, in N. Kosaric, 1993). The most intensively studied polymeric biosurfactants are emulsan and liposan and are produced by *Acinetobacter calcoaceticus* and *Candida lipolytica* respectively (Desai and Desai, in N. Kosaric, 1993).

1.1.3 Lipopeptides

Lipopeptide biosurfactants are mainly produced by *Bacillus* sp. and are characterized by a hydrophilic amino acid chain (peptide) which is linked to a fatty acid. The hydrophilic peptide is either linear or cyclic, as in the case of surfactin, a lipopeptide biosurfactant produced by *Bacillus subtilis* (Vanittanakom *et al.*, 1986). The latter also produces other lipopeptides, such as fengycin and iturin (Deleu *et al.*, 2005, Deleu *et al.*, 2008); however, surfactin is of particular importance in this study and is further discussed.

Surfactin is a nonionic lipopeptide biosurfactant produced by various strains of *B. subtilis* and is regarded as one of the most powerful biosurfactants known (Wei and Chu, 1998; Hommel, 1990). Surfactin consists of a cyclic peptide and a β -hydroxyl fatty acid (Davis *et al.*, 1999) (Figure 1-2: A surfactin molecule). The cyclic peptide consists of seven amino acids, which may differ in sequence, but in all cases it is composed of five lipophilic amino acids and two negatively charged hydrophilic ones (Buchoux *et al.*, 2008; Singh and Cameotra, 2004).

The length and structure of the fatty acid may also differ. Generally, the fatty acid consists of 13-16 carbon atoms and may be branched. Consequently, surfactin has a number of homologues (analogous to rhamnolipids). The production of surfactin by *B. subtilis* is accepted to be a mixture of homologues and the exclusive production of a single homologue is not reported in literature (see section 2.4.3). However, it has been reported that surfactin homologues with C₁₃-C₁₅ fatty acids are produced in more or less the following proportions: 50% C₁₅, 35% C₁₄ and 15% C₁₃ (Akpa *et al.*, 2001). It is further reported that the proportion of surfactin homologues produced is influenced by the growth medium (Akpa *et al.*, 2001). The fraction of C₁₅ fatty acid chain lengths increases when threonine is present in the growth medium (Akpa *et al.*, 2001).

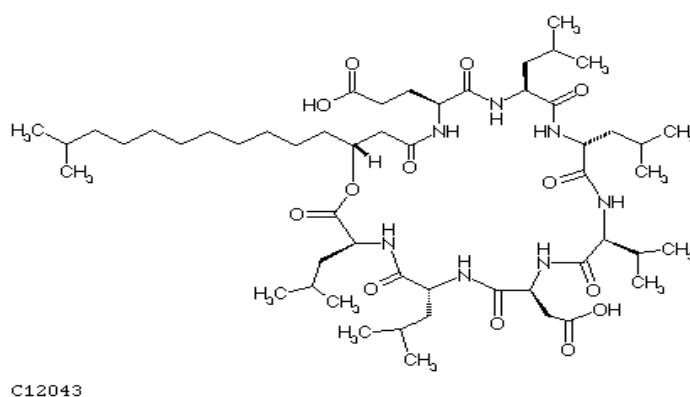


Figure 1-2: A surfactin molecule

1.2 Properties of biosurfactants

The properties of biosurfactants that make them very attractive for industrial use include pH stability, thermal stability, solubility and surface activity. In many cases, biosurfactants have shown superiority to chemically derived surfactants. Moreover, biosurfactants are also environmentally friendly, which makes these molecules particularly attractive in the modern economic climate (Kim *et al.*, 1997).

Not only do biosurfactants exhibit excellent physico-chemical properties, but also some very useful biological activities. Biosurfactants have been reported to show antimicrobial, antiviral and anticancer activities (Peypoux *et al.*, 1999). Therefore, these molecules might find useful applications in the medical industry in the future. As such, one of the focus areas of this study will be the antimicrobial activity of surfactin.

1.2.1 Surface tension

The amphiphilic structure of biosurfactants causes the molecules to align at the interface between two different phases (Desai and Banat, 1997). Therefore, at an air/water interface, the hydrophilic moiety will be immersed within the water phase with the hydrophobic moiety in the air (Maget-Dana and Ptak, 1995). As a result of the alignment of biosurfactant molecules at the interface between two different phases, it reduces surface- and interfacial tensions (Desai and Banat, 1997).

The surface tension activity of biosurfactants differs from one another. While polymeric biosurfactants do not significantly reduce the surface- and interfacial tensions, rhamnolipids and surfactin are capable of reducing the surface tension of distilled water from 72mN/m to 27mN/m (Desai and Banat, 1997; Arima *et al.*, 1968). However, the emulsification activity of rhamnolipids and surfactin are inferior to that of polymeric biosurfactants (Desai and Banat, in N. Kosaric, 1993) (see section 1.2.2).

The efficiency of the biosurfactant surface tension activity is expressed by the critical micelle concentration (CMC) (Ballot, 2009). The CMC is the concentration limit of a biosurfactant after which the addition of more biosurfactant will not cause the surface tension to be further reduced. The CMC is also defined as the solubility of a surfactant in the aqueous phase (Desai and Banat, 1997). Therefore, a biosurfactant with a low CMC is more efficient in lowering surface- and interfacial tensions than a biosurfactant with a high CMC. Biosurfactant CMCs range from 1 – 200 mg/L (Van Hamme *et al.*, 2006) and are 10 – 40 fold less than that of synthetic surfactants (Lang and Philp, 1998 in Ballot, 2009). Kim *et al.* (1997) reported that surfactin showed a lower CMC, and higher surface tension reducing activity, than the commercial surfactant sodium dodecyl sulfate (SDS). The CMC of surfactin has been reported to be as low as 21 mg/L (Peypoux *et al.*, 1999), while that of rhamnolipids has been reported to be around 40 mg/L (Zhang and Miller, 1992).

1.2.2 Emulsification activity

Emulsions are formed when one liquid phase is dispersed as microscopic droplets within another. The best studied biosurfactants that form stable emulsions are the polymeric biosurfactants emulsan and liposan, produced by *Acinetobacter calcoaticus* and *Candida lipolytica* respectively. It is reported that emulsan can form stable emulsions at concentrations as low as 0.001% – 0.01% and is regarded as one of the most powerful emulsion stabilizers known today. The excellent emulsifying properties of polymeric biosurfactants may be attributed to the high molecular weight (as high as 51400 g/mole), high viscosity, tensile strength and resistance to shear (Desai and Banat, 1997; Desai and Desai, in N. Kosaric, 1993)

However, low molecular weight biosurfactants (1000-1500 g/mole) have also been shown to form stable emulsions (Benincasa *et al.*, 2004; Makkar and Cameotra, 1998; Kim *et al.*, 1997). Benincasa *et al.* (2004) reported that rhamnolipids formed stable emulsions over a 21 day period when mixed as a 15% (m/v) aqueous solution with castor oil (EI¹ = 67%), almond oil (EI = 83%), crude oil (EI = 75%), kerosene (EI = 50%) and benzene (EI = 60%). Analogous to rhamnolipids, surfactin has also been shown to stabilize emulsions (Makkar and Cameotra, 1998; Kim *et al.*, 1997). Makkar and Cameotra (1998) showed that an EI of 33% was obtained when 4mL of culture supernatant was mixed with 6mL of motor oil.

1.2.3 Foaming activity

Foaming is another property that results from the amphiphilic structure of biosurfactants and is of considerable interest in the development of detergents and cosmetics, and also for pharmaceutical applications (Razafindralambo *et al.*, 1996). Usually, stable foams with small bubble sizes are required. Stable foams and small bubble sizes are particularly useful in the flotation (minerals processing) industry for the separation of platinum group metals from suspensions (Corné Marais, pers. comm.).

Razafindralambo *et al.* (1996) reported that surfactin showed better foam stability at low concentrations (as low as 0.05mg/L) when compared to commercial surfactants, such as sodium dodecyl sulphate (SDS) and bovine serum albumin (BSA). At a concentration of 0.1 g/L, the residual foam² of surfactin was 88%, compared to 0% achieved with SDS at the same concentration and 65% achieved with BSA at 0.2g/L. This is mainly due to the higher surface activity of surfactin as compared to SDS and BSA. These authors further reported that surfactin achieved a foaming capacity³ of 0.98 at 0.05g/L, compared with foaming capacities of 0.80 (SDS) and 0.94 (BSA) at 0.1 g/L and 0.2g/L respectively.

¹ EI – Emulsification Index

² Residual foam volume after 20 minutes

³ Foaming capacity = maximum volume of foam/volume of gas injected

1.2.4 Biological activity

1.2.4.1 Antimicrobial- and antiviral biosurfactants

Numerous biosurfactants have recently been reported to show antimicrobial properties. *Bacillus* sp. arguably produces the most antimicrobial biosurfactants. *B. subtilis*, *B. cereus*, *B. pumilus*, *B. brevis* and *B. licheniformis* have all been reported to produce antimicrobial biosurfactants (Rodriguez *et al.*, 2006). Other micro-organisms that have been reported to produce antimicrobial biosurfactants include *P. aeruginosa* (Benincasa *et al.*, 2004), *T. bombicola* (Lang and Wagner, 1992), *C. antarctica* (Kitamoto *et al.*, 1993), *Lactobacillus lactis* and *Streptococcus thermophilus* (Rodrigues *et al.*, 2004).

The biosurfactants that have been most intensively studied regarding its antimicrobial activities are rhamnolipids from *P. aeruginosa* and the lipopeptides (iturin A, fengycin and surfactin) from *B. subtilis*. Rhamnolipids and surfactin have been reported to show antimicrobial activity against Gram-positive- and Gram-negative bacteria as well as fungi. Similar MICs were reported for rhamnolipids against Gram-positive and Gram-negative bacteria, while surfactin showed superior activity against Gram-negative bacteria. Rhamnolipids showed no activity against yeasts, while no information could be found on the activity of surfactin against yeasts (Haba *et al.*, 2001; Abalos *et al.*, 2002; Benincasa *et al.*, 2004; Bechard *et al.*, 1998).

Fengycin and iturin A have been reported to show greater activity against fungi than against bacteria (Besson *et al.*, 1976; Vanittanakom *et al.*, 1986). The MICs of iturin A against the fungi *Penicillium chrysogenum* and *P. notatum* have been reported to be between 5 and 10 µg/mL respectively. The same authors reported a 150 µg/mL MIC of iturin A against the bacterium *Staphylococcus aureus*.

The greater activity of fengycin and iturin A against fungi, and the greater activity of surfactin against Gram-negative bacteria indicate that the antimicrobial potency of an antimicrobial biosurfactant is influenced by the cell structure of the target organism (see section 1.2.4.2).

A direct comparison of the antimicrobial activities between different antimicrobial biosurfactants is required to establish superiority. Unfortunately, different authors used different mechanisms to evaluate the antimicrobial potency of the various antimicrobial biosurfactants. Moreover, the different authors also did not use the same target organisms and therefore, a direct comparison of the antimicrobial activities of the various antimicrobial biosurfactants could not be made. However, since this study involves *B. subtilis* as a lipopeptide producer, the qualitative antimicrobial activity of lipopeptide biosurfactants produced by *B. subtilis* against various target organisms is shown in Table 1-1. The target organisms in Table 1-1 reported to be most susceptible to *B. subtilis* biosurfactants are *P. fluorescens*, *B. licheniformis*, *Rhodococcus globurulus* and *Staphylococcus aureus* (These target organisms are shown in bold in Table 1-1). The latter

has developed a particularly resistant strain (methicillin-resistant *Staphylococcus aureus* or MRSA) and is known to cause postsurgical infections (Walsh, 2003).

Table 1-1: Organisms susceptible to antimicrobial action of biosurfactants produced by *B. subtilis*

| Gram-negative bacteria | Source |
|--|--|
| <i>Acinetobacter calcoaceticus</i> <i>Alcaligenes eutrophus</i> <i>Pseudomonas fluorescens</i> <i>Pseudomonas proteofaciens</i> <i>Enterobacter</i> sp. strain 306 <i>Pseudomonas aeruginosa</i> <i>Escherichia coli</i> <i>Serovar typhimurium</i> <i>Pseudomonas corrugata</i> <i>Pseudomonas putida</i> <i>Erwinia amylovora</i> <i>Agrobacterium vitis</i> | Yakimov <i>et al.</i> (1995) Fernandes <i>et al.</i> (2007) Bechard <i>et al.</i> (1998) |
| Gram-positive bacteria | |
| <i>Bacillus cereus</i> <i>Bacillus licheniformis</i> <i>Bacillus subtilis</i> <i>Rhodococcus globerulus</i> <i>Staphylococcus aureus</i> <i>Enterococcus faecalis</i> | Yakimov <i>et al.</i> (1995); Fernandes <i>et al.</i> (2007) |

Table 1-1: Organisms susceptible to antimicrobial action of biosurfactants produced by *B. subtilis* (continued)

| Fungi | Source |
|---------------------------------------|---------------------------|
| <i>Chrysosporium indicum</i> | Joshi <i>et al.</i> 2008 |
| <i>Alternaria burnsii</i> | |
| <i>Fusarium oxysporum</i> | |
| <i>Fusarium udum</i> | Touré <i>et al.</i> 2004 |
| <i>Trichoderma herzanium</i> | |
| <i>Rhizoctonia bataticola</i> | |
| <i>Botrytis cinerea</i> | |
| <i>Fusarium graminearum</i> | |
| <i>Pythium ultimum</i> | |
| <i>Rhizoctonia solani</i> | |
| <i>Rhizopus</i> sp. | |
| <i>Aspergillus flavus</i> MUCLI 14109 | |
| <i>Gaeumannomyces</i> sp. | |
| <i>Mucor</i> sp. | Sabaté <i>et al.</i> 2009 |
| <i>Trichoderma reesei</i> | |
| <i>Ascosphaera apis</i> | |

Although very little is known about the antiviral activity of biosurfactants, surfactin and the succinol-trehalose lipid have been reported to show antiviral activity. Both these biosurfactants showed activity against the herpes simplex virus. The succinol-trehalose lipid also showed activity against the influenza virus, while surfactin showed activity against the vesicular stomatitis virus, the suid herpes virus and the simian immunodeficiency virus (see Table 1-2) (Kracht *et al.*, 1999; Vollenbroich *et al.*, 1997; Makkar and Cameotra, 2002).

It is reported that the antiviral activity of surfactin is strongly influenced by the length of the fatty acid chain and also the charge on the peptide moiety (Kracht *et al.*, 1999). Fatty acid chains with 13 carbon atoms showed less activity than those with 14 and 15 carbon atoms (see section 1.2.4.2).

Table 1-2: Antiviral activity of surfactin from *B. subtilis*

| Viral target | Source |
|---|---------------------------------|
| <i>Vesicular stomatitis virus</i> | Kracht <i>et al.</i> 1999 |
| <i>Semliki forest virus</i> | |
| <i>Suid herpes virus</i> | |
| <i>Herpes simplex virus (1 & 2)</i> | Vollenbroich <i>et al.</i> 1997 |
| <i>Simian immunodeficiency virus</i> | |

1.2.4.2 Mechanisms of antimicrobial- and antiviral action

The antimicrobial activity and potency of a substance depends on the mechanism by which it inhibits or kills a target organism and also on the cell structure of the target organism (Walsh, 2003). The mechanism of action of an antibiotic is certainly one of the most important factors to consider when evaluating a new antibiotic.

Antibiotics are classified according to their particular mechanism of action (Walsh, 2003). In general, four types of antimicrobial action are understood: (1) interference with cell wall biosynthesis; (2) interference with bacterial protein biosynthesis; (3) interference with DNA replication and repair and; (4) enzymatic destruction of the antibiotic (Walsh, 2003).

However, biosurfactant antimicrobial action proposes an alternative antimicrobial mechanism. Surfactin has been reported to introduce a positive curvature stress in model lipid membranes, thus compromising bi-layer stability (Carillo *et al.*, 2003). This stress can be attributed to an increase in the surface tension of the model membrane (Heerklotz and Seelig, 2004; Heerklotz and Seelig, 2007), which is mediated by the insertion of the lipid chain into the phospholipid bi-layer, causing leakage of the intracellular contents (Deleu *et al.*, 2007, Deleu *et al.*, 2008) (see figure 1.3). It is further suggested that the potency of the lipopeptide with respect to antimicrobial activity, is dependent on the chain length of the lipid and also the charge of the hydrophilic head group (Magat-Dana and Ptak, 1995). Interestingly, the presence of Ca^{2+} ions also increases the potency of the lipopeptide surfactin by the formation of surfactin- Ca^{2+} complexes (Grau *et al.*, 1999). It has been reported that the presence of Ca^{2+} could promote the formation of surfactin dimers that may lead to ion-conducting channels (Magat-Dana and Ptak, 1995; Sheppard *et al.*, 1991). These complexes are believed to insert themselves even deeper into phospholipid bi-layers, which may explain the formation of ion-conducting channels (leakage of cellular contents) in membranes (Grau *et al.*, 1999).

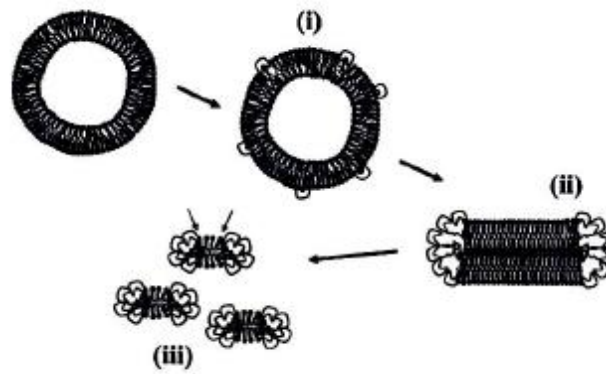


Figure 1-3: Schematic representation of membrane perturbation by fengycin (Deleu *et al.*, 2008)

The detergent-like action of fengycin, a lipopeptide produced by *B. subtilis* displayed in Figure 1-3. At a low fengycin concentration ($< 10\mu\text{M}$), the lipopeptide only inserts into the bi-layer, increasing its surface tension but not permeabilizing it. At moderate concentrations ($133\mu\text{M}$), fengycin agglomerates, causing the intracellular contents to leak. At high concentrations (5mM), micelles are formed, indicating that the bi-layer has been solubilized into the extracellular medium (Deleu *et al.*, 2008). Heerklotz and Seelig (2001) reported the same mechanism of action for surfactin on model membranes as that represented for fengycin in Figure 1-3.

The antimicrobial actions of all biosurfactants are not the same. Iturin A, a lipopeptide also produced by *B. subtilis*, passes through the cell wall and disrupts the plasma membrane with the formation of small vesicles and the aggregation of small intramembraneous particles (Thimon *et al.*, 1995). Not only does Iturin A pass through the cell membrane, but also through the plasma membrane after which it interacts with the nuclear membrane and possibly plasma membranes of other organelles (Thimon *et al.*, 1995). However, the precise mechanism of antimicrobial action of biosurfactants is not yet fully understood (Deleu *et al.*, 2005).

Analogous to the mechanism of antimicrobial activity of surfactin in bacteria, it has been reported that surfactin inserts into the lipid envelope of viruses and disrupts the cell membrane. Ultimately, the loss of viral proteins involved in virus adsorption and penetration accounts for virus inactivity (Vollenbroich *et al.*, 1997).

1.2.4.3 Resistance to antimicrobial action

The antimicrobial activity of a substance is also strongly influenced by resistance mechanisms of a target organism (Walsh, 2003).

Many micro-organisms have developed resistances to common antibiotics, such as penicillin, methicillin, vancomycin and streptomycin (Walsh, 2003). This is due to the over-use and also the misuse of antibiotics (Walsh, 2003).

Antibiotics have specific mechanisms of antimicrobial action (see section 1.2.4.2) and are influenced by the cell structure of the target organism (Walsh, 2003). Certain known antibiotics, such as vancomycin, are only effective against Gram-positive bacteria and have no effect on Gram-negative bacteria (Walsh, 2003). This is a direct result of the difference between the cell-wall structure of Gram-positive and Gram-negative organisms. The cell-wall of Gram-positive organisms lacks an outer phospholipid bi-layer membrane and consists only of an inner bi-layer membrane and a peptidoglycan layer (Walsh, 2003). Although the peptidoglycan layer in the cell-wall of Gram-negative organisms is much thinner than that of Gram-positive organisms, it has a second outer bi-layer membrane (Walsh, 2003). Two features of the outer membrane of Gram-negative organisms are responsible for its resistance to some antibiotics that are only active against Gram-positive organisms: (i) The presence of lipopolysaccharides which are attached to the outer membrane and (ii) the presence of porins in the outer membrane (Walsh, 2003). Porins are considered to be channels for the passage of certain molecules and are a possible target of certain antibiotics (Walsh, 2003).

The cell-wall features mentioned vary greatly between different bacteria. They even differ among the same genus of bacteria (Walsh, 2003). *P. aeruginosa*, which is considered to be an opportunistic human pathogen, have porins with very small pores which reduce the passage of antibiotics into the periplasmic space, making this organism less vulnerable to common antibiotics than other Gram-negative organisms (Walsh, 2003).

1.2.4.4 Specific antimicrobial resistance mechanisms

Bacteria that are antibiotics producers need protection from the harmful chemicals that they produce. The mechanisms employed by antibiotics producers vary; however, three major mechanisms are understood: (1) enzymes that either destruct or modify the antibiotic. For example, β -lactamases are known to hydrolyze β -lactam antibiotics, such as penicillin and cephalosporin (Bush and Mobashery, 1998: in Walsh, 2003), which deactivates the molecule; (2) efflux pumps that reduce the concentration of antibiotics from within the cell (Walsh, 2003). This process is mediated by transmembrane proteins which are responsible for the export of such antibiotics from the cytoplasm to the outer membrane (Walsh, 2003); (3) the modification of the drug target so that the susceptibility to the antibiotic is reduced (Walsh, 2003). This is achieved by mutation in the target gene, which may reduce sensitivity to the antibiotic (Walsh, 2003).

1.3 Applications of biosurfactants

Biosurfactants are very versatile and diverse, and are thus used in various industries. They are used for bioremediation; as antibiotics in the medical industry; for enhanced oil

recovery in the petrochemicals industry; in the minerals processing industry and also in the food industry. The use of biosurfactants in these industries show significant advantages over chemically synthesized surfactants, such as lower toxicity; enhanced biodegradability; enhanced foaming capacity; better environmental compatibility; and the ability to be synthesized from renewable feedstocks. (Desai and Banat, 1997; Mulligan *et al.*, 2001)

However, the focus of this study would be on the application of biosurfactants as antimicrobial agents for its potential use in health care.

1.3.1 Bioremediation applications

Bioremediation is the process by which pollutants or contaminants are removed from an environmentally sensitive area, usually soil, or to enhance the biodegradation of such contaminants. Usually, these contaminants have low water solubility and are more often than not hydrocarbons (Mulligan *et al.*, 2001).

Certain microorganisms, such as *B. subtilis*, *Ps. aeruginosa* and *T. bombicola*, have been reported to utilize crude oil and hydrocarbons as sole carbon sources for the production of biosurfactants and can be a useful mechanism for oil spill clean-ups in the future (Hommel and Ratledge, in N. Kosaric, 1993; Das & Mukherjee, 2006; Cubitto *et al.*, 2004; Mulligan *et al.*, 2001). Many of the existing oil decontamination processes have limited use, are expensive or are only partially effective (Das & Mukherjee, 2006). Bioremediation has been proposed to be an alternative to existing techniques. Biosurfactants also offer distinct advantages over synthetically derived compounds, such as low toxicity, biodegradability and high specificity (Mulligan *et al.*, 2001; Singh *et al.*, 2007). One particular example where a biosurfactant was used successfully for bioremediation is the Exxon Valdez oil-tanker spill (Mulligan *et al.*, 2001).

1.3.2 Agricultural applications

As a result of the antimicrobial activity of some biosurfactants, they can be applied in the biological control of postharvest diseases. It has been reported that the supernatant of a *B. subtilis* culture inhibited the growth (*in vivo*) of *Aspergillus flavus*, *A. niger*, *Penicillium oxalicum*, and *Botryodiplodia theobromae*. These organisms are all major spoilage organisms of intermediate moisture foods (Zhang *et al.*, 2008; Okigbo, 2005).

Not only may biosurfactants be used for the biological control of food spoilage organisms, but also as biological control agents of insects. Assié *et al.* (2002) incorporated various chemical surfactants, as well as iturin C₁₄, surfactin C₁₄- and C₁₅ (at 100ppm) into an artificial diet of the fruit fly *Drosophila melanogaster*. It was reported that surfactin caused an adult mortality of 92.6% after 1 day (Assié *et al.*, 2002). However, neither the chemical surfactants nor iturin showed insecticidal activity (Assié *et al.*, 2002). Therefore, more research on the potential insecticidal activity of biosurfactants is required.

1.3.3 Biomedical applications

1.3.3.1 Biosurfactants as anti-adhesives

The amphiphilic structure of biosurfactant molecules is responsible for its alignment with interfaces (Desai and Banat, 1997). Therefore, biosurfactants tend to adhere to interfaces, and consequently, biofilm forming bacteria cannot adhere to solid surfaces or to infection sites in the presence of a biosurfactant (Singh and Cameotra, 2004).

Biosurfactants have been shown to reduce the biofilm formation ability of various pathogenic bacteria, such as *Salmonella enterica*, *Escherichia coli* and *Proteus mirabilis*, which are opportunistic uropathogens (Singh and Cameotra, 2004). Biosurfactants from *Lactococcus lactis* and *Streptococcus thermophiles* reduced biofilm formation on synthetic voice prosthesis to 4% and 13% of the control respectively (Rodrigues *et al.*, 2004). Therefore, adsorbed biosurfactants onto synthetic medical prostheses can reduce the adherence of pathogens, consequently reducing infection rates and prolonging the prostheses' lifespan.

1.3.3.2 Anticancer applications

Recently, research has shown that certain biosurfactants show specific toxicity to certain cell lines (Thanomsub, 2006; Seydlova *et al.*, 2008). Rhamnolipids have shown specific activity against breast cancer cell lines (Thanomsub, 2006); sophorolipids showed specific anticancer activity against liver- lung- and leukemia cancer cell lines (Jing *et al.*, 2006); and surfactin showed activity against Ehrlich ascetic carcinoma- and human colon cancer cells (Kim *et al.*, 2007).

Although the anticancer activity of rhamnolipids is not yet understood (Thanomsub, 2006), Kim *et al.* (2007) reported that surfactin mediated anticancer effects by inducing DNA fragmentation, stimulation of morphological changes, enhanced the loss of plasma membrane polarity, apoptosis and cell cycle arrest. Similar findings were reported for the mechanism of anticancer activity of a sophorolipid produced by *Wickerhamiella domercqiae* (Jing *et al.*, 2006).

Although much research is still required, biosurfactants can possibly be applied in the treatment of various cancers.

1.3.3.3 Antimicrobial applications

Recently, Fernandes *et al.* (2007) reported that a lipopeptide biosurfactant (unnamed) from *B. subtilis* R14, showed good antimicrobial activity against eight resistant strains of *Ps. aeruginosa*. Inhibition zone diameters between 9.8 mm and 12.1 mm were reported for rhamnolipids against the resistant *Ps. aeruginosa* strains. Moreover, the same authors reported that the biosurfactant showed even better activity against resistant strains of Gram-positive cocci of *Staphylococcus aureus* and *Enterococcus faecalis*. The activity of

biosurfactants produced by *B. subtilis* against numerous micro-organisms, many of which are opportunistic human pathogens, is shown in .

Since numerous biosurfactants have been reported to exhibit antimicrobial activity against many common pathogens (see section 1.2.4.1), antimicrobial biosurfactants can possibly be applied as antibiotics against known pathogenic micro-organisms and may also be used to prevent the spread of these organisms. One of the objectives of this study is to evaluate the antimicrobial activity of surfactin against *Mycobacterium aurum*, a surrogate for *M. tuberculosis*. The latter is responsible for the illness commonly known as TB, which is currently one of the major causes of death among South Africans (Statistics South Africa).

1.4 Physiological roles of biosurfactants

The physiological roles of interest in this study are the roles of biosurfactants regarding antimicrobial activity and substrate accessibility. The low solubility of alkanes and other hydrocarbon substrates, such as vegetable oils, in water makes it rather difficult for it to be utilized by micro-organisms. It is believed that biosurfactants play a role in the emulsification of water-insoluble carbon substrates in order for them to be utilized for growth (Hommel, 1990). The appearance of biosurfactants in the culture medium is often regarded as a prerequisite for initial interactions of the microbial cell with hydrocarbons (Hommel, 1990).

Competition for survival among micro-organisms is regarded as one of the reasons for the production of inhibitory products (Van Hamme *et al.*, 2006). These inhibitory products are very often biosurfactants, which is why they tend to exhibit antimicrobial properties. The microbial competition mediated by inhibitory substances, such as biosurfactants, is called amensalism (Van Hamme *et al.*, 2006). In high cell density environments, quorum sensing⁴ is involved in amensalism and is responsible for the production of biosurfactants in order for the microbe to survive in a multi-bacterial habitat (Van Hamme *et al.*, 2006).

Another well known physiological role of biosurfactants is cell motility. One of the key properties of biosurfactants is that it is capable of reducing the surface tension between phases (see section 1.2.1) and consequently, the microbe can move along an interface more easily. This is the case for swarming motility, where populations of microorganisms migrate as a unit (Van Hamme *et al.*, 2006). Other physiological roles of biosurfactants involve the avoidance of toxic elements; cell differentiation; pathogenicity and the storage of carbon and energy (Van Hamme *et al.*, 2006).

⁴ cell communication via the production of certain substances under specific conditions

1.5 Location of biosurfactant in cell culture

The location of a biosurfactant in the cell culture is dependent on its particular physiological role. Knowledge of the location of a biosurfactant is necessary for downstream processing in order to optimize recovery. Biosurfactants are predominantly located either intracellularly or extracellularly, with a small concentration that can be located on the cell surface. Intracellular biosurfactants may be used for gene uptake, nutrient uptake or the sequestration of toxic compounds, while extracellular biosurfactants may be used for motility and quorum sensing. (Van Hamme *et al.*, 2006).

The biosurfactants from *B. subtilis* and *Ps. aeruginosa* are produced extracellularly and are thus located in the extracellular medium (Tamehiro *et al.*, 2002; Oschner *et al.*, 1995). Therefore, cells of these organisms would be separated from the culture medium to recover the produced biosurfactants from the extracellular medium.

1.6 Association of biosurfactant and cell growth phase

The production of biosurfactants has been shown to be linked to a particular growth phase (Lang and Wullbrandt, 1999). Therefore, knowledge of the associated growth phase for the production of a particular biosurfactant is of critical importance to ensure its maximum production. This is done by altering the conditions in order to prolong the growth phase in which biosurfactants are produced. The growth phases (and associated biosurfactant production) are influenced by the process conditions (Desai and Banat, 1997), the nutrients within the media (Desai and Banat, 1997), the cell density and also the excreted byproducts (Van Hamme *et al.*, 1996).

It has been shown that rhamnolipids are produced during the stationary phase of growth, which is induced by a nutrient limitation (Clarke *et al.*, 2010; Lang and Wullbrandt, 1999). Conversely, the production of surfactin by *B. subtilis* occurs during the exponential growth phase, which is in contrast to the production of other secondary metabolites (Peypoux *et al.*, 1999).

1.7 Quantification of biosurfactant characteristics

1.7.1 Surface tension

Surface activity of biosurfactants is determined by measuring surface- or interfacial tensions with a tensiometer (see Figure 2-3 and section 2.4.2). Surface tensions are mainly measured to determine the CMC, which is the lowest biosurfactant concentration that would reduce the surface tension to a minimum. However, surface tensions may also be measured to indirectly determine biosurfactant concentrations (see section 1.7.2.1).

1.7.2 Quantification of surfactin concentration

1.7.2.1 Quantification of surfactin concentration by surface tension analysis

Surface tension measurements have been used as an indication of the biosurfactant concentration within the broth by pre-determining a standard curve from pure biosurfactant solutions (Cooper *et al.*,1981; Mulligan *et al.*,1989; Sheppard and Cooper, 1990). However, this method for determining the biosurfactant concentration has its limitations, because after the CMC has been reached, the addition, or production, of more biosurfactant will not cause a further reduction in surface tension (see section 1.2.1). This problem can be overcome by preparing serial dilutions of the culture supernatant. By measuring the surface tensions of the dilutions, it could be related to concentrations used to prepare the standard curve. The biosurfactant concentration within the culture supernatant is then calculated by multiplying the surface tension concentration with the dilution factor.

This method is less time consuming than HPLC; however, there are many factors such as pH, temperature and medium components that could influence surface tensions (Zhang and Miller, 1992).

1.7.2.2 Quantification of surfactin concentration by HPLC

Surfactin concentrations can be quantified directly by HPLC and this method has been used by numerous authors (Davis *et al.*,1999; Wei and Chu, 2002; Lin *et al.*, 1998). HPLC combines the chromatographic effect (variance in retention times of molecules in HPLC column due to molecule-to-column and molecule-to-molecule interactions) and a detector (UV or IR) in order to quantify the concentration of a given substance.

Typically, a UV detector optimally detects surfactin at wavelengths of approximately 210 nm (Davis *et al.*,1999; Wei and Chu, 2002; Lin and Jaing, 1997). A series of diluted samples with known surfactin concentrations are prepared and analysed by HPLC at the specified wavelength. This yields a standard curve. The HPLC analyses of cell free culture supernatants are then compared to the standard curve to determine the surfactin concentration of the supernatant (see section 2.4.3).

The quantification of surfactin concentrations by means of HPLC is a time-consuming process, since samples have to be filtered and diluted with a mobile phase before its analysis. Moreover, each sample requires approximately 30 minutes to be analysed by HPLC. Most HPLC systems run automatically, which means that sample preparation is the only treatment required to accurately determine surfactin concentrations.

Since HPLC separates different molecules by the variance in retention times, different surfactin homologues will be detected at different times. The output of HPLC is chromatographic peaks at different times (see Appendix C), which relates to a specific homologue. Since the production of surfactin is accepted to be a mixture of different homologues (Akpa *et al.*,2001), more than one peak is observed on a surfactin

chromatogram. Unfortunately, HPLC can only distinguish between different homologues (variance in retention time), but cannot quantify their respective concentrations unless the respective homologue concentrations of the standard are known. If the respective concentrations of the different homologues are unknown, mass spectra analysis will be required to determine the respective concentrations of each homologue.

1.7.3 Emulsification activity

The emulsification activity is determined by calculating an emulsification index. The emulsification index of a surfactant is determined by emulsifying an appropriate amount of a water-insoluble substance into a surfactant solution of known concentration.

In the case of biosurfactant emulsification activity, a water-insoluble substance is emulsified with cell free culture broth after the biosurfactant concentration has been determined. The emulsification index is then determined 24 hours later by measuring the height of the emulsion layer, dividing that height by the total height of the mixture and multiplying by 100. This method was developed by Cooper & Goldenberg (1987).

1.7.4 Foaming activity

Foam stability and its liquid hold-up are quantified by image analysis and conductimetric methods (Razafindralambo *et al.*, 1996). In the minerals processing industry (flotation), foam stability is monitored by image analysis. A video camera captures the data and is analyzed with the use of specific software programs. The software statistically analyzes the bubbles sizes and stability (Corné Marais, pers. comm.).

1.7.5 Antimicrobial activity

1.7.5.1 Quantification of antimicrobial activity by the MIC method

The MIC of an antimicrobial substance is the lowest concentration at which it inhibits the growth of the target organism and is a quantitative measure of the antimicrobial potency of an antimicrobial substance. Two methods exist to determine the MIC, namely the tube dilution assay and the agar dilution assay. In the tube dilution assay, serial dilutions of an antimicrobial substance are prepared in a growth medium, which are mixed with a suspension containing the target organism. After incubation at a specified temperature over a certain time interval, the samples are analyzed for growth. The minimum concentration at which the antimicrobial substance inhibits growth is the MIC (Jorgensen & Ferraro, 1998).

Likewise, the agar dilution assay involves serial dilutions of an antimicrobial substance in an agar growth medium. A drop of a suspension containing the target organism is spread over the agar and incubated. The minimum concentration at which the antimicrobial substance inhibits growth is the MIC (Jorgensen & Ferraro, 1998).

1.7.5.2 Quantification of antimicrobial activity by disk diffusion assays

Disk diffusion assays qualitatively determine the antimicrobial activity of a substance. It is not used to determine the MIC, but rather shows zones of clearing in a petri-dish containing an agar growth medium (see section 2.5.4.1).

Disk diffusion assays can be performed in a number of ways, but the most common methods are the agar diffusion assay and radial diffusion assay. In the radial diffusion assay, wells are punched in an agar growth medium already mixed with a suspension containing the target organism. A specific volume with a known concentration of an antimicrobial substance is pipetted into the wells, after which sterile agar is overlaid on the initial agar layer. After incubation, zones of clearing around these wells indicate antimicrobial activity. In the agar diffusion assay, the antimicrobial substance is applied to sterile round paper disks. The paper disks are then placed onto an agar growth medium already mixed with a suspension containing the target organism. After incubation, zones of clearing around the paper disks indicate antimicrobial activity (Bauer *et al.*, 1966; Lehrer *et al.*, 1990; du Toit & Rautenbach, 2000).

One aspect of the disk- and radial diffusion assays that is of great concern is the rate of diffusion of the antibiotic through the agar media. Thus, a zone of clearing for two antibiotics might have the same diameter, but one antibiotic might be more potent while the other diffused at a higher rate through the agar. These methods do not provide a quantitative result, but attempts have been made to correlate the zone diameter to MIC values. Awerbuch *et al.* (1988) postulated a numerical method to determine the MICs of antibiotics directly from disc-diffusion susceptibility tests. The equation is a partial differential equation relating the changes in drug concentration, the decay of the antibiotic chemical and the 'consumption' of the antibiotic by the bacteria.

1.8 Process conditions

The preferred environmental conditions are unique to each micro-organism and are vital for achieving optimal growth and product synthesis. As this study focuses on the production of surfactin by *B. subtilis*, this section of the literature study will focus primarily on the process conditions required for growth and enhanced surfactin production. The factors influencing the environmental conditions consist of medium components and process operation.

1.8.1 Medium components

1.8.1.1 Carbon source requirements

Biosurfactants are produced from a wide variety of carbon substrates. These substrates can be divided into two main categories: carbohydrates and hydrocarbons, which include vegetable oils (Kim *et al.*, 1997). One of the main differences between these substrates is that carbohydrates are soluble in water, whereas hydrocarbons and vegetable oils are not.

In general, high cell- and biosurfactant concentrations are achieved when *B. subtilis* is grown on carbohydrate substrates, such as glucose, sucrose and starch (Kim *et al.*, 1997; Makkar & Cameotra, 1997). Consequently, most authors have used carbohydrates, especially glucose, for studies on surfactin production (see Table 1-3). The carbohydrate concentrations used range from 2-60 g/L. Surfactin production has been reported to increase almost linearly with an increase in glucose concentration up to 40 g/L, with little effect on biosurfactant production over 40 g glucose/L (Kim *et al.*, 1997; Abushady *et al.*, 2005). This trend can also be deduced from Table 1-3. It can be seen that the highest surfactin concentration reported (6450 mg/L) was obtained from a medium initially containing 40 g glucose/L, whereas the lowest reported surfactin concentration (92 mg/L) was obtained from a medium containing 2 g glucose/L.

A few studies have focused on the evaluation of different carbon sources for growth and surfactin production by *B. subtilis*. Abushady *et al.* (2005) evaluated the growth of *B. subtilis* AB01335-1 and AB02238-1 on olive-, corn-, sunflower- and castor oils and reported that the growth and surfactin production obtained was less than that obtained on carbohydrate substrates. It is reported that surfactin concentrations between 1000-1500 mg/L was achieved using vegetable oils, while concentrations of 2000-2750 mg surfactin/L were obtained from carbohydrate substrates (Abushady *et al.*, 2005). Kim *et al.* (1997) evaluated the growth of *B. subtilis* on soybean oil, and reported similar findings as that of Abushady *et al.* (2005).

Three studies referred to in Table 1-3 evaluated the growth of *B. subtilis* on *n*-hexadecane, a long chain hydrocarbon (Kim *et al.*, 1997; Makkar and Cameotra, 1997; Abushady *et al.*, 2005). It was initially found that *B. subtilis* KCTC 8701P was unable to utilize *n*-hexadecane for growth, and that the use of *n*-hexadecane inhibited biosurfactant production when used in combination with glucose (Kim *et al.*, 1997). Similar findings were reported for *B. subtilis* MTCC 1427 by Makkar and Cameotra (1997). However, in a later study by Kim *et al.* (2000), *B. subtilis* KCTC 8701P was reported to utilize hydrocarbons in combination with glucose and that *B. subtilis* KCTC 8701P degraded *n*-alkanes up to a chain length of C₁₉. Moreover, these authors reported a maximum surfactin concentration of 4200 mg/L, which is above the average maximum surfactin concentrations reported when only carbohydrates were used. Das and Mukherjee (2006) also reported the production of a biosurfactant by *B. subtilis* DM-04 from crude petroleum hydrocarbons, achieving a maximum biosurfactant concentration of 650 mg/L.

The results reported and discussed in the above paragraph indicate that the utilization of hydrocarbons for growth and biosurfactant production by *B. subtilis* is strain dependent. It is also evident that very little is known about biosurfactant production from hydrocarbons by *B. subtilis*. The utilization of hydrocarbons as a feedstock is of increasing importance in bioremediation of oil-polluted ecosystems (see section 1.3.1), since bioremediation could be less harmful to the environment than conventional methods used for hydrocarbon-spill clean-ups (Morán *et al.*, 2000). Consequently, one of the objectives of this study was to

compare the growth and biosurfactant production of *B. subtilis* ATCC 21332 on carbohydrates and hydrocarbons.

1.8.1.2 Nitrogen source requirements

Makkar and Cameotra (1997) evaluated the effect of different organic and inorganic nitrogen sources on biosurfactant production by *B. subtilis*. These authors reported that greater biosurfactant concentrations of 731mg/L and 724 mg/L were obtained when KNO_3 and NaNO_3 were used respectively. These biosurfactant concentrations are significantly higher than the 327mg/L, 458mg/L and 493mg/L biosurfactant concentrations obtained from the peptone, yeast- and beef extract organic nitrogen sources. Likewise, Abushady *et al.* (2005) also found that inorganic nitrogen sources were superior to organic nitrogen sources for surfactin production. These authors found that the use of NH_4NO_3 and NaNO_3 resulted in surfactin concentrations of 2250mg/L and 1950mg/L respectively, compared to surfactin concentrations of less than 1000mg/L when peptone, yeast- and beef extract were used. Most authors used NH_4NO_3 as the nitrogen source during studies on growth and biosurfactant production by *B. subtilis* (see Table 1-3).

The nitrogen substrate concentrations used for studies on surfactin production vary from 1- 10 g/L. Davis *et al.* (1999) showed that the maximum biomass obtained only marginally increased with a 10-fold increase (from 1-10 g/L) in NaNO_3 concentration. However, these authors do not report the effect of NaNO_3 concentration on surfactin production. Abushady *et al.* (2005) reported that surfactin production increased from approximately 1500mg/L to 2250mg/L with an increase in the NH_4NO_3 concentration from 1.5 to 4.6 g/L, with no further increase in surfactin production over this concentration.

1.8.1.3 Nutrient requirements

Nitrogen utilization, and consequently growth and surfactin production by *B. subtilis*, is reported to be strongly influenced by the availability of iron and manganese cations (Sheppard and Cooper, 1990). It is reported that the requirement of each of these nutrients (nitrogen, iron and manganese) is dependent on the availability of the other two nutrients (Sheppard and Cooper, 1990). The concentration, and thus the availability, of iron and manganese significantly increased the growth of *B. subtilis* and surfactin production (Cooper *et al.*, 1981; Wei and Chu, 1998; Wei and Chu, 2002). These authors reported that both the biomass and surfactin concentration increased 5-fold when 0.0013M $\text{FeSO}_4(\text{aq})$ was added to the culture broth, while only the surfactin concentration increased when $4 \times 10^{-6}\text{M}$ manganese was added to the culture broth. Abushady *et al.* (2005) evaluated the effect of FeSO_4 and MnSO_4 concentrations on surfactin production and found that FeSO_4 and MnSO_4 concentrations of 152mg/L and 50mg/L respectively resulted in maximum surfactin concentrations of 2450mg/L and 2500mg/L respectively.

Other salts such as MgSO_4 , CaCl_2 , Na_2HPO_4 , ZrOCl_2 and VOSO_4 have been reported to have almost no effect on either biomass or surfactin concentration (Cooper *et al.*, 1981). The

same authors also reported that ZnSO_4 suppressed growth, while CuSO_4 , NiSO_4 , CoSO_4 and $\text{Al}_2(\text{SO}_4)_3$ completely inhibited growth.

As a result of the opposing effects of certain nutrients on growth and surfactin production by *B. subtilis*, three different media were selected for this study (section 3.1). Growth and surfactin production was evaluated in each of the three selected media. The most favorable medium regarding growth and surfactin production was used for further bioreactor batch- and fed-batch experiments.

Table 1-3: List of media used in literature for biosurfactant production by *Bacillus subtilis*⁵

| Source | Carbon source (g/L) | Inorganic Nitrogen source (g/L) | Organic Nitrogen source (g/L) | Phosphate source (g/L) | Other (g/L) | Max. biosurfactant concentration (mg/L) |
|------------------------------|---|---|--|---|---|---|
| Abushady <i>et al.</i> 2005 | Glucose (5-60g/L); galactose; lactose; maltose; mannitol; sucrose; starch; fructose; sunflower oil; corn oil; castor oil; olive oil; paraffin oil; <i>n</i> -hexadecane and glycerol (concentrations not specified) | (NH ₄) ₂ SO ₄ (2-10 g/L); NH ₄ Cl; NH ₄ NO ₃ ; (NH ₄) ₂ S ₂ O ₈ ; NH ₄ Mo; (NH ₄) ₂ HPO ₄ ; NH ₄ H ₂ PO ₄ ; NH ₄ HCO ₃ ; NaNO ₃ (concentrations not specified) | Urea; beef extract; yeast extract; casein hydrosylate (concentrations not specified) | Not specified | FeSO ₄ .7H ₂ O: 0.5-8.0 mM/L MnSO ₄ .H ₂ O: 10-60 mg/L | 2750 (achieved on glucose as substrate) |
| Akpa <i>et al.</i> (2001) | Sucrose: 20 Peptone: 30 | Not specified | Yeast Extract: 7 | KH ₂ PO ₄ : 1.9 | MgSO ₄ : 0.45, Trace element solution: 9mL -(CuSO ₄ : 0.001), (FeCl ₃ : 0.005), (NaMnO ₄ : 0.004), (KI: 0.002), (ZnSO ₄ : 0.014), (H ₃ BO ₃ : 0.01), (MnSO ₄ : 0.0036), (Citric acid: 10) | Not specified |
| Bechard <i>et al.</i> (1998) | Dextrose: 20 | Not specified | DL-Glutamic acid: 5 | K ₂ HPO ₄ : 1 | KCl: 0.5, MgSO ₄ .7H ₂ O: 1.02, Trace element solution: 1mL - (MnSO ₄ .H ₂ O: 5), (CuSO ₄ .5H ₂ O: 1.6), (FeSO ₄ .7H ₂ O: 0.15) | Not specified |
| Chen <i>et al.</i> (2006) | Glucose: 2 | NH ₄ Cl: 1 | Not specified | KH ₂ PO ₄ : 3 Na ₂ HPO ₄ : 6 | NaCl: 5, MgSO ₄ : 1 mmol/L, CaCl ₂ : 0.1 mmol/L | 92 |
| Cooper <i>et al.</i> (1981) | Glucose: 40 | NH ₄ NO ₃ : 0.05 M | Not specified | KH ₂ PO ₄ : 0.03 M Na ₂ HPO ₄ : 0.04 M | MgSO ₄ : 8x10 ⁻⁴ M, CaCl ₂ : 7x10 ⁻⁶ M, Na ₂ -EDTA: 4x10 ⁻⁶ M, FeSO ₄ : 4x10 ⁻⁶ M | Not specified |

⁵All units are in g/L unless otherwise stated

Table 1-3: List of media used in literature for biosurfactant production by *Bacillus subtilis*(continued)

| Source | Carbon source (g/L) | Inorganic Nitrogen source (g/L) | Organic Nitrogen source (g/L) | Phosphate source (g/L) | Other (g/L) | Max. biosurfactant concentration (mg/L) |
|--------------------------------|---|---|-------------------------------|---|--|--|
| Das and Mukherjee (2005) | Not specified | NH ₄ NO ₃ : 1 | Not specified | KH ₂ PO ₄ : 3 Na ₂ HPO ₄ : 6 | NaCl: 1, MgSO ₄ .7H ₂ O: 0.245, CaCl ₂ : 0.014, thiamine-HCl _(aq) : 1 mL, Micronutrients solution: 1 mL | Not specified |
| Fernandes <i>et al.</i> (2007) | Glucose: 40 | (NH ₄) ₂ SO ₄ : 8.5 NaNO ₃ : 8.5 | Not specified | KH ₂ PO ₄ : 4 K ₂ HPO ₄ : 13.6 | MgSO ₄ .7H ₂ O: 0.5, Trace element solution: 10mL -(CaCl ₂ : 0.42), (FeSO ₄ .7H ₂ O: 2.29), (MnCl ₂ .4H ₂ O: 0.10), (ZnCl ₂ : 0.17), (CuCl ₂ : 0.03) (CoCl ₂ .6H ₂ O: 0.06) (Na ₂ MoO ₄ .2H ₂ O: 0.06) | 2000 |
| Kim <i>et al.</i> (1997) | Glucose: 40 Soybean oil: NS Hexadecane: NS Glu+SO: NS Glu+Hex: NS | NH ₄ NO ₃ : 0.05 M | Yeast extract: 0.5 | KH ₂ PO ₄ : 0.03 M Na ₂ HPO ₄ : 0.04 M | MgSO ₄ : 8x10 ⁻⁴ M, CaCl ₂ : 7x10 ⁻⁶ M, FeSO ₄ : 4x10 ⁻⁶ M | 4500 (achieved on glucose as substrate) |
| Makkar and Cameotra (1998) | Glucose: 20 Starch: 20 Sucrose: 20 Sodium pyruvate: 20 Sodium acetate: 20 Dodecane: 20 Hexadecane: 20 Pristane: 20 | NH ₄ NO ₃ :3 (NH ₄) ₂ SO ₄ : 3 NaNO ₃ : 3 | Urea: 3 | KH ₂ PO ₄ : 0.14 Na ₂ HPO ₄ : 2.2 | KNO ₃ : 3, NaCl: 0.01, MgSO ₄ : 0.6, CaCl ₂ : 0.04, FeSO ₄ : 0.02, Trace element solution: 0.1mL - (ZnSO ₄ .7H ₂ O: 2.32), (MnSO ₄ .4H ₂ O: 1.78), (H ₃ BO ₃ : 0.56), (KI: 0.66), (CuSO ₄ .5H ₂ O: 1), (Na ₂ MoO ₄ .2H ₂ O: 0.39), (CoCl ₂ .6H ₂ O: 0.42), (EDTA: 1), | 808 (achieved on glucose as substrate) |

Table 1-3: List of media used in literature for biosurfactant production by *Bacillus subtilis*(continued)

| Source | Carbon source (g/L) | Inorganic Nitrogen source (g/L) | Organic Nitrogen source (g/L) | Phosphate source (g/L) | Other (g/L) | Max. biosurfactant concentration (mg/L) |
|----------------------------|---------------------|--|-------------------------------|---|--|---|
| Sen and Swaminathan (1997) | Glucose: 36.5 | NH ₄ NO ₃ : 4.5 | Not specified | KH ₂ PO ₄ : 0.03 M Na ₂ HPO ₄ : 0.04 M | MgSO ₄ : 0.8 mM, CaCl ₂ : 7 μM, EDTA: 4 μM, FeSO ₄ : 14.5 μM, MnSO ₄ : 1.63 mM | 1100 |
| Sheppard and Cooper (1990) | Glucose: 15 | (NH ₄) ₂ HPO ₄ : 0.002- 0.006 M | Not specified | KH ₂ PO ₄ : 0.03 M | MgSO ₄ ·7H ₂ O: 0.0008 M, CaCl ₂ : 7×10 ⁻⁶ M, Na ₂ -EDTA: 0.001 M, FeSO ₄ ·7H ₂ O: 0.1 - 0.2 mM, MnSO ₄ ·H ₂ O: 0 - 0.3 mM | Not specified |
| Wei and Chu (2002) | Glucose: 40 | NH ₄ NO ₃ : 50 mM | Not specified | KH ₂ PO ₄ : 30 mM Na ₂ HPO ₄ : 40 mM | CaCl ₂ : 7 μM Na ₂ -EDTA: 4 μM FeSO ₄ ·7H ₂ O: 4 μM | 2600 |
| Yeh <i>et al.</i> (2006) | Glucose: 40 | NH ₄ NO ₃ : 50 mM | Not specified | KH ₂ PO ₄ : 30 mM Na ₂ HPO ₄ : 30 mM | MgSO ₄ ·7H ₂ O: 800 μM, CaCl ₂ : 7 μM, Na ₂ -EDTA: 4 μM, FeSO ₄ ·7H ₂ O: 2 mM | 6450 |

1.8.1.4 Anaerobic growth of *B. subtilis* in the presence of nitrate

Prior to 1993, *B. subtilis* was believed to be a strict aerobe. However, Priest (1993) reported growth of *B. subtilis* under anaerobic conditions for the first time (Nakano and Zuber, 1998). Studies have shown that *B. subtilis* can grow by anaerobic respiration during which nitrate is utilized as the terminal electron acceptor, as opposed to oxygen during aerobic respiration (Glaser *et al.*, 1995; Nakano *et al.*, 1997; Nakano and Zuber, 1998; Hoffman *et al.*, 1998). It is reported that nitrate is the preferred terminal electron acceptor under anaerobic conditions because of its high midpoint redox potential ($E'^0 = 430$ mV) relative to that of oxygen ($E'^0 = 820$ mV) (Nakano and Zuber, 1998). The same authors also reported that nitrate- and nitrite respiration are the only forms of anaerobic respiration known for *B. subtilis*.

In general, two distinct ways exist in which nitrate is utilized by micro-organisms – *assimilation* and *dissimilation* (Painter, 1970). During assimilation, nitrate is reduced to ammonia for its subsequent conversion to nitrogenous cell constituents (see Figure 1-4) (Painter, 1970). During nitrate dissimilation, or respiration, nitrate is reduced to any one of the following end products without the formation of nitrogenous cell constituents: nitrite, ammonia, nitrous oxide or nitrogen (Painter, 1970). If nitrous oxide or nitrogen is formed, the process is called *denitrification* (Painter, 1970). If ammonia is formed (via nitrite), the process is called *ammonification* (Hoffman *et al.*, 1998).

Hoffman *et al.* (1998) reported that neither nitrous oxide nor nitrogen were observed in the end products during anaerobic growth of *B. subtilis*, indicating that *B. subtilis* is an ammonifying facultative aerobe. Moreover, both assimilation (Ogawa *et al.*, 1995) and dissimilation (Hoffman *et al.*, 1998) of nitrate via two distinct nitrate reductases have been reported for growth of *B. subtilis* under anaerobic conditions (Nakano and Hulett, 1997). Therefore, nitrate serves as the terminal electron acceptor during anaerobic respiration and the nitrate-nitrogen is also consumed into cell constituents.

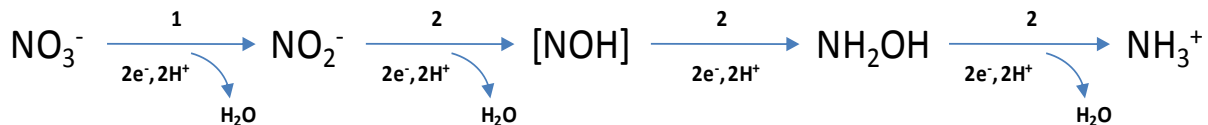


Figure 1-4: Assimilatory nitrate reduction pathway: Present in all bacteria that reduce nitrate to ammonia for subsequent conversion to nitrogenous cell constituents. Enzymes: 1 – nitrate reductase; 2 – nitrite reductase (Redrawn from White, 2007)

1.8.1.5 Influence of oxygen availability on growth and surfactin production by *B. subtilis*

In order to optimize the production of surfactin on a large scale, the influence of oxygen availability on the growth and surfactin production by *B. subtilis* needs to be known. Clements

et al. (2002) found that, in the presence of nitrate, the maximum cell density obtained under anaerobic conditions is inferior to that obtained under aerobic conditions. These authors reported a maximum optical density (at 600nm) of 0.12 under anaerobic conditions, compared to a maximum optical density of 3.00 under aerobic conditions. However, Clements *et al.* (2002) did not report the influence of oxygen availability on surfactin production.

Abushady *et al.* (2005) evaluated the influence of oxygen availability on surfactin production and found that surfactin production increased with an increase in the volumetric oxygen concentration. These authors found that the achieved surfactin concentration increased from approximately 1200 mg/L at 30% volumetric oxygen, to approximately 2100 mg/L at 90% volumetric oxygen. In contrast to Clements *et al.* (2002) and Abushady *et al.* (2005), Kim *et al.* (1997) reported that higher cell densities and higher biosurfactant concentrations were obtained under oxygen-limited conditions. Kim *et al.* (1997) found that the biomass doubled and that the rate of biosurfactant production increased 3-fold under oxygen-limiting conditions. It is further reported that a maximum biosurfactant concentration of 4500 mg/L was achieved under oxygen-limiting conditions, compared to only 1300 mg/L under oxygen-sufficient conditions (Kim *et al.*, 1997).

Neither Abushady *et al.* (2005) nor Kim *et al.* (1997) provides a clear explanation regarding the effect of oxygen concentration on surfactin production. Kim *et al.* (1997) reported that surfactin production was growth-associated. Considering that these authors also reported that the biomass doubled under oxygen-limiting conditions, the higher biomass concentration achieved under those conditions resulted in the higher reported surfactin concentration (4500 mg/L). Unfortunately, Abushady *et al.* (2005) did not report the effect of volumetric oxygen on the cell concentration and therefore, a clear explanation for this paradox could not be deduced.

Most reactor studies on surfactin production were performed under oxygen-sufficient conditions (see Table 1-4, Table 1-5 and section 1.8.2.1). Typically, the dissolved oxygen (DO) concentration was controlled to remain above 20% saturation. The maximum surfactin concentrations achieved vary greatly, with concentrations between 136 – 6450 mg/L being reported under oxygen-sufficient conditions.

1.8.2 Process operation

1.8.2.1 Environmental operating conditions

Environmental factors, such as pH, temperature, agitation and aeration also influence cell growth and biosurfactant production (Güerra-Santos *et al.*, 1986). Therefore, an understanding of the influence of each of these factors on cell growth of *B. subtilis* and surfactin production is required. Most authors have used a temperature of 30°C, a pH between 6.5 and 7.2, an

agitation rate between 150 and 400 rpm, and an aeration rate between 0.25 and 1.5 vvm (see Table 1-4)

In an optimization study, it has been reported that the optimum environmental conditions required for enhanced surfactin production by *B. subtilis* strain DSM 3256 were as follows: temperature – 37.4°C; pH – 6.75; agitation – 140 rpm and aeration - 0.75 vvm (Sen and Swaminathan, 1997). These authors reported a maximum surfactin concentration of 1100mg/L, obtained under the reported optimum environmental conditions. Except for temperature, the optimum environmental conditions reported by Sen and Swaminathan (1997) are within the range used by most authors.

Surfactin production by various *B. subtilis* strains has also been found to be strain dependent (Abushady *et al.*, 2005) and consequently the optimum environmental operating conditions may also be strain dependent. However, Abushady *et al.* (2005) showed similar optimum environmental conditions for two *B. subtilis* strains (AB01335-1 and AB02338-1) that produced a high yield of surfactin. These authors reported the optimum environmental conditions for maximum surfactin production as follows: temperature - 30°C; pH – 6.5-7; volumetric oxygen 90% and agitation – 200 rpm.

Table 1-4: Process operating conditions and modes of operation used for *B. subtilis* culture from literature

| Source | Product | Carbon source concentration (g/L) | Mode of operation | Working volume (L) | Temperature (°C) | pH | Agitation (rpm) | Aeration (vvm) | Max. biosurfactant production (mg/L) | Yield (g biosurfactant / g carbon source) |
|--------------------------------|---------------------------------|-----------------------------------|-----------------------------|--------------------|------------------|---------------|-------------------|----------------|--------------------------------------|---|
| Akpa <i>et al.</i> (2001) | Iturins, Fengycin and surfactin | 20 | Shake flask | 100mL | 30 | 7 | 130 | Not specified | Not specified | Not specified |
| Chen <i>et al.</i> (2006) | Surfactin | 0.25-2 | Reactor (Continuous) | 1 | 30 | 7 | 200 | 0.4 | 136 | 0.068 |
| Chen <i>et al.</i> (2006) | Surfactin | 2 | Shake flask/Reactor (Batch) | 1 | 30 | 7 | 200 (shake flask) | Not specified | 92/136 | 0.068 |
| Sheppard and Cooper (1990) | Surfactin | 15 | Reactor (Batch) | 0.8 | 30 | 6.7 | Not specified | Not specified | Not specified | Not specified |
| Chenikher <i>et al.</i> (2010) | Mycosubtilin (lipopeptide) | 10 | Reactor (Fed-batch) | 5 (max) | 30 | 6.5 | 200-500 | 0.75L/min | 336 | Not specified |
| Cooper <i>et al.</i> (1981) | Surfactin | 40 | Reactor (Batch) | 20 / 12 | 30 | Not specified | 200 | 0.5/0.9 | 800 | 0.025 |
| Bechard <i>et al.</i> (1998) | Unspecified Biosurfactant | 20 | Shake flask | 100mL | 30 | Not specified | 150 | Not specified | Not specified | Not specified |
| Makkar and Cameotra (1997) | Unspecified Biosurfactant | 20 | Shake flask | 200mL | 45 | Not specified | 200 | Not specified | 652 | Not specified |
| Fernandes <i>et al.</i> (2007) | Lipopeptide biosurfactant | 40 | Shake flask | 225mL | 30 | Not specified | 150 | Not specified | 2000 | Not specified |

Table 1-4: Process operating conditions and modes of operation used for *B. subtilis* culture from literature (continued)

| Source | Product | Carbon source concentration (g/L) | Mode of operation | Working volume (L) | Temperature (°C) | pH | Agitation (rpm) | Aeration (vvm) | Max. biosurfactant production (mg/L) | Yield (g biosurfactant / g carbon source) |
|---------------------------------|---------------------------|-----------------------------------|---------------------|--------------------|------------------|---------------|-----------------|----------------|--------------------------------------|---|
| Davis <i>et al.</i> (1999) | Surfactin | 10 | Reactor (Batch) | 1 | 32 | 7 | 300 | 1 | 439 | 0.015 |
| Sen and Swaminathan (1996) | Surfactin | 36.5 | Reactor (Batch) | 2 | 10 - 50 | 5 - 9 | 0 - 400 | 0 - 1.1 | 1100 | 0.030 |
| Das and Mukherjee (2005) | Unspecified Biosurfactant | Not specified | Reactor (Batch) | 3 | 45 - 55 | 7 - 8 | 200 | Not specified | Not specified | Not specified |
| Kim <i>et al.</i> (1997) | Lipopeptide biosurfactant | 40 | Reactor (Batch) | 1.5 | 30 | 6.8 | 300 | 0.1 or 1 | 4500 | 0.113 |
| Suwansukho <i>et al.</i> (2008) | Unspecified Biosurfactant | 5-25g/L | Reactor (Batch) | 1 | 30 | uncontrolled | 200 | 1 | 320 | 0.032 |
| Joshi <i>et al.</i> (2008) | Unspecified Biosurfactant | 20 | Reactor (Batch) | 3 | 30 | 6.8-7.2 | 300 | 1 | Not specified | Not specified |
| Guez <i>et al.</i> (2007) | Mycosubtilin | 40 | Reactor (Fed-batch) | 5 | 30 | 6.5 | 200 - 400 | 0.25 | Not specified | Not specified |
| Wei <i>et al.</i> (1998) | Surfactin | 40 | Shake flask | 200mL | 30 | Not specified | 200 | Not specified | 3500 | Not specified |

Table 1-4: Process operating conditions and modes of operation used for *B. subtilis* culture from literature (continued)

| Source | Product | Carbon source concentration (g/L) | Mode of operation | Working volume (L) | Temperature (°C) | pH | Agitation (rpm) | Aeration (vvm) | Max. biosurfactant production (mg/L) | Yield (g biosurfactant / g carbon source) |
|----------------------------|------------------------|-----------------------------------|--|--------------------|------------------|---------------|--|----------------|--------------------------------------|---|
| Yeh <i>et al.</i> (2006) | Surfactin | 40 | Reactor (Batch) | 2 | 30 | Not specified | 200 - 350 | 0.5 - 1.5 | 6450 | 0.161 |
| Oh <i>et al.</i> (2002) | Subtilisin | 5 | Reactor (Fed-batch) | 2 | 37 | 6.8 | oxygen controlled by agitation and aeration to above 20% | | Not specified | Not specified |
| Ohno <i>et al.</i> (1995) | Iturin A and Surfactin | Not specified | Solid state fermentation in shake flasks | Not specified | 23-48 | Not specified | 0 | Not specified | Not specified | 0.002 g/g dry weight |
| Matar <i>et al.</i> (2009) | Antagonistic compound | 10 | Reactor (Fed-batch) | 1.9 | 30 | 7 | 150-900 | 0.5-1.0 | Not specified | Not specified |

1.8.2.2 Mode of operation

The environmental conditions, discussed in section 1.8.2.1 above, are best evaluated in bioreactor studies, because environmental conditions such as temperature, pH, aeration and agitation can be rigorously controlled. Consequently, a fair number of studies on surfactin production were conducted under batch conditions in instrumented bioreactors (see Table 1-4). Surfactin concentrations achieved in bioreactor batch studies range from 136 – 6450 mg/L, the latter being the maximum surfactin concentration reported in literature.

Since surfactin production is reported to be growth-associated (Davis *et al.*, 1999; Peypoux *et al.*, 1999; Yeh *et al.*, 2006), the maximum surfactin concentrations were achieved at the onset of the stationary phase. The stationary phase is usually induced by a nutrient limitation, which could be avoided by the addition of nutrients during fed-batch culture. Fed-batch culture involves the continuous or sequential addition of nutrients to a batch process to either avoid or control substrate-associated growth inhibition, and consequently to extend the period of product formation (Lee *et al.*, 1999; Ding and Tan, 2006). During fed-batch culture, nutrients may be added to the culture broth according to a number of different feeding strategies which depend on the objective of the addition of nutrients. Typical objectives of fed-batch culture are to maintain a constant- pH (pH-stat) (Chen *et al.*, 2007); dissolved oxygen concentration (DO-stat) (Chia *et al.*, 2008); nutrient concentration (Vuolanto *et al.*, 2001; Cayuela *et al.*, 1993) and specific growth rate (Seok Oh *et al.*, 2002).

During pH- and DO-stat fed-batch culture, the pH and DO respectively is indirectly controlled at a certain set point by controlling the concentration of a specific nutrient within the culture broth. pH-stat fed-batch fermentation of *Ps. aeruginosa* has been used for the production of rhamnolipids (Chen *et al.*, 2007), as it has been found that pH severely affects rhamnolipid production (Guerra-Santos *et al.*, 1997). Excessive glucose feeding to a *Ps. aeruginosa* culture enhances the formation of acidic metabolites, causing a severe decrease in pH (Chen *et al.*, 2007). Therefore, the *Ps. aeruginosa* culture pH can be indirectly controlled with glucose feeding to ensure enhanced rhamnolipid productivity (Chen *et al.*, 2007). Similarly, DO-stat fed-batch fermentation of *Ps. aeruginosa* has been used for the production of 2-keto-D-gluconic acid from glucose, as the metabolic pathway for the formation of 2-keto-D-gluconic acid from glucose requires oxygen (Chia *et al.*, 2008). Therefore, a rapid rise in DO would signal the controller to increase the feed of glucose to stimulate the formation of 2-keto-D-gluconic acid from glucose.

Predetermined feeding strategies, such as constant and exponential feeding strategies, are arguably the strategies that are most often applied to fed-batch systems (Ding and Tan, 2006; Cheniker *et al.*, 2010; Seok Oh *et al.*, 2002). A constant feeding strategy implies that the flow rate of nutrients to the culture broth is constant, whereas an exponential feeding strategy implies that the flow rate of nutrients increases exponentially.

Chapter 1: Literature review

Exponential feeding strategies are mainly used to maintain a constant specific growth rate, which under pseudo steady-state conditions is equal to the dilution rate (see Appendix A: Fed-batch Kinetics). The specific growth rate is one of the most important process parameters during fermentations, as it indicates the dynamic behavior of the micro-organism (Seok Oh *et al.*, 2002). The specific growth rate is usually controlled by a limiting nutrient (such as glucose) which is exponentially fed to the reactor to control the specific growth rate.

Typically, the feed rate of exponential feeding strategies is applied according to a mass balance equation of cells and the limiting nutrient (Seok Oh *et al.*, 2002), which has the following form (derivation in Appendix A):

$$F(t) = \frac{\mu}{Y_{XS}(s_i - s)} x_0 V_0 e^{\mu t} \quad \text{Equation 1-1}$$

The advantage of the use of this equation is that the specific growth rate can be controlled to be equal to the selected dilution rate. However, the disadvantages of this equation is that it requires the biomass yield on substrate to be constant and to be known, and it also requires the concentration of the limiting nutrient within the reactor to be known. These problems are usually overcome by assuming a constant biomass yield on substrate based on preliminary experiments and by taking regular samples to determine the concentration of the limiting nutrient within the reactor (Seok *et al.*, 2002; Guez *et al.*, 2007).

Various feeding strategies applied during fed-batch culture of *B. subtilis* are shown in Table 1-5. Seok Oh *et al.* (2002) applied exponential feeding strategies to maintain the specific growth rate at 0.2-0.5 h⁻¹ to evaluate the optimal specific growth rate for maximum subtilisin (a protein-digesting enzyme) expression. These authors found that subtilisin expression increased with an increase in the specific growth rate up to 0.35 h⁻¹, after which subtilisin expression decreased. Similarly, Chen *et al.* (2006) evaluated the optimal specific growth rate of *B. subtilis* for maximum surfactin productivity during continuous culture. These authors reported that surfactin production by *B. subtilis* was optimal at a specific growth rate of 0.2 h⁻¹ and that surfactin production decreased with a further increase in the specific growth rate. Matar *et al.* (2009) evaluated the use of constant and exponential feeding strategies on the production of an unnamed antimicrobial compound during fed-batch culture of *B. subtilis*. These authors applied a constant feed flow rate of 16.2 mL/h and an exponential feeding rate of 8.4 – 16.2 mL/h and reported a 3.2- and 3.8-fold higher biomass concentration when compared to bioreactor batch culture. These authors also reported that the use of constant and exponential feeding strategies resulted in a 4-fold increase in the inhibition activity of the inhibitory compound.

Chapter 1: Literature review

In the case of predetermined feeding strategies, the fed-batch phase is typically started at the end of the exponential growth phase (Seok Oh *et al.*, 2002; Matar *et al.*, 2009; Patel *et al.*, 2004). The medium that is fed to the reactor may contain only certain nutrients, such as the limiting nutrient and a few others (Seok Oh *et al.*, 2002), or may contain all nutrients initially supplied during the batch phase (Matar *et al.*, 2009). The concentration of the nutrients that is fed to the reactor is usually much higher than the initial nutrient concentrations during the batch phase. The batch phase medium used by Seok Oh *et al.* (2002) initially contained (among others) glucose and peptone at 5g/L respectively. However, the medium that was fed to the reactor during the fed-batch phase contained only glucose and peptone at concentrations of 200 g/L and 400 g/L respectively. Similarly, the batch phase medium of Matar *et al.* (2009) contained glucose and peptone (among others) at concentrations of 10 g/L respectively, while in the feeding medium the glucose and peptone concentrations were 300 g/L respectively.

A major objective of this study was to evaluate the effect of constant- and exponential feeding strategies during fed-batch culture of *B. subtilis* ATCC 21332 as a process strategy for enhanced surfactin production.

Table 1-5: Feeding strategies applied for fed-batch culture of *B. subtilis* from literature

| Source | Product | Fed-batch feeding strategy | Dilution rates/Specific growth rates (h^{-1}) | Initial volume (L) | Maximum reactor volume (L) | Temperature ($^{\circ}C$) | pH | Agitation (rpm) | Aeration (vvm) | Comments |
|--------------------------------|--|--|---|--------------------|----------------------------|-----------------------------|-----|-----------------|----------------|---|
| Oh <i>et al.</i> (2002) | Subtilisin | Exponential | 0.2, 0.3, 0.4, 0.5 | 2 | 7 | 37 | 6.8 | See comments | See comments | oxygen controlled by agitation and aeration to above 20% saturation |
| Vuolanto <i>et al.</i> (2001) | Phytase | Glucose controlled | Not specified | 1 | 2 | 37 | 7 | See comments | See comments | oxygen controlled by agitation aeration and oxygen enriched air to above 25% saturation |
| Chenikher <i>et al.</i> (2010) | Mycosubtilin (lipopeptide) | Exponential feeding started when substrate concentration reached a value of 0.001g/L | 0.05 | Not specified | 5 | 30 | 6.5 | 200-500 | 0.75L/min | oxygen controlled by agitation and aeration to above 15% saturation |
| Cho <i>et al.</i> (2010) | Nattokinase | pH-stat by addition of nutrients when pH rose above 7.0 | Not specified | 2 | 5 | 37 | 7 | 500-900 | Not specified | oxygen controlled by agitation and aeration to above 20% saturation |
| Shene <i>et al.</i> (2000) | Recombinant β -1,4-endoglucanase | Constant and exponential feeding strategies | 0.04-0.12 | Not specified | Not specified | 37 | 7 | Not specified | Not specified | No comment |

Table 1-5: Feeding strategies applied for fed-batch culture of *B. subtilis* from literature(continued)

| Source | Product | Fed-batch feeding strategy | Dilution rates/Specific growth rates (h^{-1}) | Initial volume (L) | Maximum reactor volume (L) | Temperature ($^{\circ}C$) | pH | Agitation (rpm) | Aeration (vvm) | Comments |
|-------------------------------|---|---|---|--------------------|----------------------------|-----------------------------|-----|-----------------|----------------|--|
| Cayuela <i>et al.</i> (1993) | Unnamed insecticide | Glucose controlled | Not specified | 0.9 | 1.4 | 30 | 7 | 150-400 | see comments | oxygen maintained at 3 - 5 ppm by varying agitation, aeration and supply of pure |
| Martínez <i>et al.</i> (1998) | β -galactosidase from <i>Escherichia coli</i> | Exponential feeding started after initial 2h batch mode | 0.058-0.35 | 1 | 1.6 | 37 | 7 | Not specified | 1L/min | oxygen controlled to above 20% saturation |
| Matar <i>et al.</i> (2009) | Unnamed antagonistic and inhibitory product | Constant (0.27ml/min) and exponential feeding (0.14-0.27ml/min) strategies. Feeding commenced after glucose depletion in batch mode | Not specified | 1.9 | 3 | 30 | 7 | 150-900 | 0.5-1.0 | oxygen controlled to above 20% saturation |
| Guez <i>et al.</i> (2007) | Mycosubtilin | Exponential | 0.008 - 0.086 | Not specified | 5 | 30 | 6.5 | 200 - 400 | 0.25 | No comment |

1.8.3 Preferred process conditions for growth of *B. subtilis* and associated surfactin production

Based on the literature cited, the preferred process conditions for growth of *B. subtilis* and associated surfactin production is summarized below:

1. In general, high cell- and surfactin concentrations have been reported when *B. subtilis* was grown on carbohydrates (Kim *et al.*, 1997; Makkar & Cameotra, 1997)
2. Surfactin production has been reported to increase almost linearly with an increase in glucose concentration up to 40 g/L, with little effect on biosurfactant production over 40 g glucose/L (Kim *et al.*, 1997; Abushady *et al.*, 2005)
3. Little is known about biosurfactant production from hydrocarbons by *B. subtilis*
4. Higher biosurfactant concentrations from *B. subtilis* have been reported for cultivations when inorganic nitrogen sources were used as opposed to organic nitrogen sources
5. Most authors used NH_4NO_3 as the nitrogen source during studies on growth and biosurfactant production by *B. subtilis* (see Table 1-3)
6. Nitrogen source concentrations were typically between 1 and 10 g/L
7. Nitrogen utilization, and consequently growth and surfactin production by *B. subtilis*, is reported to be strongly influenced by the availability of iron and manganese cations (Sheppard and Cooper, 1990).
8. Studies have shown that *B. subtilis* can grow by anaerobic respiration during which nitrate is utilized as the terminal electron acceptor, as opposed to oxygen during aerobic respiration (Glaser *et al.*, 1995; Nakano *et al.*, 1997; Nakano and Zuber, 1998; Hoffman *et al.*, 1998).
9. Clements *et al.* (2002) found that, in the presence of nitrate, the maximum cell density obtained under anaerobic conditions is inferior to that obtained under aerobic conditions.
10. Abushady *et al.* (2005) evaluated the influence of oxygen availability on surfactin production and found that surfactin production increased with an increase in the volumetric oxygen concentration. In contrast to Clements *et al.* (2002) and Abushady *et al.* (2005), Kim *et al.* (1997) reported that higher cell densities and higher biosurfactant concentrations were obtained under oxygen-limited conditions. Neither Abushady *et al.*

(2005) nor Kim *et al.* (1997) provides a clear explanation regarding the effect of oxygen concentration on surfactin production.

11. Most authors have used a temperature of 30°C, a pH between 6.5 and 7.2, an agitation rate between 150 and 400 rpm, and an aeration rate between 0.25 and 1.5 vvm (see Table 1-4)
12. No literature could be found regarding fed-batch culture used explicitly for surfactin production by *B. subtilis*. A brief summary of available literature regarding the use of fed-batch culture of *B. subtilis* for other means is given in section 1.8.2.2. From this literature, it would seem that higher dilution rates/growth rates were preferred.

1.9 Hypotheses

Based on the literature review in sections 1.1-1.8 above, the following hypotheses are made:

1. *B. subtilis* ATCC 21332 is able to utilize both hydrocarbons and carbohydrates as sole carbon sources for growth and surfactin production
2. Surfactin from *B. subtilis* ATCC 21332 has antimicrobial activity against *Mycobacterium aurum*
3. Active growth of *B. subtilis* and associated surfactin production can be extended during fed-batch culture
 - a. High constant dilution rate strategies are superior to low constant dilution rate strategies for growth of *B. subtilis* ATCC 21332 and associated surfactin production during fed-batch culture
 - b. High constant feed rate strategies are superior to low constant feed rate strategies for growth of *B. subtilis* ATCC 21332 and associated surfactin production during fed-batch culture

1.10 Objectives

The objectives of this study are to prove or disprove the hypotheses stated above by performing the following experiments:

1. Shake flask studies to evaluate the growth of *B. subtilis* ATCC 21332 and associated surfactin production on *n*-hexadecane (hydrocarbon) and glucose (carbohydrate) as the sole carbon sources. This will be done to establish whether *B. subtilis* ATCC 21332 is able to utilize hydrocarbons for growth and surfactin production and also whether similar cell- and surfactin concentrations can be achieved when grown on hydrocarbons and carbohydrates respectively.
2. Disk diffusion antimicrobial assays to establish whether surfactin has antimicrobial activity against *Mycobacterium aurum*.
3. Bioreactor fed-batch culture experiments to establish whether active growth of *B. subtilis* ATCC 21332 and associated surfactin production can be extended during fed-batch culture. Various constant dilution rate- and constant feed rate strategies will be

applied to establish superiority regarding growth of *B. subtilis* ATCC 21332 and surfactin production during fed-batch culture.

2 Materials and Methods

As this study focuses on the production of surfactin by *B. subtilis* ATCC 21332, this section will focus on the process conditions and analytical methods applied for that organism and surfactin.

2.1 Micro-organisms and culture maintenance

Biosurfactant production experiments were performed using *B. subtilis* ATCC 21332. The culture collection strain was obtained from the American Type Culture Collection (ATCC). *B. subtilis* ATCC 21332 produces the lipopeptide surfactin and is described in Section 1.1.3.

The antimicrobial activity of surfactin was determined by using *Mycobacterium aurum* as the target organism. The latter is a surrogate for *M. tuberculosis*, the most common causative agent of tuberculosis.

Cultures were stored in 30 % (v/v) glycerol at -20 °C and were recovered from the frozen stocks by aseptically transferring one loopful to 25 mL nutrient broth. The culture was incubated in an orbital shaker incubator (Labcon®) at 37°C and 200 rpm. Nutrient agar (Biolab®) plates were prepared by aseptically spreading one droplet of the 48 h culture over the surface. Cultures were then transferred from the plate to nutrient agar slants. The slants were kept in a refrigerator at 4 °C for a maximum of 3 months.

2.2 Culture Media

2.2.1 Liquid media

Three minimal salts media (MSM) were selected for *B. subtilis* growth and surfactin production studies:

- A MSM, reported to be nitrogen limited; Medium A (Sim *et al.*, 1997)
- A MSM demonstrated to be phosphate limited; Medium B (Ballot, 2009)
- A nutrient rich MSM containing excess nitrogen and phosphate; Medium C (Fernandes *et al.*, 2007)

The glucose concentration of Media A and B was modified from that in literature (Sim *et al.*, 1997) to contain only 1.2% carbon (equivalent to 3% glucose) instead of 6% carbon source

(Ballot, 2009). Therefore, in order for the C/N and C/P ratios to remain the same as that in literature, the nitrogen and phosphate concentrations had to be adjusted accordingly.

Medium A and B only differed in the type of buffer used while maintaining equal buffering capacity (see Table 2-1). Medium A contained phosphate buffer whereas Medium B contained Tris (tris(hydroxymethyl)aminomethane) buffer. Medium C was phosphate buffered with equal buffering capacity.

The major differences between Medium A, Medium B and Medium C are the higher glucose, nitrogen and phosphate concentrations (with similar buffering capacity) in Medium C (see Table 2-3).

Table 2-1: Medium A and Medium B media components

| Component | Concentration [g/L] |
|--------------------------------------|---------------------|
| Glucose | 30 |
| NaNO ₃ | 3.6 |
| Yeast Extract | 0.5 |
| KCl | 1.1 |
| NaCl | 1.1 |
| FeSO ₄ ·7H ₂ O | 0.00028 |
| MgSO ₄ ·7H ₂ O | 0.5 |
| *KH ₂ PO ₄ | 0.87 |
| *K ₂ HPO ₄ | 1.124 |
| [†] Tris-HCl | 14.54 |
| Trace element solution (mL) | 5 mL |

*Medium A [†]Medium B

The trace element solution for Medium A and Medium B (see Table 2-2) was added aseptically by means of filtering through a 0.22 µm Millipore syringe filter to the media, since autoclaving would cause precipitation of the compounds. The combined phosphate, sulphate and yeast extract was also autoclaved separately from the other compounds in order to prevent precipitation.

Table 2-2: Trace element solution components for Medium A and Medium B

| Component | Concentration [g/L] |
|--------------------------------------|---------------------|
| ZnSO ₄ ·7H ₂ O | 0.29 |
| CaCl ₂ ·4H ₂ O | 0.24 |
| CuSO ₂ ·5H ₂ O | 0.25 |
| MnSO ₄ ·H ₂ O | 0.17 |

Table 2-3: Medium components of Medium C

| Component | Concentration [g/L] |
|---|---------------------|
| Glucose or <i>n</i> -Hexadecane | 40 or 18.8 |
| (NH ₄) ₂ SO ₄ | 8.5 |
| NaNO ₃ | 8.5 |
| K ₂ HPO ₄ | 13.6 |
| KH ₂ PO ₄ | 4 |
| MgSO ₄ ·7H ₂ O | 0.5 |
| Trace element solution (mL) | 10 mL |

The trace element solution for Medium C was added aseptically as before (Table 2-4). Similarly, the combined phosphates and sulphates were autoclaved separately.

Table 2-4: Trace element solution components for Medium C

| Component | Concentration [g/L] |
|--------------------------------------|---------------------|
| CaCl ₂ ·4H ₂ O | 0.42 |
| FeSO ₄ ·7H ₂ O | 2.29 |
| MnCl ₂ ·4H ₂ O | 0.1 |
| ZnCl ₂ | 0.17 |
| CuCl ₂ | 0.03 |
| CoCl ₂ ·6H ₂ O | 0.06 |

2.2.1.1 Alkane media

In experiments where alkanes were used as the only carbon source, glucose in Medium C was replaced by *n*-hexadecane. The *n*-hexadecane concentration was adjusted to contain the same amount of carbon atoms as that of its glucose counterpart (see Table 2-1). This was done in order for the C/N and C/P ratios to remain the same (Ballot, 2009). The total carbon, nitrogen

and phosphate percentages as well as the C/N and C/P ratios of the three minimal salts media are given in Table 2-5 below.

Table 2-5: Derived media used for growth and biosurfactant production studies

| Medium | Total Carbon [%] | Total Nitrogen [%] | Total Phosphate [%] | C/N | C/P |
|----------|------------------|--------------------|---------------------|-------|-------|
| Medium A | 1.2 | 0.06 | 0.04 | 18.64 | 30.17 |
| Medium B | 1.78 | 0.2 | 0 | 9.03 | NA |
| Medium C | 1.6 | 0.32 | 1.05 | 5 | 1.52 |

The alkane source was added aseptically, by means of filtering through a 0.22µm Millipore syringe filter, after cooling of the autoclaved media.

2.2.2 Solid media

The solid media used for *B. subtilis* culture were nutrient agar and alkane agar plates. Alkane agar plates were prepared by supplementing Medium A with 1% pure hexadecane instead of glucose, and 1.5% agar (Biolab®). *B. subtilis* grown on nutrient agar plates were used to inoculate media containing glucose as the sole carbon source, while *B. subtilis* grown on alkane agar plates were used to inoculate media containing alkanes as sole carbon source. The plates were incubated at 37 °C for 48 hours. Nutrient agar plates were used for growth of *M. aurum*. These plates were also incubated at 37°C for 48 hours.

2.3 Experimental protocol

2.3.1 Inoculum development

B. subtilis cultured in Medium A was used to inoculate all test flasks containing MSM. Therefore, traces of phosphate were present in Medium B. Test flasks containing alkane media were inoculated with *B. subtilis* cultured in Medium A which contained either hexadecane or glucose as the sole carbon source.

Two loops of *B. subtilis* were transferred aseptically from nutrient agar plates and alkane agar plates for glucose and alkane based experiments respectively. The liquid media for the different inocula were prepared according to Table 2-1 and Table 2-2. Inoculum volumes of 100 mL were prepared in 500 mL Erlenmeyer test flasks for each of the different media used. Inocula were incubated at 200 rpm and 37°C.

A two-stage inoculum procedure was followed, whereby a second inoculum was prepared by aseptically transferring 10 mL from the first inoculum to 90 mL of sterile medium after 16 hours of incubation. The second inoculum was incubated for four hours after which an inoculum volume of 15 mL (equivalent to 10% v/v) was transferred aseptically to 135 mL of test flask media. The use of a two-stage inoculum would ensure a more consistent final inoculum culture.

A two-stage inoculum procedure was also followed for bioreactor studies. The first inoculum was prepared as for shake flask studies and was incubated for 16 hours. The second inoculum was prepared by aseptically transferring 20 mL (equivalent to 10% v/v) from the first inoculum to 180 mL of sterile media in a 1 L shake flask and was incubated for 4 hours. The 1 L shake flask had a bottom exit tube port, to which a 30 cm piece of autoclavable silicone tubing was connected. A 0.22 μ m vent filter (Acro[®]) was connected to the silicone tube and the silicone tube was clamped before inoculation to avoid wetting of the filter. For bioreactor studies, a 200 mL inoculum, corresponding to 10% (v/v), was used to inoculate 1.8 L of sterile media.

2.3.2 Test flask experiments

Test flask experiments were conducted in 1L Erlenmeyer test flasks. The experiments were conducted in duplicate and the flasks contained 200mL of the desired medium (including inoculum). The flasks were incubated at 37 °C and 200 rpm.

2.3.3 Bioreactor experiments

2.3.3.1 Batch operation

Batch and fed-batch culture experiments were performed in a 7.5 L instrumented modular bench-top fermentor (Bioflo 110, New Brunswick Scientific[®]), with minimum and maximum working volumes of 1.5 L- and 5.6 L respectively. The temperature was controlled at 37°C using a heating jacket and cooling water which flows through a tube that was submerged in the culture broth. The pH was controlled at 6.8 by the addition of sterile 2M NaOH_(aq) by means of an automatic peristaltic pump. The DO concentration was controlled by a cascade system which was linked to agitation. The dissolved oxygen concentration was set to be 10% at a constant aeration rate of 0.8 vvm and controlled agitation, with minimum and maximum revolutions per minute of 50 and 400 respectively. Agitation was supplied by a Rushton impeller.

The physical setup of the fermentor included two 0.22 μ m air filters (Acro[®]) that were connected at both the air inlet and outlet to ensure uncontaminated reactor runs. The setup also included a vapor condenser before the air outlet. The condenser ensured that no liquid vapor condensed on the filter, consequently reducing the risk of a pressure build-up and loss of liquid from the culture.

Temperature, pH (Mettler Toledo®) and dissolved oxygen probes (Mettler Toledo®) were inserted into the culture broth. The temperature probe was inserted into a hollow tube filled with glycerol (80% v/v) before it was inserted into the culture broth. The dissolved oxygen probe was calibrated after sterilization while the pH probe was calibrated before sterilization.

A 10% (v/v) solution of sterile Antifoam A (30% aqueous polymer solution, Fluka®) was added manually by means of a peristaltic pump to reduce and inhibit foam formation.

2.3.3.2 Fed-batch operation

Fed-batch experiments were performed at the same environmental conditions (pH, temperature and DO concentration) as that for batch fermentation, with the exception of a sterile feed solution being added during the experiment. The composition of the sterile feed solution was exactly the same for all six fed-batch experiments and consisted of all components of Medium C, as given in Table 2-3 and Table 2-4. However, the concentrations (and amount of trace element solution) of the components were twice as much as given in Table 2-3.

The addition of sterile feed solution commenced at the cessation of the exponential growth phase. The flow rate of the sterile feed solution was either constant or controlled to increase exponentially according to a predetermined dilution rate. Six predetermined feeding strategies were applied for fed-batch culture. The predetermined flow rates and dilution rates for the fed-batch runs are given in Table 2-6.

Table 2-6: Predetermined feeding strategies for fed-batch fermentation

| Fed-batch run | Conditions | Dilution rate (1/h) | Flow rate (L/h) |
|---------------|-------------------------|---------------------|-----------------|
| 1 | Constant feed flow rate | 0.2-0.071 | 0.4 |
| 2 | Constant feed flow rate | 0.063-0.025 | 0.125 |
| 3 | Constant dilution rate | 0.4 | 0.8-1.57 |
| 4 | Constant dilution rate | 0.15 | 0.3-0.8 |
| 5 | Constant dilution rate | 0.1 | 0.2-0.52 |
| 6 | Constant dilution rate | 0.05 | 0.1-0.25 |

During the constant dilution rate fed-batch experiments, the flow rate of the sterile feed was increased exponentially over time to maintain the predetermined constant dilution rate. The feed flow rate was predetermined according to the following equation:

$$F = DV$$

Equation 2-1

According to Equation 2-1, the dilution rate would decrease as the volume increases as a result of nutrients being added to the reactor. Equation 2-1 was used to predict what the flow rate of

the sterile feed should be at a given volume to maintain the selected dilution rate and accordingly, the flow rate of the sterile feed was increased exponentially to maintain a constant dilution rate (see Appendix B).

By predetermining the feed flow rate according to Equation 2-1, no assumptions had to be made regarding the biomass yield on substrate or concentration of the limiting nutrient in the culture broth. The flow rate of the feed solution was increased hourly following a stepwise procedure. As an example, Figure 2-1 illustrates the stepwise increase in the feed flow rate to approximately maintain a constant dilution rate of 0.15 h^{-1} . The mathematical derivations regarding fed-batch culture are explained in Appendix A: Fed-batch Kinetics.

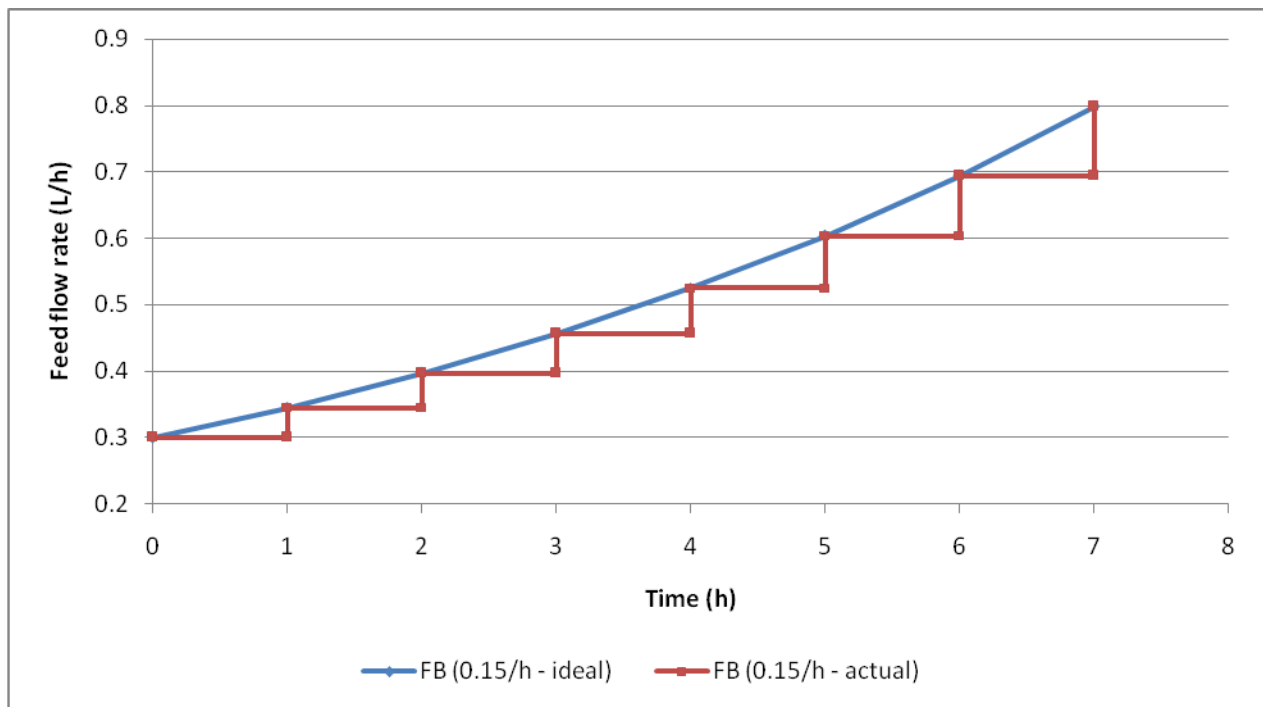


Figure 2-1: Illustration of stepwise increase in sterile feed flow rate to maintain a constant dilution rate

2.4 Analytical Methods

2.4.1 Cell concentration

The cell concentration was determined according to two different methods; cell dry weight and absorbance measurements (see section 2.4.1.1 and section 2.4.1.2). These methods are further discussed separately in sections 2.4.1.1 and 2.4.1.2 below.

2.4.1.1 Cell dry weight (CDW)

The CDW was determined for bioreactor studies only because it requires a sample volume which would be too large for the small volume contained in the shake flasks. 10 mL samples were withdrawn from the reactor and filtered to separate the cells from the supernatant. A Buchner vacuum filter (Millipore®) and filter paper disks with a pore size of 0.2µm (Anatech®) were used for filtration. Each filter paper disk was dried in a vacuum oven (SHEL LAB) at 60°C for 24 hours and weighed (OHAUS adventurer®) after cooling in a desiccator before it was used for filtration. After filtration, the wet paper disk containing the separated cells was dried in a vacuum oven at 60°C for 24 hours. After drying, the paper disc was cooled and weighed as before, and the difference in weight before and after filtration is the CDW.

2.4.1.2 Absorbance

The absorbance was measured with a spectrophotometer (Varian®) at 621nm (visible light region). The following procedure was followed for absorbance measurements:

- A 1mL sample was withdrawn from the test flask and pipetted into a micro-centrifuge tube
- This sample was centrifuged (Eppendorf® Minispin Plus) for 10 minutes at 6800 rcf
- The supernatant was separated from the cell pellet and resuspended in physiological saline (0.85% m/v NaCl solution) by means of vortexing
- The absorbance of this suspension was measured with a spectrophotometer at 621nm
- The linear region of absorbance versus cell concentration was determined to be between 0 - 0.80
- If absorbance values higher than 0.80 were obtained, the sample was diluted in order to obtain an absorbance value in the linear region
- The blank used for cell density measurements was sterile physiological saline

2.4.1.3 Relationship between CDW and absorbance

Cell densities of all experiments were measured according to the absorbance of the culture broth. Since this method is an indirect method for measuring the cell concentration, the relationship between the direct CDW method and absorbance was determined to quantify all absorbance measurements. It is evident from Figure 2-2 that the relationship between CDW and absorbance is linear. Therefore, all absorbance measurements were converted to CDW by multiplying the absorbance measurement with the gradient of the trendline (equal to 0.467) in Figure 2-2.

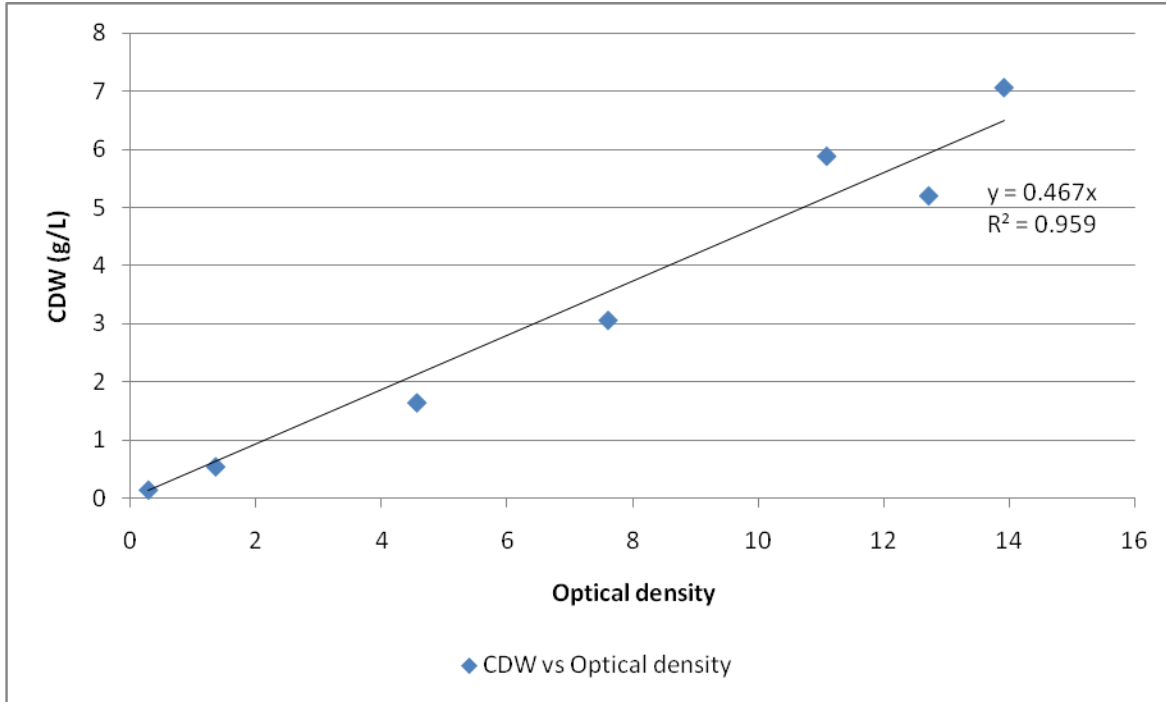


Figure 2-2: Relationship between CDW and Optical density

2.4.2 Surface tension

2.4.2.1 Surface tension measurement

The surface tension measurements were conducted by using a du Noüy ring type tensiometer (Figure 2-3). The tensiometer was calibrated before surface tension measurements were performed. The calibration procedure (with reference to Figure 2-3) is given below:

- The platinum ring (B) was hung from a precision balance (C) and the scale value (D) noted when the precision balance was in a horizontal position
- A small piece of foil (approximately 100mg) was placed onto the platinum ring while the precision beam is kept horizontal by adjusting D and the scale value noted
- The calibration factor (dimensionless), equal to $\frac{mg}{Rl}$ was then calculated, with m being the mass of the piece of foil, g being gravitational acceleration, l being the contact perimeter of the ring and R being the difference in measurements with and without the piece of foil.

Surface tension measurements were then conducted by the following procedure:

- The platinum ring was hung from the precision balance and the scale value (“zero” value) was noted
- A 3 mL sample was poured into a container and placed on platform A

- The container was then lifted by lifting platform A until the platinum ring was fully submerged under the liquid surface
- The platinum ring was kept at a horizontal position ensuring that the force measured was the vertical pull
- Platform A was lowered while simultaneously keeping the precision balance at a horizontal position. This was done by increasing the tension on the scale
- When the platinum ring released from the liquid, the final value on the scale was noted
- The difference between the two scale values noted before and after measurements, multiplied by the calibration factor is equal to the surface tension of the sample (units – mN/m)

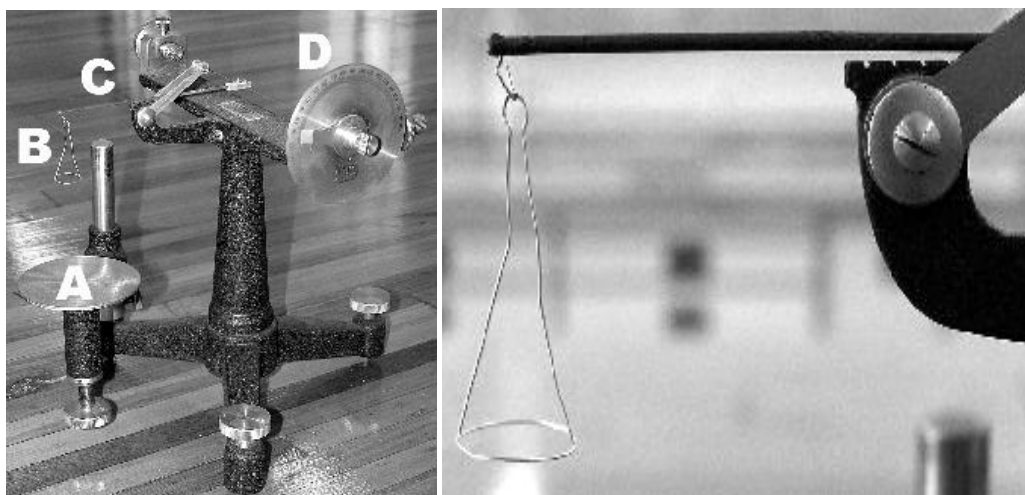


Figure 2-3: The du Noüy Tensiometer (With permission: University of Stellenbosch, Chemistry 324 Practical Guide 2009)

2.4.2.2 Critical micelle concentration (CMC)

The critical micelle concentration was determined by measuring the surface tensions of serial dilution of supernatant obtained from a culture broth. The serial dilution was carried out by diluting the filtered (0.22 μ m syringe filter) supernatant with phosphate buffer at pH 7.00. This dilution was carried out as follows:

- 6mL of supernatant was obtained by filtering a sample through a 0.22 μ m syringe filter
- The surface tension of this sample was measured first
- 3mL of the first sample was diluted with 3mL of pH 7 phosphate buffer
- The surface tension of the second sample was then measured, and repeated

2.4.3 Surfactin concentration

The concentration of surfactin was determined using High Pressure Liquid Chromatography (HPLC). The HPLC specifications are given in Table 2-7.

Table 2-7: Specifications of the HPLC column, mobile phase and absorbance

| HPLC specifications | |
|---------------------|---|
| Column | Phenomenex Luna 5 μ m C18 column (150 x 4.6 mm) |
| Detector | Thermo Separation Products, SpectraSYSTEM UV1000 detector |
| Mobile phase A | 0.1% (v/v) Trifluoroacetic acid (Fluka [®]) in water |
| Mobile phase B | 0.1% (v/v) Trifluoroacetic acid in Acetonitrile (Chromasolv, Sigma-Aldrich [®]) |
| Mobile phase ratio | 80% mobile phase A: 20% mobile phase B |
| Flow rate | 0.5 mL/min |
| Absorbance | 210 nm |

A standard absorption curve for surfactin was constructed each time samples were analysed. Pure surfactin was obtained from Sigma-Aldrich[®]. The following procedure was followed for the construction of the standard curve:

- 10 mg of pure surfactin was dissolved in methanol to prepare a 1 x 10 000 mg/L solution (dissolving 10 mg of pure surfactin in 1 mL of methanol)
- Serial dilutions with concentrations ranging from 0 – 5000 mg/L surfactin were prepared from the 10 000 mg/L solution
- 10 μ L samples were injected into the column and eluted with the mobile phase
- The absorbancy of the eluent was monitored at 210 nm for the construction of the chromatogram (see
- Six major peaks (peaks 1-6 in Appendix C: HPLC chromatograms) were observed on the chromatogram and corresponds to different surfactin homologues (see section 1.1.3). The sequence of the peptide ring and also the length of fatty acid moiety of surfactin homologues may differ and interacts differently with the column. Hence the six major peaks at different retention times. Some variation in the retention times of the six peaks were observed and may be ascribed to column effects. However, the relative times between the six peaks were very similar.
- The areas under the chromatograms were plotted against the standard surfactin concentrations to obtain the surfactin standard curve (see Figure 2-4)

The error bars in Figure 2-4 indicate the difference in the surfactin standard curves obtained from different runs. The percentage error on all data points was less than 5% between the different runs, indicating good reproducibility of the analysis.

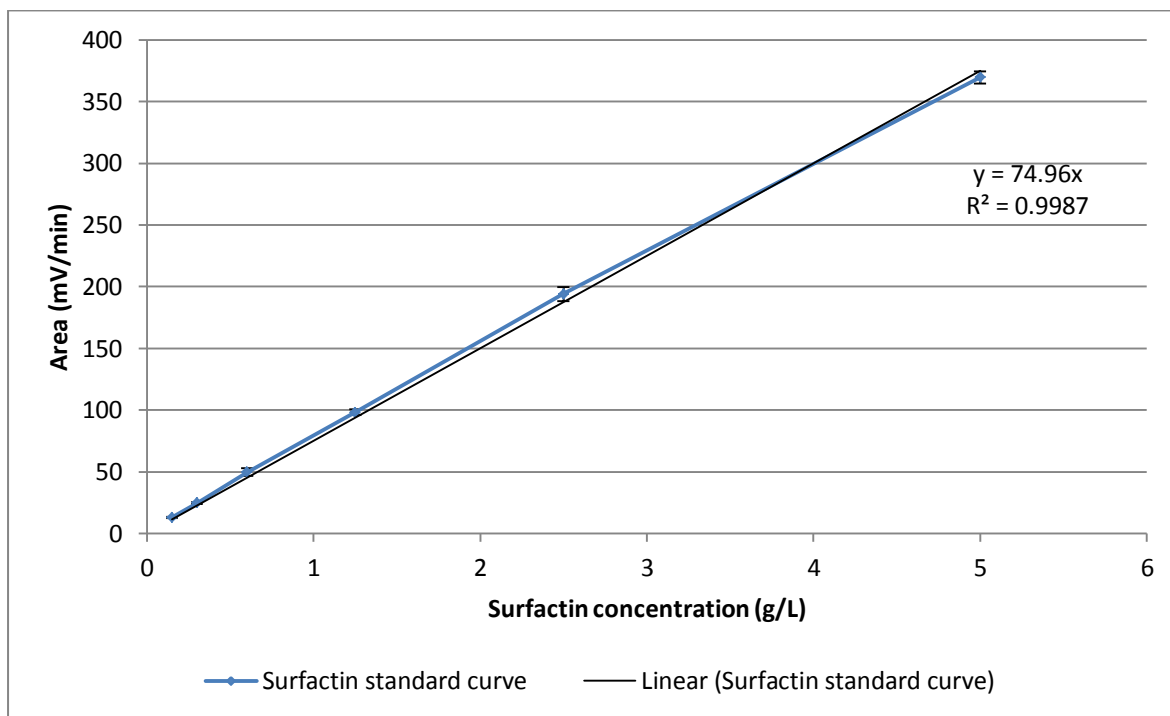


Figure 2-4: Surfactin standard curve

Sample preparation to determine the surfactin concentration within the culture broth:

- Samples from the culture broth were centrifuged for 10 minutes at 6700 rcf to remove most of the cells from the culture broth, leaving a supernatant
- The supernatant was filtered through a 0.22 μm syringe filter (Anatech®) to ensure that all cells are removed from the supernatant
- 400 μL of filtered supernatant was added to 1600 μL acetonitrile (Anatech®) to allow precipitation (unknown precipitate⁶; however, surfactin concentration was not affected)
- This mixture was filtered through a 0.22 μm syringe filter
- 100 μL of the supernatant/acetonitrile mixture was injected into the column
- The absorbancy of the eluent was monitored at 210 nm
- Digital software compared the absorption peaks obtained from the supernatant to that of the standard curve and automatically related it to the surfactin concentration within the supernatant

⁶ It was found that the unknown precipitate obstructed the flow through the HPLC column

Six absorbance peaks were observed when culture supernatant was analyzed for surfactin and also had similar retention times to those of the surfactin standards. Therefore the surfactin analysis was reliable and accurate.

2.4.4 Glucose concentration

The glucose concentration was also determined using HPLC analyses. The HPLC specifications for the glucose analyses are given in Table 2-8:

Table 2-8: HPLC specifications for glucose analyses

| HPLC specifications | |
|---------------------|---|
| Column | Prevail Carbohydrate ES 5 I (250 mm, 4.6 mm) column (Grace Davison Discovery Sciences, Deerfield, IL, USA) connected to All-Guard Cartridge System (Grace Davison Discovery Sciences, Deerfield, IL, USA) |
| Mobile phase | 55% acetonitrile, 15% acetone, 30% water (isocratic separation) |
| Sample volume | 10 μ L |
| Flow rate | 1 mL/min |
| Detector | Evaporative light-scattering detector |

A standard absorption curve was constructed each time before samples were analysed. Pure D-Glucose was obtained from Sigma-Aldrich®. The following procedure was followed to obtain the standard curve:

- 5 glucose standards with concentrations of 2.08, 1.04, 0.52, 0.26 and 0.13 g/L were prepared in deionised water
- 10 μ L of each of the prepared standards were injected into the column and eluted with the mobile phase
- A standard curve was constructed from the absorbance outputs and standard concentrations (Figure 2-5)

Since a glucose standard curve was prepared each time before samples were analysed, the error bars in Figure 2-5 correspond to the difference between the standard curves obtained for the different runs. The percentage error for low glucose concentrations of 0.08 – 0.13 g/L were 13% and 10% respectively, while that of glucose concentrations of 0.16 – 2.08 g/L were all less than 5%.

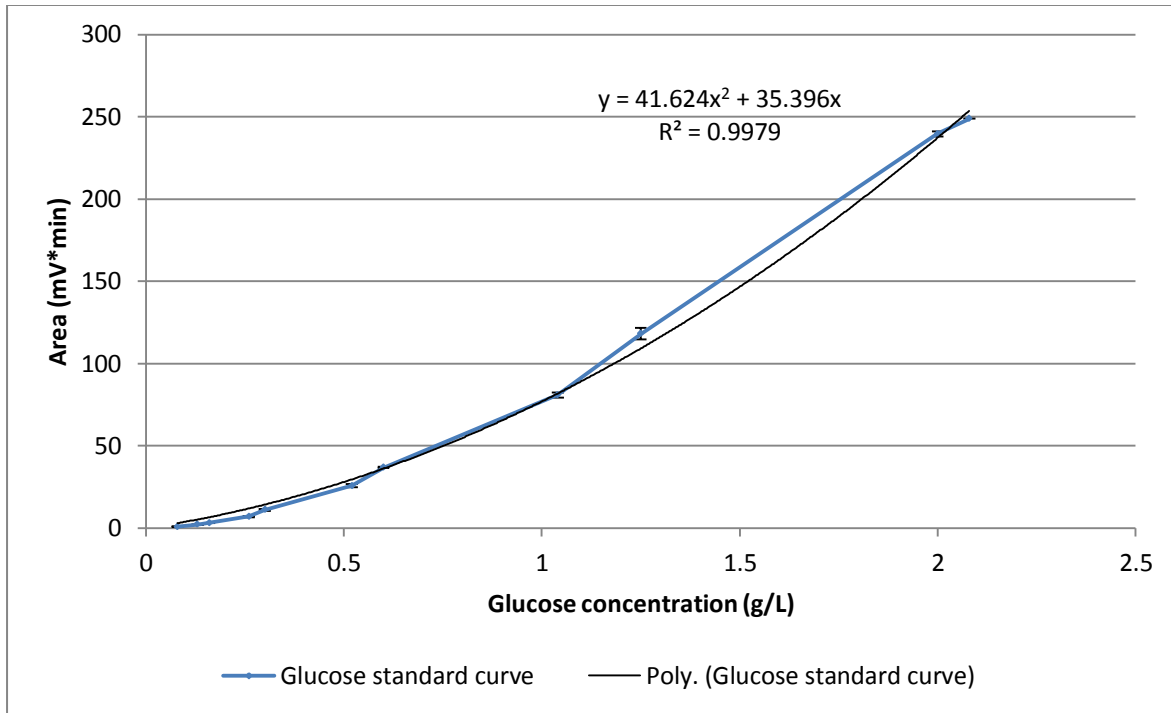


Figure 2-5: Glucose standard curve

Samples for the glucose analyses were prepared as follows:

- Samples from the culture broth were centrifuged for 10 minutes at 6700 rcf to remove most of the cells from the culture broth, leaving a supernatant
- The supernatant was filtered through a 0.22 μm syringe filter to ensure that all cells are removed from the supernatant
- 400 μL of filtered supernatant was added to 1600 μL acetonitrile (Anatech[®]) to allow precipitation
- This mixture was filtered through a 0.22 μm syringe filter
- 10 μL of the supernatant/acetonitrile mixture was injected into the column.
- Digital software compares the absorption peaks obtained from the supernatant to that of a standard curve and automatically relates it to the glucose concentration within the supernatant

2.4.5 Nitrate- and phosphate concentrations

Nitrate- and phosphate concentrations were analysed on a Dionex[®] Ion Chromatograph equipped with a conductivity detector. The following settings were used:

Table 2-9: Ion Chromatograph specifications for nitrate- and phosphate analyses

| | |
|------------------|--|
| Separator column | IonPac AS4A-SC 4mm |
| Mobile phase | 1.80mM Na ₂ CO ₃ / 1.70mM NaHCO ₃ |
| Flow rate | 1.0 ml/min |
| Regenerant | 25mM H ₂ SO ₄ |

The ion chromatograph had to be calibrated before samples were analysed. The calibration procedure was as follows:

- 10, 20, 50, 100 mg/L nitrate/phosphate standards were prepared in deionised water
- 50µL of each of the standards were injected into the column and eluted with the mobile phase
- The response of the detector, in the form of absorption peaks, were used to construct a standard curve (see Figure 2-6 and Figure 2-7)

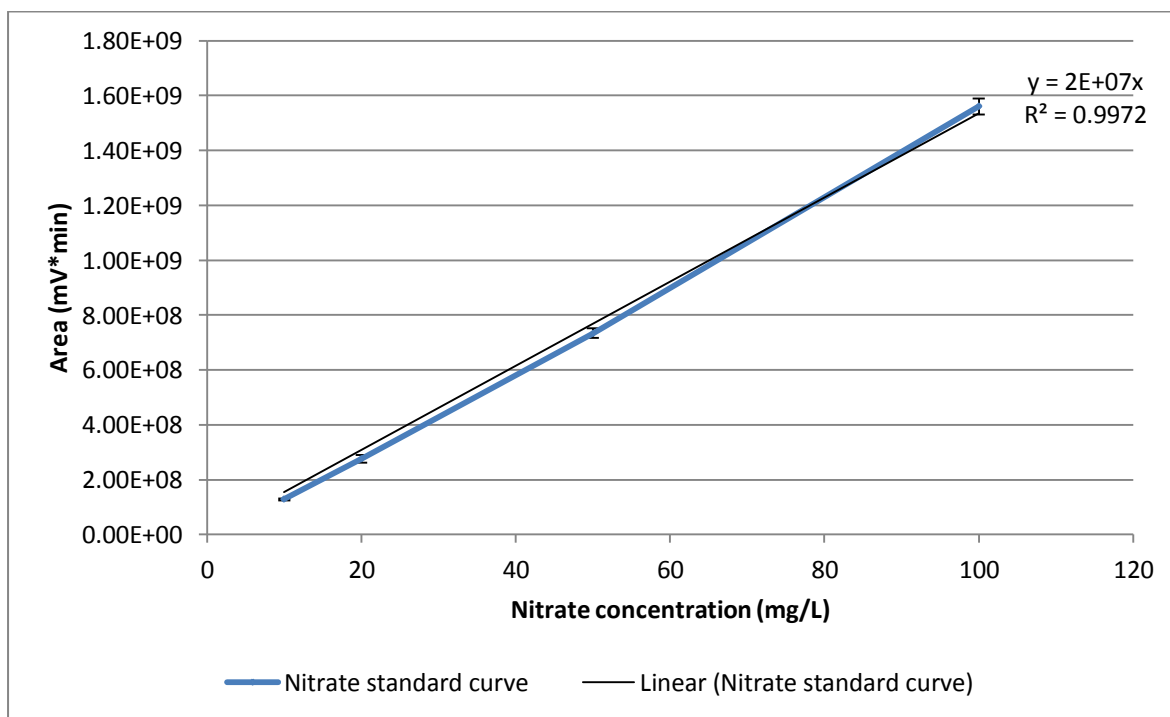


Figure 2-6: Nitrate standard curve

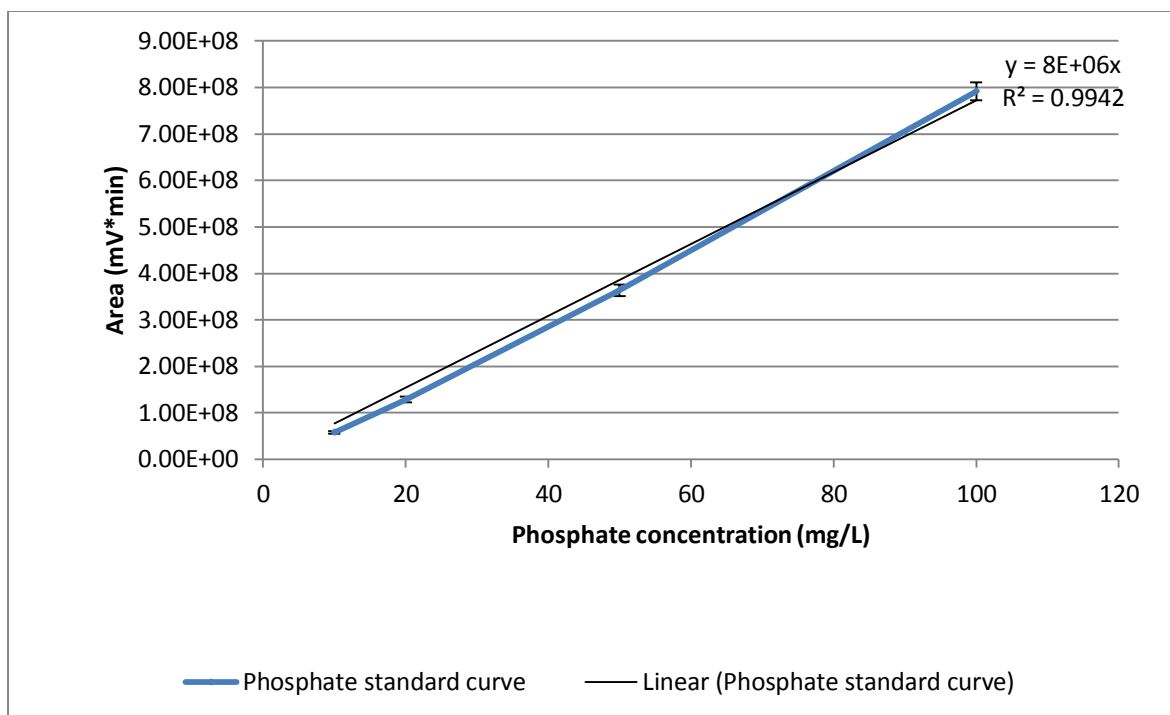


Figure 2-7: Phosphate standard curve

Samples for the nitrate- and phosphate analyses were prepared as follows:

- Samples from the culture broth were centrifuged for 10 minutes at 6700 rcf to remove most of the cells from the culture broth, leaving a supernatant
- The supernatant was filtered through a 0.22 μm syringe filter to ensure that all cells are removed from the supernatant
- The supernatant was filtered through a 0.22 μm syringe filter
- The supernatant was diluted either 50x or 100x to ensure that the detector was not saturated
- 50 μL of the diluted supernatant mixture was injected into the column
- Digital software compared the absorption peaks obtained from the supernatant to that of the nitrate- and phosphate standard curves and automatically related it to the nitrate- and phosphate concentrations within the supernatant

2.4.6 Antimicrobial activity

2.4.6.1 Determination of antimicrobial activity by soft agar overlay method

The soft agar overlay method developed by du Toit and Rautenbach (2000) was modified by Ballot (2009). The modified method was used for the determination of antimicrobial activity of surfactin. The procedure for determining antimicrobial activity of surfactin is given below:

- The test organism, *Mycobacterium aurum*, was grown on solid nutrient agar plates
- After 48 hours of incubation at 37°C, colonies of *Mycobacterium aurum* were suspended aseptically into sterile physiological saline (0.85% w/v) until an optical density, as measured by a spectrophotometer (Varian) of 0.3 was achieved
- A soft nutrient agar solution was prepared (nutrient broth with 7.5% agar)
- 2mL of the saline suspension of *Mycobacterium aurum* was added to 10mL of soft nutrient agar solution
- The combined solution was then vortexed for approximately 30 seconds
- The cut-off back ends of sterile pipette tips were placed in Petri-dishes, 3 per plate and evenly spaced
- The vortexed solution was then carefully poured into the Petri-dish and allowed to settle around the cut-off back ends of the pipette tips
- The back ends were removed with sterile forceps, leaving three wells in the agar
- Test samples were filter sterilized with a 0.22µm syringe filter (Millipore®)
- 40µL of the filtered solution was pipetted into two of the wells and 40µL of sterile physiological saline was pipette into the third well which served as the control.
- The plates were incubated for 48 hrs at 37°C
- The inhibition zone diameters were measured after 48hours and is defined as the difference between the diameter of the inhibition zone and the well diameter (seeFigure 2-8)

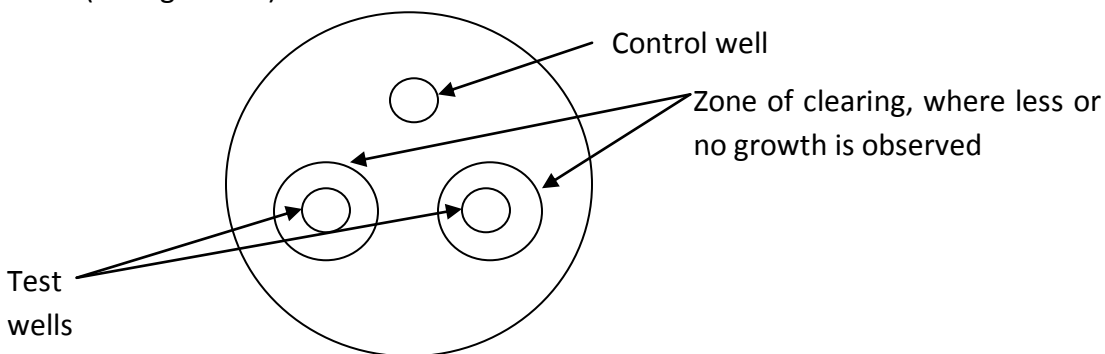


Figure 2-8: Schematic representation of antimicrobial inhibition zones

3 Results and Discussion

3.1 Media requirements for growth and biosurfactant production

3.1.1 Media selection

Three different media were selected to evaluate the growth and surfactin production by *B. subtilis* (see section 2.2.1 for media compositions). The objective for selecting these media was to evaluate the different nutrient requirements for good growth and biosurfactant production. Two of the selected media, media A- and B, were used in a previous study on the production of rhamnolipids by *Ps. aeruginosa* (Ballot, 2009). Medium A has been reported to be nitrogen-limiting (Sim *et al.*,1997), whereas medium B has been demonstrated to be phosphate-limiting (Ballot, 2009).

Medium C has been selected to serve as a benchmark for the other selected media, since it has been used previously for biosurfactant production by *B. subtilis* (Fernandes *et al.*,2007). Medium C has a C:N ratio of 5 and a C:P ratio of 1.52, which is substantially lower than that of the other selected media (see Table 2-5). The effect of excess nitrogen and phosphate on growth and biosurfactant production will be compared to the effect of low nitrogen- and phosphate concentrations on growth and surfactin production.

Growth and surfactin production in the selected media were evaluated in 1L shake flasks. This was done to select the most appropriate medium for further bioreactor batch- and fed-batch studies. All shake flask experiments were performed in duplicate and therefore, the error bars presented indicate the standard deviation between the samples withdrawn from the duplicate flasks. The reproducibility of the shake flask experiments is discussed in section 3.6.1.

3.1.2 Quantification of cell dry weight and surfactin concentration in selected glucose media

B. subtilis responded well to media A and C, reaching maximum CDWs of 7.71 g/L and 12.6 g/L at the start of the stationary phase after 21 and 30 hours respectively (Figure 3-1). These CDWs are 1.5- and 2.5- fold higher than the maximum CDW (5.09 g/L) achieved in medium B.

The maximum CDWs achieved in all media are in accordance with that in literature, which range from 2 g/L to approximately 9 g/L (Kim *et al.*, 1997; Makkar and Cameotra, 1997; Davis *et al.*, 1999; Cooper *et al.*, 1981; Fernandes *et al.*, 2007). The maximum CDW of 12.6 g/L achieved in medium C is higher than the reported maximum CDW of 8.0 g/L by Fernandes *et al.* (2007). This difference in maximum CDW could possibly be ascribed to the difference in incubation temperature, which was higher by 7°C in this study.

It can be seen in Figure 3-1 that growth of *B. subtilis* was accompanied by surfactin production. Relatively high maximum surfactin concentrations of 730 mg/L and 652 mg/L were achieved in media B- and C, while a poor maximum surfactin concentration of 172 mg/L was achieved in medium A. The surfactin concentrations achieved are in accordance with the surfactin concentrations in literature (see Table 1-4), which range from 31.2 mg/L (Davis *et al.*, 1999) to 6450 mg/L (Yeh *et al.*, 2006). However, the latter was achieved in a bioreactor under controlled conditions.

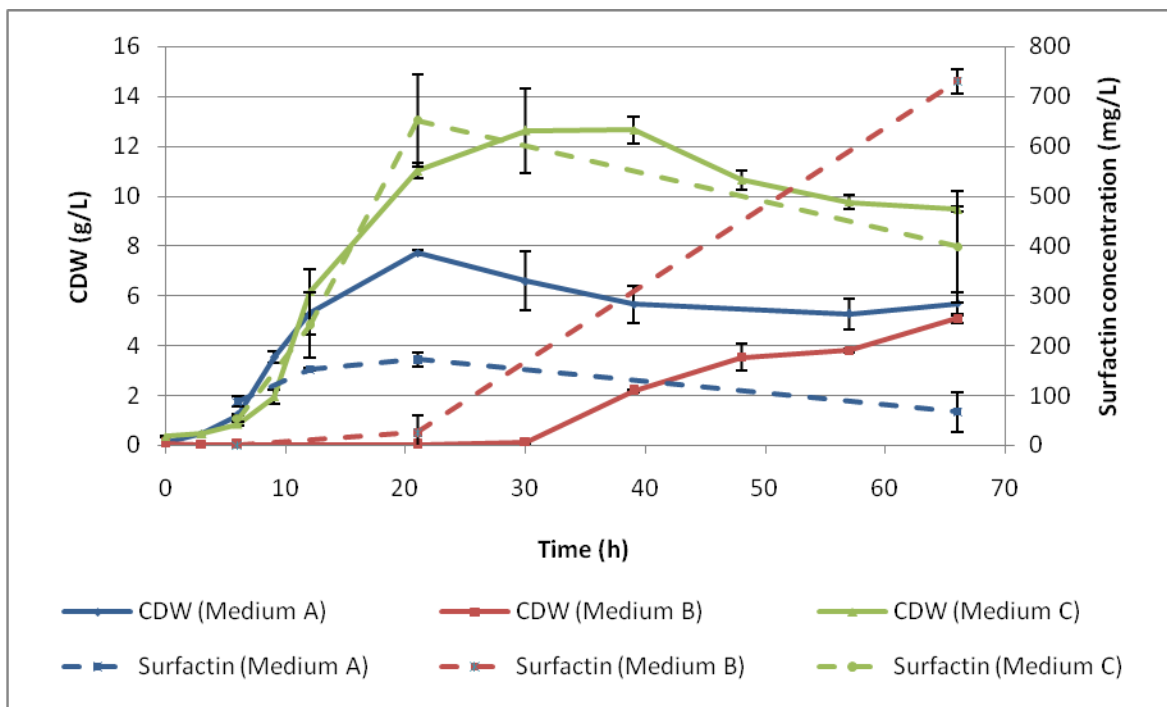


Figure 3-1: Growth and surfactin production by *B. subtilis* ATCC 21332 from selected media

3.1.3 Influence of nutrient conditions on cell dry weight and surfactin concentration during shake flask culture

3.1.3.1 Medium A

Glucose, nitrate and phosphate were measured during experiments. Neither of these nutrients were near depletion at the cessation of active growth in medium A (Figure 3-2). Active growth ceased after 21 hours and coincided with glucose, nitrate and phosphate concentrations of 18.08 g/L, 1370mg/L and 1213 mg/L respectively. This indicated that none of these nutrients were responsible for the growth limitation in this medium and therefore, some other nutrient (eg. trace element) could have limited the growth in this medium.

Although good growth was observed in medium A, surfactin production was poor compared to that observed in media B- and C. The maximum surfactin concentration of 172 mg/L achieved after 21 hours of growth in Medium A was 4- and 3-fold less than that achieved in media B- and C respectively. Since all the measured nutrients were in excess during the first 21 hours of growth in Medium A, the reason for the low surfactin concentration achieved in medium A could not be determined.

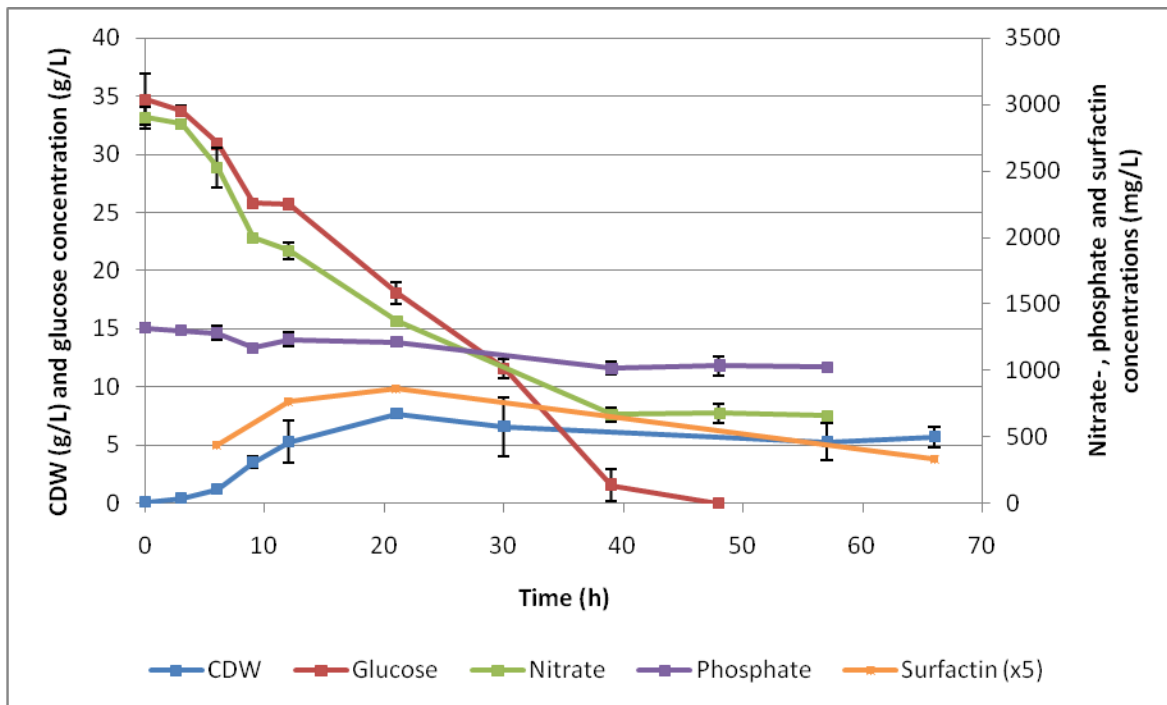


Figure 3-2: Influence of nutrient conditions on growth and surfactin production in medium A

3.1.3.2 Medium B

A 30 h lag phase was observed when *B. subtilis* was cultured in medium B, which only contained traces of phosphate from the inoculum (see Figure 3-3). Since the inocula for all shake flask

studies were prepared in medium A, the observed lag phase was probably due to the inoculation from a phosphate rich environment to a phosphate deficient medium.

After the 30 h lag phase, the CDW slowly increased from 0.1 g/L to 5.1 g/L between 30 and 66 hours of incubation. Although poor growth was observed in medium B, the highest surfactin concentration of 730 mg/L was produced from this medium, indicating a high surfactin yield on biomass. This surfactin concentration is 4-fold higher than the maximum surfactin concentration (172 mg/L) produced in medium A, while the only difference between these two media is the phosphate concentration.

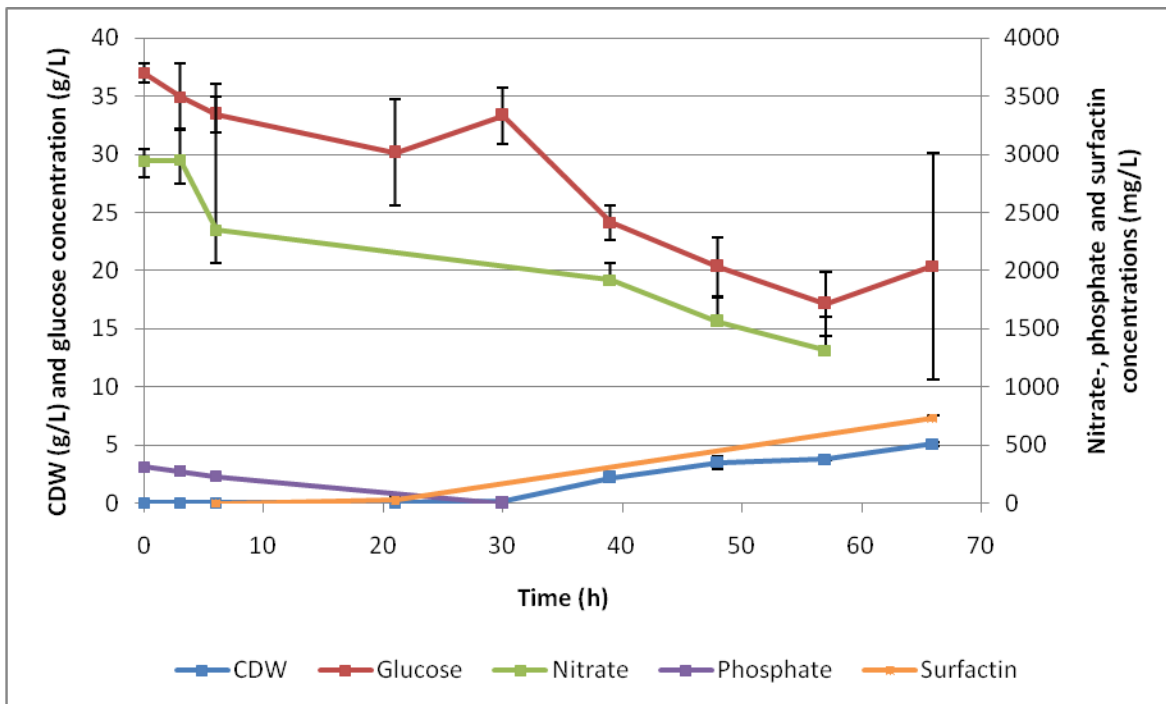


Figure 3-3: Influence of nutrient conditions on growth and surfactin production in medium B

In Figure 3-3 it can be seen that phosphate in medium B was depleted after 30 hours, while glucose and nitrate were in excess for the duration of the experiment. Growth and surfactin production in this medium only started after 30 hours of incubation in medium B, indicating that a phosphate deficiency does not limit surfactin production by *B. subtilis*, but seems to enhance it.

A fourth medium, medium D, derived from medium A, was used to evaluate whether the lag phase observed in medium B could be reduced by supplementing medium A with 0.35 g/L KH_2PO_4 and 0.45 g/L K_2HPO_4 . These concentrations correspond to 40% of the KH_2PO_4 and K_2HPO_4 concentrations used in medium A. The lag phase observed in medium B was reduced by 20 hours when *B. subtilis* was cultured in medium D (Figure 3-4). This supports the fact that the

lag phase observed in medium B was caused by a phosphate deficiency. Although the lag phase was reduced by 20 hours, the shape of the growth curves of media B- and D were very similar. A maximum CDW of 5.74 g/L was reached in medium D, which compared well with the maximum CDW of 5.09 g/L achieved in medium B. The maximum surfactin concentrations achieved in media B- and D were also very similar. A maximum surfactin concentration of 627 mg/L was achieved after 69 hours in medium D, while the maximum surfactin concentration achieved in medium B was 730 mg/L.

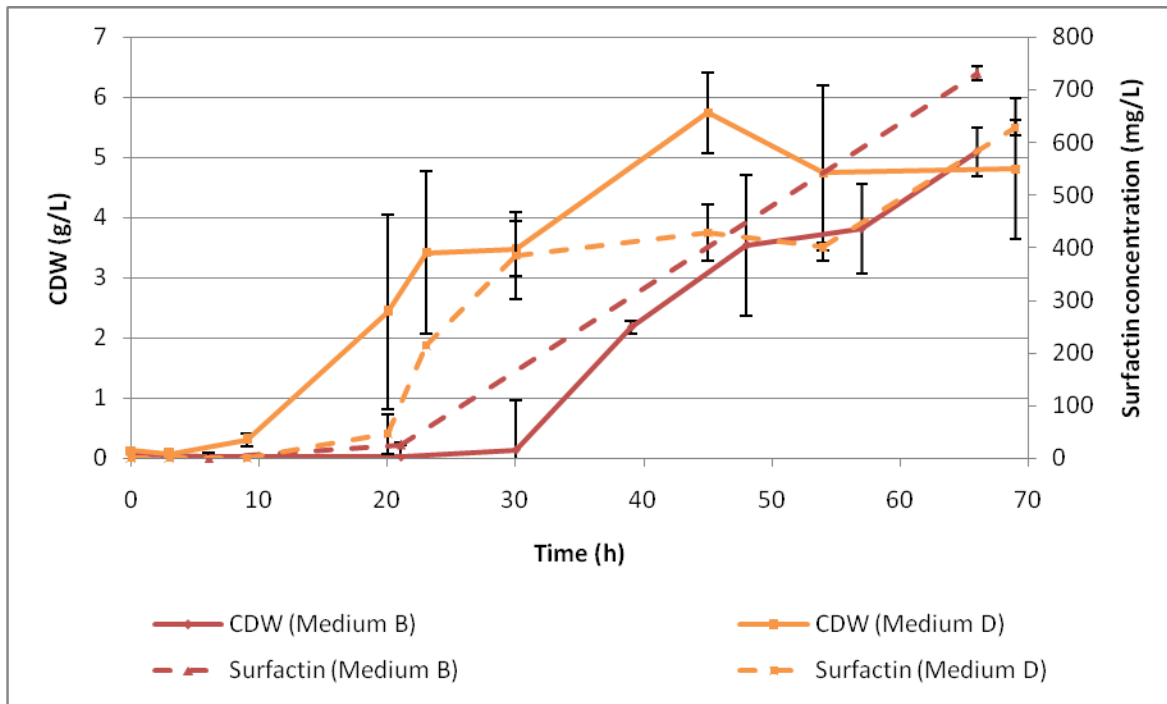


Figure 3-4: Evaluation of the effect of phosphate concentration on lag phase

Growth in medium D ceased after 45 hours, and coincided with glucose depletion (Figure 3-5). However, the surfactin concentration increased from 428 mg/L to 627 mg/L during the stationary phase between 45 and 69 hours of growth. This indicates that surfactin was excreted from within the cell, since surfactin could not be synthesized as a result of glucose depletion. It also indicates that surfactin is excreted from within the cell during the stationary phase under low phosphate concentrations, since this effect has not been observed in media A- and C. Further research is required to confirm these results.

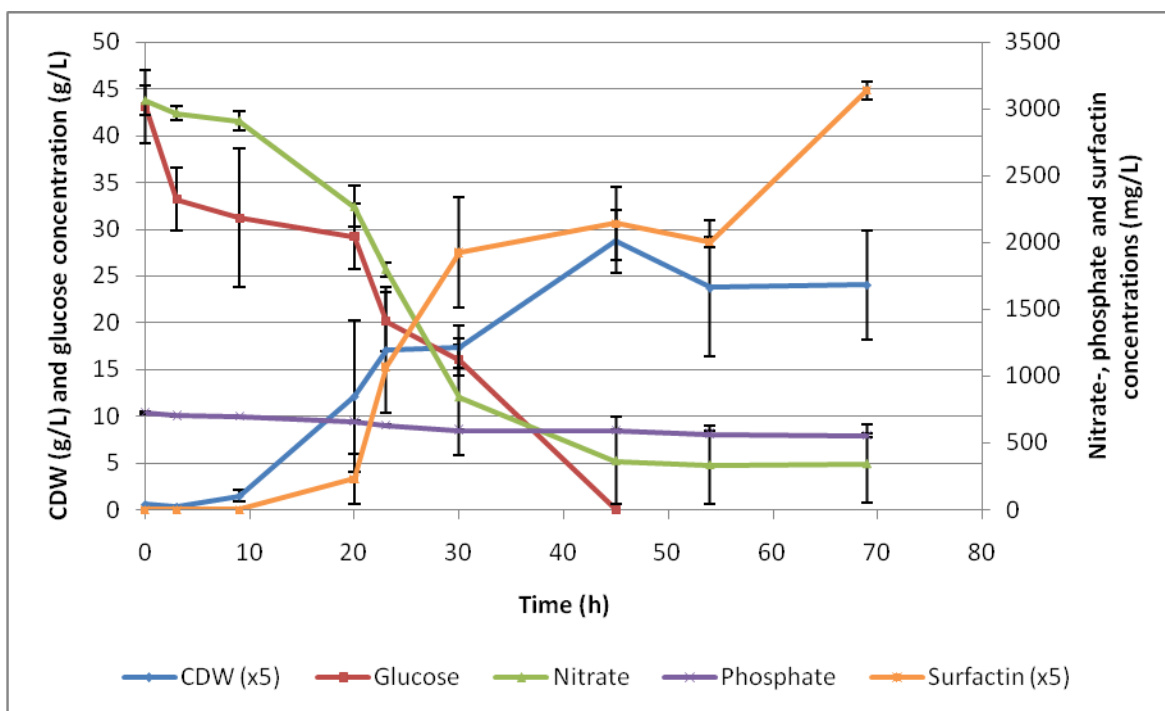


Figure 3-5: Influence of nutrient conditions on growth and surfactin production in medium D

3.1.3.3 Medium C

A maximum CDW of 12.6 g/L and maximum surfactin concentration of 652 mg/L were achieved in medium C. The high CDW and surfactin concentration achieved in medium C is a result of the higher glucose- and nutrient concentrations, compared to the other selected media (see section 2.2.1). All selected media contained similar Mn^{2+} concentrations; however, medium C contained an 82-fold higher Fe^{2+} concentration than that in the other selected media. Higher concentrations of iron and manganese have been shown to significantly increase the growth and surfactin production by *B. subtilis* (Cooper *et al.*, 1981) (see section 1.8.1.2).

Nitrate and glucose were rapidly consumed as a result of the higher CDW achieved in medium C and was depleted after 21 and 39 hours of growth respectively (Figure 3-6). It can be seen that growth continued after the nitrate depletion between 21 and 30 hours of growth, before being limited by the low residual glucose concentration. However, surfactin production ceased after 21 hours of growth which coincided with nitrate depletion, indicating that surfactin production is possibly limited by nitrate depletion (Figure 3-6). This is in contrast to the effect of phosphate depletion observed in medium B (see section 3.1.3.2).

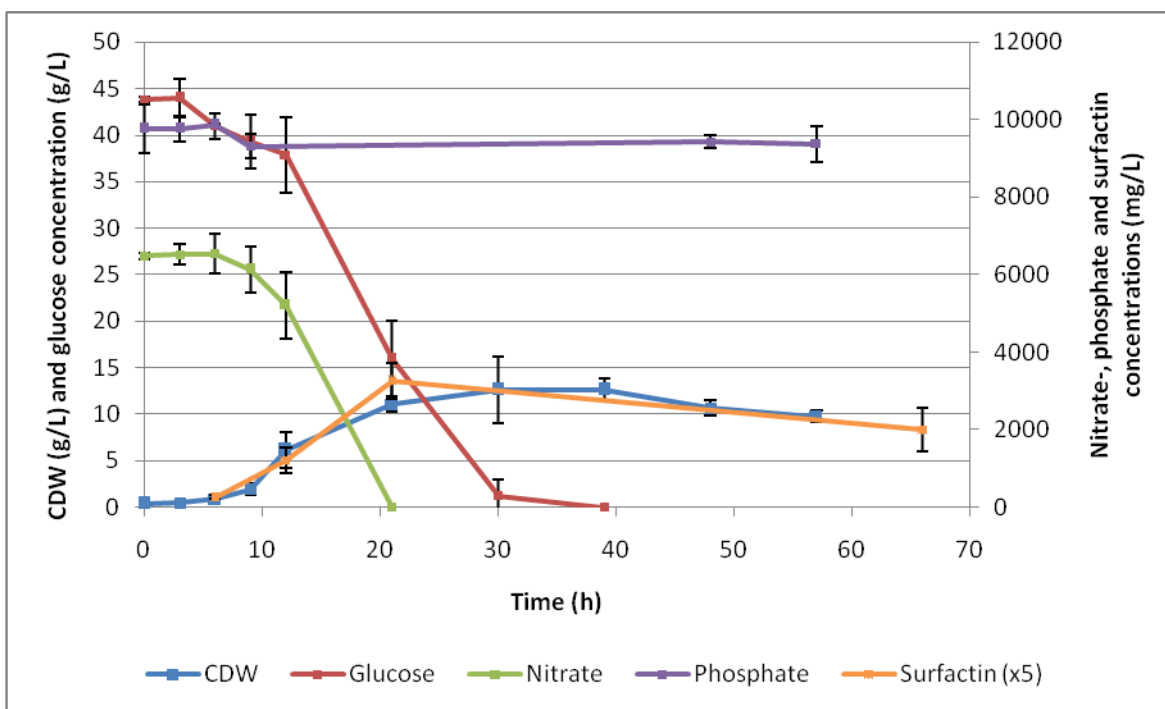


Figure 3-6: Influence of nutrient conditions on growth and surfactin production in medium C

The maximum CDWs and maximum surfactin concentrations achieved in the selected media is shown in Table 3-1. It is shown that the maximum CDW achieved during shake flask culture was achieved in medium C (12.6 g/L), while a relatively high surfactin concentration of 652 mg/L was also achieved in this medium. Although a surfactin concentration of 730 mg/L was achieved in medium B, growth only started after a 30h lag phase. Therefore, medium C has been selected for further bioreactor batch- and fed-batch experiments.

Table 3-1: Maximum CDWs and maximum surfactin concentrations achieved in selected media

| Medium | Max. CDW achieved (g/L) | Maximum surfactin concentration achieved (mg/L) |
|--------|-------------------------|---|
| A | 7.71 | 172 |
| B | 5.09 | 730 |
| C | 12.6 | 652 |

3.1.4 Quantification of cell dry weight and surfactin concentration in alkane media

Growth of *B. subtilis* ATCC 21332 on alkane media was evaluated to establish whether *B. subtilis* ATCC 21332 is able to grow and produce surfactin from alkanes. Since the best results on glucose media were achieved in Medium C, this medium was selected for alkane based experiments. However, glucose in Medium C was replaced by *n*-hexadecane (see section 2.2.1.1) and the concentration of *n*-hexadecane was altered to contain the same amount of carbon atoms as its glucose counterpart.

As depicted in Figure 3-7, *B. subtilis* ATCC 21332 was unable to utilize *n*-hexadecane for growth. The CDW after inoculation was 0.41 g/L and remained at concentrations near 0.40 g/L for 119 hours. These findings are in accordance to that of Kim *et al.* (1997) and Makkar and Cameotra (1997). Since *B. subtilis* ATCC 21332 was unable to utilize *n*-hexadecane for growth, no further analyses were performed on samples.

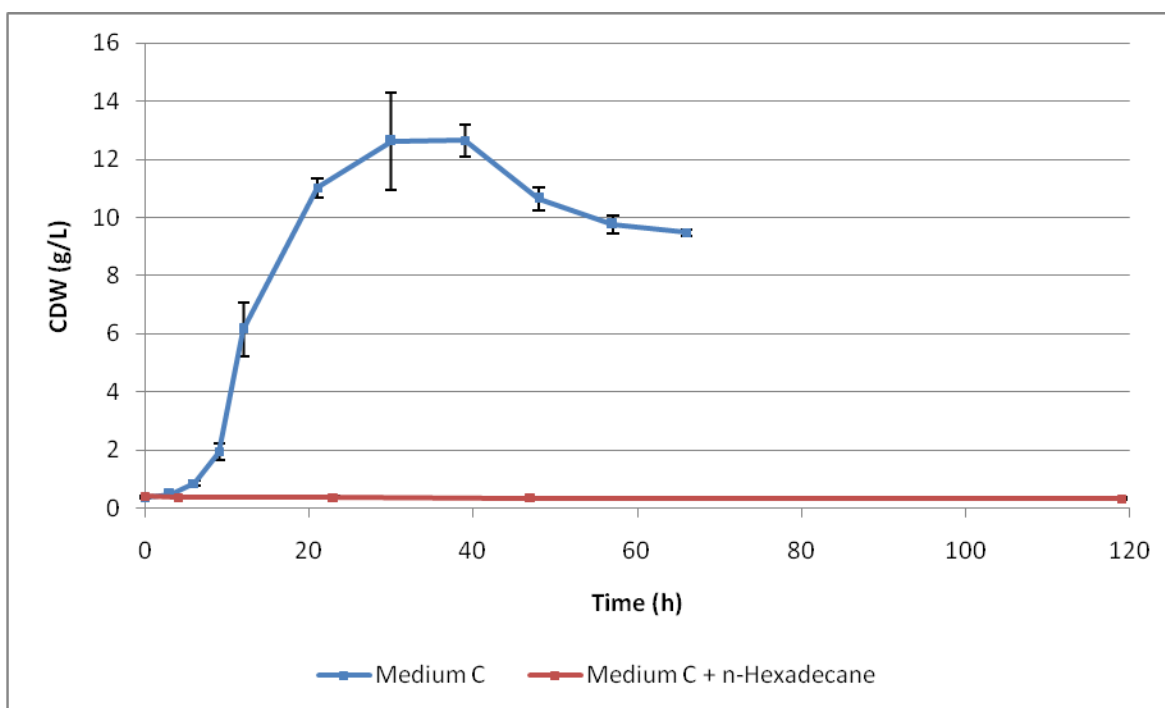


Figure 3-7: Comparison of growth profiles between growth on glucose- and alkane media

3.2 Bioreactor batch culture of *B. subtilis* ATCC 21332

Based on the effect of environmental conditions on growth and surfactin production, and the preferred environmental conditions reported (1.8.2.1), bioreactor batch experiments were performed in an instrumented bioreactor at the following conditions: temperature - 37°C; pH – 6.8; aeration - 0.8 vvm and agitation between 50 - 400 rpm. Bioreactor experiments were performed since the environmental conditions can be rigorously controlled. DO was controlled by agitation to above 10% of the saturation concentration, with only one impeller submerged in the culture broth. Medium C (Table 2-3) was chosen as the most suitable medium for bioreactor experiments, due to its superior performance to the other selected media. The results from the bioreactor batch experiments were used later to develop feeding strategies for fed-batch operation.

The bioreactor experiments were not performed in duplicate as the shake flask studies and therefore, the profiles relating to them are without error bars. However, all bioreactor experiments were started as a batch and as such, the batch phases of the bioreactor batch experiments and those from the fed-batch experiments were all performed under the same conditions. Therefore, the batch phases of the bioreactor experiments will be used to evaluate reproducibility. A dedicated discussion on the reproducibility of experiments is given in section 3.6.

3.2.1 Cell dry weight and surfactin concentration in bioreactor batch culture

Two bioreactor configurations were evaluated for growth and biosurfactant production. In the first reactor configuration, the impeller was situated at the liquid surface to promote surface aeration. In the second configuration, the impeller was situated approximately 50mm below the liquid surface.

The growth and surfactin concentration profiles obtained from the two bioreactor configuration experiments are shown in Figure 3-8. From the gradients of the profiles, it can be seen that growth and surfactin production were superior in the bioreactor with configuration 1, achieving a maximum CDW of 27.0 g/L and a maximum surfactin concentration of 1737 mg/L after 16 and 12 hours of growth respectively. After 16 hours of growth in the bioreactor with configuration 2, a CDW of 5.5 g/L and a surfactin concentration of 401 mg/L were achieved. These concentrations are approximately 5- and 4-fold less than that achieved in the bioreactor with configuration 1, respectively.

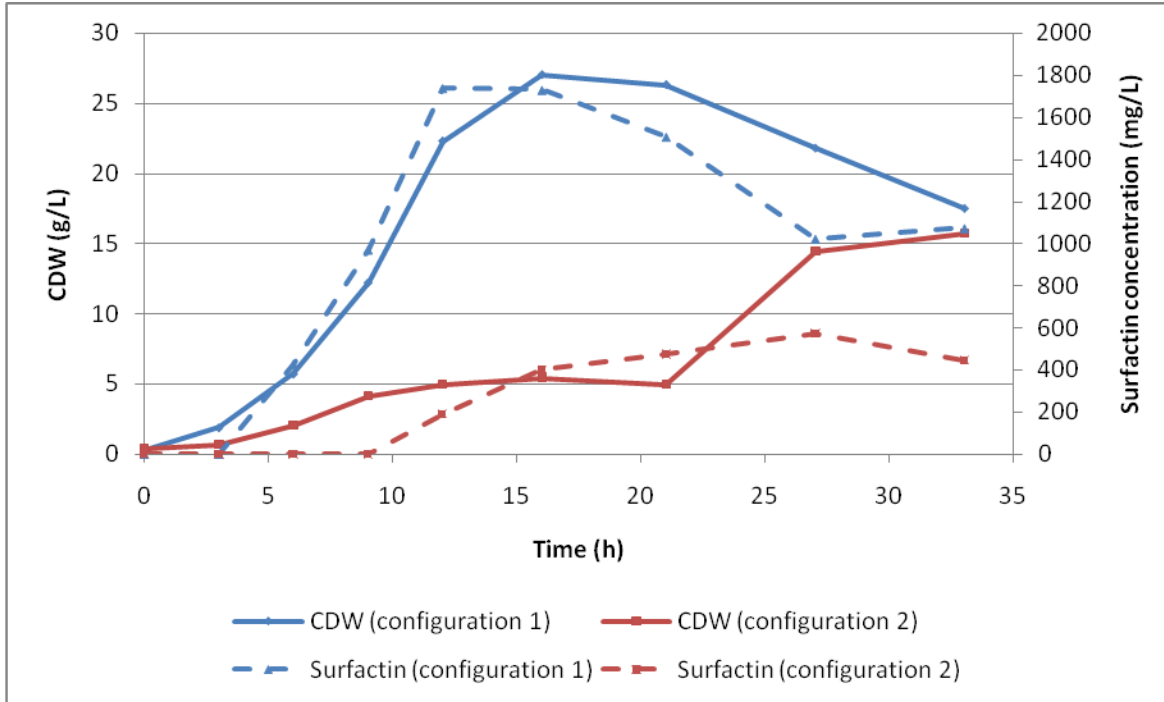


Figure 3-8: CDW profiles of bioreactor batch experiments (configuration 1 and 2)

The reason for the poor growth achieved in the bioreactor with configuration 2 is poor oxygen transfer. The DO profiles obtained from the two bioreactor batch experiments are shown in Figure 3-9. It can be seen that the DO concentration is well maintained at the set-point of 10% for the first 12 hours of growth in the bioreactor with configuration 1. Thereafter, the DO concentration decreased below the 10% set-point as a result of continued growth and the high CDW of 27.0 g/L achieved. However, the DO concentration in the bioreactor with configuration 2 decreased to 0.7% within the first 5 hours of growth, indicating insufficient oxygen transfer. Even though the agitation rate increased to its maximum set-point of 400 rpm, the DO concentration in the bioreactor with configuration 2 remained below 1% of saturation for the duration of the experiment.

A stationary phase between 12 and 21 hours of growth was observed in the bioreactor with configuration 2. This may have been due to the synthesis of enzymes for oxygen-limited growth, since the DO concentration was very low. This is in agreement with the findings of Nakano and Hulett (1997), who reported that a nitrate reductase enzyme was induced under oxygen-limiting conditions. After this stationary phase, the CDW increased from 5.0 g/L to 15.7 g/L between 21 and 33 hours. Despite the increase in the CDW during this period, the surfactin concentration remained approximately 500 mg/L during this period.

Since growth and surfactin production were superior in the bioreactor with configuration 1, it was used for all subsequent bioreactor fed-batch experiments.

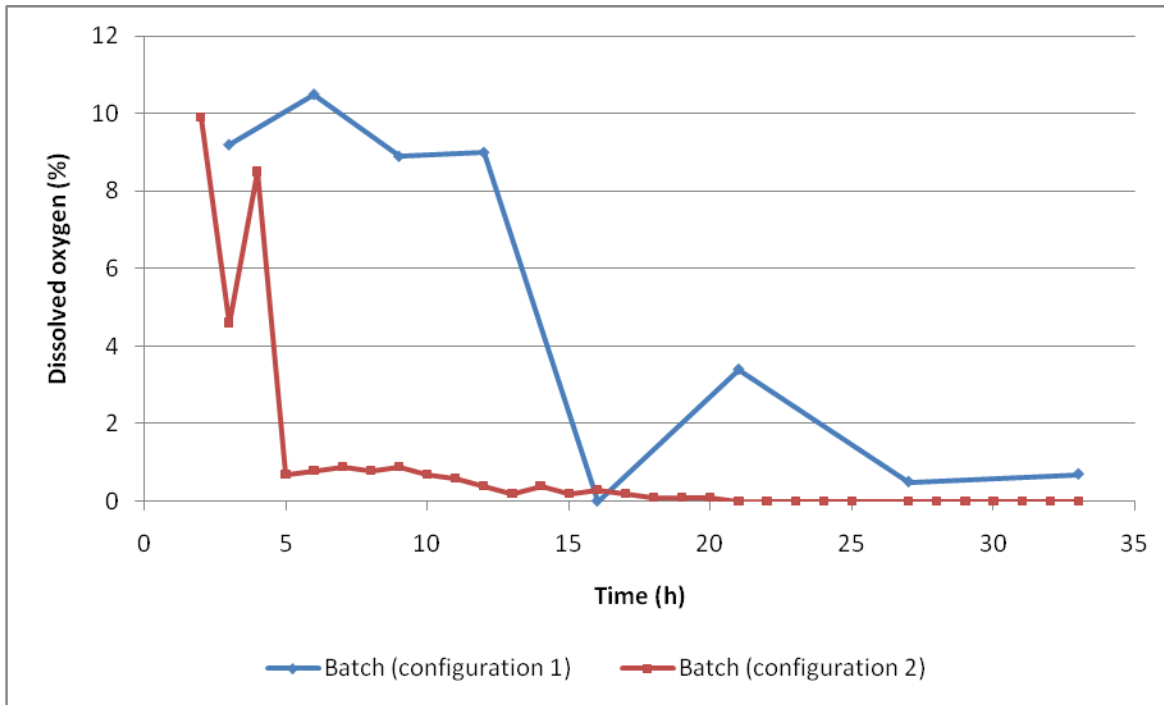


Figure 3-9: Dissolved oxygen concentration profiles of bioreactor batch experiments

3.2.2 Influence of nutrient conditions on cell dry weight and surfactin concentration in bioreactor batch culture

As discussed in section 3.2.1, growth and surfactin production were superior in the bioreactor with configuration 1. A maximum CDW of 27.0 g/L and a maximum surfactin concentration of 1737 mg/L were achieved after 16 and 12 hours of growth respectively. Growth ceased shortly after 16 hours as a result of glucose depletion and the CDW decreased from 27.0 g/L to 17.5 g/L between 16 and 33 hours (Figure 3-10).

Surfactin production ceased after 12 hours of growth in the bioreactor with configuration 1. After 12 hours of growth, the residual glucose concentration was 16.4 g/L, while the nitrate concentration was near depletion (628 mg/L), indicating that the nitrate concentration possibly influenced surfactin production. These results are consistent with the shake flask results of medium C. However, the DO concentration in the bioreactor with configuration 1 decreased from 9% to 0% saturation between 12 and 16 hours, indicating that the DO concentration could also have affected surfactin production. Therefore, it was unclear as to which nutrient, oxygen or nitrate, was the limiting nutrient in the bioreactor with configuration 1.

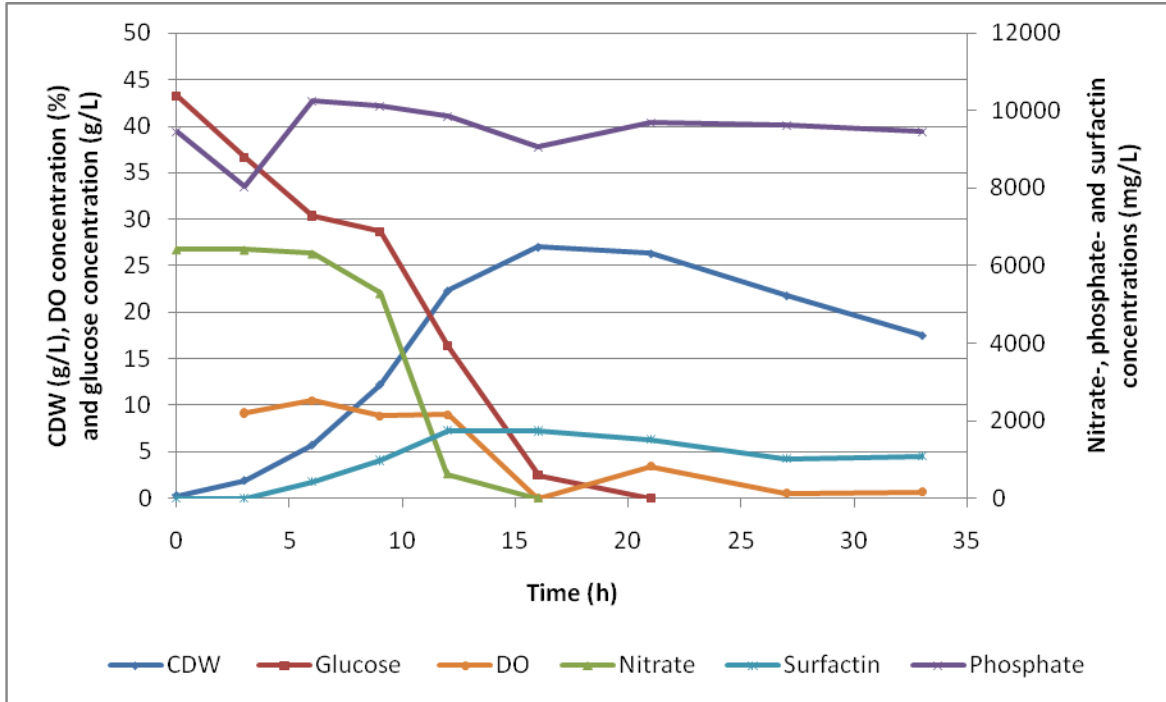


Figure 3-10: Nutrient concentration profiles of batch culture in the bioreactor with configuration 1

By definition, only one nutrient can be the limiting nutrient. Considering the results obtained from the bioreactor with configuration 2, all nutrients were in excess except for oxygen. It can be seen in Figure 3-11 that the DO concentration in the bioreactor with configuration 2 decreased to a concentration below 0.7% of saturation within 5 hours and decreased to even lower values during the experiment. Nitrate and glucose in the bioreactor with configuration 2 were only depleted after 27 and 33 hours of growth respectively. *B. subtilis* was able to grow and produce surfactin under the low oxygen conditions. However, growth and surfactin production under these conditions were inferior to that achieved under oxygen sufficient conditions and therefore, growth and surfactin production was oxygen-limited in the bioreactor with configuration 2.

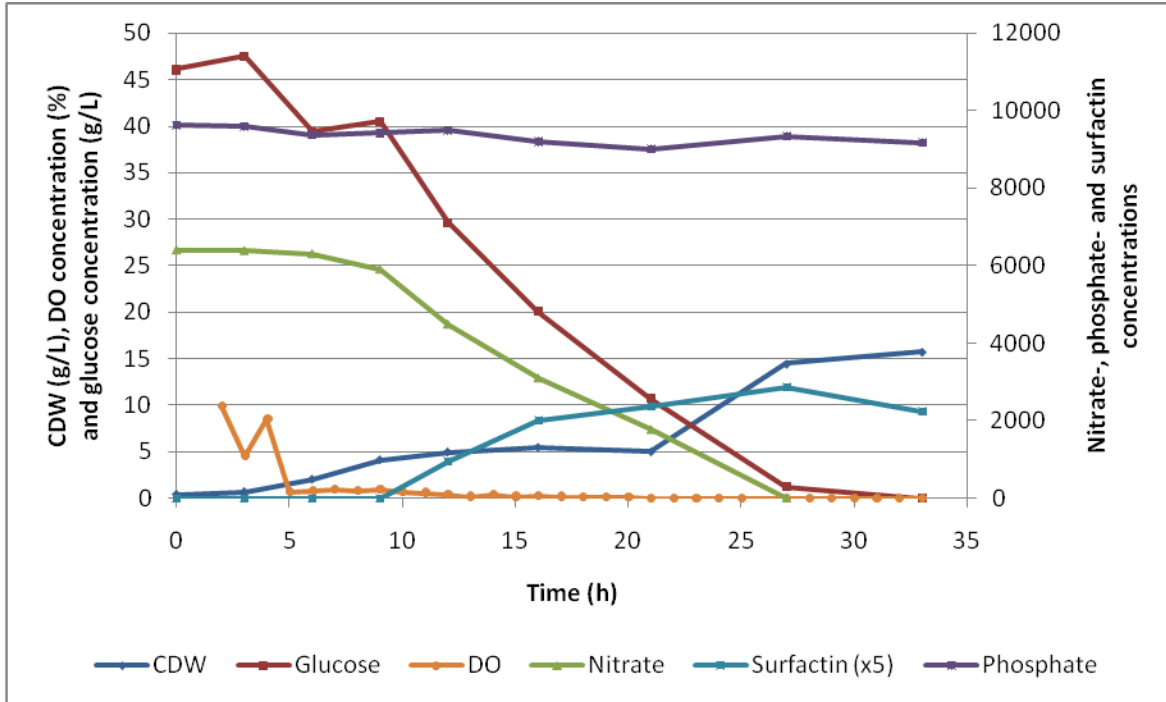


Figure 3-11: Nutrient concentration profiles of batch culture in the bioreactor with configuration 2

3.2.3 Quantification of kinetics parameters of bioreactor batch cultures

3.2.3.1 Specific growth rate

The specific growth rate was calculated from the slope of the natural logarithm profile of $CDW(x \times V)$ (Figure 3-12) according to Equation 3-1 below and is shown graphically in Figure 3-13:

$$\mu = \frac{\ln(x_1 V_1 / x_2 V_2)}{(t_1 - t_2)}$$

Equation 3-1

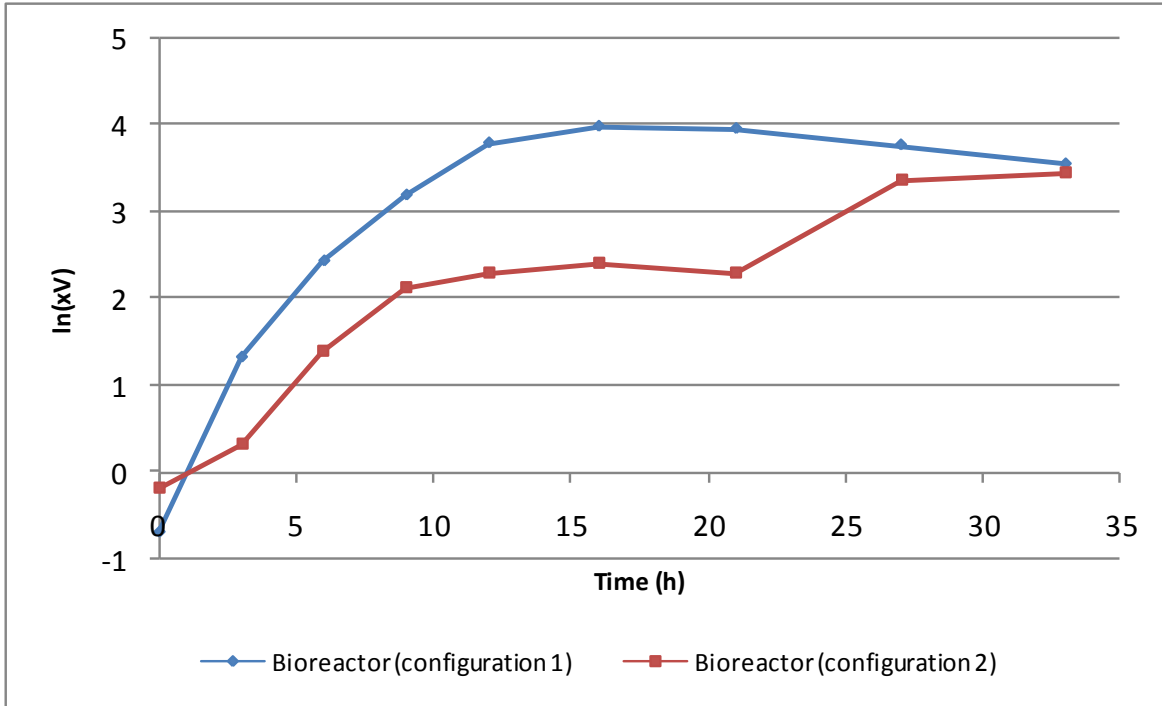


Figure 3-12: $\ln(xV)$ versus time profiles of bioreactor batch experiments

In Figure 3-13 it is shown that after inoculation, the specific growth rate of *B. subtilis* was 0.67 h^{-1} in the bioreactor with configuration 1, while the specific growth rate was less than 0.2 h^{-1} after inoculation in the bioreactor with configuration 2. This difference observed was not a result of any nutrient limitation, but rather a result of variance in the lag time after inoculation. The specific growth rate in the bioreactor with configuration 2 increased to a maximum specific growth rate of 0.36 h^{-1} during the onset of active growth. This maximum specific growth rate was equal to the specific growth rate achieved in the bioreactor with configuration 1 over the same period (3–6 hours). Thereafter, the specific growth rate in the bioreactor with configuration 2 decreased rapidly between 6 and 12 hours as a result of an oxygen-limitation.

A stationary phase was observed between 12 and 21 hours of growth in the bioreactor with configuration 2 and consequently, the specific growth rate decreased from 0.07 h^{-1} to zero during this period. However, between 21 and 27 hours of growth, the specific growth rate increased to 0.18 h^{-1} as a result of oxygen-limited growth. The maximum specific growth rate achieved in the bioreactor with configuration 1 (0.67 h^{-1}) was 2.4- and 1.4 fold higher respectively than that reported by Chen *et al.* (2006) and Kim *et al.* (1997).

These results indicate that an oxygen-limitation severely affects the specific growth rate of *B. subtilis* and consequently affects surfactin production.

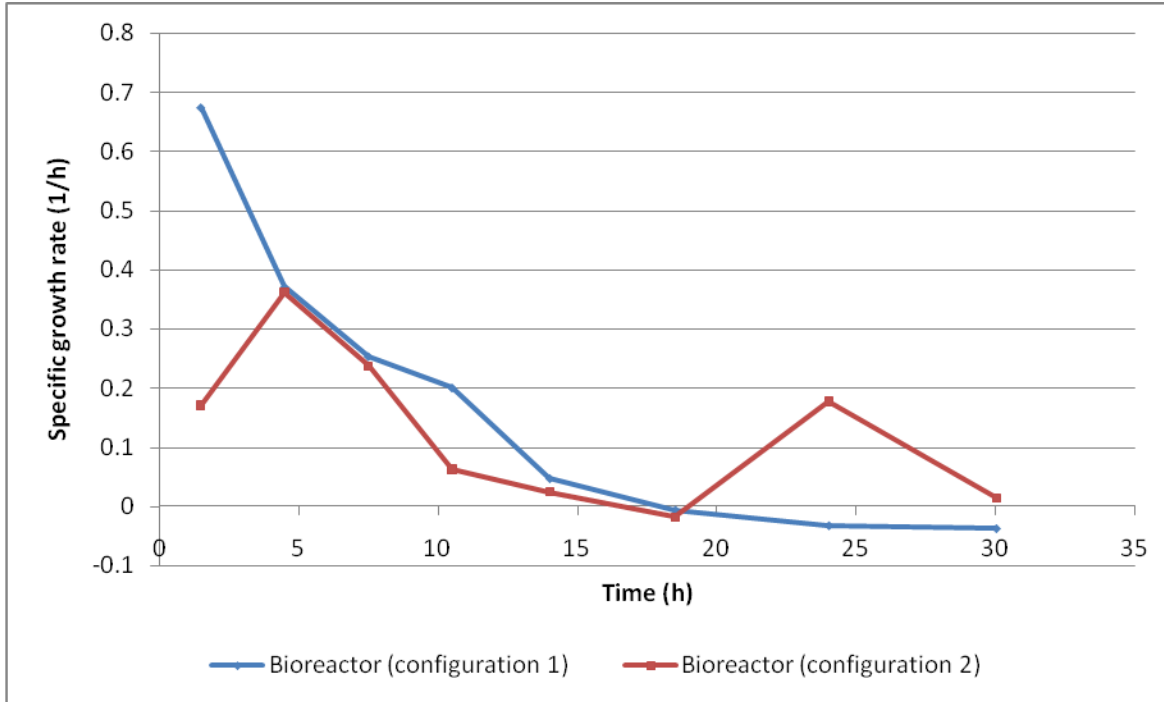


Figure 3-13: Specific growth rate profiles of bioreactor batch experiments

3.2.3.2 Biomass yield on substrate

The biomass yield on substrate indicates the efficiency of the utilization of the substrate for growth. A high biomass yield on substrate would indicate very efficient use of the substrate for growth and *vice versa*. The biomass yield on substrate was calculated by dividing the total increase in CDW (from the time of inoculation into bioreactor to time i) by the total decrease in substrate quantity over the same period and is given by Equation 3-2

$$Y_{x/s} = \frac{X_i - X_0}{S_0 - S_i} \quad \text{Equation 3-2}$$

It can be seen in Figure 3-14 that the biomass yield on glucose was superior in the bioreactor with configuration 1. The biomass yield on glucose increased to a maximum of 0.82 after 12 hours of growth and was to be expected since this period coincided with active growth (Figure 3-8). After 12 hours of growth, the biomass yield on substrate decreased from 0.82 to 0.60 during the stationary phase. The maximum biomass yield on substrate achieved is approximately 3- and 2-fold higher than the biomass yield reported by Chen *et al.* (2006) and Kim *et al.* (1997).

The biomass yield on glucose in the bioreactor with configuration 2 increased to a maximum of 0.67 after 9 hours of growth. Thereafter, the biomass yield on substrate decreased rapidly between 9 and 16 hours as a result of an oxygen limitation (Figure 3-9). During this period, the

CDW marginally increased from 4.12 g/L to 5.47 g/L (Figure 3-8), while the glucose concentration decreased significantly from 40.5 g/L to 20.0 g/L (Figure 3-11). This was probably due to the consumption of glucose for maintenance and the formation of enzymes for oxygen-limited growth (Nakano and Hulett, 1997) due to the low DO concentration. The biomass yield on glucose increased to 0.33 between 21 and 33 hours of growth, indicating a much lower biomass yield on glucose during oxygen limited growth when compared to the 0.82 achieved under oxygen sufficient conditions (configuration 1).

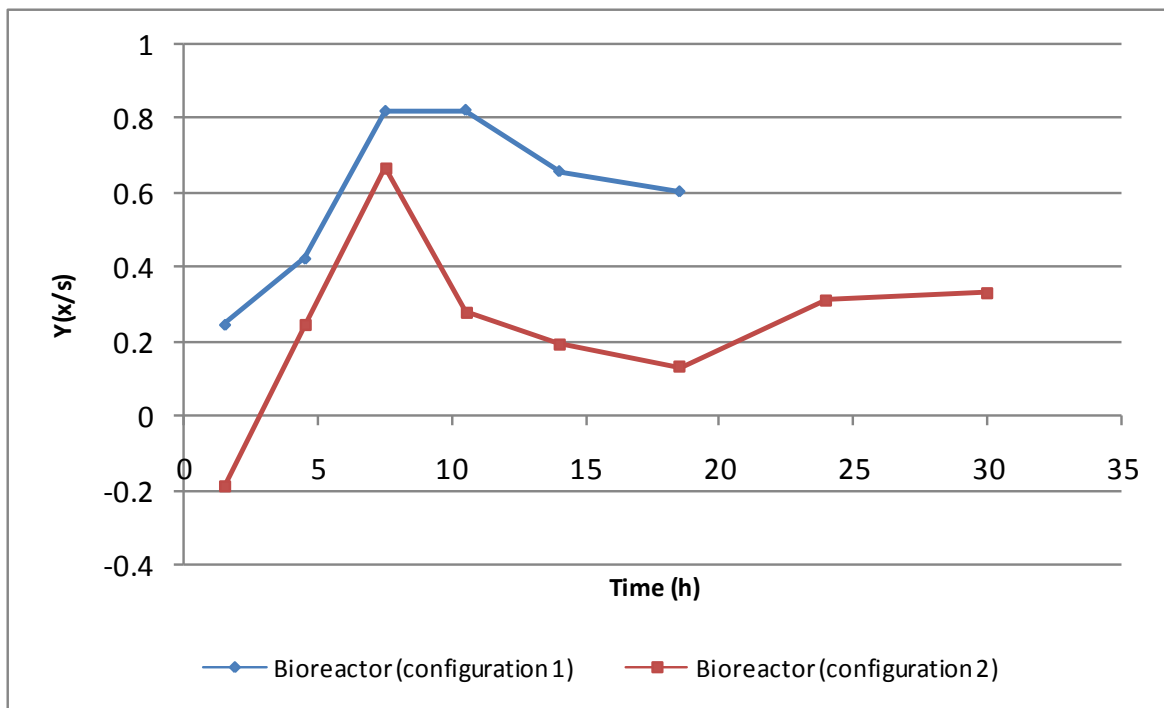


Figure 3-14: Biomass yield on glucose profiles of bioreactor batch experiments

3.2.3.3 Surfactin yield on substrate

In order to select an appropriate process strategy for surfactin production, one of the important kinetic parameters to consider is the surfactin yield on substrate. A high surfactin yield on substrate would indicate very efficient use of the substrate for surfactin synthesis, whereas a low surfactin yield on substrate would indicate the opposite. By evaluating the surfactin yield on substrate, it can be deduced whether the substrate being used is effective for product formation or not.

The surfactin yield on substrate was calculated according to Equation 3-3:

$$Y_{P/S} = \frac{P_i - P_0}{S_0 - S_i}$$

Equation 3-3

The surfactin yield on substrate was calculated by dividing the total surfactin increase (from the time of inoculation into bioreactor to time i) by the total decrease in substrate quantity over the same period. The surfactin yield on glucose profiles of the bioreactor batch experiments are shown in Figure 3-15 and it is evident that the surfactin yield on glucose was superior in the bioreactor with configuration 1. The surfactin yield on glucose increased to a maximum of approximately 0.07 (i.e. 7% (w/w) of the glucose was converted to surfactin) between 6 and 9 hours and coincided with the active growth phase (Figure 3-8). Thereafter, the surfactin yield on glucose decreased as a result of a significant decrease (from 0.20 h^{-1} to 0.048 h^{-1}) in the specific growth rate (Figure 3-13). The surfactin yield on substrate further decreased after 16 hours as a result of glucose depletion (Figure 3-10). After glucose depletion, the surfactin concentration decreased from 1728 mg/L to 1072 mg/L between 16 and 33 hours. One of the physiological roles of biosurfactants has been reported to be energy storage (van Hamme *et al.*, 2006) and the decrease in the surfactin concentration may have been as a result of it being used as substrate. However, further research is required to confirm the use of surfactin as an energy storage molecule.

The surfactin yield on glucose in the bioreactor with configuration 2 only marginally increased between 9 and 16 hours of growth, which coincided with the onset of the stationary phase (Figure 3-8). A maximum surfactin yield on glucose of only 0.015 was achieved with this configuration, which was approximately 4.4-fold less than that achieved in the bioreactor with configuration 1. The low surfactin yield on substrate achieved in the bioreactor with configuration 2 was a result of the oxygen-limitation during this experiment (Figure 3-9).

The surfactin yields on glucose achieved in this study (configuration 1) compared well with the 0.076 and 0.046 reported by Kim *et al.* (1997) and Chen *et al.* (2006) respectively. Moreover, these results further indicate that the surfactin yield on glucose is superior under oxygen sufficient conditions.

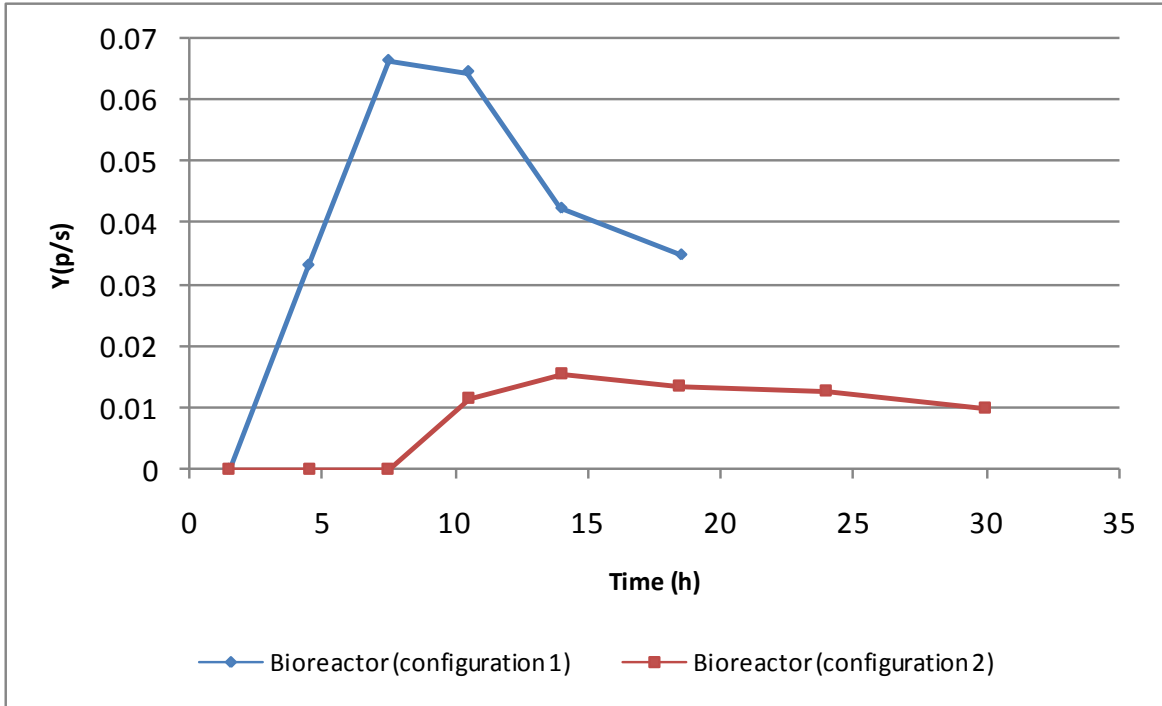


Figure 3-15: Surfactin yield on glucose ($Y_{p/s}$) profiles of bioreactor batch experiments

3.2.3.4 Surfactin yield on biomass

The surfactin yield on biomass indicates the amount of surfactin produced (g) per gram of cells formed. The surfactin yield on biomass was calculated by dividing the total surfactin increase (from the time of inoculation into bioreactor to time i) by the total increase in CDW over the same period, and is mathematically expressed by Equation 3-4.

$$Y_{P/X} = \frac{P_i - P_0}{X_i - X_0}$$

Equation 3-4

The surfactin yield on biomass increased to a maximum of 0.081 during the active growth phase in the bioreactor with configuration 1 (Figure 3-16). However, no surfactin was produced during the active growth phase in the bioreactor with configuration 2. Surfactin was only produced from the onset of the stationary phase, where the surfactin yield on biomass increased to approximately 0.1. Similar results have been found for growth of *B. subtilis* under phosphate-limiting conditions (see section 3.1.3.2). Although the surfactin yield on biomass was higher under oxygen-limiting conditions, the total amount of surfactin produced under these conditions was approximately 4-fold less than that achieved under oxygen-sufficient conditions. However, further research is required on the enhanced surfactin yield on biomass under nutrient-limiting conditions.

The surfactin yields on biomass achieved in this study compared well to the 0.071 reported by Chen *et al.* (2006). However, the surfactin yield on biomass of 0.38 reported by Kim *et al.* (1997) is greater than the results of this study. The surfactin yield on biomass reported by Kim *et al.* (1997) was achieved for growth under oxygen-limiting conditions. Therefore, more research on surfactin production under nutrient-limiting conditions is required to quantify the underlying mechanisms of surfactin production under these conditions.

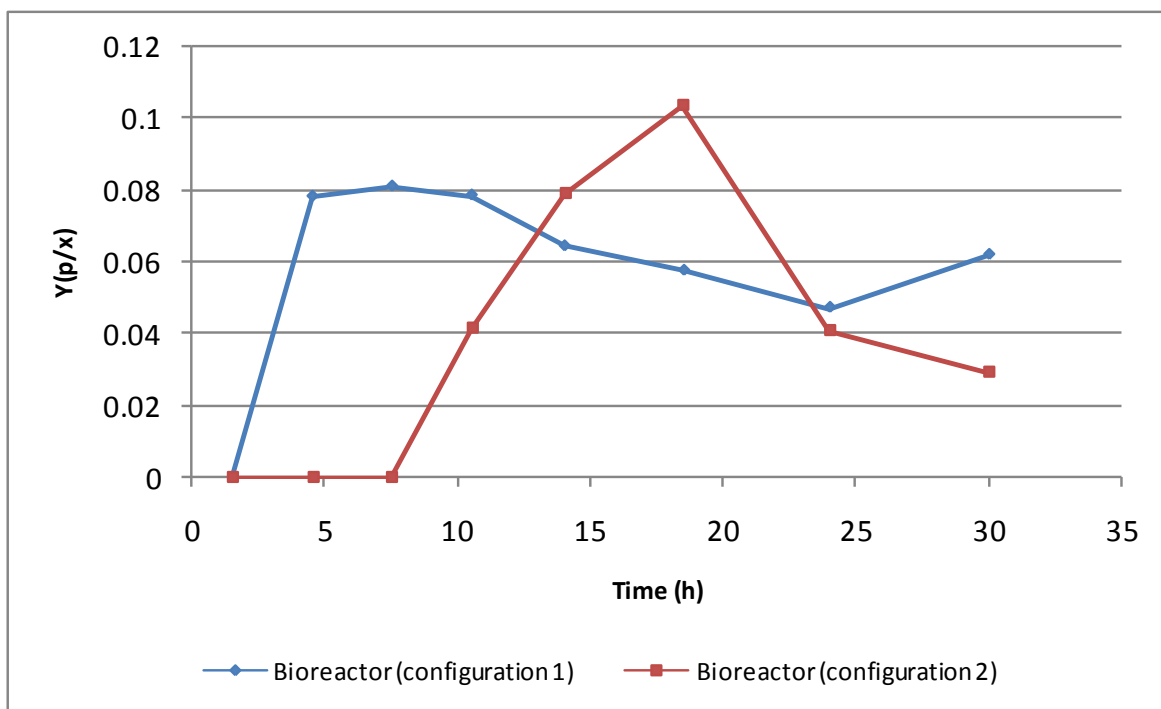


Figure 3-16: Surfactin yield on biomass profiles of bioreactor batch experiments

3.2.3.5 Surfactin productivity and specific productivity

Productivity and specific productivity indicate the rate of product formation and are key parameters in selecting a process strategy for improved process economics. Surfactin productivity increased rapidly to a maximum productivity of 255 mg/L/h during the active growth phase in the bioreactor with configuration 1 (Figure 3-17). Thereafter, surfactin production ceased as the organism entered the stationary phase after 12 hours of growth, indicating that surfactin production is growth-associated.

Since surfactin production only started after 9 hours of growth in the bioreactor with configuration 2, surfactin productivity remained zero during this period. Surfactin productivity increased to a maximum of 63 mg/L/h between 9 and 12 hours, which was 4-fold less than that achieved in the bioreactor with configuration 1. Thereafter, surfactin productivity decreased to approximately 15 mg/L/h during the observed stationary phase between 12 and 21 hours and became negative after 21 hours of growth as a result of glucose depletion. The difference

between the maximum surfactin productivities achieved is a result of the difference in the achieved cell densities of the two bioreactors.

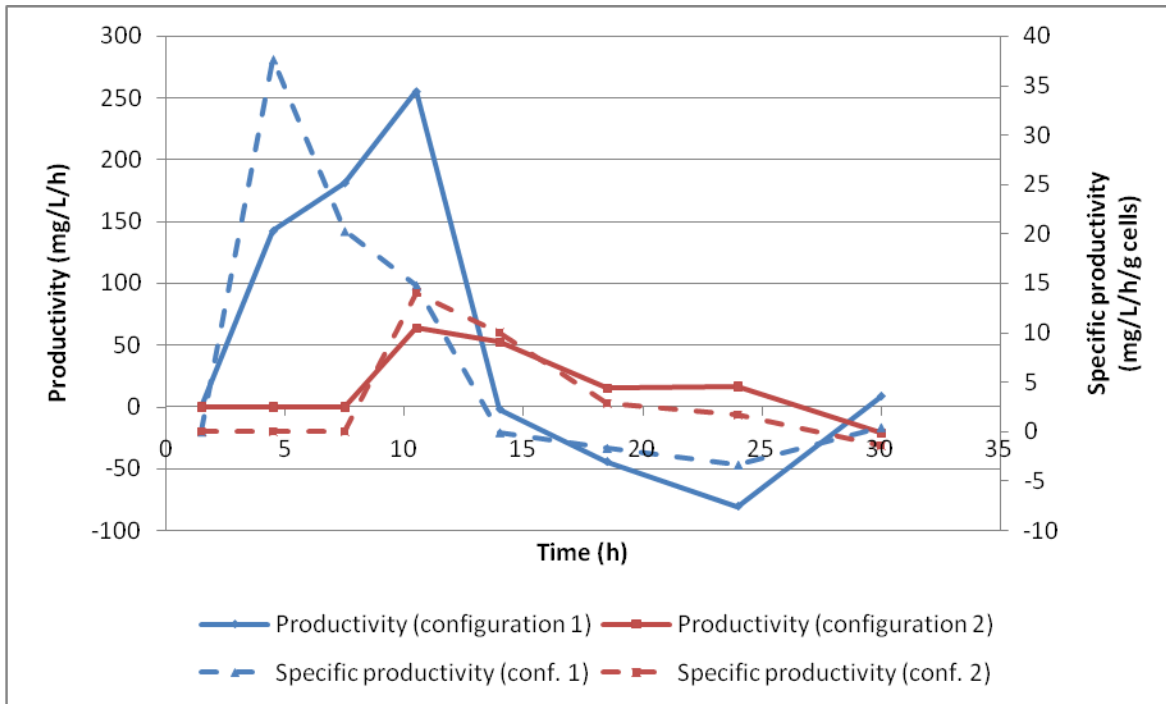


Figure 3-17: Surfactin productivity and specific productivity profiles of bioreactor batch experiments

It is evident from Figure 3-17 that the specific surfactin productivity was greater during the active growth phase when compared to that achieved during the stationary phase. The specific surfactin productivity in the bioreactor with configuration 1 reached a maximum of $38 \text{ mg/L/h/g}_{\text{cells}}$ between 3 and 6 hours of growth. Thereafter, the specific surfactin productivity decreased steadily between 6 and 12 hours, but was still higher than the maximum specific surfactin productivity ($14 \text{ mg/L/h/g}_{\text{cells}}$) achieved in the bioreactor with configuration 2.

The maximum specific surfactin productivity of $14 \text{ mg/L/h/g}_{\text{cells}}$ was achieved between 9 and 12 hours in the bioreactor with configuration 2, and coincided with the onset of the stationary phase. Since all nutrients except oxygen were in excess during the first 12 hours, these results indicate that surfactin productivity and specific productivity is severely influenced by an oxygen limitation. Therefore, the specific surfactin productivity of *B. subtilis* is greater during the active growth phase under oxygen-sufficient conditions when compared to oxygen-limited conditions.

3.2.4 Comparison of cell dry weight and surfactin concentration between bioreactor batch- and shake flask studies

Growth and surfactin production in the bioreactor with configuration 1 was greater than the growth and surfactin production in shake flask experiments (Figure 3-18). The maximum CDW achieved in the bioreactor with configuration 1 was twice the maximum CDW achieved in shake flask studies and was achieved in half the time. Similarly, the maximum surfactin concentration achieved in the bioreactor with configuration 1 was approximately 2.5-fold higher than that achieved in shake flasks.

These results indicate that high CDWs and surfactin concentrations can be achieved under improved conditions (especially w.r.t. oxygen transfer) in instrumented bioreactors. Moreover, enhanced growth and surfactin production can be achieved over smaller periods of time in instrumented bioreactors, thus indicating higher biomass and surfactin productivities.

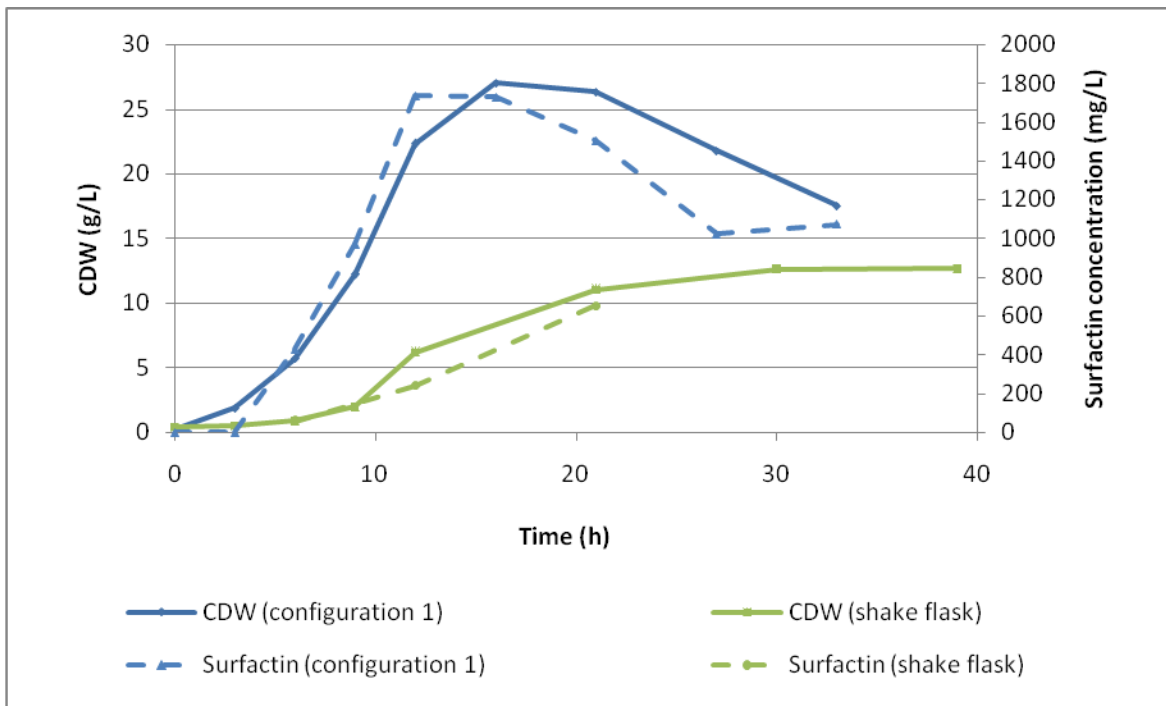


Figure 3-18: Comparison of growth and biosurfactant production in shake flasks and bioreactor

3.2.5 Comparison of nutrient concentrations between bioreactor batch- and shake flask studies

The glucose- and nitrate concentration profiles of the bioreactor batch and shake flask studies are given in Figure 3-19 below. It is evident that glucose and nitrate were consumed at a higher

rate during bioreactor culture. Nitrate was depleted after 16 hours and glucose after 21 hours in the bioreactor, while these nutrients were depleted after 21 and 39 hours respectively during shake flask culture. The reason for the significant difference observed in the nutrient profiles is the difference in CDW achieved in the bioreactor and shake flasks respectively. These results correspond to a higher cell growth rate, and hence higher nutrient rate in the bioreactor compared with shake flask culture.

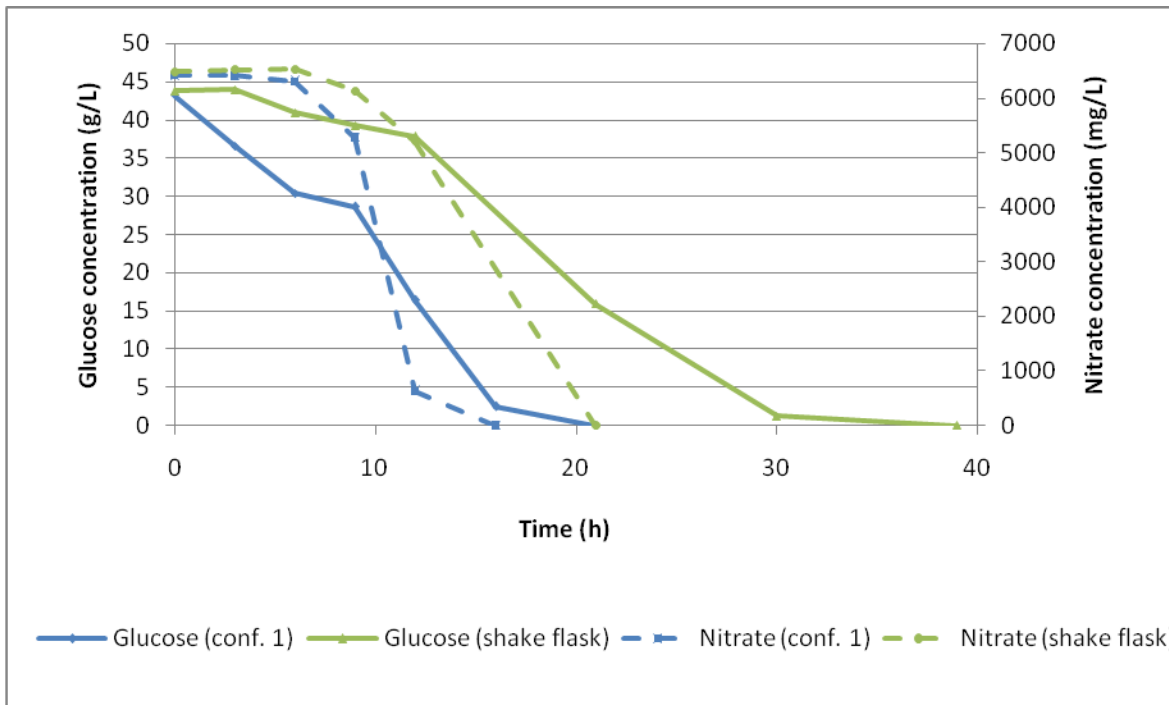


Figure 3-19: Comparison of glucose- and nitrate concentration profiles between bioreactor batch and shake flask studies

Since surfactin production is influenced by the availability of nitrate and glucose, the addition of these nutrients to the culture broth could possibly enhance surfactin production. It has already been shown in section 3.1.2 that surfactin production is growth associated and enhanced surfactin production may result by extending the active growth phase of *B. subtilis* ATCC 21332. Therefore, fed-batch operation would be a suitable option to extend the active growth phase of *B. subtilis* ATCC 21332 by the addition of fresh nutrients as soon after they are depleted during batch growth.

A concentrated medium should be added at the end of a batch culture (fed-batch) to stimulate growth and consequently surfactin production. A concentrated medium is required since the nutrient concentrations are very low at the end of a batch culture and usually the substrate is depleted. Moreover, the cell concentration is usually at a maximum at the end of a batch culture, which means that there would be a very high demand for fresh nutrients.

The concentration of the feed during fed-batch culture is not the only factor governing the quantity of nutrients entering the reactor, but also the flow rate of the feed stream. These two factors (concentrations of nutrients and feed flow rate) ultimately control the fed-batch culture kinetics. In section 3.3 below the fed-batch culture of *B. subtilis* ATCC 21332 is discussed, with particular emphasis on the effect of the feed flow rate on growth and surfactin production and also its effect on *B. subtilis* culture kinetics.

3.3 Bioreactor fed- batch culture of *B. subtilis* ATCC 21332

Bioreactor fed-batch experiments were performed in order to evaluate whether active growth of *B. subtilis* could be sustained and consequently sustain the production of surfactin when additional nutrients are supplied at the end of a batch culture. Four constant dilution rate- and two constant flow rate predetermined feeding strategies were applied during fed-batch culture (see Table 2-6). These feeding strategies were selected to evaluate the effect of different feeding strategies on growth and surfactin production during fed-batch culture.

Fed-batch experiments were performed under the same environmental conditions as the bioreactor batch experiments. Since growth and surfactin production was superior in the bioreactor with configuration 1, fed-batch experiments were performed with the same configuration, the only difference being the addition of a sterile feed to the bioreactor during fed-batch culture. The composition of the feed stream was that of Medium C; however, the concentration of each component was double the concentrations given in Table 2-3.

All fed-batch cultures were started as a batch culture (0-12 hours) and feeding only started at the onset of the stationary phase (after 12 hours of batch growth).

3.3.1 Quantification of cell dry weight and surfactin concentration in constant dilution rate fed-batch experiments

The four different dilution rates that were evaluated for growth and surfactin production during fed-batch culture of *B. subtilis* were 0.40 h^{-1} , 0.15 h^{-1} , 0.10 h^{-1} and 0.05 h^{-1} . The selected dilution rates were maintained by applying four different exponential feeding strategies.

The CDW profiles of the constant dilution rate fed-batch experiments are shown in Figure 3-20. The CDW profiles of the batch phases of the fed-batch experiments (0-12 hours in Figure 3-20) are very similar and show good reproducibility (see section 3.6). The average CDW achieved after 12 hours of batch culture was 24.7 g/L (Figure 3-20) and compared well to the CDW of 22.4 g/L achieved after 12 hours in the batch (bioreactor configuration 1) experiment (Figure 3-8). These CDWs are superior to all CDWs reported in literature regarding surfactin production

by *B. subtilis*, which range from approximately 2 g/L to 9 g/L (Kim *et al.*, 1997; Makkar and Cameotra, 1997; Davis *et al.*, 1999; Cooper *et al.*, 1981), and is twice as high as that reported by Fernandes *et al.* (2007).

It is evident from Figure 3-20 that the CDWs decreased during the fed-batch phases (from 12 hours) with the magnitude of the decrease dependant of the specific dilution rate applied. The higher flow rate range of the $D=0.40\text{h}^{-1}$ experiment showed the fastest decrease in CDW, while the slowest decrease in CDW was observed in the 0.05h^{-1} experiment. The CDW decreased from 23.4 g/L to 13.5 g/L within 3 hours during the fed-batch phase of the $D=0.40\text{h}^{-1}$ experiment, while a similar decrease in CDW took more than 14 hours during the fed-batch phase of the $D=0.05\text{h}^{-1}$ experiment.

A cell balance during fed-batch culture would yield the following equation (see Appendix A: Fed-batch Kinetics

$$\frac{dx}{dt} = x(\mu - D) \quad \text{Equation 3-5}$$

Since the CDWs decreased during the fed-batch phases, the specific growth rate was less than the selected dilution rates according to Equation 3-5 (see section 3.3.4.1). The specific growth rate is a function of the limiting substrate, and assuming that growth follows Monod kinetics, this relationship is expressed by the following equation:

$$\mu = \frac{\mu_{\max} s}{K_s + s} \quad \text{Equation 3-6}$$

During fed-batch culture, the volume of the culture broth increases according to the applied dilution rate (if a continuous feed is supplied). If the applied dilution rate is higher than the specific growth rate as governed by the limiting substrate, the cell concentration would decrease (see Appendix A: Fed-batch Kinetics). Therefore, the results of the fed-batch phases in Figure 3-20 indicated that a limiting nutrient caused the specific growth rate to decrease to less than the applied dilution rate (see sections 3.3.3 and 3.3.4.1)

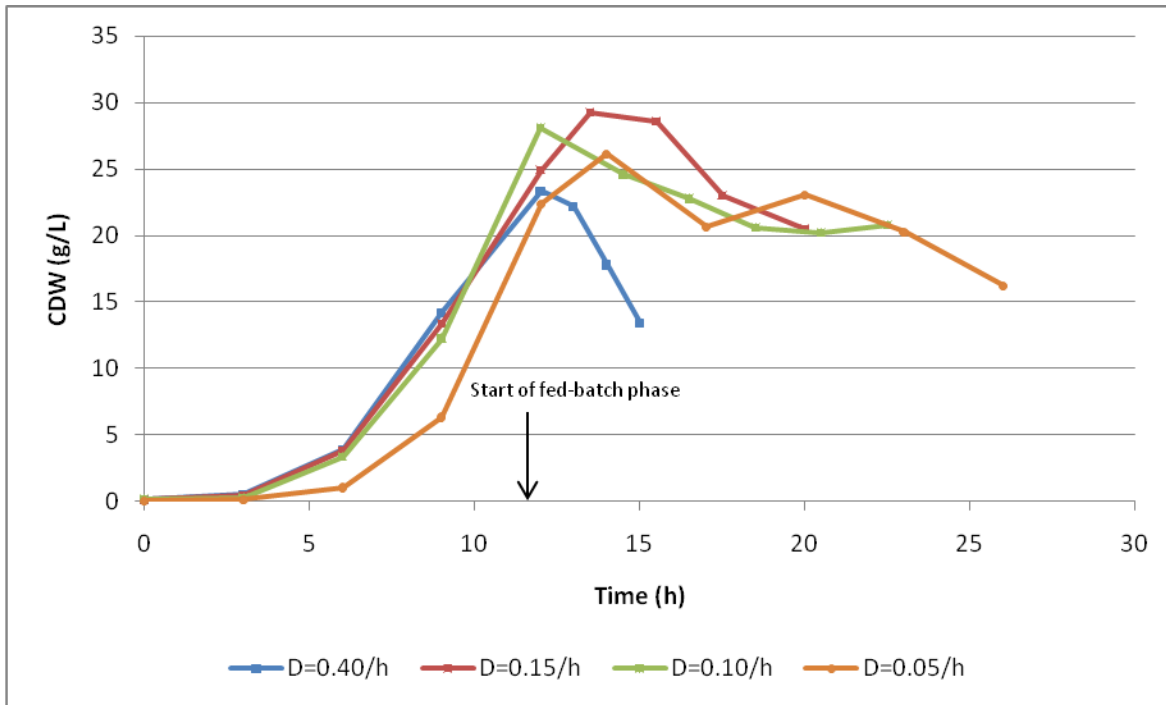


Figure 3-20: CDW profiles of fed-batch cultures (from 12 hours) during which exponential feeding strategies were applied

Although the CDWs decreased during the fed-batch phases, the total biomass (CDW x Volume) increased during the fed-batch phases (Figure 3-21). This indicated that active growth of *B. subtilis* was maintained during the fed-batch phases. The most significant biomass increases occurred in the $D=0.40\text{h}^{-1}$ and $D=0.15\text{h}^{-1}$ experiments. The biomass increased by 58.1% and 51.7% respectively between 12 and 15 hours in the $D=0.40\text{h}^{-1}$ and $D=0.15\text{h}^{-1}$ experiments. The biomass increases in the $D=0.10\text{h}^{-1}$ and $D=0.05\text{h}^{-1}$ were 18.6% between 12 and 16.5 hours and 23.6% between 12 and 17 hours respectively.

Unfortunately, the $D=0.40\text{h}^{-1}$ experiment was limited by the reactor volume after 15 hours, which meant that the experiment could not be extended beyond 15 hours. The $D=0.15\text{h}^{-1}$ experiment was extended for a further 4.5 hours to 20 hours, but no further biomass increase was observed during this period. The $D=0.10\text{h}^{-1}$ was limited by the reactor volume after 22.5 hours and reached a total biomass of 93 g, 25 g higher than that achieved in the $D=0.05\text{h}^{-1}$ experiment over the same period. These results indicate that the rate of biomass increase increases with the dilution rate (see section 3.3.4.1)

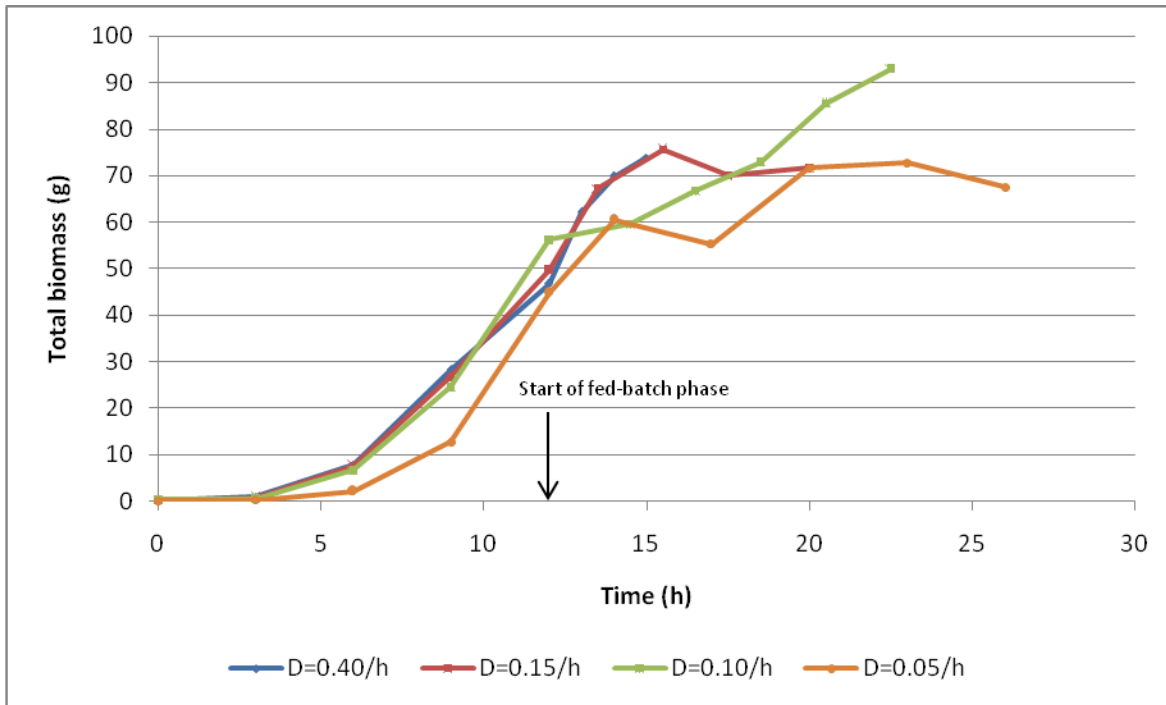


Figure 3-21: Total biomass profiles of fed-batch cultures during which exponential feeding strategies were applied

Active growth of *B. subtilis* was accompanied by surfactin production during all fed-batch experiments. The surfactin concentration profiles were very similar to the CDW profiles. The surfactin concentrations increased rapidly during the batch phases of the fed-batch experiments, and reached an average surfactin concentration of 1918 mg/L at the end of the batch phases. The surfactin concentrations achieved during the batch phases of the fed-batch experiments presented here compared well to the 1737 mg/L achieved during the bioreactor batch experiment (Figure 3-8).

Analogous to CDW, the surfactin concentrations also decreased during the fed-batch phases at a rate proportional to the applied dilution rate (Figure 3-22). The fastest decrease in the surfactin concentration was observed in the $D=0.40\text{h}^{-1}$ experiment, while the slowest decrease in surfactin concentration occurred in the $D=0.05\text{h}^{-1}$ experiment.

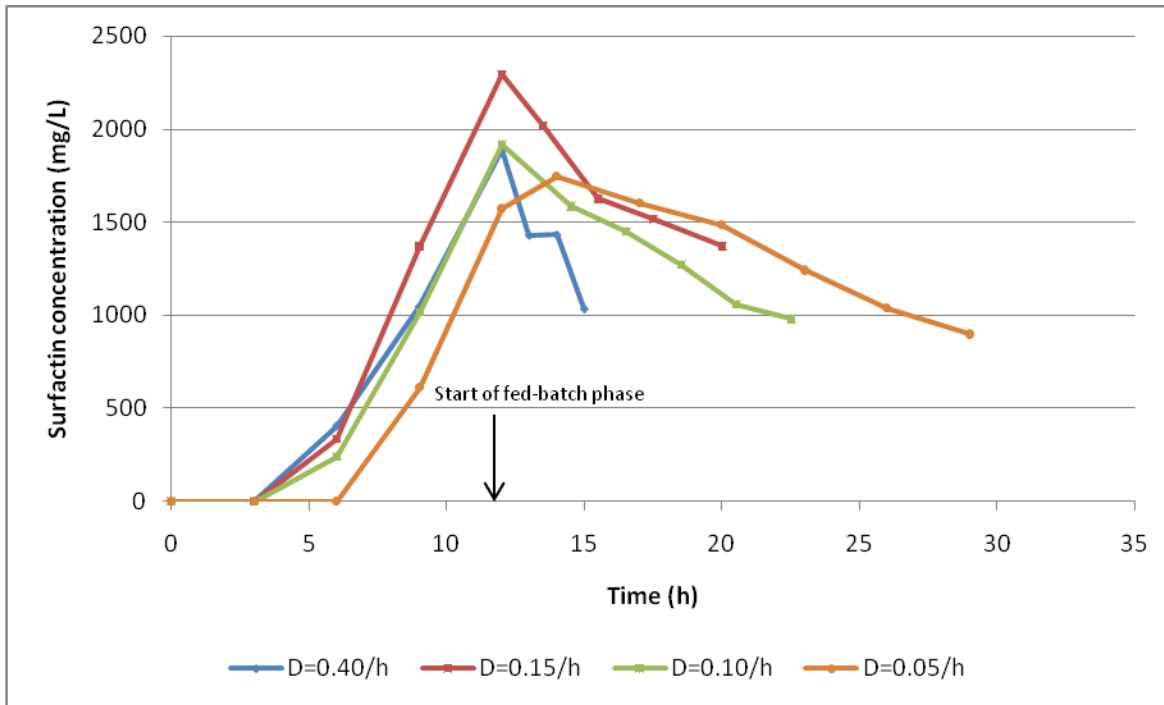


Figure 3-22: Surfactin concentration profiles of fed-batch cultures during which exponential feeding strategies were applied

Although the surfactin concentrations decreased, the total amounts of surfactin (surfactin concentration \times volume) increased during the fed-batch phases and were a direct result of the achieved biomass increase (Figure 3-23). The most significant surfactin increase occurred in the $D=0.40\text{h}^{-1}$ experiment, where the total amount of surfactin increased from 3775 mg to 5675 mg between 12 and 15 hours. This increase is equivalent to 50.3% and was achieved in only three hours. The total amount of surfactin increased only marginally from 4587 mg to 4795 mg (4.5%) between 12 and 20 hours in the $D=0.15\text{h}^{-1}$ experiment. The total surfactin increased from 3838 mg to 5084 mg between 12 and 22.5 hours in the $D=0.10\text{h}^{-1}$ experiment, while an increase from 3492 mg to 3981 mg was observed between 12 and 17 hours in the $D=0.05\text{h}^{-1}$ experiment. These results indicate that surfactin production by *B. subtilis* can be sustained as a result of active growth during fed-batch culture. Moreover, the average rate of surfactin production increases with an increase in the dilution rate, and is proportional to the average rate of biomass increase (see section 3.3.2).

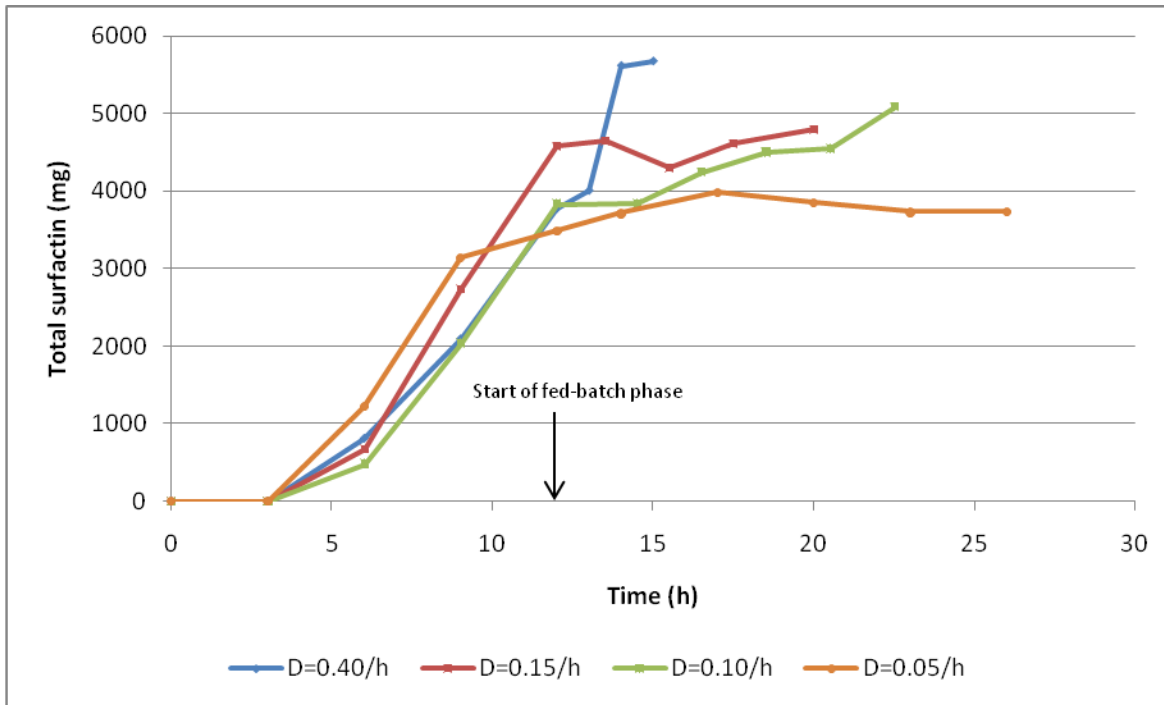


Figure 3-23: Total surfactin profiles of fed-batch cultures during which exponential feeding strategies were applied

3.3.2 Comparison of rate of total biomass- and rate of total surfactin increase in constant dilution rate fed-batch experiments

In Figure 3-24, it can be seen that a high constant dilution rate strategy is superior to low constant dilution rate strategies in terms of amount of cells and surfactin produced. However, it can be seen in Figure 3-20 and Figure 3-22 that a high constant dilution rate strategy is inferior to low constant dilution rate strategies in terms of cell- and surfactin concentrations. The average rate of biomass increase and average rate of surfactin production were calculated as the difference in the total biomass and total surfactin achieved during the fed-batch phase respectively, and was divided by the duration of the fed-batch phase. These are shown in Figure 3-24.

The average rate of biomass increase was 3.5-, 3.1- and 5.3-fold higher during the fed-batch phase of the $D=0.40\text{h}^{-1}$ experiment compared to the fed-batch phases of the $D=0.15\text{h}^{-1}$, $D=0.10\text{h}^{-1}$ and $D=0.05\text{h}^{-1}$ experiments respectively. The average rate of surfactin production was 29.4-, 5.4- and 34.2-fold higher during the fed-batch phase of the $D=0.40\text{h}^{-1}$ experiment compared to the fed-batch phases of the $D=0.15\text{h}^{-1}$, $D=0.10\text{h}^{-1}$ and $D=0.05\text{h}^{-1}$ experiments respectively. These findings indicate that a high constant dilution rate could be applied as a process strategy for enhanced cell and surfactin production during fed-batch culture.

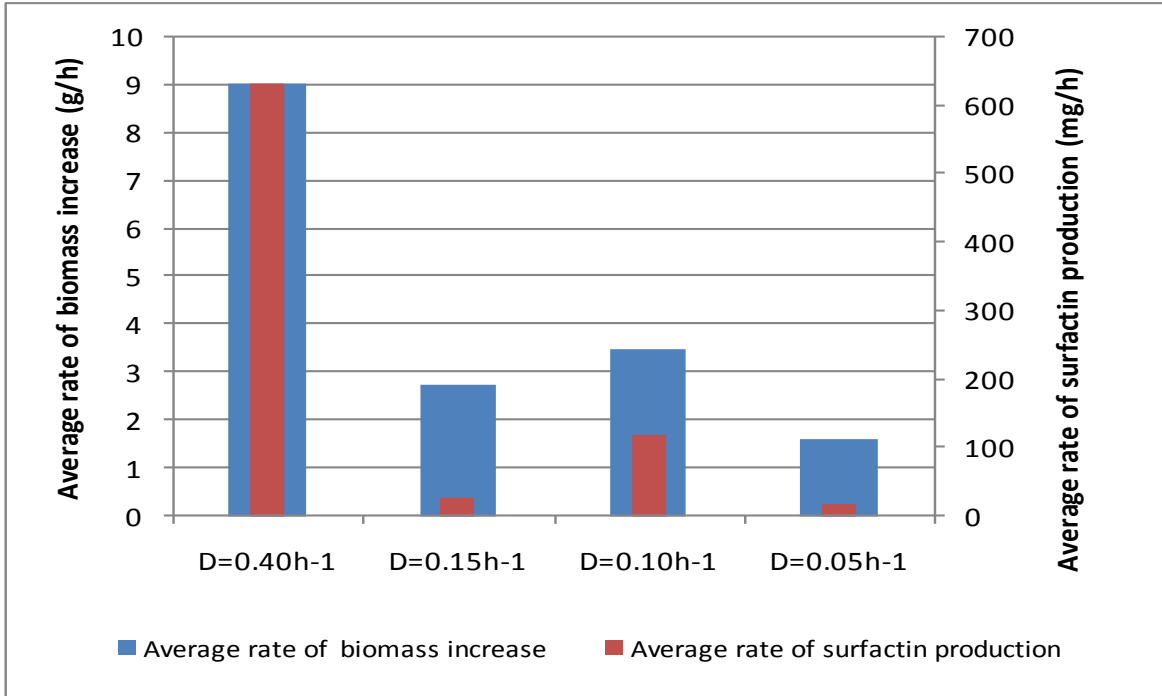


Figure 3-24: Average rate of biomass increase and average rate of surfactin production during fed-batch phases of constant dilution rate fed-batch experiments

3.3.3 Influence of nutrient conditions on cell dry weight and surfactin concentration in constant dilution rate fed-batch cultures

Glucose and nitrate were rapidly consumed during the batch phases and were either depleted or very near depletion at the start of the fed-batch phases (see Figure 3-25 and Figure 3-26). After the start of the fed-batch phases, the glucose concentration increased immediately in the D=0.40h⁻¹, D=0.15h⁻¹ and D=0.10h⁻¹ experiments. The increases observed were dependent on the glucose concentration in the feed (maintained constant) as well as the dilution rates that were applied. This indicated that the glucose consumption rate was less than the glucose feed rate during the fed-batch phases of these experiments. During the first 12 hours of the fed-batch phase of the D=0.05h⁻¹ experiment, the glucose concentration remained zero, indicating that the glucose consumption rate was equal to the glucose feed rate at this low dilution rate.

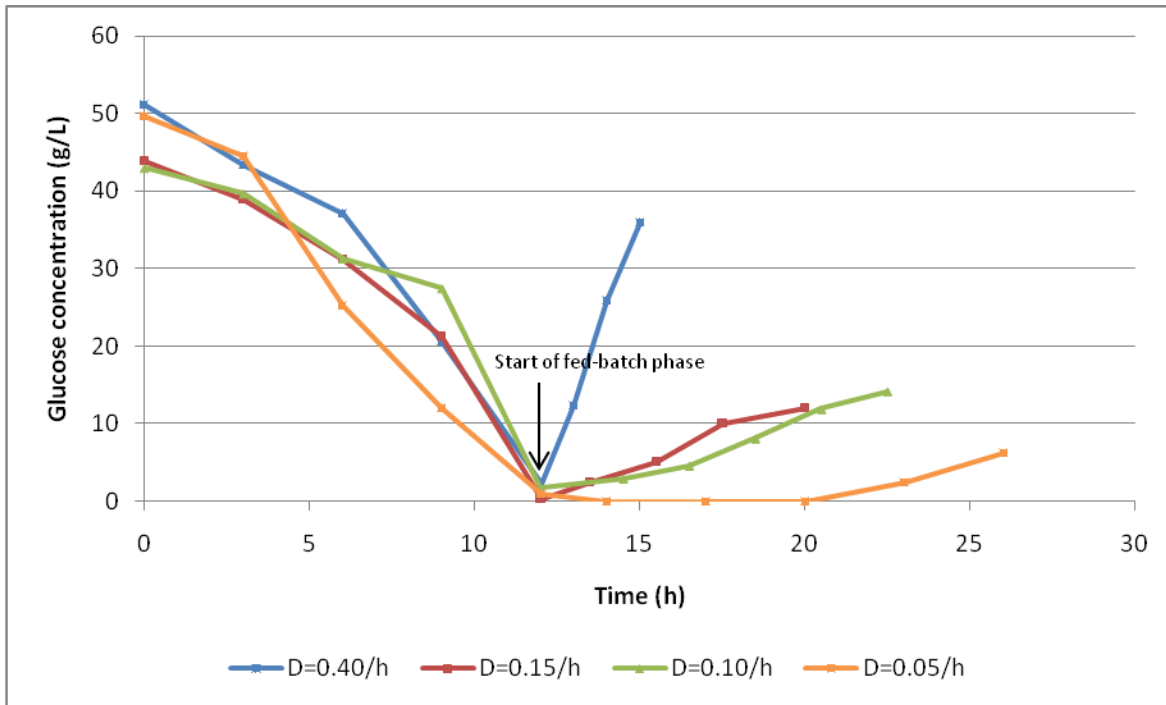


Figure 3-25: Glucose concentration profiles of fed-batch cultures during which exponential feeding strategies were applied

Unlike the glucose concentration profiles, the nitrate concentration essentially remained zero during the fed-batch phases of all four constant dilution rate experiments (Figure 3-26).

In section 1.8.1.4 the anaerobic growth of *B. subtilis* was discussed and it was mentioned that *B. subtilis* can grow under anaerobic conditions in the presence of nitrate. It has been reported that *B. subtilis* can utilize nitrate as both the terminal electron acceptor during anaerobic respiration and as a nitrogen source for cell constituents. Considering the $D=0.10\text{h}^{-1}$ experiment, the biomass increased by 36.8 g during the fed-batch phase (12-22.5 hours). During the same period, 59.8 g NaNO_3 and 59.8 g $(\text{NH}_4)_2\text{SO}_4$ was added to the reactor. Nitrogen contributed 9.85 g and 12.66 g of the 59.8 g NaNO_3 and 59.8 g $(\text{NH}_4)_2\text{SO}_4$ respectively. The combined total mass of nitrogen fed to the reactor during the fed-batch phase of the $D=0.10\text{h}^{-1}$ experiment was 22.51 g. If all the nitrogen fed to the reactor during the fed-batch phase was consumed for cell constituents, nitrogen contributed 61% of the newly formed biomass. It is improbable that 61% of the total biomass increase resulted from nitrate accumulation. Therefore, nitrate was possibly co-consumed as a terminal electron acceptor during the fed-batch phase. However, further research regarding the consumption of nitrate and nitrite as terminal electron acceptors by *B. subtilis* is required.

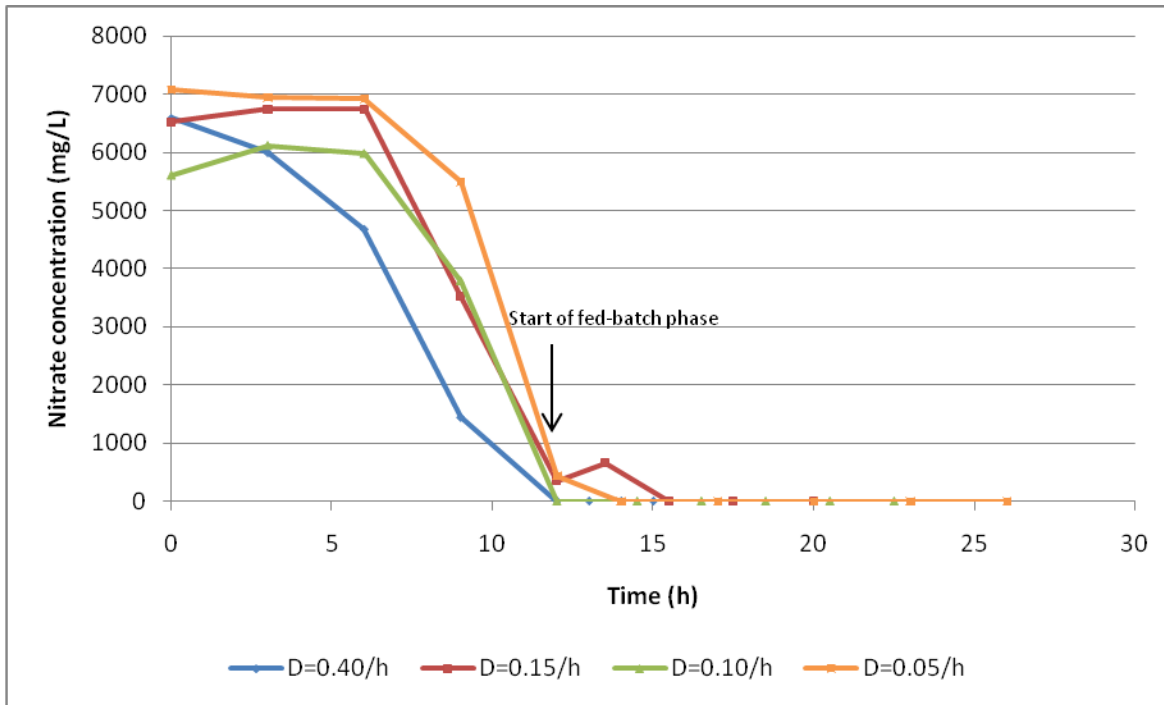


Figure 3-26: Nitrate concentration profiles of fed-batch cultures during which exponential feeding strategies were applied

The DO concentration profiles (Figure 3-27) of the batch phases of the fed-batch experiments were very similar and showed that the DO concentration decreased to zero during the first 9 hours. The nitrate concentrations of the batch phases showed a very rapid decrease between 6 and 12 hours. These results indicate that the use of nitrate as a terminal electron acceptor increased as the DO concentration decreased.

The DO concentration profiles also indicate that oxygen was in excess during the fed-batch phases of the $D=0.40\text{h}^{-1}$, $D=0.10\text{h}^{-1}$ and $D=0.05\text{h}^{-1}$ experiments. During the fed-batch phases of the $D=0.10\text{h}^{-1}$ and $D=0.05\text{h}^{-1}$ experiments, the DO concentration increased to well above 20% of saturation. Only the $D=0.15\text{h}^{-1}$ experiment showed a DO concentration of zero throughout the fed-batch phase. Since the DO concentrations did not increase to 100% of saturation and the nitrate concentrations remained zero during the fed-batch phases, these results indicate that both oxygen and nitrate were utilized as terminal electron acceptors.

Nitrate remained limiting during the fed-batch phases of all constant dilution rate fed-batch experiments. Surprisingly, the DO concentrations of the $D=0.40\text{h}^{-1}$, $D=0.10\text{h}^{-1}$ and $D=0.05\text{h}^{-1}$ experiments increased during the fed-batch phases of these experiments. However, the DO concentrations did not increase to 100% of saturation, which indicated that both nitrate and oxygen were utilized. Since nitrate was the limiting nutrient, these results further indicate that nitrate was the preferred electron acceptor.

It is accepted that different organisms utilize electron transport systems that employ a variety of electron-donor/electron-acceptor pairs and often occurs simultaneously (Moat and Foster, 1995). Since it has been reported that nitrate, nitrite and oxygen are the only electron acceptors used by *B. subtilis* (Nakano and Hulett, 1997), these results indicate that growth of *B. subtilis* and associated surfactin production may have been limited by the availability of nitrate as a terminal electron acceptor during the fed-batch phases (see section 3.3.4).

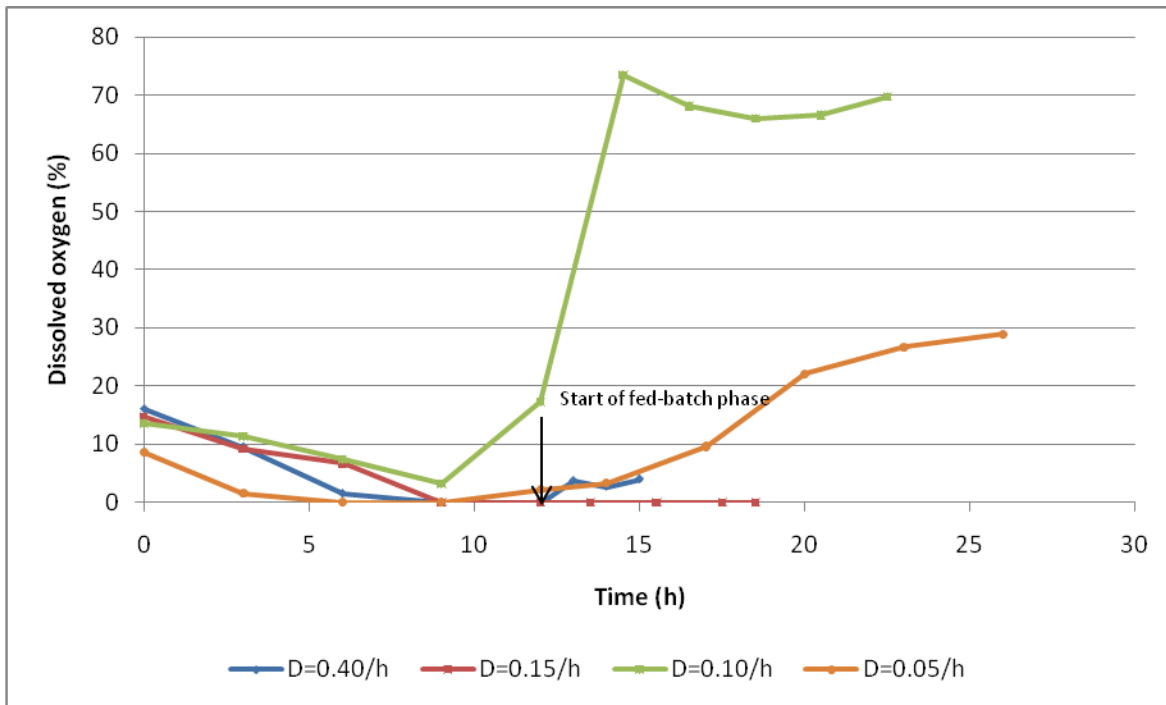


Figure 3-27: DO concentration profiles of fed-batch cultures during which exponential feeding strategies were applied

3.3.4 Quantification of kinetic parameters of constant dilution rate fed batch cultures

3.3.4.1 Specific growth rate

The specific growth rate of *B. subtilis* reached a maximum between 3 and 6 hours of growth, which coincided with the onset of active growth. The maximum specific growth rate achieved over this period was approximately 0.7 h^{-1} and corresponds to a biomass doubling time of approximately 1 hour. The specific growth rate of *B. subtilis* remained high at an average specific growth rate 0.47 h^{-1} during the active growth phase (between 3 and 12 hours), and subsequently decreased as the organism entered the stationary phase (12 hours) at which time a feed was initiated to maintain a constant dilution rate.

It is shown in Figure 3-28 that the specific growth rates achieved during the fed-batch phases of the constant dilution rate fed-batch experiments were less than the applied dilution rates. Since the specific growth rate is a function of the limiting substrate, these results indicate that growth was limited during the fed-batch phases of the constant dilution rate fed-batch experiments. Referring to section 3.3.3, it has already been shown that growth may have been nitrate-limited during the fed-batch phases of the constant dilution rate experiments.

According to the mass balance derivations in Appendix A: Fed-batch Kinetics, the specific growth rate is equal to the dilution rate under pseudo steady-state conditions. Since the specific growth rates of the constant dilution rate experiments were not equal to the applied dilution rates, pseudo steady-state was not achieved during these experiments.

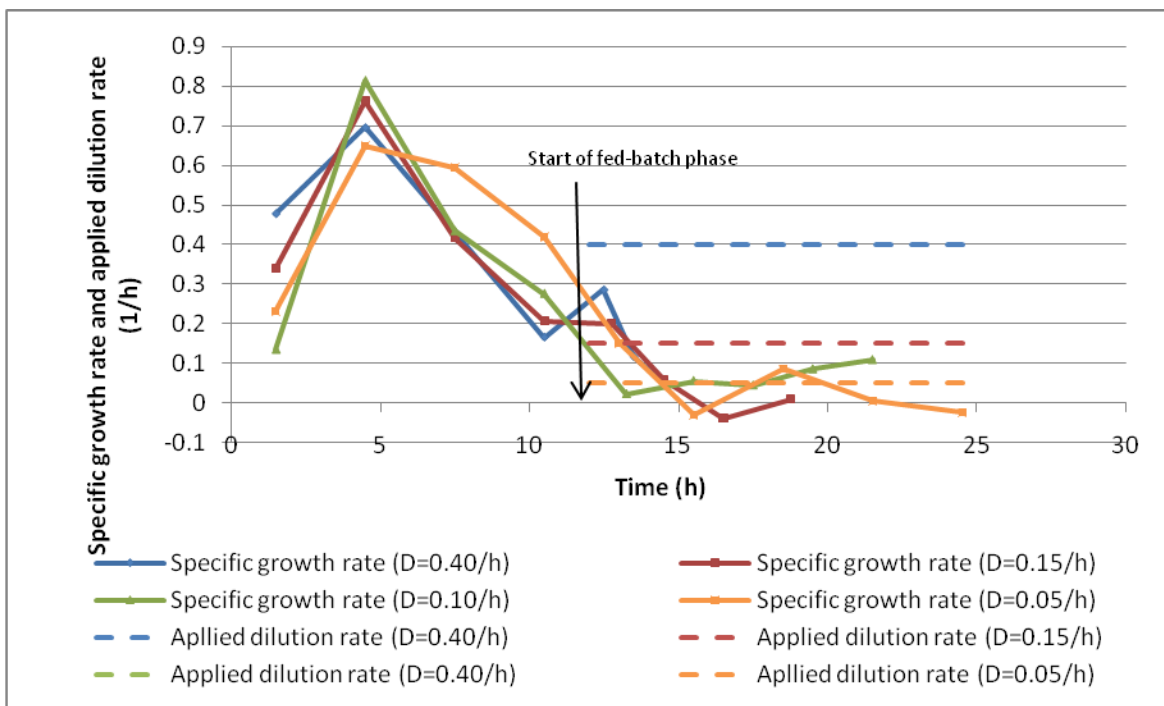


Figure 3-28: Specific growth rate profiles of fed-batch cultures during which exponential feeding strategies were applied

3.3.4.2 Biomass yield on substrate

During fed-batch culture, nutrients are continuously added to the culture broth. In order to calculate the biomass yield on substrate during fed-batch culture, an additional term needs to be added to the denominator of Equation 3-2. This term, S_{fed} , is the cumulative amount of substrate that was added during the fed-batch phase (from the start of fed-batch phase to time i) and can be seen in Equation 3-7.

$$Y_{x/s} = \frac{X_i - X_0}{S_0 + S_{fed} - S_i}$$

Equation 3-7

The biomass yield on substrate increased during the growth phase and reached an average maximum biomass yield on substrate of 0.75 at the end of active growth during the batch phase (Figure 3-29). This value is approximately 2.9- and 1.6-fold higher than the 0.26 and 0.46 biomass yields on substrate reported by Chen *et al.* (2006) and Davis *et al.* (1999) respectively.

After the onset of the fed-batch phases, the biomass yields on glucose decreased possibly as a result of slow growth caused by the nitrate-limitation (Figure 3-26). The biomass yields on glucose achieved during the fed-batch phases were very similar and decreased to values less than 0.4. These results indicate that a high biomass on substrate yield is achieved during active growth under nutrient sufficient conditions.

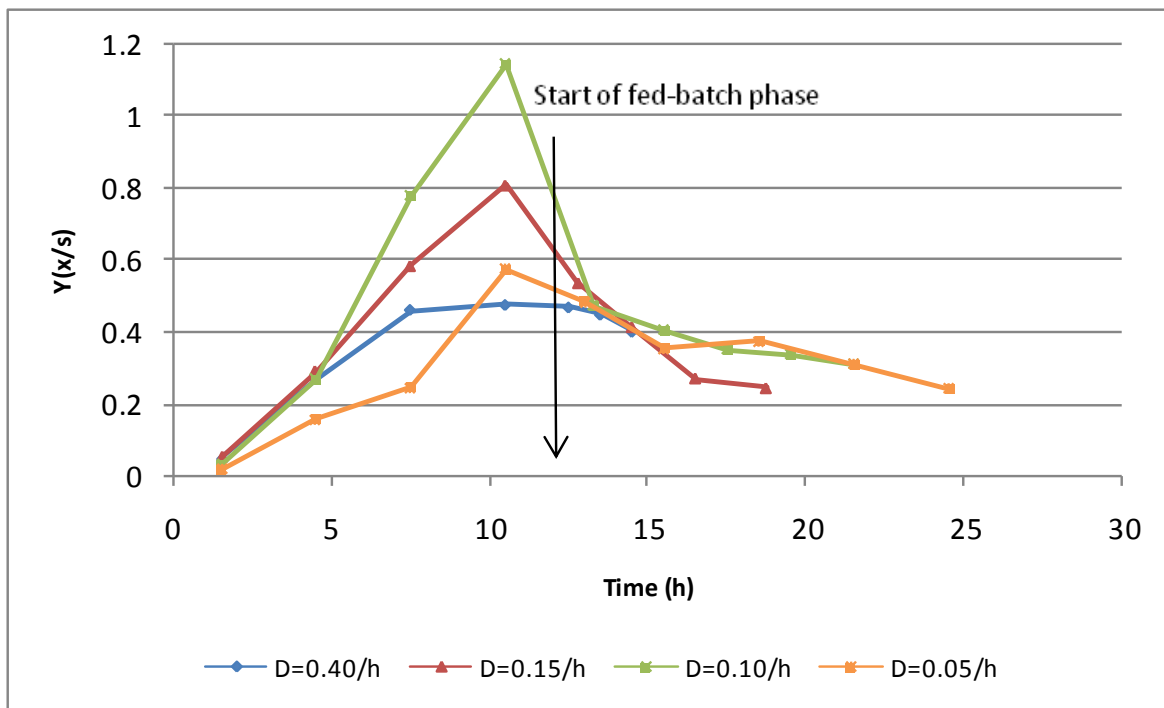


Figure 3-29: Biomass yield on glucose profiles of fed-batch cultures during which exponential feeding strategies were applied

3.3.4.3 Surfactin yield on substrate

The surfactin yield on substrate during the fed-batch experiments were calculated according to Equation 3-8, which contains an additional S_{fed} term in the denominator to account for the addition of substrate during the fed-batch phases (from the start of fed-batch phase to time i).

$$Y_{P/S} = \frac{P_i - P_0}{S_0 + S_{fed} - S_i}$$

Equation 3-8

The surfactin yield on glucose was superior prior to feeding and ranged between 0.045 and 0.075, with the exception of one data point of the $D=0.05\text{h}^{-1}$ experiment between 3 and 6 hours (Figure 3-30). The surfactin yield on glucose in the $D=0.05\text{h}^{-1}$ experiment increased to 0.096 between 3 and 6 hours. This value is a result of changes in local gradients of concentration profiles and give a false representation of the actual gradient, since the average surfactin yield on substrate of the $D=0.40\text{h}^{-1}$, $D=0.15\text{h}^{-1}$ and $D=0.10\text{h}^{-1}$ experiments were 0.025. The surfactin yield on glucose achieved during the batch phases in this study compared well with the 0.076 and 0.046 reported by Kim *et al.* (1997) and Chen *et al.* (2006) respectively.

The surfactin yields on glucose decreased to values less than 0.04 at the onset of the stationary phase and only the $D=0.40\text{h}^{-1}$ showed an increase of 0.006 in the surfactin yield on glucose during the fed-batch phase between 13 and 14 hours. This increase was a result of the availability of glucose and nitrate over this period. However, the large increase in total biomass over the same period increased the demand for glucose and nitrate, after which nitrate then became the limiting nutrient and caused the surfactin yield on glucose to decrease. The surfactin yield on glucose in the $D=0.15\text{h}^{-1}$, $D=0.10\text{h}^{-1}$ and $D=0.05\text{h}^{-1}$ experiments remained approximately 0.02 during the fed-batch phases as a result of slow growth caused by nitrate-limitation. These results indicate that a high surfactin yield on glucose is obtained during active growth.

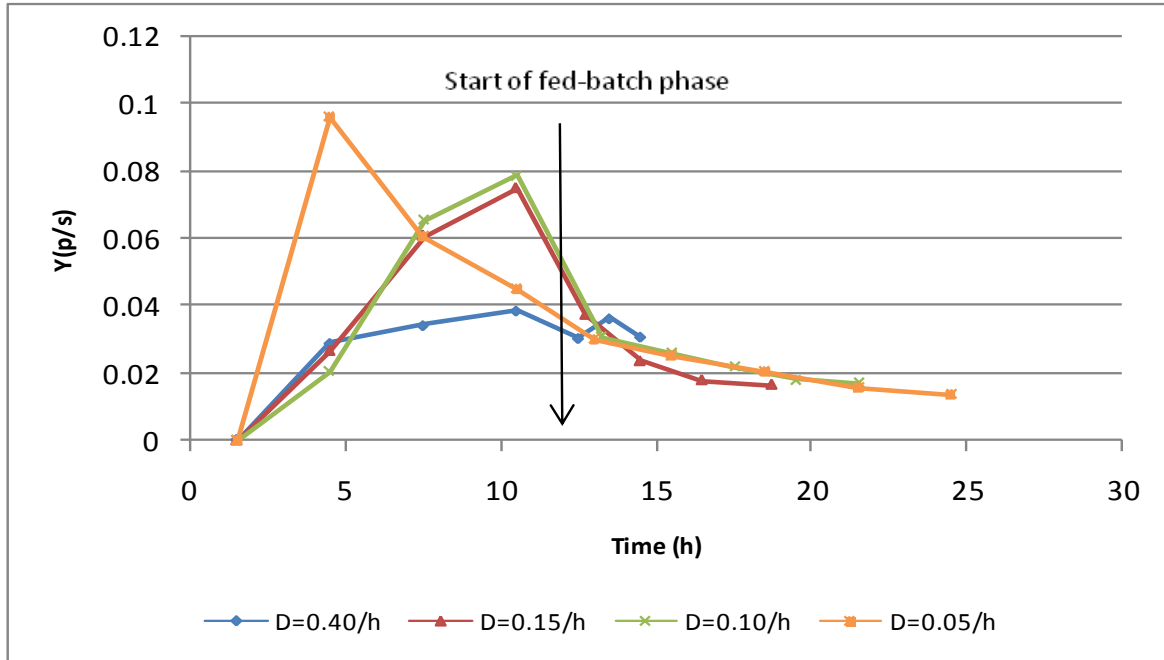


Figure 3-30: Surfactin yield on glucose profiles of fed-batch cultures during which exponential feeding strategies were applied

3.3.4.4 Surfactin yield on biomass

The $D=0.40\text{h}^{-1}$ experiment showed a significant increase in the surfactin yield on biomass after the onset of the fed-batch phase (Figure 3-31). The surfactin yield on biomass increased from $65\text{ mg/g}_{\text{cells}}$ to $80\text{ mg/g}_{\text{cells}}$ between 13 and 14 hours as a result of the high amount of glucose and nitrate fed to the reactor during this period. Thereafter, the yield of surfactin on biomass decreased as a result of a growth limitation.

The surfactin yield on biomass of the $D=0.15\text{h}^{-1}$ experiment initially decreased after the onset of the fed-batch phase as a result of a decrease in the total surfactin, but increased to approximately $67\text{ mg/g}_{\text{cells}}$ between 17.5 and 20 hours. The surfactin yield on biomass in the $D=0.10\text{h}^{-1}$ experiment decreased to approximately $55\text{ mg/g}_{\text{cells}}$, which was $25\text{ mg/g}_{\text{cells}}$ less than that of the $D=0.40\text{h}^{-1}$ experiment. The surfactin yield on biomass of the $D=0.05\text{h}^{-1}$ experiment marginally increased from $61\text{ mg/g}_{\text{cells}}$ to $72\text{ mg/g}_{\text{cells}}$ between 12 and 17 hours. Thereafter, the surfactin yield on biomass in the $D=0.05\text{h}^{-1}$ experiment decreased to approximately $55\text{ mg/g}_{\text{cells}}$. These results indicate that a high surfactin yield on biomass is achieved during active growth and also indicates that the surfactin yield on biomass increases with an increase in the dilution rate during fed-batch culture.

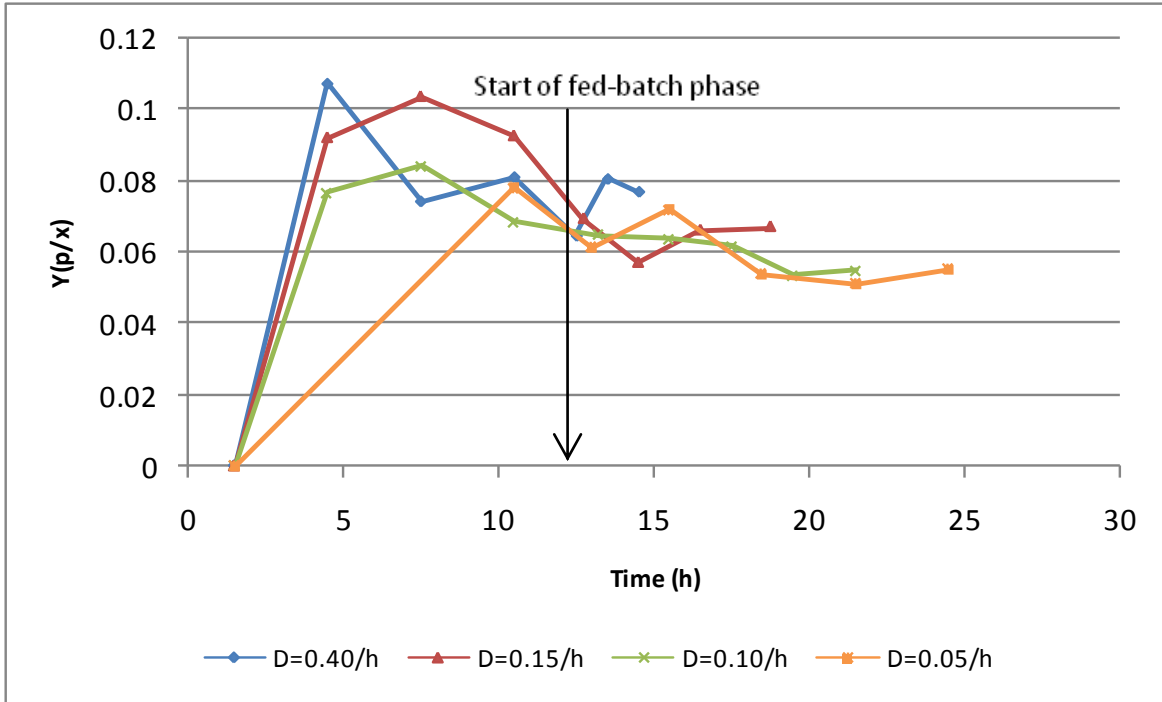


Figure 3-31: Surfactin yield on biomass profiles of fed-batch cultures during which exponential feeding strategies were applied

Although not very clear in Figure 3-31, Figure 3-32 shows that a linear relationship exists between surfactin concentration and CDW during active growth of *B. subtilis*. The slopes of the surfactin concentration versus CDW profiles indicate that the average yield of surfactin on biomass was 0.081 prior to feeding. Very few authors have reported yields and productivities, which makes a direct comparison difficult. However, the surfactin yield on biomass obtained in this study compared well with the surfactin yield on biomass of 0.071 reported by Chen *et al.* (2006), but is far less than the 0.38 reported by Kim *et al.* (1997).

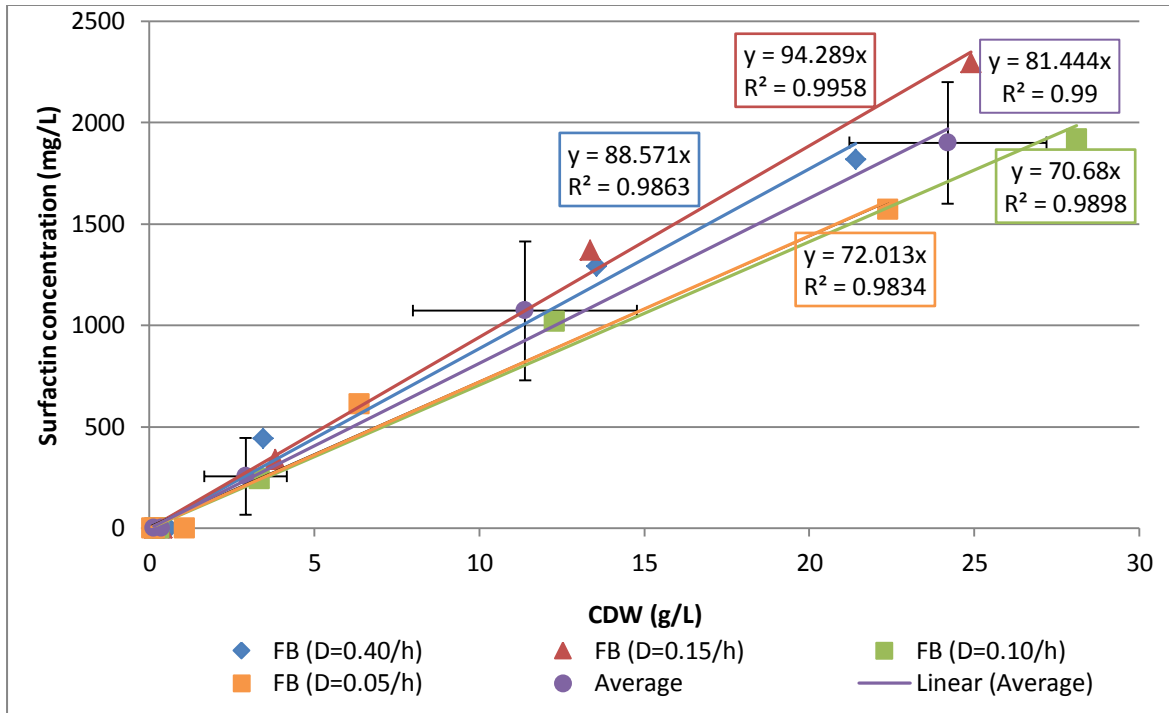


Figure 3-32: Relationship between CDW and surfactin concentration during batch phases of fed-batch cultures during which exponential feeding strategies were applied

3.3.4.5 Surfactin productivity and specific productivity

The productivity of the fed-batch experiments has been calculated without the culture volume and is reported as mg/h. This was done to eliminate the effect of different rates of volume increases in the different experiments. Similarly, the specific productivity was calculated as mg/h/g_{cells}.

The surfactin productivity increased as the total biomass increased during the batch phases of the fed-batch experiments and reached an average maximum productivity (of all four constant dilution rate experiments) of 604 mg/h between 9 and 12 hours of growth (Figure 3-33). This value is greater than the 7.6 mg/h and 124 mg/h (calculated from literature) reported for batch culture by Chen *et al.* (2006) and Kim *et al.* (1997) respectively. The reason for the greater surfactin productivity achieved in this study is the high CDWs achieved.

The $D=0.40h^{-1}$ experiment showed a significant increase in surfactin productivity after the onset of the fed-batch phase (at 12 hours). The surfactin productivity increased to 1613 mg/h between 12 and 13 hours in this experiment and subsequently decreased to 58 mg/h between 13 and 15.5 hours. The increase observed between 12 and 13 hours might be as a result of the large amount of fresh nutrients, particularly nitrate, being added to the culture. The surfactin productivity of the $D=0.15h^{-1}$ and $D=0.10h^{-1}$ experiments decreased to between 0 mg/h and 200 mg/L during the fed-batch phases, while the surfactin productivity of the $D=0.05h^{-1}$ experiment

decreased to approximately zero. These results indicate that a high dilution rate strategy is superior to low dilution rate strategies for surfactin production with respect to productivity during fed-batch culture of *B. subtilis*.

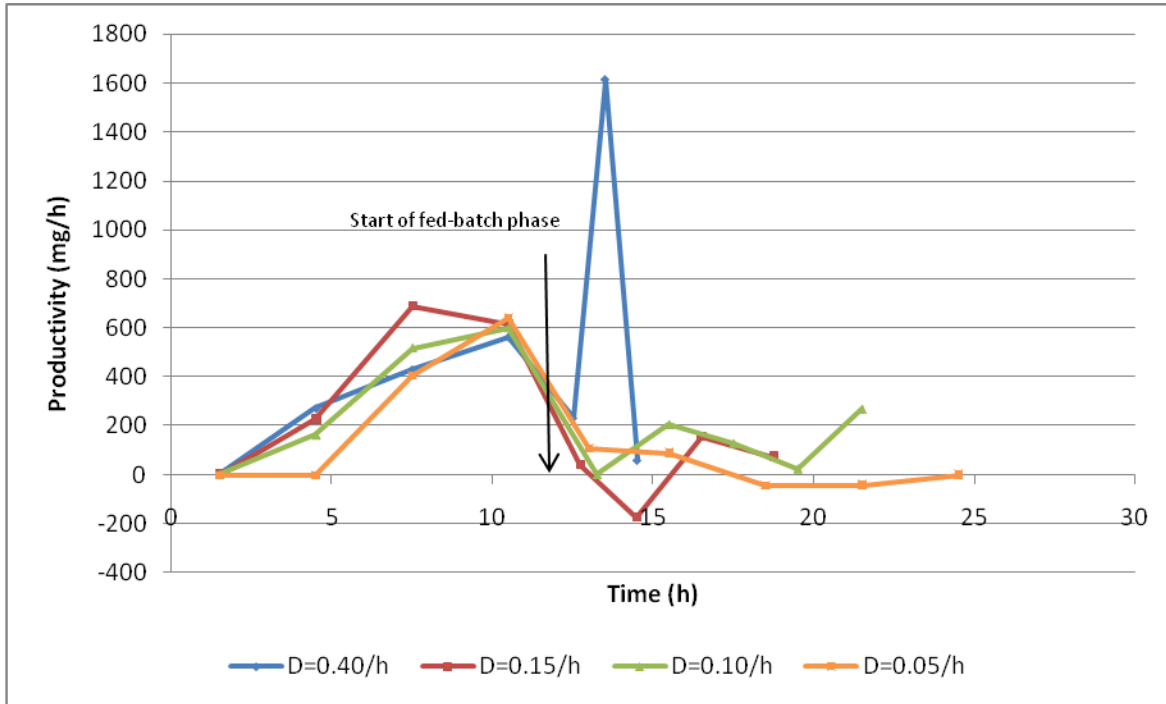


Figure 3-33: Surfactin productivity profiles of fed-batch cultures during which exponential feeding strategies were applied

The specific surfactin productivity profiles (Figure 3-34) follow similar trends to those of the specific growth rate profiles (Figure 3-28), indicating that the specific surfactin productivity is proportional to the specific growth rate. Analogous to the maximum specific growth rate, the maximum specific surfactin productivity was achieved between 3 and 6 hours of growth. The average of the maximum specific surfactin productivities achieved over this period during the batch phases of the four constant dilution rate experiments was 54 mg/h/g_{cells}. No studies could be found which report specific surfactin productivities and therefore, the specific surfactin productivities achieved in this study could not be compared to others.

Only the $D=0.40\text{h}^{-1}$ experiment showed an increase in the specific surfactin productivity at the onset of the fed-batch phase. The specific surfactin productivity in this experiment increased from 4 mg/h/g_{cells} to 24 mg/h/g_{cells} between 12 and 13 hours, and subsequently decreased possibly as a result of a nitrate-limitation. The specific surfactin productivities during the fed-batch phases of the $D=0.15\text{h}^{-1}$, $D=0.10\text{h}^{-1}$ and $D=0.05\text{h}^{-1}$ were all less than 5 mg/h/g_{cells} and were also possibly the result of nitrate-limitation which limited growth and consequently surfactin production (Figure 3-26).

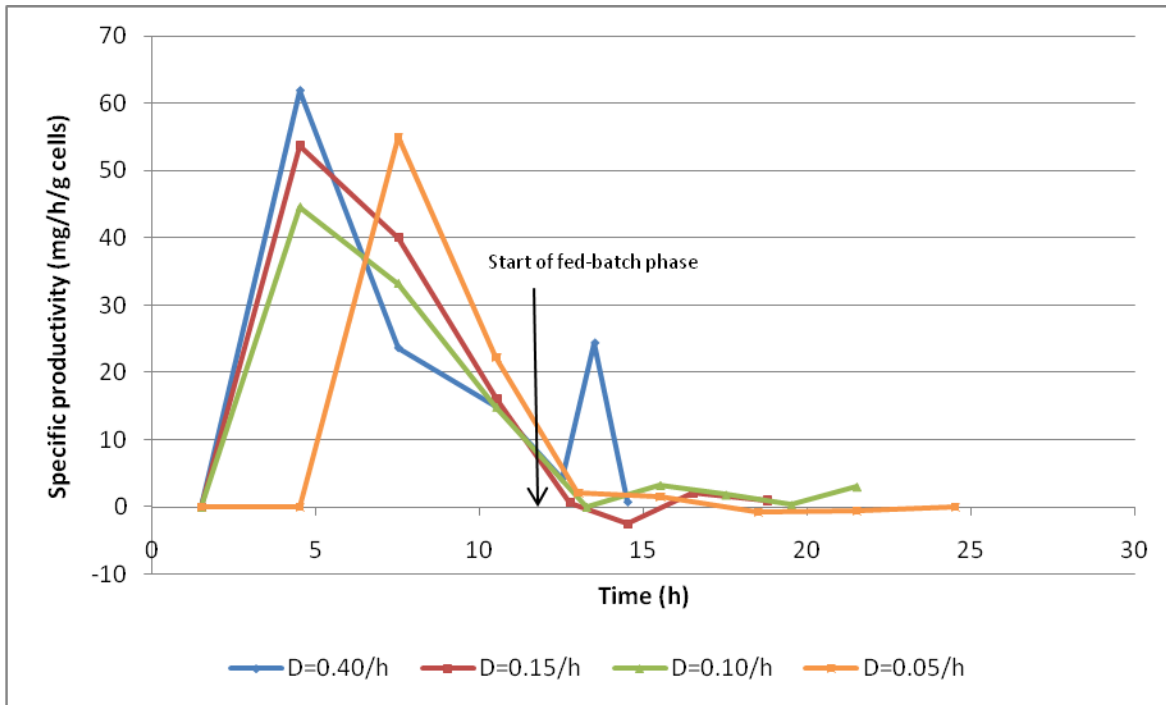


Figure 3-34: Surfactin specific productivity profiles of fed-batch cultures during which exponential feeding strategies were applied

3.3.5 Quantification of cell dry weight and surfactin concentration in constant feed rate fed-batch cultures

Two constant feeding rate strategies were applied during fed-batch culture of *B. subtilis*. The flow rates of the two constant feeding strategies were 0.125 L/h and 0.4 L/h. These flow rates have been selected to evaluate the effect of high- and low constant feeding rate strategies on growth and surfactin production during fed-batch culture.

It is shown in Figure 3-35 that the CDW increased to maxima of 26.2 g/L and 21.4 g/L at the end of the batch phases of the $F=0.125\text{L/h}$ and $F=0.40\text{L/h}$ experiments respectively. These maxima compare well with the 22.4 g/L achieved after 12 hours during the bioreactor batch experiment (Figure 3-8) and also compares well with the average CDW of 24.7 g/L achieved during the batch phases of the constant dilution rate experiments (Figure 3-20). The CDW during the $F=0.125\text{L/h}$ experiment increased from 26.2 g/L to 35.5 g/L during the fed-batch phase between 12 and 24 hours (Figure 3-35), while the CDW of the $F=0.40\text{L/h}$ experiment remained constant at approximately 23 g/L during the fed-batch phase. These results are different to that of the constant dilution rate experiments, since the CDWs of the constant flow rate experiments did not decrease during the fed-batch phases. The reason for this difference is that since the feed flow rates remained constant during the constant feeding rate experiments, the dilution rate of the culture broth decreased with time and the culture dilution was decreased.

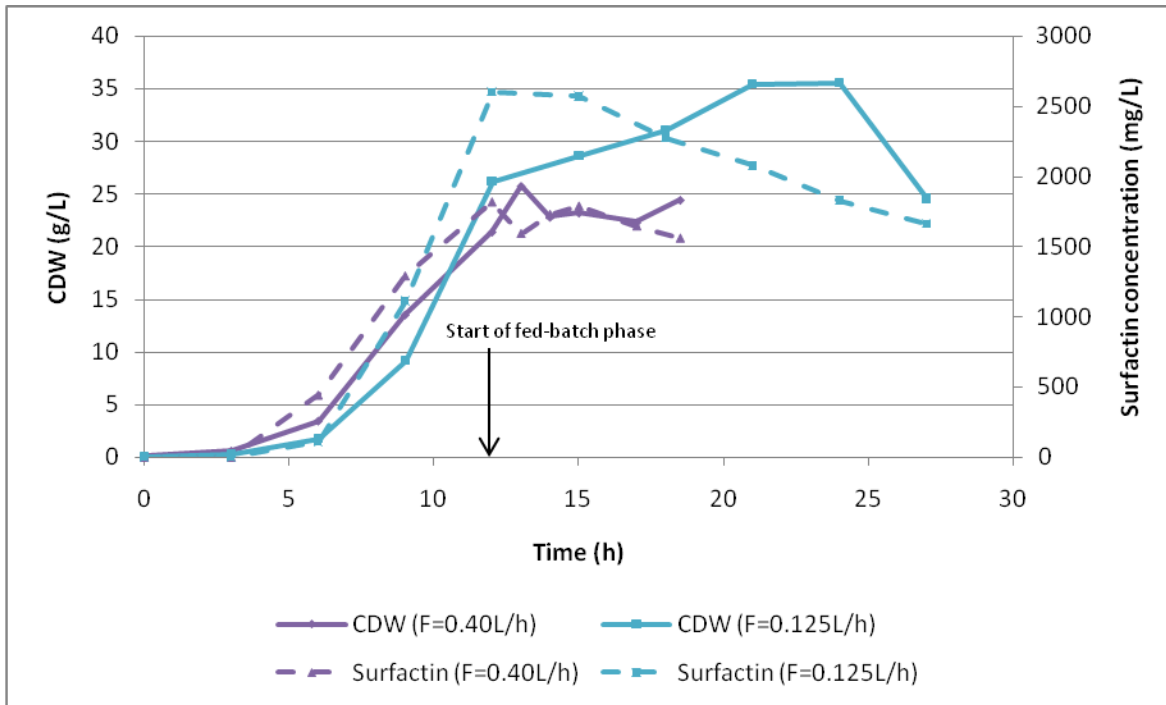


Figure 3-35: CDW and surfactin concentration profiles of fed-batch cultures during which constant feeding strategies were applied

Although the CDW of the $F=0.125\text{L/h}$ experiment increased during the fed-batch phase, the surfactin concentration decreased from 2600 mg/L to 1662 mg/L (Figure 3-35). This indicated that the rate of surfactin production significantly decreased during the fed-batch phase of the $F=0.125\text{L/h}$ experiment (see section 3.3.8.5). The surfactin concentration in the $F=0.40\text{L/h}$ experiment only marginally decreased from 1818 mg/L to 1560 mg/L during the fed-batch phase.

Analogous to the constant dilution rate experiments, the total biomass and total amount of surfactin increased during the fed-batch phases of the constant feeding rate experiments (Figure 3-36). The total biomass of the $F=0.125\text{L/h}$ experiment increased from 52.3 g to 124.4 g (138%) over 12 hours during the fed-batch phase. However, the total surfactin of the $F=0.125\text{L/h}$ experiment only increased from 5200 mg to 6441 mg (23.1%) over the same period. The total biomass of the $F=0.40\text{L/h}$ experiment increased from 42.9 g to 112.4 g (equivalent to 166%) over a shorter period of only 6.5 hours during its fed-batch phase. A total surfactin increase from 3636 mg to 7177 mg (equivalent to 97.4%) was achieved between 12 and 18.5 hours in the $F=0.40\text{L/h}$ experiment. These results indicate that the rate of biomass and the rate of surfactin production increases with an increase in the feed rate of constant feeding rate strategies.

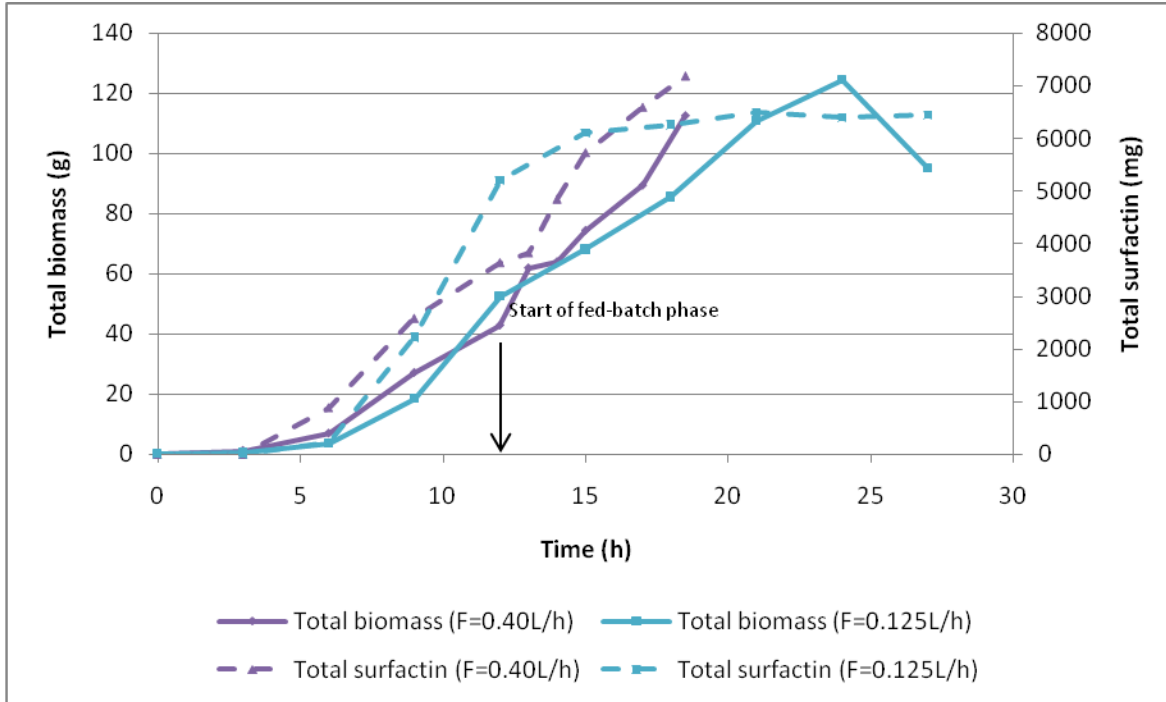


Figure 3-36: Total biomass and total surfactin profiles of fed-batch cultures during which constant feeding strategies were applied

3.3.6 Comparison of rate of total biomass- and rate of total surfactin increase in constant feed rate fed-batch experiments

A comparison of the average rate of biomass increase and average rate of surfactin production between the fed-batch phases of the two constant feed rate fed-batch experiments is shown in Figure 3-37. These were calculated as the increase in the total biomass and total surfactin during the fed-batch phases respectively, divided by the duration of the respective fed-batch phases.

It is evident that a higher constant feed flow rate strategy results in a higher average rate of biomass increase and average rate of surfactin production. The average rate of biomass increase during the fed-batch phase of the $F=0.40\text{L/h}$ experiment was 1.8-fold higher than that of the $F=0.125\text{L/h}$ experiment, while the average rate of surfactin production of the $F=0.40\text{L/h}$ experiment was 9.4 fold higher than that of the $F=0.125\text{L/h}$ experiment. These results indicate that a high constant feed rate strategy should be considered as a process strategy for enhanced surfactin production.

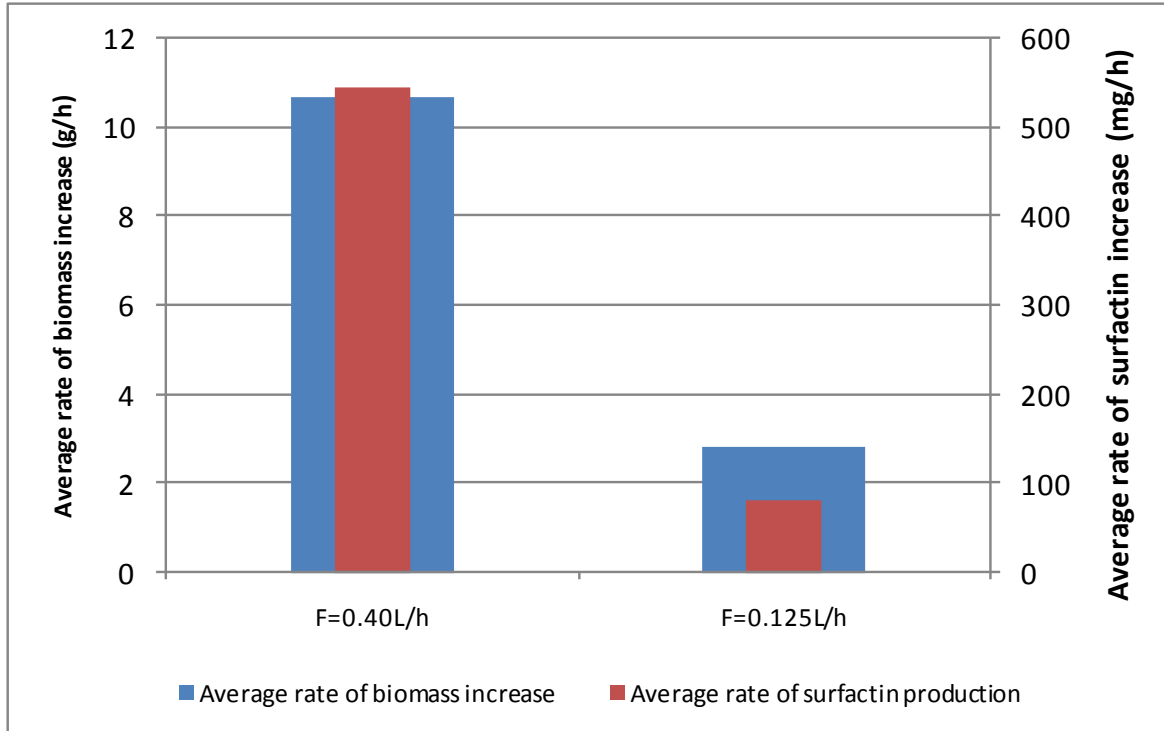


Figure 3-37: Average hourly rate of biomass- and surfactin increases during the fed-batch phases of the constant feed rate fed-batch experiments

3.3.7 Influence of nutrient conditions on cell dry weight and surfactin concentration in constant feed rate fed-batch cultures

The glucose, nitrate and DO concentration profiles of the constant feeding rate fed-batch experiments showed similar trends as those of the constant dilution rate experiments (Figure 3-38). The glucose concentration increased from 2.6 g/L to 10.6 g/L between 12 and 17 hours during the fed-batch phase of the F=0.40L/h experiment as a result of the high constant feed flow rate. This indicated that the glucose feed rate was higher than the glucose consumption rate over this period. Thereafter, the glucose concentration remained steady at approximately 10 g/L in the F=0.40L/h experiment between 13 and 18.5 hours, indicating that the glucose consumption rate was equal to the glucose feed rate. The glucose concentration in the F=0.125L/h experiment decreased to zero between 12 and 15 hours and remained zero for the rest of the fed-batch phase, indicating that the glucose consumption rate was equal to the glucose feed rate during its fed-batch phase.

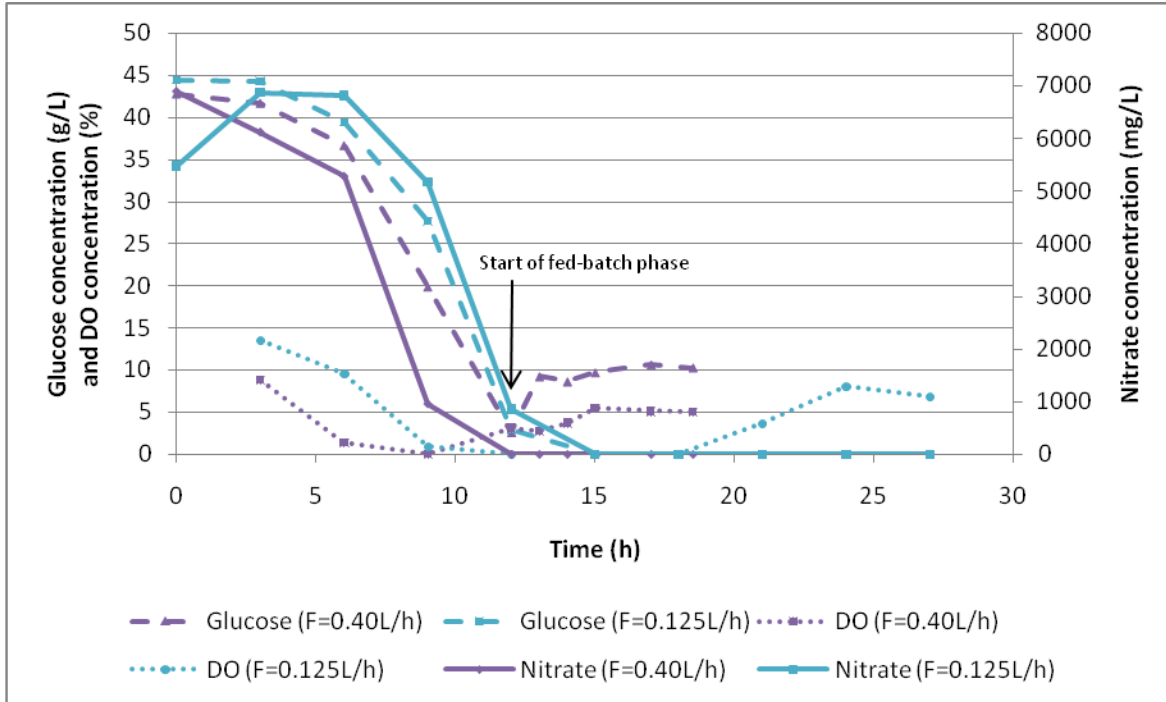


Figure 3-38: Glucose-, nitrate- and dissolved oxygen concentration profiles of fed-batch cultures during which constant feeding strategies were applied

Analogous to the constant dilution rate experiments, the DO concentrations of the F=0.40L/h and F=0.125L/h experiments decreased to zero within 9 hours (Figure 3-38). This was followed by very rapid nitrate utilization between 6 and 12 hours, suggesting that nitrate was utilized as a terminal electron acceptor as a result of the low DO concentrations. The nitrate concentrations of the F=0.40L/h and F=0.125L/h experiments remained zero after depletion, while the DO concentration increased to 5% and 6.8% during the respective fed-batch phases. Since the nitrate concentrations did not increase as the DO increased, it had to be assumed that nitrate was still being utilized as a terminal electron acceptor (in combination with DO) during the fed-batch phases, confirming earlier findings of this behavior (see section 3.3.3).

3.3.8 Quantification of kinetic parameters of constant feed rate fed-batch cultures

3.3.8.1 Specific growth rate

The specific growth rate profiles of the batch phases of the constant feed rate fed-batch experiments show similar trends as those of the constant dilution rate experiments. The specific growth rates increased to maxima of 0.59 h^{-1} between 3 and 6 hours in the F=0.40L/h and F=0.125L/h experiments respectively and subsequently decreased toward the onset of the fed-batch phase (Figure 3-39).

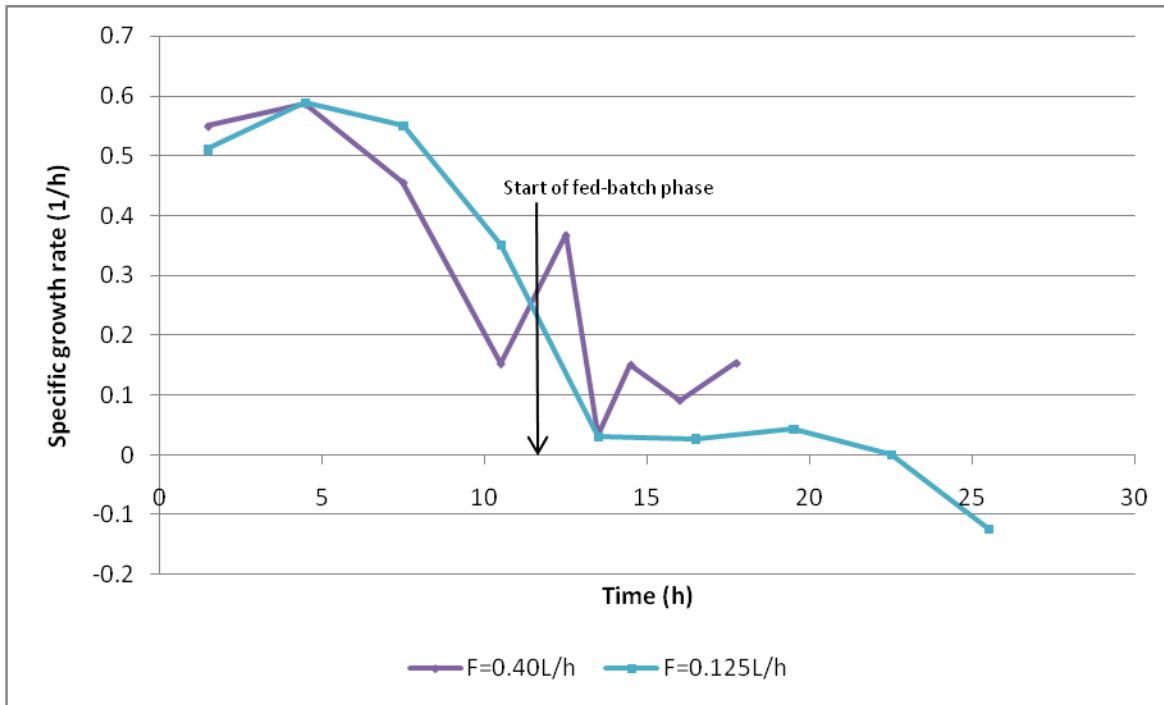


Figure 3-39: Specific growth rate profiles of fed-batch cultures during which constant feeding strategies were applied

After the onset of the fed-batch phase, the specific growth rate of the $F=0.40\text{L/h}$ experiment increased to 0.37 h^{-1} between 12 and 13 hours as a result of the high amounts of glucose and nitrate fed to the reactor (Figure 3-39). As a result the biomass increased by 19 g over the same period and the demand for nutrients increased. However, the nutrient feed rate (feed flow rate) was constant and thus the added nutrients were consumed at a higher rate. Consequently, the specific growth rate decreased to approximately 0.15 h^{-1} between 15 and 18.5 hours.

The specific growth rate of the $F=0.125\text{L/h}$ experiment decreased during the fed-batch phase to approximately 0.03 h^{-1} between 12 and 21 hours. The low specific growth rate during this phase was caused by the very low glucose and nitrate concentrations during this period (Figure 3-38).

3.3.8.2 Biomass yield on substrate

The biomass yields on glucose of the constant feed rate experiments were calculated according to Equation 3-7 and were very similar over the batch phases. Biomass yields on glucose of approximately 0.6 were achieved over this period. These values are in accordance to that achieved during the batch phases of the constant dilution rate experiments (Figure 3-29).

The biomass yield on glucose of the $F=0.40\text{L/h}$ experiment increased after the onset of the fed-batch phase from 0.53 to 0.64 between 12 and 15 hours as a result of the addition of glucose

and nitrate (Figure 3-38). Thereafter, the biomass yield on glucose stabilized at approximately 0.50 between 15 and 24 hours. The biomass yield on substrate of the $F=0.125\text{L/h}$ experiment decreased from 0.63 to 0.57 after the onset of the fed-batch phase and remained relatively stable between 15 and 24 hours.

The biomass yields on glucose achieved after the onset of the fed-batch phases of the constant feed rate fed-batch experiments are different from that achieved in the constant dilution rate experiments. The biomass yields on glucose are stable during the constant feed rate fed-batch phases (Figure 3-40), whereas the biomass on glucose yields continuously decrease during the constant dilution rate fed-batch phases (Figure 3-29).

The difference in the achieved biomass yields on glucose between the fed-batch phases of the constant feed rate and constant dilution rate experiments is a direct result of the applied dilution rates. In the constant dilution rate experiments, the total biomass increases as the glucose feed rate increases, while in the constant feed rate experiments, the total biomass increases while a constant glucose feed rate is applied. This means that in the constant dilution rate experiments, less biomass was formed relative to the amount of glucose that was added during the fed-batch phases. During the constant dilution rate fed-batch experiments, the biomass yield on substrate decreases, even though glucose is added exponentially to the culture broth. However, during the constant feed rate fed-batch experiments, the biomass yield on substrate remains relatively constant, while glucose is fed at a constant rate.

These results indicate that the biomass yield on glucose can be increased during fed-batch culture if constant feed rate strategies are applied.

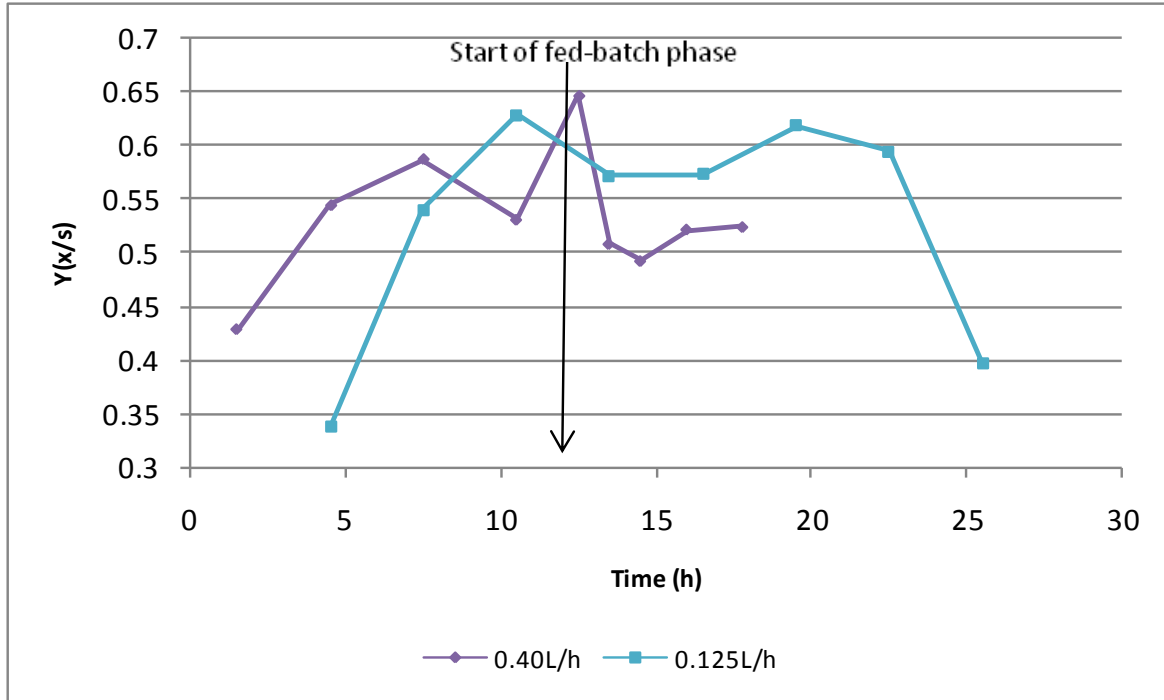


Figure 3-40: Biomass yield on glucose profiles of fed-batch cultures during which constant feeding strategies were applied

3.3.8.3 Surfactin yield on substrate ($Y_{p/s}$)

Since surfactin production predominated during active growth, the maximum surfactin yield on substrate occurred over this period. The surfactin yields on glucose of the constant feed rate fed-batch experiments are similar to those of the constant dilution rate experiments (Figure 3-30). The maximum surfactin yields on glucose of the $F=0.40\text{L/h}$ and $F=0.125\text{L/h}$ experiments are 0.07 and 0.066 respectively (Figure 3-41), while those of the constant dilution rate experiments varied between 0.039 and 0.079 (Figure 3-30).

The maximum surfactin yields on glucose of the constant feed rate fed-batch experiments were achieved at the onset of active growth between 3 and 9 hours. Thereafter, the surfactin yield on glucose of the $F=0.125\text{L/h}$ experiment continuously decreased. The decrease observed during the $F=0.125\text{L/h}$ was a result of a decrease in the growth rate (Figure 3-39), which has already been shown to decrease surfactin production (Figure 3-1).

The surfactin yield on glucose of the $F=0.40\text{L/h}$ experiment also decreased as a result of a decrease in the specific growth rate. However, Figure 3-41 shows that the surfactin yield on glucose of the $F=0.40\text{L/h}$ experiment stabilized after the onset of the fed-batch phase. The surfactin yield on glucose remained stable at approximately 0.38 between 12 and 17 hours during the $F=0.40\text{L/h}$ experiment.

When compared to the surfactin yields on glucose achieved during the fed-batch phases of the constant dilution rate experiments (excluding the $D=0.40\text{h}^{-1}$ experiment) (Figure 3-30), the surfactin yields on glucose were higher in the constant feed rate experiments. Glucose is fed at a constant feed rate during the constant feed rate experiments, whereas glucose is fed exponentially in the constant dilution rate experiments. These results indicate that the utilization of glucose for surfactin production is more efficient during constant feed rate fed-batch operation.

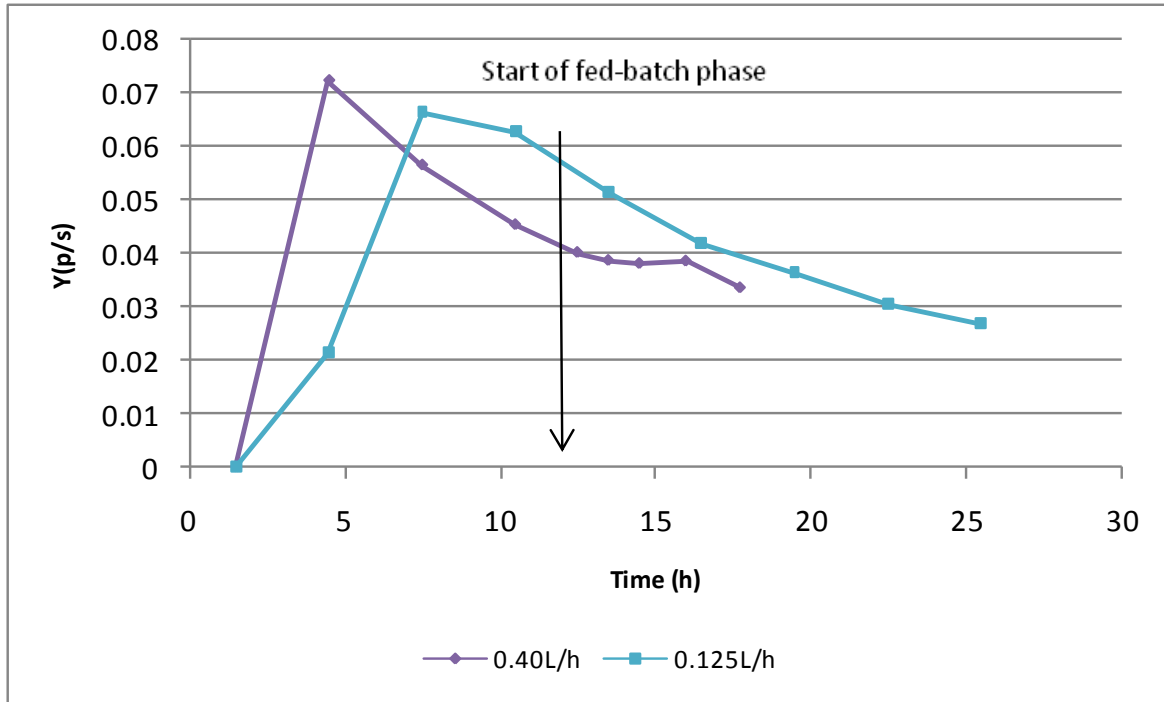


Figure 3-41: Surfactin yield on glucose profiles of fed-batch cultures during which constant feeding strategies were applied

3.3.8.4 Surfactin yield on biomass

The surfactin yields on biomass profiles of the two constant feed rate fed-batch experiments are very similar over the batch phase (Figure 3-42). The maximum surfactin yields on biomass achieved in the $F=0.40\text{L/h}$ and $F=0.125\text{L/h}$ experiments were 0.13 and 0.12 respectively. These maxima are slightly higher than that achieved in the constant dilution rate experiments. However, this observation should be regarded as variance in the surfactin yield on biomass during the batch phases, since the operating conditions during the batch phases of all experiments (using configuration 1) were the same.

Analogous to the $D=0.40\text{h}^{-1}$ experiment, the $F=0.40\text{L/h}$ showed a significant increase in the surfactin yield on biomass after the onset of the fed-batch phase. This was a direct result of the high glucose and nitrate feed rate to the bioreactor culture. The surfactin yield on biomass

increased from 0.062 to 0.076 between 13 and 14 hours, and subsequently decreased as a result of the high total biomass achieved and the high nitrate demand. It has already been suggested in section 3.3.3 that nitrate was consumed as a terminal electron acceptor. Nitrate is required to complete the electron transport chain and as such, if nitrate is limited, the process of energy production is limited.

No increase in the surfactin yield on biomass was observed during the fed-batch phase of the $F=0.125\text{L/h}$ experiment. The surfactin yield on biomass of this experiment decreased from 0.089 to 0.051 between 12 and 24 hours, indicating that the feed rate of fresh nutrients was too slow to maintain a high product yield. This is confirmed in Figure 3-38, where it can be seen that both the glucose and nitrate concentrations remained zero after the onset of the fed-batch phase. However, the surfactin yield on biomass increased after 24 hours from 0.051 to 0.067 as a result of an increase in the glucose concentration.

These results confirm earlier results, which indicated that the surfactin yield on biomass is higher during active growth. Moreover, these results indicate that high feed flow rates should be applied to increase the surfactin yield on biomass during fed-batch culture.

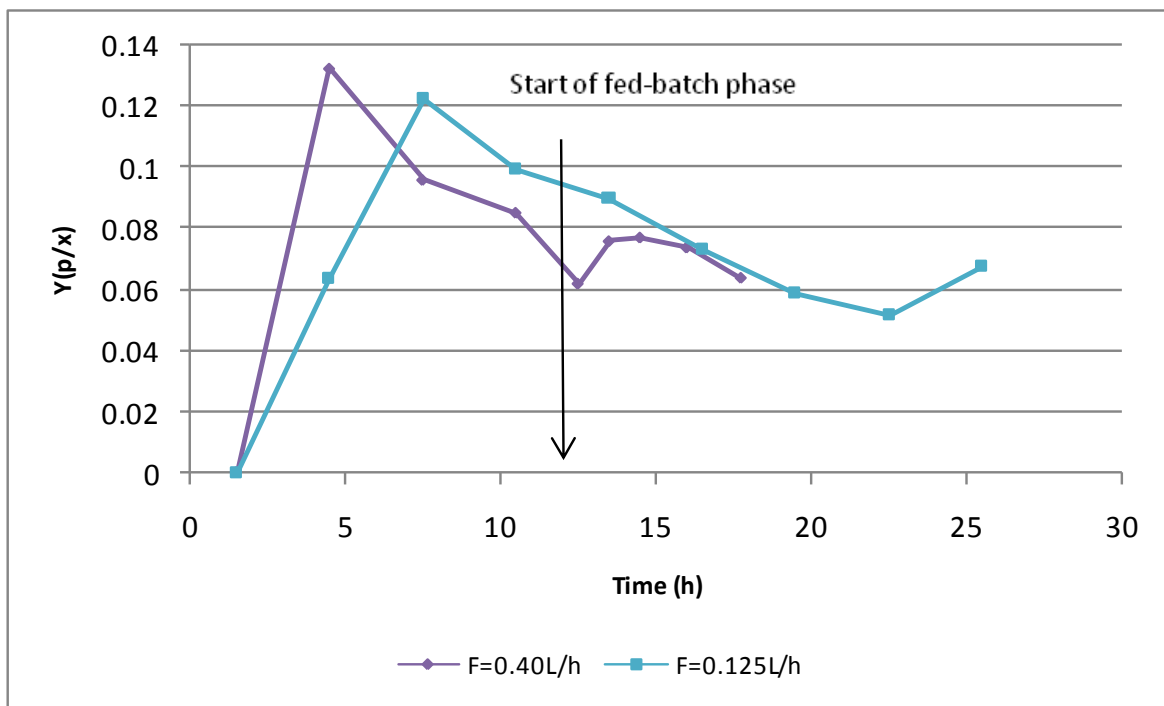


Figure 3-42: Surfactin yield on biomass profiles of fed-batch cultures during which constant feeding strategies were applied

3.3.8.5 Surfactin productivity and specific productivity

The surfactin productivity and specific surfactin productivity profiles (Figure 3-43) of the constant feed rate fed-batch experiments show similar trends as those of the constant dilution fed-batch experiments (see section 3.3.4.5). The productivity profiles indicate that a higher surfactin productivity was achieved in the $F=0.125\text{L/h}$ experiment when compared to the $F=0.40\text{L/h}$ experiment, but should be regarded as variance in the achieved productivity of the batch phases, since the batch phases were conducted under the same conditions. Only the $F=0.40\text{L/h}$ experiments showed an increase in the surfactin productivity and specific productivity at the onset of the fed-batch phase. These increases can be ascribed to large amounts of glucose and nitrate being added after the onset of the stationary phase. As the biomass increased, the demand for nitrate (to act as a terminal electron acceptor and complete the electron transport chain) increased which limited growth and ultimately caused the surfactin productivity and specific productivity to decrease.

The maximum specific surfactin productivities were achieved over the same period at which the maximum specific growth rates (Figure 3-39) were achieved. Similar findings were reported for the constant dilution rate experiments and thus confirm earlier results of a proportional relationship between specific surfactin productivity and specific growth rate.

The surfactin productivity and specific productivity of the $F=0.125\text{L/h}$ experiment decreased to approximately zero after the onset of the fed-batch phase, indicating very little surfactin production during this phase. These results indicate that a high constant feed rate is superior to a low constant feed rate for enhanced surfactin production during fed-batch culture.

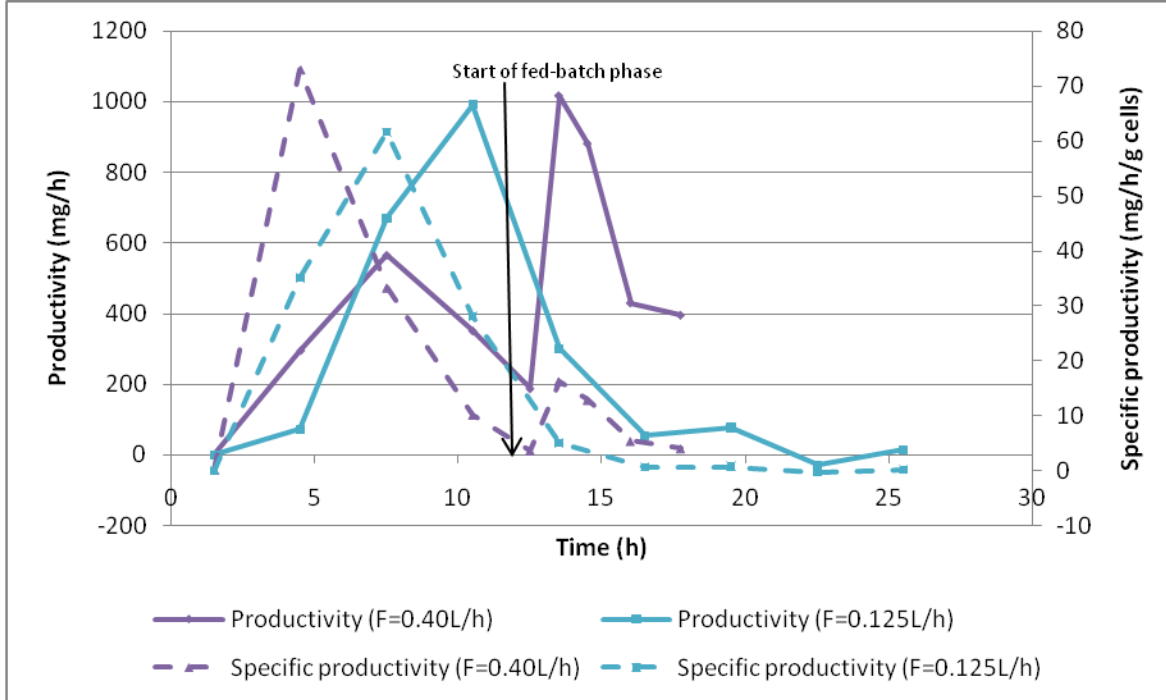


Figure 3-43: Surfactin productivity and specific productivity profiles of fed-batch cultures during which constant feeding strategies were applied

3.4 Surface activity of surfactin

One of the properties that characterize a surfactant is its ability to lower surface- and interfacial tensions. Culture supernatant of a sample withdrawn at the end of the batch phase of the $D=0.40h^{-1}$ experiment was used to evaluate the surface activity of surfactin. The surfactin concentration of this sample was determined to be 1662 mg/L and serial dilutions of this sample were prepared using pH 7.0 KH_2PO_4 buffer. A pH buffer was used since pH is known to affect surface tensions. The surface tension of each of the prepared dilutions was measured and the results are given in Figure 3-44.

The surface tensions of the prepared dilutions were all very similar, except for the sample which contained no surfactin and only pH 7.0 KH_2PO_4 buffer. The surface tension of the pH 7.0 buffer decreased from 67 mN/m to approximately 35 mN/m at a surfactin concentration of 13 mg/L. No further reduction in the surface tension was observed at higher surfactin concentrations. This indicated that the CMC of surfactin was approximately 13 mg/L. Generally, the CMC is determined from a semilog plot of surface tension versus the surfactant concentration. A semilog plot of the surface tension results would be of the same shape as that of Figure 3-44. It is evident from Figure 3-44 that the CMC of surfactin is 13 mg/L, which is less

than the minimum surfactin CMC of 21 mg/L reported by Peypoux *et al.* (1999). The difference may be due to small dilution errors in the preparation of the serial dilutions. However, a difference of 8 mg/L after 7 dilutions is an error of approximately 1 mg/L per dilution and may be considered insignificant.

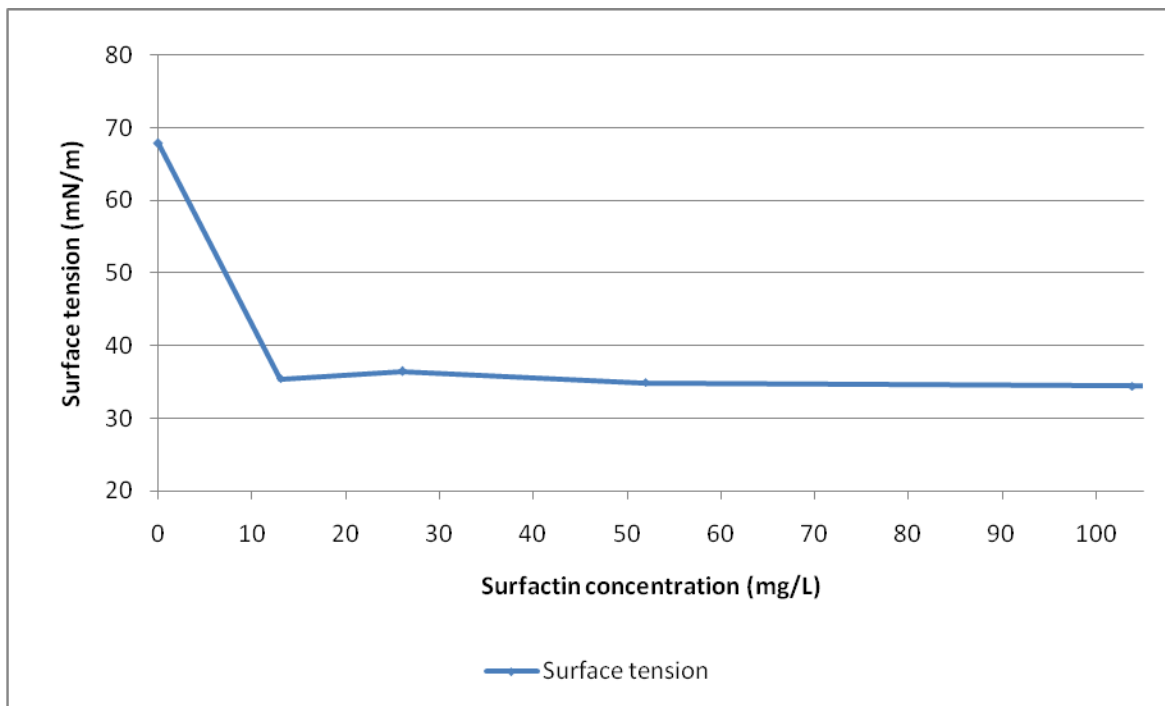


Figure 3-44: Plot of surface tension versus surfactin concentration

3.5 Antimicrobial activity of surfactin against *Mycobacterium aurum*

Surfactin has been reported to exhibit antimicrobial properties against numerous bacteria and fungi (see section 1.2.4.1). One of the objectives of this study was to determine whether surfactin showed antimicrobial activity against *M. aurum*. This organism is used as a surrogate for *M. tuberculosis*, the causative bacteria of the illness Tuberculosis, commonly known as TB.

Since surfactin is produced extracellularly, culture supernatant was tested for antimicrobial activity against *M. aurum*. Antimicrobial susceptibility assays of surfactin against *M. aurum* were performed based on the method described in section 2.4.6. Culture supernatant of a sample withdrawn at the end of the batch phase of the $D=0.40h^{-1}$ experiment was used for the antimicrobial assays. The surfactin concentration of this sample was determined to be 1662 mg/L. Serial dilutions of this sample were prepared using physiological saline (0.85% w/v) to determine a possible relationship between the surfactin concentration and the inhibition zone diameter.

In Figure 3-45 it is shown that surfactin exhibited antimicrobial activity against *M. aurum*. It can be seen that surfactin was unable to inhibit *M. aurum* growth at a surfactin concentration of 104 mg/L and that *M. aurum* growth was only inhibited from a surfactin concentration of 208 mg/L. This indicates that the MIC of surfactin against *M. aurum* lies somewhere between 104 mg/L and 208 mg/L. It is evident from Figure 3-45 that there could be a linear relationship between the surfactin concentration and the inhibition diameter. The inhibition diameter linearly increased from 4 mm at a surfactin concentration of 208 mg/L to 24 mm at a surfactin concentration of 1662 mg/L.

The inhibition diameters observed against *M. aurum* are in accordance with the inhibition zone diameters reported in literature against other bacteria. Typical reported inhibition zone diameters of surfactin against bacteria vary between 10 mm and 30 mm (Yakimov *et al.* 1995; Fernandes *et al.* 2007; Bechard *et al.* 1998). The different authors have used different disk diffusion assays to evaluate the antimicrobial activity of surfactin, and therefore the results obtained against *M. aurum* cannot be directly compared to that in literature. However, the antimicrobial activity results of surfactin against *M. aurum* indicate that surfactin can be applied as an antimicrobial agent against *M. aurum* to prevent the spread of this disease.

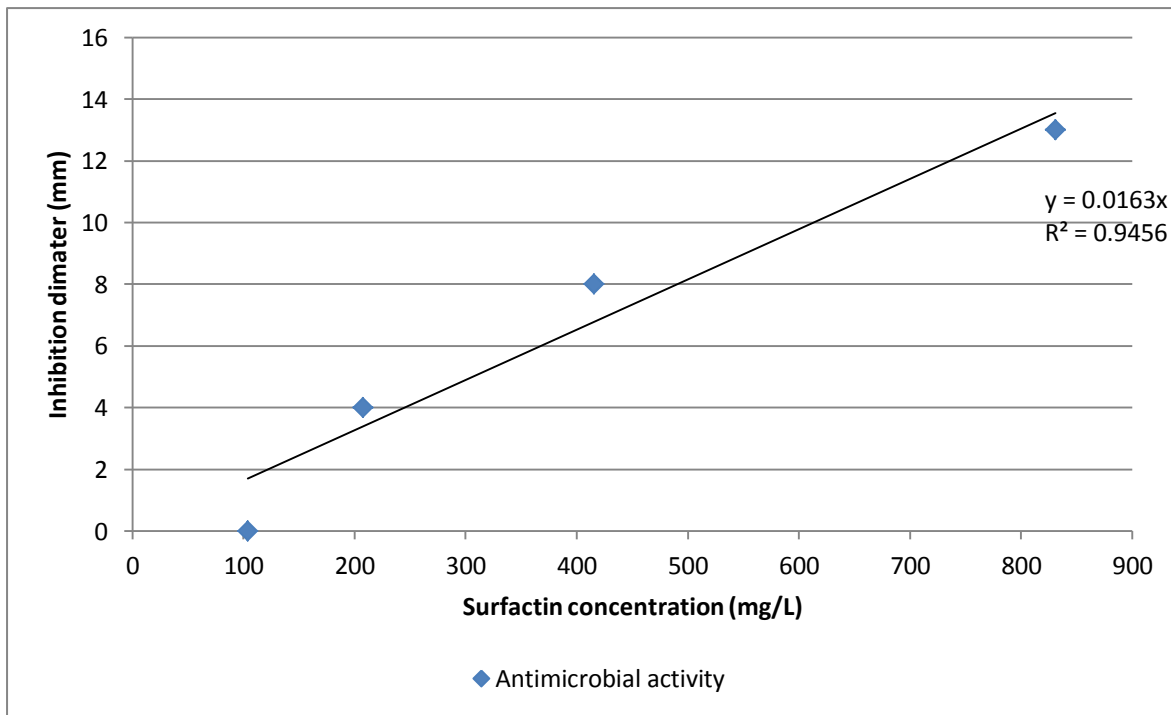


Figure 3-45: Relationship between surfactin concentration and antimicrobial activity (inhibition diameter) against *M. aurum*

3.6 Reproducibility of experiments

3.6.1 Shake flask experiments

The shake flask experiments were performed in duplicate to evaluate reproducibility. The reproducibility of the duplicate shake flask experiments was evaluated by considering the variance between certain key parameters, such as initial CDW; maximum CDW achieved; maximum surfactin concentration achieved; the initial glucose concentration; and the initial nitrate concentration. The reproducibility of these parameters is reported as the percentage reproducibility, which was calculated according to the following equation:

$$\text{Percentage reproducibility} = \left(1 - \frac{\text{stdev}}{\text{average}}\right) \times 100 \dots\dots\dots(\text{Equation 3-9})$$

Therefore, a percentage reproducibility of 100 would indicate perfect reproducibility, while a percentage reproducibility of 0 would indicate no reproducibility. The percentage reproducibility of the selected key parameters of the shake flask experiments is shown in Figure 3-46. It is evident that the shake flask experiments showed very good reproducibility, since the percentage reproducibility of most of the selected key parameters was greater than 90%. The reproducibility of the shake flask experiments indicate that the results discussed in section 3.1 are accurate and that the conclusions drawn from these results are valid.

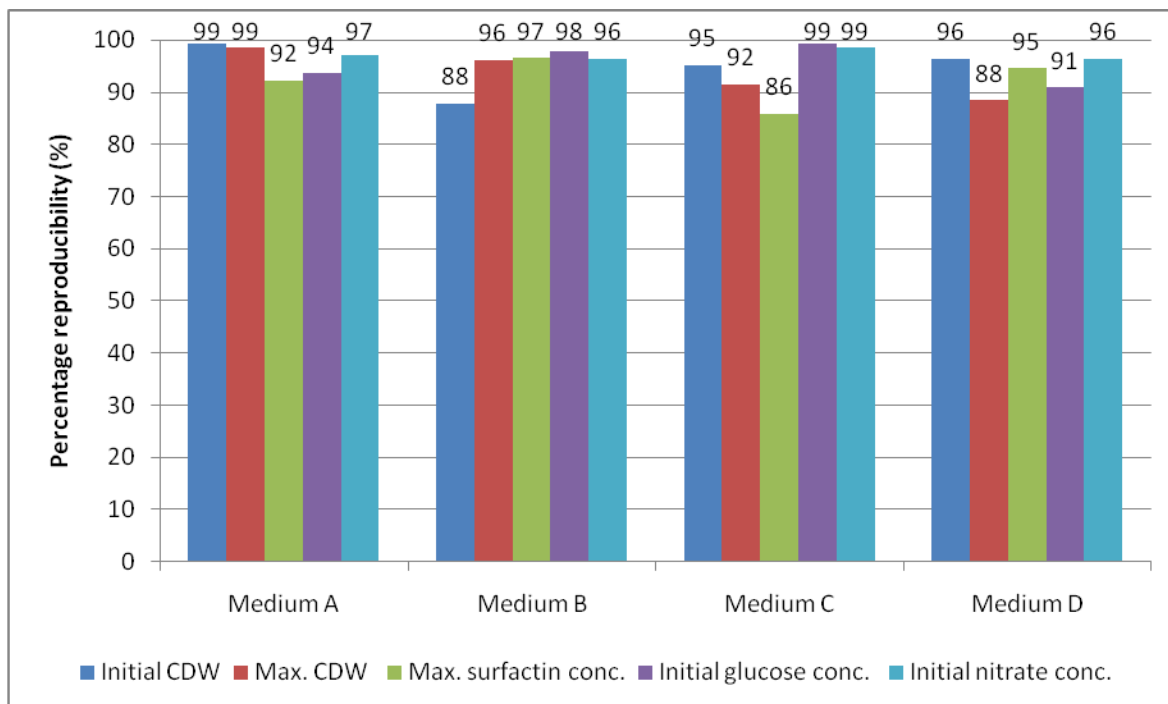


Figure 3-46: Percentage reproducibility of key parameters of shake flask experiments

3.6.2 Bioreactor experiments

A total of 7 bioreactor experiments (1 batch experiment and 6 batch phases of fed-batch experiments) were performed using configuration 1 during this study. Since the fed-batch phases of the fed-batch experiments were only started after the onset of the stationary phase, the batch phases of the 7 bioreactor experiments were performed under the same conditions. Therefore, the reproducibility of the bioreactor experiments was evaluated by considering the reproducibility of certain key parameters of the 7 batch phases.

The percentage reproducibility of the initial CDW (CDW at time of inoculation); the maximum CDW achieved; the maximum surfactin concentration achieved; the maximum surfactin productivity achieved; the initial glucose concentration (at time of inoculation) in the culture broth; and the initial nitrate concentration (at time of inoculation) in the culture broth are shown in Figure 3-47. It is evident from Figure 3-47 that all key parameters evaluated for reproducibility, except for the initial CDW, showed a percentage reproducibility of approximately 90%, indicating very good reproducibility. The low percentage reproducibility (52.14%) of the initial CDW is likely to be a result of sampling errors due to the low CDW at the time of inoculation. The reproducibility of the bioreactor experiments indicate that the experimental protocols followed for bioreactor experiments were reproducible and that the results obtained and discussed are accurate.

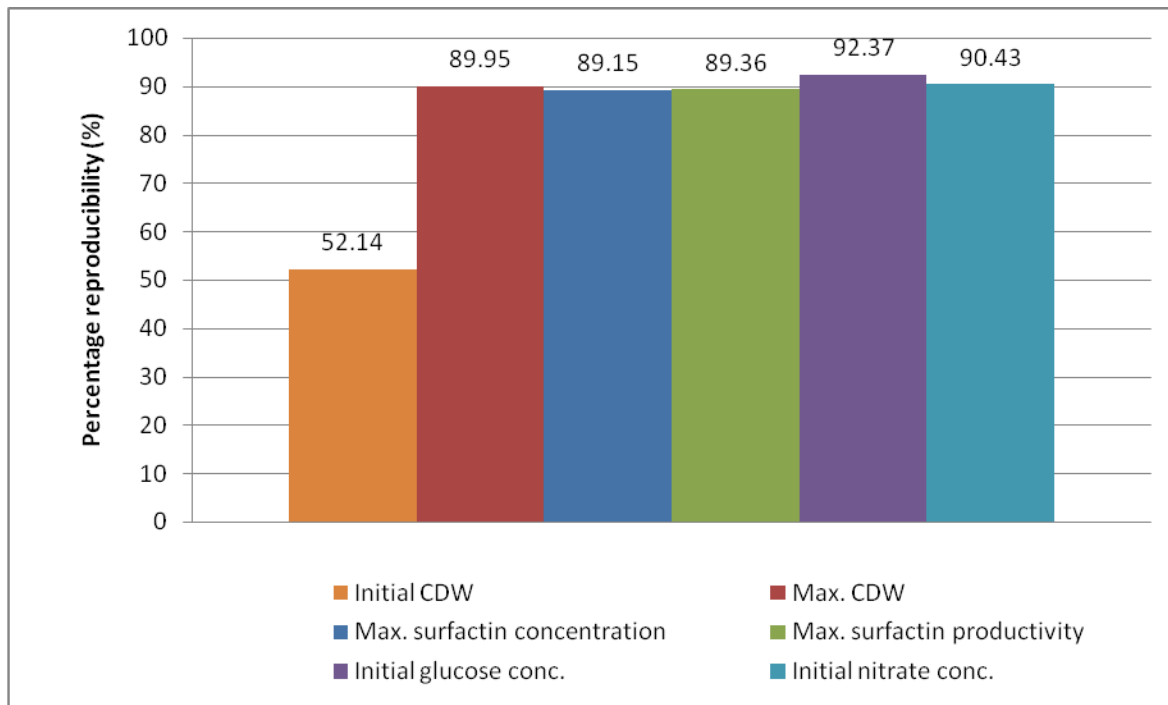


Figure 3-47: Percentage reproducibility of key parameters of bioreactor experiments

3.6.3 Antimicrobial activity

The antimicrobial activity of surfactin against *M. aurum* was evaluated according to the disk diffusion method described in section 2.4.6. Serial dilutions of a sample initially containing 1662 mg surfactin/L were prepared and evaluated for antimicrobial activity (see section 3.5). Since two wells per assay (see Figure 2-8) were evaluated for antimicrobial activity of surfactin, the reproducibility of the antimicrobial activity was evaluated by considering the variance of the inhibition zone diameters between the duplicate wells. However, no variance was observed between the inhibition zone diameters measured for each concentration of surfactin evaluated for antimicrobial activity. Thus, the antimicrobial assay used during this study was reproducible and reliable.

4 Conclusions

Based on the stated hypotheses and the results and discussion above, the following conclusions were drawn:

1. ***B. subtilis* ATCC 21332 was unable to utilize *n*-hexadecane for growth and surfactin production**

B. subtilis ATCC 21332 was inoculated into a medium containing only *n*-hexadecane as the sole carbon source. The cell concentration of this organism did not increase over a period of 119 h, which indicated that *B. subtilis* ATCC 21332 is unable to utilize *n*-hexadecane for growth and surfactin production.

2. **Surfactin from *B. subtilis* ATCC 21332 shows antimicrobial activity against *Mycobacterium aurum***

Surfactin showed antimicrobial activity against *M. aurum* at concentrations equal to and above 208 mg/L. An inhibition zone diameter of 4 mm was observed at a surfactin concentration of 208 mg/L and linearly increased to 24 mm at a surfactin concentration of 1662 mg/L.

The antimicrobial activity of surfactin against *M. aurum* indicates that this biosurfactant has the potential to be used as an antimicrobial agent against *M. tuberculosis*. The latter is a major cause of death in South Africa and has developed very resistant strains over recent years. Therefore, surfactin has the potential to be used in the medical industry to reduce the spread of this, and other deadly diseases.

3. **Active growth of *B. subtilis* ATCC 21332 and associated surfactin production can be maintained by applying constant- and exponential feeding rate strategies during fed-batch culture**

The total biomass and total amount of surfactin increased after the onset of the fed-batch phases of all fed-batch experiments. These results indicated that active growth and surfactin production was maintained during the fed-batch phases and therefore, fed-batch culture of *B. subtilis* ATCC 21332 can be used as a process strategy for improved surfactin production.

During the fed-batch phase of the $D=0.40\text{ h}^{-1}$ experiment, the average rate of biomass increase was shown to be 9 g/h. This average rate of biomass increase was 3.5-, 3.1- and 5.3-fold higher than that achieved during the fed-batch phases of the $D=0.15\text{ h}^{-1}$,

$D=0.10\text{h}^{-1}$ and $D=0.05\text{h}^{-1}$ experiments respectively. The average rate of surfactin production during the fed-batch phase of the $D=0.40\text{h}^{-1}$ experiment was shown to be 633 mg/h, which was 29.4-, 5.4- and 34.2-fold higher than that achieved during the fed-batch phases of the $D=0.15\text{h}^{-1}$, $D=0.10\text{h}^{-1}$ and $D=0.05\text{h}^{-1}$ experiments respectively.

The average rate of biomass increase during the fed-batch phase of the $F=0.40\text{L/h}$ experiment was shown to be 10.7 g/h. This average rate of biomass increase was 1.8-fold higher than that achieved during fed-batch phase of the $F=0.125\text{L/h}$ experiment. Analogously, the average rate of surfactin production in the $F=0.40\text{L/h}$ experiment was shown to be 545 mg/h, which was approximately 9-fold higher than that of the $F=0.125\text{L/h}$ experiment. These findings show that fed-batch culture of *B. subtilis* ATCC 21332 can be applied for enhanced surfactin production and further indicate that high feed flow rates show higher rates of biomass increase and higher rates of surfactin production.

The use of high feed flow rate strategies also show favorable kinetics. The surfactin yield on substrate, the surfactin yield on biomass as well as surfactin specific- and overall productivities have all been shown to be superior during the fed-batch phase of the $D=0.40\text{h}^{-1}$ experiment when compared to those of the $D=0.15\text{h}^{-1}$, $D=0.10\text{h}^{-1}$ and $D=0.05\text{h}^{-1}$ experiments. Similarly, the surfactin yield on substrate, the surfactin yield on biomass as well as surfactin specific- and overall productivities were all superior during the fed-batch phase of the $F=0.40\text{L/h}$ experiment when compared to that of the $F=0.125\text{L/h}$ experiment.

The improved surfactin specific- and overall productivities would decrease the large-scale production time of this biosurfactant. The improved yields indicate a higher conversion of substrate to product, which would ultimately reduce the cost of large-scale surfactin production.

5 Recommendations

Based on the results and discussion and the conclusions drawn, the following recommendations are made:

1. Ensure that nitrate in culture broth is in excess

- It was found that growth of *B. subtilis* ATCC 21332 and associated surfactin production was nitrate-limited during the fed-batch phases. Therefore, growth and surfactin production can be enhanced by increasing the nitrate feed concentration so that the nitrate concentration, as well as all other nutrients within the culture broth, is in excess.

2. Ensure that oxygen does not become limited

- An oxygen-limitation significantly affects growth and surfactin production by *B. subtilis*. Therefore, it is recommended that pure oxygen be combined with air to increase the oxygen concentration supplied to the culture broth to avoid an oxygen-limitation

3. Determine whether nitrate consumption increases as oxygen concentration decreases

It has been mentioned in section 1.8.1.4 that nitrate, nitrite and oxygen are the only terminal electron acceptors utilized by *B. subtilis*. However, the extent to which the consumption of one of these nutrients influences the other is still unknown.

4. Determine which terminal electron acceptor between oxygen, nitrate and nitrite is the preferred electron acceptor

- Compare the effect of the presence-; absence- and combinations of terminal electron acceptor(s) to establish which electron acceptor(s) has the greatest effect on growth of *B. subtilis* ATCC 21332 and associated surfactin production

-

5. Determine the influence of an oxygen-limitation to the preference for inorganic nitrogen sources

- Compare the influence of an oxygen-limitation on the rate of inorganic nitrogen source utilization by independently evaluating different inorganic nitrogen sources

6. Extend range of target organisms

- The antimicrobial activity of surfactin should be evaluated against common food pathogens (*in vivo*) to establish whether it can be used commercially to increase food security
- Compare the antimicrobial activity of surfactin against food spoilage micro-organisms to the antimicrobial activity of currently used antimicrobial agents to establish whether similar, or perhaps enhanced, antimicrobial activity can be achieved from antimicrobial biosurfactants

7. Time stability of surfactin

- The stability of surfactin surface- and antimicrobial activity over time should be investigated
- Long term storage possibilities for surfactin should be investigated

8. Continuous culture of *B. subtilis* ATCC 21332 as a process strategy for enhanced surfactin production

- Continuous culture can be used to maintain active growth at predetermined specific growth rates. Since surfactin production by *B. subtilis* ATCC 21332 is growth associated, the influence of the specific growth rate on surfactin production can be accurately determined by using continuous culture.
- Optimization studies on surfactin production during continuous culture to determine the process conditions optimizing surfactin yields and productivities

9. Evaluate other suitable hydrocarbons for growth and surfactin production by *B. subtilis* ATCC 21332

- Evaluate whether other hydrocarbons, e.g. benzene, kerosene and other linear alkanes, could be utilized by *B. subtilis* ATCC 21332 for growth and surfactin production. More available data regarding growth of *B. subtilis* on hydrocarbon substrates would indicate whether this organism will be a suitable choice for bioremediation

References

- Abalos, A., A. Pinazo, M.R. Infante, M. Casals, F. García and A. Manresa. 2000. Physicochemical and Antimicrobial Properties of New Rhamnolipids Produced by *Pseudomonas aeruginosa* AT10 from Soybean Oil Refinery Wastes. *Langmuir* 17: 1367-1371.
- Abushady, H.M., A.S. Bashandy, N.H. Aziz and H.M.M. Ibrahim. 2005. Molecular characterization of *Bacillus subtilis* surfactin producing strain and the factors affecting its production. *Int J Agri Biol* 7: 337-344.
- Akpa, E., P. Jacques, B. Wathélet, M. Paquot, R. Fuchs, H. Budzikiewicz and P. Thonart. 2001. Influence of Culture Conditions on Lipopeptide Production by *Bacillus subtilis*. *Applied Biochemistry and Biotechnology* 93: 551-561.
- Arima, K., A. Kakinuma and G. Tamura. 1968. Surfactin, a crystalline peptide lipid surfactant produced by *Bacillus subtilis*: isolation, characterization and its inhibition of fibrin clot formation. *Biochem Biophys Res Commun* 31: 488-494.
- Assié, L.K., M. Deleu, L. Arnaud, M. Paquot, P. Thonart, Ch. Gasper and E. Haubruge. 2002. Insecticide activity of surfactins and iturins from a biopesticide *Bacillus subtilis* cohn (S499 strain). *Med. Fac. Landbouww. Univ. Gent*.67/3.
- Awerbuch, T.E., L. Lustman and J.M. Piret. 1989. A numerical method to determine minimal inhibitory concentrations (MICs) of antibiotics directly from disc-diffusion susceptibility tests. *Journal of Microbiological Methods* 9:1-7.
- Ballot, F. 2009. Bacterial production of antimicrobial biosurfactants. *MScEng thesis*. University of Stellenbosch.
- Bauer, A.W., W.M. Kirby, J.C. Sherris and M. Turck. 1966. Antibiotic susceptibility testing by a standardized single disk method. *American Journal of Clinical Pathology* 45: 493-496.
- Bechard, J., K.C. Eastwell, P.L. Sholberg, G. Mazza and B. Skura. 1998. Isolation and Partial Chemical Characterization of an Antimicrobial Peptide Produced by a Strain of *Bacillus subtilis*. *J. Agric. Food Chem.* 46: 5355-5361.
- Benincasa, M., A. Abalos, I. Oliveira and A. Manresa. 2004. Chemical structure, surface properties and biological activities of the biosurfactant produced by *Pseudomonas aeruginosa* LBI from soapstock. *Antonie van Leeuwenhoek* 85: 1-8.
- Besson, F., F. Peypoux, G. Michel and L. Delcambe. 1976. Characterization of Iturin A in Antibiotics from various strains of *Bacillus subtilis*. *The Journal of Antibiotics*.XXIX No. 10: 1043-1049.
- Buchoux, S., J. Lai-Kee-Him, M. Garnier, P. Tsan, F. Besson, A. Brisson and E.J. Dufourc. 2008. Surfactin-Triggered Small Vesicle Formation of Negatively Charged Membranes: A Novel Membrane-Lysis Mechanism. *Biophysical Journal* 95: 3840-3849.

- Carillo, C., J.A. Tereul, F.J. Aranda and A. Ortiz. 2003. Molecular mechanism of membrane permeabilization by the peptide antibiotic surfactin. *Biochimica et Biophysica Acta* 1611: 91-97.
- Cayuela, C., K. Kai, Y.S. Park, S. Iijima and T. Kobayashi. 1993. Insecticide production by recombinant *Bacillus subtilis* 1A96 in fed-batch culture with control of glucose concentration. *Journal of Fermentation and Bioengineering*. Vol. 75, No. 5: 383-386.
- Chen, C-Y., S.C. Baker and R.C. Darton. 2006. Batch production of biosurfactant with foam fractionation. *Journal of Chemical Technology and Biotechnology* 81: 1923-1931.
- Chen, C-Y., S.C. Baker and R.C. Darton. 2006. Continuous production of biosurfactant with foam fractionation. *Journal of Chemical Technology and Biotechnology* 81: 1915-1922
- Chen, S-Y., Y-H. Wei and J-S. Chang. 2007. Repeated pH-stat fed-batch fermentation for rhamnolipid production with indigenous *Pseudomonas aeruginosa* S2. *Appl. Microbiol. Biotechnol.* 76: 67-74.
- Chenikher, S., J.S. Guez, F. Coutte, M. Pekpe, P. Jacques and J.P. Cassar. 2010. Control of the specific growth rate of *Bacillus subtilis* for the production of biosurfactant lipopeptides in bioreactors with foam overflow. *Process Biochemistry*. (Article in Press).
- Chia, M., T.B.C. Nguyen and W.J. Choi. 2008. DO-stat fed-batch production of 2-keto-D-gluconic acid from cassava using immobilized *Pseudomonas aeruginosa*. *Appl. Microbiol. Biotechnol.* 78: 759-765.
- Cho, Y-H., J.Y. Song, K.M. Kim, M.K. Kim, I.Y. Lee, S.B. Kim, H.S. Kim, N.S. Han, B.H. Lee and B.S. Kim. 2010. Production of nattokinase by batch and fed-batch culture of *Bacillus subtilis*. *New Biotechnology*. Vol. 27, No. 4: 341-346.
- Clarke, K. G., F. Ballot and S.J. Reid. 2010. Enhanced rhamnolipid production by *Pseudomonas aeruginosa* under phosphate limitation. *World Journal of Microbial Biotechnology* 26: 2179-2184.
- Clements, L. D. B. S. Miller and U. N. Streips. 2002. Comparative growth analysis of the facultative anaerobes *Bacillus subtilis*, *Bacillus licheniformis* and *Escherichia coli*. *Systematic and Applied Microbiology* 25: 284-286.
- Cooper, D.G. and J.E. Zajic. 1980. Surface active compounds from microorganisms. *Adv Appl Microbiol* 26: 229-256.
- Cooper, D.G., C.R. MacDonald, S.J.B. Duff and N. Kosaric. 1981. Enhanced production of surfactin from *Bacillus subtilis* by continuous product removal and metal cation additions. *Applied and Environmental Microbiology* 42: 408-412.
- Cooper, D.G., B.G. Goldenberg. 1987. Surface-active agents from two *Bacillus* species. *Appl Environ Microbiol* 53 (2): 224-229.
- Cubitto, M.A., A.C. Moran, M. Commendatore, M.N. Chiarello, M.D. Baldini and F. Siñeriz. 2004. Effects of *Bacillus subtilis* O9 on the bioremediation of crude oil-polluted soils. *Biodegradation* 15: 281-287.

- Das, K. and A.K. Mukherjee. 2006. Crude petroleum-oil biodegradation efficiency of *Bacillus subtilis* and *Pseudomonas aeruginosa* strains isolated from a petroleum-oil contaminated soil from North-East India. *Bioresource Technology* 98: 1339-1345.
- Davis, D.A., H.C. Lynch and J. Varley. 1999. The production of Surfactin in batch culture by *Bacillus subtilis* ATCC 21332 is strongly influenced by the conditions of nitrogen metabolism. *Enzyme and Microbial Technology* 25: 322-329.
- Deleu, M., M. Paquot and T. Nylander. 2008. Effect of Fengycin, a Lipopeptide Produced by *Bacillus subtilis*, on Model Biomembranes. *Biophysical Journal* 94: 2667-2679.
- Deleu, M., M. Paquot and T. Nylander. 2005. Fengycin interaction with monolayers at the air-aqueous interface – implications for the effect of fengycin on biological membranes. *Journal of Colloid and Interface Science* 283: 358-365.
- Deleu, M., H. Razafindralambo, Y. Popineau, P. Jacques, P. Thonart and M. Paquot. 1999. Interfacial and emulsifying properties of lipopeptides from *Bacillus subtilis*. *Colloids and Surfaces. A: Physicochemical and Engineering Aspects* 152: 3-10.
- Desai, J.D. and I.M. Banat. 1997. Microbial Production of Surfactants and Their Commercial Potential. *Microbiology and Molecular Biology Reviews*. Vol. 61, No. 1: 47-64.
- Déziel, E., G. Paquette, R. Villemur, F. Lépine and J. Bisailon. 1996. Biosurfactant production by a soil *Pseudomonas* strain growing on polyaromatic hydrocarbons. *Appl Environ Microbiol* 62: 1908-1912.
- Ding, S. and T. Tan. 2006. L-lactic acid production by *Lactobacillus casei* fermentation using different fed-batch feeding strategies. *Process Biochemistry* 41: 1451-1454.
- du Toit, E.A. and M. Rautenbach. 2000. A sensitive standardised micro-gell well diffusion assay for the -determination of antimicrobial activity. *Journal of Microbial Methods* 42: 159-165.
- Fernandes, P.A.V., I.R. de Arruda, A.F.A.B. dos Santos, A.A. de Araújo, A.M.S. Maior and E.A. Ximenes. 2007. Antimicrobial activity of surfactants produced by *Bacillus subtilis* R14 against multidrug-resistant bacteria. *Brazilian Journal of Microbiology* 38: 704-709.
- Glaser, P., A. Dunchin, F. Kunst, P. Zuber and M.M. Nakano. 1995. Identification and isolation of a gene required for nitrate assimilation and anaerobic growth of *Bacillus subtilis*. *Journal of Bacteriology*. Vol. 177, No. 4: 1112-1115.
- Grau, A., J.C. Gómez Fernández, F. Peypoux and A. Ortiz. 1999. A study on the interactions of surfactin with phospholipid vesicles. *Biochimica et Biophysica Acta* 1418: 307-319.
- Guerra-Santos, L.H., O. Käppeli and A. Fiechter. 1986. Dependence of *Pseudomonas aeruginosa* continuous culture biosurfactant production on nutritional and environmental factors. *Appl Microbiol Biotechnol* 24:443–448.
- Guez, J.S., S. Chenikher, J.Ph. Cassar and P. Jacques. 2007. Setting up and modeling of overflowing fed-batch cultures of *Bacillus subtilis* for the production and continuous removal of lipopeptides. *Journal of Biotechnology* 131: 67-75.

- Haba, E., A. Pinazo, O. Jauregui, M.J. Espuny, M.R. Infante and A. Manresa. 2003. Physicochemical characterization and antimicrobial properties of rhamnolipids produced by *Pseudomonas aeruginosa* 47T2 NCIB 40044. *Biotechnology and Bioengineering* 81: 316-322.
- Heerklotz, H. and J. Seelig. 2001. Detergent-Like Action of the Antibiotic Peptide Surfactin on Lipid membranes. *Biophysical Journal* 81: 1547-1554.
- Heerklotz, H. and J. Seelig. 2007. Leakage and Lysis of lipid membranes induced by the lipopeptide surfactin. *Eur. Biophys. J.* 36: 305-314.
- Heerklotz, H., T. Wieprecht and J. Seelig. 2004. Membrane Perturbation by the Lipopeptide Surfactin and Detergents as Studied by Deuterium NMR. *J. Phys. Chem. B.* 108: 4909-4915.
- Hoffman, T., B. Troup, A. Szabo, C. Hungerer and D. Jahn. 1995. The anaerobic life of *Bacillus subtilis*: Cloning of the genes encoding the respiratory nitrate reductase system. *FEMS Microbiology Letters* 131: 219-225.
- Hommel, R.K. 1990. Formation and physiological role of biosurfactants produced by hydrocarbon-utilizing microorganisms. *Biodegradation* 1: 10-119.
- Itoh, S., H. Honda, F. Tomita and T. Suzuki. 1971. Rhamnolipids produced by *Pseudomonas aeruginosa* grown on n-paraffin (mixture of C₁₂, C₁₃ and C₁₄ fractions). *Journal of Antibiotics* 24: 855.
- Jing, C., S. Xin, Z. Hui and Q. Yinbo. 2006. Production, structure elucidation and anticancer properties of sophorolipids from *Wickerhamiella domercqiae*. *Enzyme and Microbial Technology* 39: 501-506.
- Jorgensen, J.H. and M.J. Ferraro. 1998. Antimicrobial susceptibility testing: General principles and contemporary practices. *Clinical Infectious Diseases* 26: 973-980.
- Joshi, S., C. Bharucha and A.J. Desai. 2008. Production of biosurfactant and antifungal compound by fermented food isolate *Bacillus subtilis* 20B. *Bioresource Technology* 99: 4603-4608.
- Kakinuma, A., M. Hori, M. Isono, G. Tamura and K. Arima. 1969(a). Determination of amino acid sequence in surfactin, a peptidelipid surfactant produced by *Bacillus subtilis*. *Agric. Biol. Chem.* 33: 971-972.
- Kakinuma, A., M. Hori, H. Sugino, I. Yoshida, M. Isono, G. Tamura and K. Arima. 1969(b). Determination of the location of lactone ring in surfactin. *Agric. Biol. Chem.* 33: 1523-1534.
- Kakinuma, A., H. Sugino, I. Yoshida, M. Isono, G. Tamura and K. Arima. 1969(c). Determination of fatty acid in surfactin and elucidation of total structure of surfactin. *Agric. Biol. Chem.* 33: 973-976.

- Kim, H-S., S-B.Kim, S-H.Park, H-M. Oh, Y-I. Park, C-K.Kim, T. Katsuragi, Y. Tani and B-D.Yoon. 2000. Expression of *sfp* gene and hydrocarbon degradation by *Bacillus subtilis*. *Biotechnology Letters* 22: 1431-1436.
- Kim, H-S., B-D.Yoon, C-H.Lee, H-H.Suh, H-M. Oh, T. Katsuragi and Y. Tani. 1997. Production and properties of a lipopeptide biosurfactant from *Bacillus subtilis* C9. *Journal of Fermentation and Bioengineering*. Vol. 84, No. 1: 41-46.
- Kim, S-y., J.Y. Kim, S-H. Kim, H.J. Bae, H. Yi, S.H. Yoon, B.S. Koo, M. Kwon, J.Y. Cho, C-E. Lee and S. Hong. 2007. Surfactin from *Bacillus subtilis* displays anti-proliferative effect via apoptosis induction, cell cycle arrest and survival signaling suppression. *FEBS Letters* 581: 865-871.
- Kitamoto, D., H. Yanagishita, T. Shinbo, T. Nakane, C. Kamisawa and T. Nakahara. 1993. Surface active properties and antimicrobial activities of mannosylerythritol lipids as biosurfactants produced by *Candida Antarctica*. *Journal of Biotechnology* 29: 91-96.
- Kosaric, N. 1993. *Biosurfactants: Production, properties, applications*. CRC Press.
- Kracht, M., H. Rokos, M. Özel, M. Kowall, G. Pauli and J. Vater. 1999. Antiviral and hemolytic activities of surfactin isoforms and their methyl ester derivatives. *The Journal of Antibiotics*. Vol. 52, No. 7: 613-619.
- Lang, S. and J.C. Philp. 1998. Surface-active lipids in rhodococci. *Antonie van Leeuwenhoek* 74: 59-70.
- Lang, S. and D. Wullbrandt. 1999. Rhamnose-lipids – biosynthesis, microbial production and application potential. *Applied Microbiology and Biotechnology* 51: 22-32.
- Lee, J. S.Y. Lee, S. Park and A.P.J. Middelberg. 1999. Control of fed-batch fermentations. *Biotechnology Advances* 17: 29-48.
- Lehrer, R.I., M. Rosenman, S.S.S.L. Harwig, R. Jackson and P. Eisenhauer. 1991. Ultrasensitive assays for endogenous antimicrobial polypeptides. *Journal of Immunological Methods* 137: 167-173.
- Lin, S-C. and H-J. Jaing. 1997. Recovery and purification of the lipopeptide biosurfactant of *Bacillus subtilis* by ultrafiltration. *Biotechnology Techniques*. Vol. 11, No. 6: 413-416.
- Maget-Dana, R. and M. Ptak. 1995. Interactions of Surfactin with Membrane Models. *Biophysical Journal*. Vol. 68: 1937-1943.
- Makkar, R.S. and S.S. Cameotra. 2002. An update on the use of unconventional substrates for biosurfactant production and their new applications. *Applied Microbiology and Biotechnology* 58: 428-434.
- Makkar, R.S. and S.S. Cameotra. 1997. Biosurfactant production by a thermophilic *Bacillus subtilis* strain. *Journal of Industrial Microbiology and Biotechnology* 18: 37-42.
- Makkar, R.S. and S.S. Cameotra. 1998. Production of Biosurfactant at mesophilic and thermophilic conditions by a strain of *Bacillus subtilis*. *Journal of Industrial Microbiology and Biotechnology* 20: 48-52.

- Makkar, R.S. and S.S. Cameotra. 1997. Utilization of Molasses for Biosurfactant Production by Two *Bacillus* Strains at Thermophilic Conditions. *JAOCS*. Vol. 74, No. 7: 887-889.
- Matar, S.M., S.A. El-Kazzaz, E.E. Wagih, A.I. El-Diwany, H.E. Moustafa, M.A. El-Saadani, G.A. Abo-Zaid and E.E. Hafez. 2009. Bioprocessing and scaling-up cultivation of *Bacillus subtilis* as a potential antagonist to certain plant pathogenic fungi, III. *Biotechnology*. Vol. 8, No. 1: 138-143.
- Marais, C. Chemical engineer, MScEng graduate 2010, Department of Process Engineering, University of Stellenbosch.
- Martínez, A., O.T. Ramírez and F. Valle. 1998. Effect of growth rate on the production of β -galactosidase from *Escherichia coli* in *Bacillus subtilis* using glucose-limited exponentially fedbatch cultures. *Enzyme and Microbial Technology* 22: 520-526.
- Moat, A.G., J.W. Foster. 1995. *Microbial Physiology*. Wiley-Liss Inc.
- Morán, A.C., N. Olivera, M. Comondatore, J.L. Esteves and F. Siñeriz. 2000. Enhancement of hydrocarbon waste biodegradation by addition of a biosurfactant from *Bacillus subtilis* O9. *Biodegradation* 11: 65-71.
- Mulligan, C.N., G. Mahmoudides and B.F. Gibbs. 1989. The influence of phosphate metabolism on biosurfactant production by *Pseudomonas aeruginosa*. *Journal of Biotechnology* 12: 199-210.
- Mulligan, C.N., R.N. Yong and B.F. Gibbs. 2001. Heavy metal removal from sediments by biosurfactants. *Journal of Hazardous Materials* 85: 111-125.
- Mulligan, C.N., R.N. Yong and B.F. Gibbs. 2001. Surfactant-enhanced remediation of contaminated soil: a review. *Engineering geology* 60: 371-380.
- Nakano, M.M., Y.P. Dailly, P. Zuber and D.P. Clark. 1997. Characterization of anaerobic fermentative growth of *Bacillus subtilis*: Identification of fermentation end products and genes required for growth. *Journal of Bacteriology*. Vol. 179, No. 21: 6749-6755.
- Nakano, M.M. and F. M. Hulett. 1997. Adaptation of *Bacillus subtilis* to oxygen limitation. *FEMS Microbiology Letters* 157: 1-7.
- Nakano, M.M and P. Zuber. 1998. Anaerobic growth of a "strict" aerobe (*Bacillus subtilis*). *Annu. Rev. Microbiol.* 52: 165-190.
- Ochsner, U., J. Reiser, A. Fiechter and B. Witholt. 1995. Production of *Pseudomonas aeruginosa* rhamnolipid biosurfactants in heterologous hosts. *Appl Environ Microbiol.* 68: 3503-3506.
- Ogawa, K., E. Akagawa, K. Yamane, Z.W. Sun, M. LaCelle, P. Zuber and M.M. Nakano. 1995. The nasB operon and nasA gene are required for nitrate/nitrite assimilation in *Bacillus subtilis*. *Journal of Bacteriology* Vol. 177, No. 5: 1409-1413.
- Oh, J.S., B-G. Kim and T.H. Park. 2002. Importance of specific growth rate for subtilisin expression in fed-batch cultivation of *Bacillus subtilis* *spoilG* mutant. *Enzyme and Microbial Technology* 30: 747-751.

- Ohno, A., T. Ano and M. Shoda. 1995. Effect of temperature on production of lipopeptide antibiotics, Iturin A and Surfactin by a dual producer, *Bacillus subtilis* R14, in solid-state fermentation. *Journal of Fermentation and Bioengineering*. Vol. 80, No. 5: 517-519.
- Okigbo, R.N. 2005. Biological control of postharvest fungal rot of yam (*Dioscorea* spp.) with *Bacillus subtilis*. *Mycopathologia* 159: 307-314.
- Painter, H.A. 1970. A review of literature on inorganic nitrogen metabolism in microorganisms. *Water Research* 4: 393-450.
- Patel, V.J., S.R. Tendulkar and B.B. Chattoo. 2004. Bioprocess development for the production of an antifungal molecule by *Bacillus licheniformis* BC98. *Journal of Bioscience and Bioengineering*. Vol. 98, No. 4: 231-235.
- Peypoux, F., J.M. Bonmatin and J. Wallach. 1999. Recent trends in the biochemistry of surfactin. *Appl. Microbiol. Biotechnol.* 51: 553-563.
- Razafindralambo, H., M. Paquot, A. Baniel, Y. Popineau, C. Hbid, P. Jacques and P. Thonart. 1996. Foaming Properties of Surfactin, a Lipopeptide Biosurfactant from *Bacillus subtilis*. *JAOCS* 73: 149-151.
- Rodrigues, L., H.C. van der Mei, J. Teixeira and R. Oliveira. 2004. Influence of biosurfactants from probiotic bacteria on formation of biofilms on voice prostheses. *Applied and Environmental Microbiology*. Vol. 70, No. 7: 4408-4410.
- Rodrigues, L.R., J.A. Teixeira, H.C. van der Mei and R. Oliveira. 2006. Physicochemical and functional characterization of a biosurfactant produced by *Lactobacillus lactis* 53. *Colloids and Surfaces B: Biointerfaces* 49: 79-86.
- Sabaté, D.C., L. Carillo and M.C. Audisio. 2009. Inhibition of *Paenibacillus larvae* and *Ascosphaera apis* by *Bacillus subtilis* isolated from honeybee gut and honey samples. *Research in Microbiology* 160: 193-199.
- Sen, R. and T. Swaminathan. 1997. Application of response-surface methodology to evaluate the optimum environmental conditions for the enhanced production of surfactin. *Appl. Microbiol. Biotechnol.* 47: 358-363.
- Sen, R. and T. Swaminathan. 2004. Response surface modeling and optimization to elucidate and analyze the effects of inoculum age and size on surfactin production. *Biochemical Engineering Journal* 21: 141-148.
- Seydlová, G., J. Svobodová. 2008. Review of surfactin chemical properties and the potential biomedical applications. *Central European Journal of Medicine*. Vol. 3, No. 2: 123-133.
- Shene, C., N. Mir, B.A. Andrews and J.A. Asenjo. 2000. Effect of the growth conditions on the synthesis of a recombinant β -1,4-endoglucanase in continuous and fed-batch culture. *Enzyme and Microbial Technology* 27: 248-253.
- Sheppard, J.D., C. Jumarie, D.G. Cooper and R. Laprade. 1991. Ionic channels induced by surfactin in planar lipid bilayer membranes. *Biochimica et Biophysica Acta – Biomembranes* 1064: 13-23.

- Sheppard, J.D. and D.G. Cooper. 1990. The response of *Bacillus subtilis* ATCC 21332 to manganese during continuous-phased growth. *Applied Microbiology and Biotechnology* 35: 72-76.
- Sheppard, J.D. and C.N. Mulligan. 1987. The production of surfactin by *Bacillus subtilis* grown on peat hydrolysate. *Applied Microbiology and Biotechnology* 27: 110-116.
- Sim, L., O.P. Ward and Z-Y. Li. 1997. Production and characterization of a biosurfactant isolated from *Pseudomonas aeruginosa* UW-1. *Journal of Industrial Microbiology and Biotechnology* 19: 232-238.
- Singh, A., J.D. Van Hamme and O.P. Ward. 2007. Surfactants in microbiology and biotechnology: Part 2. Application aspects. *Biotechnology Advances* 25: 99-121.
- Singh, P. and S.S. Cameotra. 2004. Potential applications of microbial surfactants in biomedical sciences. *TRENDS in Biotechnology*. Vol. 22, No. 3: 142-146.
- Statistics South Africa. <http://www.statssa.gov.za/publications/statkeyfindings>. P0309.3. Mortality and causes of death in South Africa – Findings from death notification, 2007.
- Suwansukho, P., V. Rukachisirikul, F. Kawai and A.H-Kittikun. 2008. Production and applications of biosurfactant from *Bacillus subtilis* MUV4. *Songklanakarin Journal of Science and Technology* 30: 87-93.
- Tamehiro, N., Y. Okamoto-Hosoya, S. Okamoto, M. Ubukata, M. Hamada, H. Naganawa and K. Ochi. 2002. Bacilysoicin, a Novel Phospholipid Antibiotic Produced by *Bacillus subtilis* 168. *Antimicrobial Agents and Chemotherapy*. Vol. 46, No. 2: 315-320.
- Thanomsub, B., W. Pumeechockchai, A. Limtrakul, P. Arunrattiyakorn, W. Petchleelaha, T. Nitoda and H. Kanzaki. 2006. Chemical structures and biological activities of rhamnolipids produced by *Pseudomonas aeruginosa* B189 isolated from milk factory waste. *Bioresource Technology* 97: 2457-2461.
- Thimon, L., F. Peypoux, J. Wallach and G. Michel. 1995. Effect of lipopeptide antibiotic, iturin A, on morphology and membrane ultrastructure of yeast cells. *FEMS Microbiology Letters* 128: 101-106.
- Touré, Y., M. Ongena, P. Jacques, A. Guiro and P. Thonart. 2004. Role of lipopeptides produced by *Bacillus subtilis* GA1 in the reduction of grey mold disease caused by *Botrytis cinerea* on apple. *Journal of Applied Microbiology* 96: 1151-1160.
- Van Hamme, J.D., A. Singh, O.P. Ward. 2006. Physiological aspects: Part 1 in a series of papers devoted to surfactants in microbiology and biotechnology. *Biotechnology Advances* 24: 604-620.
- Vanittanakom, N., W. Loeffler, U. Koch and G. Jung. 1986. Fengycin – A Novel Antifungal Lipopeptide Antibiotic Produced by *Bacillus subtilis* F-29-3. *The Journal of Antibiotics*. Vol. XXXIX, No. 7: 888-901.

- Vollenbroich, D., M. Özel, J. Vater, R.M. Kamp and G. Pauli. 1997. Mechanism of Inactivation of enveloped viruses by the biosurfactant surfactin from *Bacillus subtilis*. *Biologicals* 25: 289-297.
- Vuolanto, A., N. von Weymarn, J. Kerovu, H. Ojamo and M Leisola. 2001. Phytase production by high cell density culture of recombinant *Bacillus subtilis*. *Biotechnology Letters* 23: 761-766.
- Walsh, C. 2003. *Antibiotics – Actions, Origins, Resistance*. ASM Press.
- Wei, Y-H., C-C.Lai and J-S.Chang. 2007. Using Taguchi experimental design methods to optimize trace element composition for enhanced surfactin production by *Bacillus subtilis* ATCC 21332. *Process Biochemistry* 42: 40-45.
- Wei, Y-H. and I-M. Chu. 2002. Mn²⁺ improves surfactin production by *Bacillus subtilis*. *Biotechnology Letters* 24: 479-482.
- Wei, Y-H. and I-M. Chu. 1998. Enhancement of surfactin production in iron-enriched media by *Bacillus subtilis* ATCC 21332. *Enzyme and Microbial Technology* 22: 724-728.
- Wei, Y-H., L-F Wang, J-S.Chang and S-S Kung. 2003. Identification of Induced Acidification in Iron-Enriched Cultures of *Bacillus subtilis* during Biosurfactant Fermentation. *Journal of Bioscience and Bioengineering*. Vol. 96, No. 2: 174-178.
- White, D. 2007. *The Physiology and Biochemistry of Prokaryotes*. Oxford University Press.
- Yakimov, M.M., K.N. Timmis, V. Wray and H.L. Fredrickson. 1995. Characterization of a new lipopeptide surfactant produced by thermotolerant and halotolerant subsurface *Bacillus licheniformis* BAS50. *Applied and Environmental Microbiology*. Vol. 61, No. 5: 1706-1713.
- Yeh, M-S., Y-H.Wei and J-S.Chang. 2006. Bioreactor design for enhanced carrier-assisted surfactin production with *Bacillus subtilis*. *Process Biochemistry* 41: 1799-1805.
- Zhang, Y. and R.M. Miller. 1992. Enhanced octadecane dispersion and biodegradation by a *Pseudomonas* rhamnolipid surfactant (biosurfactant). *Appl Environ Microbiol* 58: 3276-3282.
- Zhang, T., Z-Q.Shi, L-B.Hu, L-G.Cheng and F. Wang. 2008. Antifungal compounds from *Bacillus subtilis* B-FS06 inhibiting the growth of *Aspergillus flavus*. *World J Microbiol Biotechnol* 24: 783-788.

Appendix A: Fed-batch Kinetics

Derivation of unsteady-state rate equations

During fed-batch culture, nutrients are continuously added to maintain desired process conditions. Due to the addition of nutrients to the culture broth, the volume increases with time. As there is no flow out of the reactor during fed-batch culture, a total mass balance over the fed-batch system is derived as follows:

$$\frac{d(\rho V)}{dt} = F_i \rho_i - F_o \rho_o \quad \text{Equation A-1}$$

where ρ is the density of the reactor contents.

Equation A-1 may be simplified by assuming a constant density of the reactor contents and also no flow out of the reactor. Applying these assumptions to Equation A-1 would then yield Equation A-2:

$$\frac{dV}{dt} = F_i \quad \text{Equation A-2}$$

A cell- and limiting substrate balance is required to evaluate kinetic parameters. A cell balance may be derived in a similar way to that of the total mass balance. However, the rate of biomass generation, equal to $\mu x V$ shall be included in the derivation. The cell balance is given by the following equation:

$$\frac{d(xV)}{dt} = Fx_i + \mu x V \quad \text{Equation A-3}$$

where μ is the specific growth rate.

The differential on the left-hand side of Equation A-3 is expanded by applying the product rule. This is done because V cannot be cancelled as it is a function of time. This yields Equation A-4.

$$x \frac{dV}{dt} + V \frac{dx}{dt} = Fx_i + \mu x V \quad \text{Equation A-4}$$

Substituting Equation A-2 into Equation A-4 gives:

$$xF + V \frac{dx}{dt} = Fx_i + \mu x V \quad \text{Equation A-5}$$

Dividing Equation A-5 through by V and rearranging yields Equation A-6.

$$\frac{dx}{dt} = \frac{F}{V} x_i + x(\mu - \frac{F}{V}) \quad \text{Equation A-6}$$

However, the dilution rate, D , may be defined as follows:

$$D = \frac{F}{V} \quad \text{Equation A-7}$$

Therefore, substituting Equation A-7 into Equation A-6 gives:

$$\frac{dx}{dt} = Dx_i + x(\mu - D) \quad \text{Equation A-8}$$

For most applications, however, it may be assumed that the feed material is sterile and therefore $x_i = 0$. Applying this assumption to Equation A-8 then gives:

$$\frac{dx}{dt} = x(\mu - D) \quad \text{Equation A-9}$$

From Equation A-9 it is clear that if the dilution rate is greater than the specific growth rate, $\frac{dx}{dt}$ will be negative and the cell concentration would decrease. Therefore, the flow rate of the feed stream should be chosen in such a way that the dilution rate is equal to or lower than the maximum specific growth rate to maintain or increase the cell concentration.

A material balance on the limiting substrate is further required for the evaluation of kinetic parameters. By performing a material balance on the limiting substrate, Equation A-10 is derived.

$$\frac{d(sV)}{dt} = Fs_i - r_s V \quad \text{Equation A-10}$$

where r_s is the rate of substrate uptake.

However, r_s is influenced by the growth rate, rate of product synthesis and the rate of substrate uptake for maintenance (Doran, 2004) and may be expressed as follows:

$$r_s = (\text{Rate of substrate uptake for growth}) + (\text{Rate of substrate uptake for product synthesis}) + (\text{Rate of substrate uptake for maintenance}) \quad \text{Equation A-11}$$

The three terms on the right-hand side of Equation A-11 are mathematically expressed as follows:

$$\text{Rate of substrate uptake for growth} = \frac{r_x}{Y_{XS}} \quad \text{Equation A-12}$$

where r_x is the volumetric rate of biomass production and Y_{XS} is the true yield of biomass from substrate.

$$\text{Rate of substrate uptake for product synthesis} = \frac{r_p}{Y_{PS}} \quad \text{Equation A-13}$$

where r_p is the volumetric rate of product formation and Y_{PS} is the true yield of product from substrate.

$$\text{Rate of substrate uptake for maintenance} = m_s x \quad \text{Equation A-14}$$

Where m_s is the specific rate of substrate uptake for maintenance activities, also known as the *maintenance coefficient*.

The volumetric rate of biomass production, r_x , is a function of the specific growth rate, μ , and the cell concentrations, and can be described by the following equation:

$$r_x = \mu x \quad \text{Equation A-15}$$

Similarly, the volumetric rate of product formation, r_p , is a function of the specific rate of product formation, q_p , and the cell concentration, and is given by the following equation:

$$r_p = q_p x \quad \text{Equation A-16}$$

Equation A-11 is thus re-written as follows:

$$r_s = \left(\frac{\mu}{Y_{XS}} + \frac{q_p}{Y_{PS}} + m_s \right) x \quad \text{Equation A-17}$$

Finally, the material balance on the limiting substrate (Equation A-10) can be re-written as:

$$\frac{d(sV)}{dt} = F_{S_i} - \left(\frac{\mu}{Y_{XS}} + \frac{q_p}{Y_{PS}} + m_s \right) xV \quad \text{Equation A-18}$$

Once again expanding the differential on the left-hand side of Equation A-18 and applying Equation A-2 and Equation A-7, gives:

$$\frac{ds}{dt} = D(s_i - s) - x\left(\frac{\mu}{Y_{XS}} + \frac{q_P}{Y_{PS}} + m_S\right)$$

Equation A-19

Quasi-steady-state fed-batch operation

If the reactor is first operated in batch-mode until the stationary phase has been reached, and fed-batch operation is only started when the limiting substrate is almost depleted, Equation A-9 and Equation A-19 can be simplified. When fed-batch operation is started, the added nutrients will continuously be converted into biomass and synthesized products. At the same time, the volume of the culture broth would increase. From Equation A-9, if the growth rate is equal to the dilution rate applied during the fed-batch phase ($\mu \approx D$), the cell concentration

will remain constant and $\frac{dx}{dt} \approx 0$. Furthermore, *pseudo steady-state operation* is achieved if D is constant. This can be achieved by exponentially increasing the inlet flow rate. If the inlet flow rate is constant, D will rapidly decrease and then much slower at longer times (Blanch and Clark, 1997)

Assuming that growth follows Monod kinetics, and substituting $\mu \approx D$ into the Monod expression, would yield the following equation:

$$D \approx \frac{\mu_{\max} x}{K_S + s}$$

Equation A-20

After rearranging, Equation A-21 yields an expression for substrate concentration as a function of dilution rate:

$$s \approx \frac{DK_S}{\mu_{\max} - D}$$

Equation A-21

Moreover, if it is assumed that maintenance is negligible and that product synthesis is directly coupled with energy metabolism, then Equation A-19 is simplified to:

$$\frac{ds}{dt} = D(s_i - s) - x\left(\frac{\mu}{Y_{XS}}\right)$$

Equation A-22

If a high cell density is achieved, the substrate concentration entering the reactor at the start of fed-batch operation is much higher than that inside the reactor. Furthermore, the nutrients entering the reactor are almost instantly consumed, and $\frac{ds}{dt} \approx 0$ (Doran, 2004). However, to

achieve $\frac{ds}{dt} \approx 0$ the specific substrate utilization rate ($g_{\text{substrate}}/L/hr/g_{\text{cells}}$) should be known, so that the feed concentration can be chosen to be of such a concentration that the nutrient feed rate is equal to the nutrient consumption rate.

By applying the relationships $\frac{ds}{dt} \approx 0$ and $\mu \approx D$, an expression for cell concentration is derived and is given by:

$$x = Y_{XS} S_i$$

Equation A-23

The condition of fed-batch operation when $\frac{dx}{dt} \approx 0$, $\frac{ds}{dt} \approx 0$ and $\frac{dp}{dt} \approx 0$, yields *quasi-steady state operation*.

Derivation of exponential feed flow rate equation

The exponential feed flow rate can be calculated explicitly if the specific growth rate is assumed constant. Equation A-3 is a cell balance over the fed-batch system. If it is assumed that the cell concentration in the feed is zero, Equation A-3 reduces to:

$$\frac{d(xV)}{dt} = \mu xV$$

Equation A-24

When μ is constant, Equation A-24 may be solved in xV as follows:

$$\int \frac{d(xV)}{xV} = \int \mu xV dt$$

Equation A-25

Solving the integral, Equation A-25 is simplified to Equation A-26

$$\ln xV - \ln x_0V_0 = \mu t$$

Equation A-26

Solving Equation A-26 yields Equation A-27:

$$xV = x_0V_0 e^{\mu t}$$

Equation A-27

Substituting Equation A-27 into Equation A-22 and assuming $\frac{ds}{dt} \approx 0$ yields Equation A-28:

$$D(s_i - s) = \frac{x_0V_0 e^{\mu t}}{V}$$

Equation A-28

Since $D=F/V$, Equation A-28 can be simplified to, from which the feed flow rate can be calculated as a function of time:

$$F(t) = \frac{\mu x_0 V_0 e^{\mu t}}{Y_X (s_i - s)}$$

Equation A-29

Figure A-1 below shows the exponential increase in the feed flow rate (according to Equation A-29) while the dilution rate, substrate concentration and cell concentration is maintained constant.

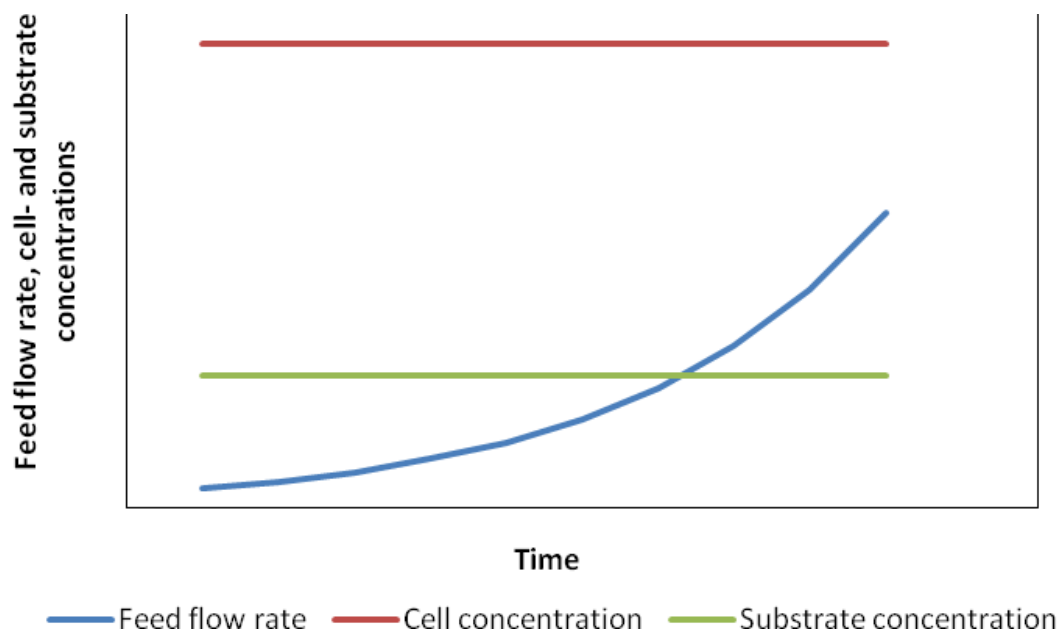


Figure A-1: Exponential increase in feed flow rate, while cell- and substrate concentration remains constant

Equation A-29 was not used in this study to predict the feed flow rate, since it requires the biomass yield on substrate to be constant and to be known. It also requires the concentration of the limiting nutrient within the reactor to be known.

Alternatively, the feed flow rate (to maintain a constant dilution rate) can be calculated from Equation A-7. By assuming a constant dilution rate, and rearranging Equation A-7, the flow rate can be calculated from $F = DV$. However, as fresh nutrient are added to the reactor, the volume increases. Accordingly, the flow rate should be increased to maintain the desired dilution rate. In this study, the feed flow rate was increased hourly following a stepwise

procedure (see Figure 2-1). The stepwise increases in the feed flow rate are calculated as follows:

- The initial feed flow rate is calculated according to Equation A-7 using the predetermined dilution rate and initial culture broth volume and is maintained constant for a constant time interval. The time interval selected for this study was 1 hour ($\Delta t=1$).
- After 1 hour, the increase in culture broth volume is calculated from the following equation:

$$\Delta V = F \Delta t \quad \text{Equation A-30}$$

- Therefore, the volume of the culture broth after 1 hour is calculated according to the following equation:

$$V = V_0 + \Delta V \quad \text{Equation A-31}$$

- After calculating the volume of the culture broth after 1 hour of fed-batch operation, Equation A-7 is used to re-calculate the feed flow rate.
- This methodology is repeated after every constant time interval

Appendix B shows the predicted feed flow rates of the constant dilution rate fed-batch experiments, which was based on the alternative method described above.

Variation of dilution rate with constant feed rate

For the special case where the inlet flow rate is constant, the volume of the culture broth increases linearly with time and is described by the following equation:

$$V = V_0 + Ft \quad \text{Equation A-32}$$

If the inlet flow rate is constant and $\mu \approx D$ when $\frac{dx}{dt} \approx 0$, the change in the dilution rate with time is derived as follows:

$$\frac{d\left(\frac{F}{V}\right)}{dt} = \frac{d\left(\frac{F}{V_0 + Ft}\right)}{dt} = \frac{-F^2}{(V_0 + Ft)^2} \quad \text{Equation A-33}$$

Figure A-2 below shows the initial rapid decrease in the dilution rate, followed by a slower decrease over a longer period of time.

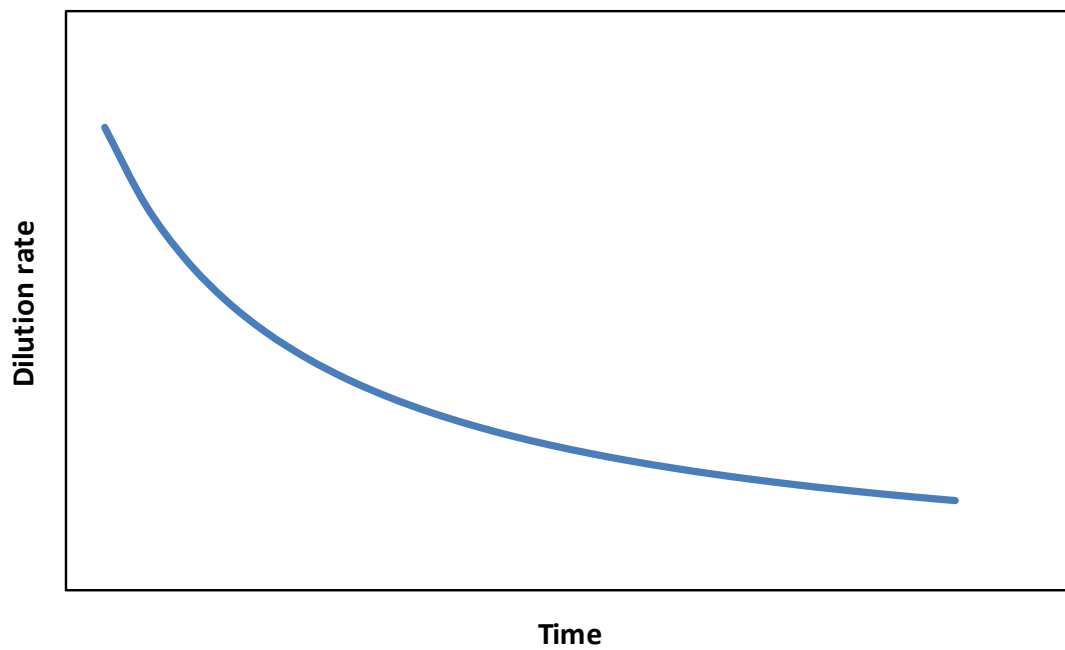


Figure A-2: Change of dilution rate with time when a constant feed rate strategy is applied

Appendix B: Predicted feed flow rates of constant dilution rate experiments

The flow rates of the constant dilution rate fed-batch experiments were determined according to the following procedure:

- The dilution rate to be applied was selected, and using Equation 2-1, the initial feed flow rate was calculated by assuming a starting culture broth volume of $V_0=2\text{L}$.
- The feed flow rate was run at the calculated initial flow rate for 1h.
- Using the equation, $\Delta V=F\Delta t$, the change in culture volume was determined after $\Delta t=1\text{h}$.
- The volume after 1h was calculated by adding ΔV to the initial volume of 2L ($V=V_0+\Delta V$)
- Thereafter, Equation 2-1 was used to recalculate the desired flow rate to maintain the selected dilution rate.
- The newly calculated flow rate was run for $\Delta t=1\text{h}$ and this procedure was repeated until $V=5.6\text{L}$, which is the limiting working volume of the bioreactor used for experiments.

The predicted feed flow rates to maintain constant dilution rates of 0.05 h^{-1} , 0.10 h^{-1} , 0.15 h^{-1} and 0.4 h^{-1} are shown in Table B-1

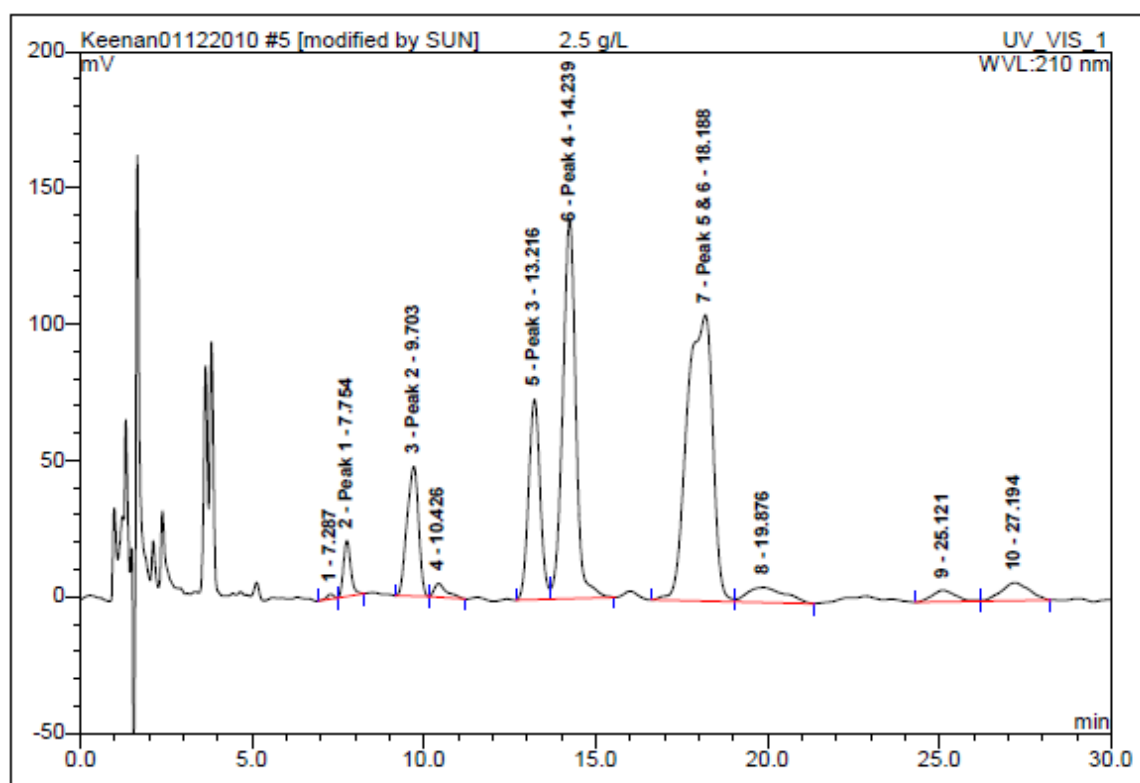
Table B-1: Predicted feed flow rates according to Equation 2-1 to maintain a constant dilution rate of 0.05 h^{-1} , 0.10 h^{-1} , 0.15 h^{-1} and 0.4 h^{-1}

| Predicted feed flow rates to maintain a constant dilution rate of 0.05 h^{-1} | | | | |
|---|-----------------------|-------|------------|---------|
| t (h) | D (h^{-1}) | V (L) | ΔV | F (L/h) |
| 0.00 | 0.05 | 2.00 | | 0.10 |
| 1.00 | 0.05 | 2.10 | 0.10 | 0.11 |
| 2.00 | 0.05 | 2.21 | 0.11 | 0.11 |
| 3.00 | 0.05 | 2.32 | 0.11 | 0.12 |
| 4.00 | 0.05 | 2.43 | 0.12 | 0.12 |
| 5.00 | 0.05 | 2.55 | 0.12 | 0.13 |
| 6.00 | 0.05 | 2.68 | 0.13 | 0.13 |
| 7.00 | 0.05 | 2.81 | 0.13 | 0.14 |
| 8.00 | 0.05 | 2.95 | 0.14 | 0.15 |
| 9.00 | 0.05 | 3.10 | 0.15 | 0.16 |
| 10.00 | 0.05 | 3.26 | 0.16 | 0.16 |
| 11.00 | 0.05 | 3.42 | 0.16 | 0.17 |
| 12.00 | 0.05 | 3.59 | 0.17 | 0.18 |
| 13.00 | 0.05 | 3.77 | 0.18 | 0.19 |
| 14.00 | 0.05 | 3.96 | 0.19 | 0.20 |
| 15.00 | 0.05 | 4.16 | 0.20 | 0.21 |
| 16.00 | 0.05 | 4.37 | 0.21 | 0.22 |
| 17.00 | 0.05 | 4.58 | 0.22 | 0.23 |
| 18.00 | 0.05 | 4.81 | 0.23 | 0.24 |
| 19.00 | 0.05 | 5.05 | 0.24 | 0.25 |
| 20.00 | 0.05 | 5.31 | 0.25 | 0.27 |

Table B-1: Predicted feed flow rates according to Equation 2-1 to maintain a constant dilution rate of 0.05 h⁻¹, 0.10 h⁻¹, 0.15 h⁻¹ and 0.4 h⁻¹(continued)

| Predicted feed flow rates to maintain a constant dilution rate of 0.10 h ⁻¹ | | | | |
|--|----------------------|-------|------|---------|
| t (h) | D (h ⁻¹) | V (L) | ΔV | F (L/h) |
| 0.00 | 0.10 | 2.00 | | 0.20 |
| 1.00 | 0.10 | 2.20 | 0.20 | 0.22 |
| 2.00 | 0.10 | 2.42 | 0.22 | 0.24 |
| 3.00 | 0.10 | 2.66 | 0.24 | 0.27 |
| 4.00 | 0.10 | 2.93 | 0.27 | 0.29 |
| 5.00 | 0.10 | 3.22 | 0.29 | 0.32 |
| 6.00 | 0.10 | 3.54 | 0.32 | 0.35 |
| 7.00 | 0.10 | 3.90 | 0.35 | 0.39 |
| 8.00 | 0.10 | 4.29 | 0.39 | 0.43 |
| 9.00 | 0.10 | 4.72 | 0.43 | 0.47 |
| 10.00 | 0.10 | 5.19 | 0.47 | 0.52 |
| Predicted feed flow rates to maintain a constant dilution rate of 0.15 h ⁻¹ | | | | |
| t (h) | D (h ⁻¹) | V (L) | ΔV | F (L/h) |
| 0.00 | 0.15 | 2.00 | | 0.30 |
| 1.00 | 0.15 | 2.30 | 0.30 | 0.35 |
| 2.00 | 0.15 | 2.65 | 0.35 | 0.40 |
| 3.00 | 0.15 | 3.04 | 0.40 | 0.46 |
| 4.00 | 0.15 | 3.50 | 0.46 | 0.52 |
| 5.00 | 0.15 | 4.02 | 0.52 | 0.60 |
| 6.00 | 0.15 | 4.63 | 0.60 | 0.69 |
| 7.00 | 0.15 | 5.32 | 0.69 | 0.80 |
| Predicted feed flow rates to maintain a constant dilution rate of 0.40 h ⁻¹ | | | | |
| t (h) | D (h ⁻¹) | V (L) | ΔV | F (L/h) |
| 0.00 | 0.40 | 2.00 | | 0.80 |
| 1.00 | 0.40 | 2.80 | 0.80 | 1.12 |
| 2.00 | 0.40 | 3.92 | 1.12 | 1.57 |
| 3.00 | 0.40 | 5.49 | 1.57 | 2.20 |

Appendix C: HPLC chromatograms



| No. | Ret. Time min | Peak Name | Height mV | Area mV*min | Rel.Area % | Amount ug/ml | Type |
|---------------|------------------|------------|--------------|----------------|---------------|-----------------|------|
| 1 | 7.29 | n.a. | 1.825 | 0.398 | 0.18 | n.a. | BMb* |
| 2 | 7.75 | Peak 1 | 20.453 | 5.029 | 2.25 | 1.593 | bMB* |
| 3 | 9.70 | Peak 2 | 47.528 | 18.524 | 8.30 | 1.505 | BMB |
| 4 | 10.43 | n.a. | 5.046 | 2.116 | 0.95 | n.a. | BMB |
| 5 | 13.22 | Peak 3 | 73.485 | 28.577 | 12.80 | 1.594 | BM |
| 6 | 14.24 | Peak 4 | 139.145 | 61.186 | 27.41 | 1.628 | MB |
| 7 | 18.19 | Peak 5 & 6 | 104.974 | 90.717 | 40.64 | 1.615 | BM |
| 8 | 19.88 | n.a. | 5.476 | 7.062 | 3.16 | n.a. | MB |
| 9 | 25.12 | n.a. | 4.245 | 3.375 | 1.51 | n.a. | BM |
| 10 | 27.19 | n.a. | 6.634 | 6.232 | 2.79 | n.a. | MB |
| Total: | | | 408.811 | 223.218 | 100.00 | 7.936 | |

Figure C-1: HPLC chromatogram of a 2.5 g/L surfactin standard

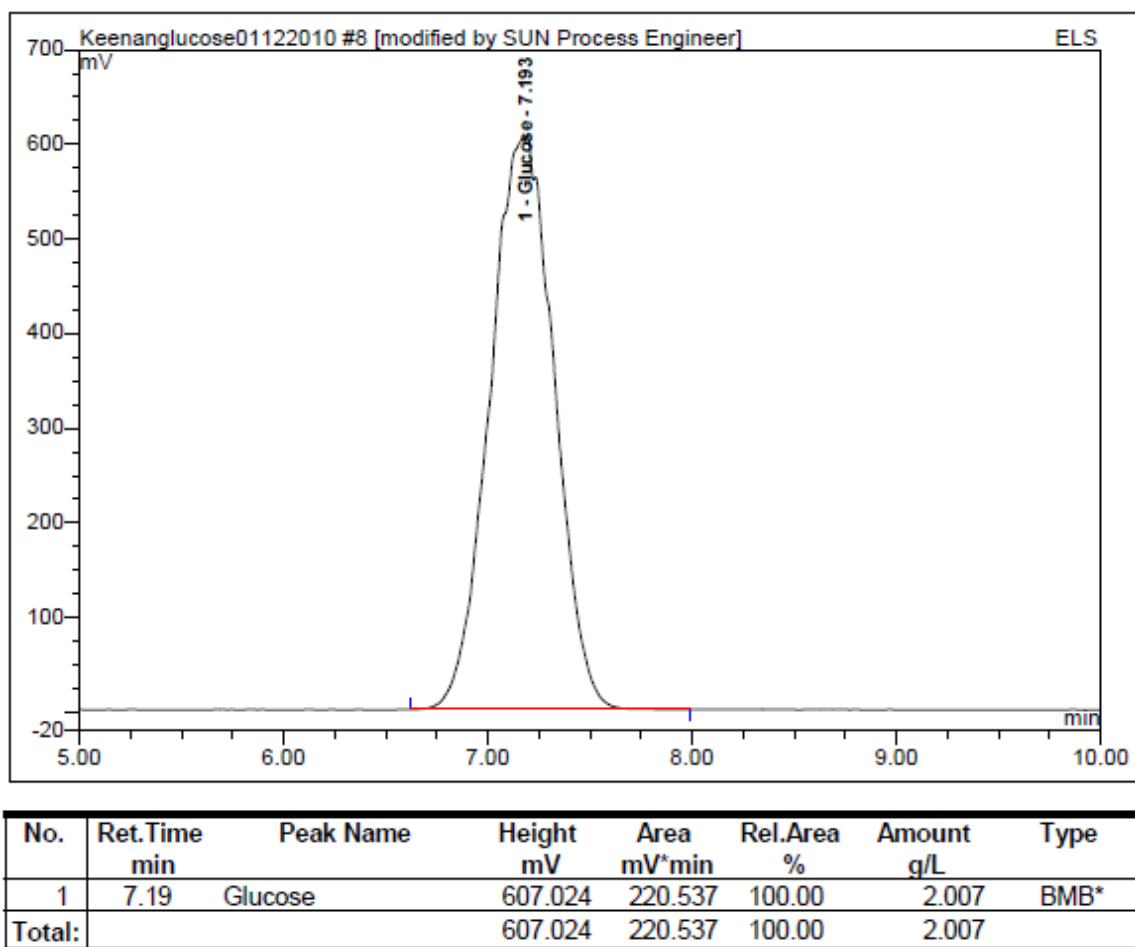


Figure C-2: HPLC chromatogram of a 2.0352 g/L glucose standard